Nuclear Science

ISBN 92-64-02331-3
NEA/NSC/DOC(2006)23

NEA NUCLEAR SCIENCE COMMITTEE
NEA COMMITTEE ON SAFETY OF NUCLEAR INSTALLATIONS

BOILING WATER REACTOR TURBINE TRIP (TT) BENCHMARK

Volume III: Summary Results of Exercise 2

November 2006

by

Bedirhan Akdeniz, Kostadin N. Ivanov
Nuclear Engineering Program
The Pennsylvania State University
University Park, PA, 16802 USA

Andy M. Olson
Exelon Nuclear
200 Exelon Way, KSA2-N
Kennett Square, PA, 19348 USA

NEA No. 5437

NUCLEAR ENERGY AGENCY
ORGANISATION FOR ECONOMIC CO-OPERATION AND DEVELOPMENT
US NUCLEAR REGULATORY COMISSION

ORGANISATION FOR ECONOMIC CO-OPERATION AND DEVELOPMENT

The OECD is a unique forum where the governments of 30 democracies work together to address the economic, social and environmental challenges of globalisation. The OECD is also at the forefront of efforts to understand and to help governments respond to new developments and concerns, such as corporate governance, the information economy and the challenges of an ageing population. The Organisation provides a setting where governments can compare policy experiences, seek answers to common problems, identify good practice and work to co-ordinate domestic and international policies.

The OECD member countries are: Australia, Austria, Belgium, Canada, the Czech Republic, Denmark, Finland, France, Germany, Greece, Hungary, Iceland, Ireland, Italy, Japan, Korea, Luxembourg, Mexico, the Netherlands, New Zealand, Norway, Poland, Portugal, the Slovak Republic, Spain, Sweden, Switzerland, Turkey, the United Kingdom and the United States. The Commission of the European Communities takes part in the work of the OECD.

OECD Publishing disseminates widely the results of the Organisation's statistics gathering and research on economic, social and environmental issues, as well as the conventions, guidelines and standards agreed by its members.

* * *

This work is published on the responsibility of the Secretary-General of the OECD. The opinions expressed and arguments employed herein do not necessarily reflect the official views of the Organisation or of the governments of its member countries.

NUCLEAR ENERGY AGENCY

The OECD Nuclear Energy Agency (NEA) was established on 1st February 1958 under the name of the OEEC European Nuclear Energy Agency. It received its present designation on 20th April 1972, when Japan became its first non-European full member. NEA membership today consists of 28 OECD member countries: Australia, Austria, Belgium, Canada, the Czech Republic, Denmark, Finland, France, Germany, Greece, Hungary, Iceland, Ireland, Italy, Japan, Luxembourg, Mexico, the Netherlands, Norway, Portugal, Republic of Korea, the Slovak Republic, Spain, Sweden, Switzerland, Turkey, the United Kingdom and the United States. The Commission of the European Communities also takes part in the work of the Agency.

The mission of the NEA is:

- to assist its member countries in maintaining and further developing, through international co-operation, the scientific, technological and legal bases required for a safe, environmentally friendly and economical use of nuclear energy for peaceful purposes, as well as
- to provide authoritative assessments and to forge common understandings on key issues, as input to government decisions on nuclear energy policy and to broader OECD policy analyses in areas such as energy and sustainable development.

Specific areas of competence of the NEA include safety and regulation of nuclear activities, radioactive waste management, radiological protection, nuclear science, economic and technical analyses of the nuclear fuel cycle, nuclear law and liability, and public information. The NEA Data Bank provides nuclear data and computer program services for participating countries.

In these and related tasks, the NEA works in close collaboration with the International Atomic Energy Agency in Vienna, with which it has a Co-operation Agreement, as well as with other international organisations in the nuclear field.

FOREWORD

The OECD Nuclear Energy Agency (NEA) completed under US Nuclear Regulatory Commission (NRC) sponsorship a PWR main steam line break (MSLB) benchmark against coupled system three-dimensional (3-D) neutron kinetics and thermal-hydraulic codes. Another OECD/NRC coupled-code benchmark was completed for a BWR turbine trip (TT) transient and is the object of the present report. Turbine trip transients in a BWR are pressurisation events in which the coupling between core space-dependent neutronic phenomena and system dynamics plays an important role. The data made available from actual experiments carried out at the Peach Bottom 2 plant make the present benchmark particularly valuable. While defining and co-ordinating the BWR TT benchmark, a systematic approach and multi-level methodology was developed, which not only allowed for a consistent and comprehensive validation process, but also contributed to the study of key parameters of pressurisation transients. The benchmark consists of three separate exercises, two steady states and five transient scenarios.

The BWR TT benchmark is being published in four volumes as OECD/NEA reports. CD-ROMs will also be prepared and will include the four reports and the transient boundary conditions, decay heat values as a function of time, cross-section libraries and supplementary tables and graphs not published in the paper versions. *BWR TT Benchmark – Volume I: Final Specifications* was issued in 2001 [NEA/NSC/DOC(2001)1]. The benchmark team – Pennsylvania State University (PSU) in co-operation with Exelon Nuclear and the OECD/NEA – was responsible for co-ordinating benchmark activities, answering participants' questions and assisting participants in developing their models, as well as analysing submitted solutions and providing reports summarising the results for each phase. The benchmark team was also involved in the technical aspects of the benchmark, including sensitivity studies for the different exercises. In performing these tasks, the PSU team has been collaborating with Andy M. Olson and Kenneth W. Hunt of Exelon Nuclear. Lance J. Agee, of the Electric Power Research Institute (EPRI), also provided technical assistance for this international benchmark project. *BWR TT Benchmark – Volume II: Summary Results of Exercise 1* was published in 2004 [NEA/NSC/DOC(2004)21]. It summarised the results for Exercise 1 of the benchmark and identified the key parameters and important issues concerning the thermal-hydraulic system modelling of the TT transient with specified core average axial power distribution and fission power (or reactivity) time transient history. Exercise 1 helped the participants initialise and test their system code models for further use in Exercise 3 on coupled 3-D kinetics/system thermal-hydraulics simulations.

Volume III summarises the results for Exercise 2 of the benchmark and identifies the key parameters and important issues concerning the coupled neutronics/thermal-hydraulic core modelling with provided core inlet and outlet boundary conditions. Exercise 2 helped the participants initialise and test their core models for further use in Exercise 3 on coupled 3-D kinetics/system thermal-hydraulics simulations.

Acknowledgements

The authors would like to thank Prof. J. Aragonés (UPM), Drs. T. Lefvert and S. Langenbuch (GRS) and Dr. F. Eltawila (US NRC), whose support and encouragement in establishing this benchmark are invaluable.

This report is the sum of many efforts, the participants, the funding agencies and their staff – the US Nuclear Regulatory Commission and the Organisation of Economic Co-operation and Development. Special appreciation is due to: L. Agee (EPRI), Professor T. Downar (Purdue) University, B. Aktas (ISL Inc.), Drs. G. Gose and C. Peterson (CSA), Dr. A. Hotta (TEPSYS), Dr. P. Coddington (PSI) and Dr. U. Grundmann (FZR). Their technical assistance, comments and suggestions have been very valuable. We would like to thank them for the effort and time involved.

Of particular note are the efforts of Dr. F. Eltawila assisted by Drs. J. Han and J. Uhle of the US Nuclear Regulatory Commission. Through their efforts, funding was secured for this project. We also thank them for their invaluable technical advice and assistance.

Special appreciation goes to the report reviewers: Dr. A. Hotta, Dr. U. Grundman and Professor G. Verdú (UPV). Their comments and suggestions were very valuable and significantly improved the quality of this report.

The authors wish to express their sincere appreciation for the outstanding support offered by Dr. E. Sartori, who is providing efficient administration, organisation and valuable technical advice.

Authors wish to specially thank all of the OECD/NEA BWR Turbine Trip Benchmark participants for their valuable support, comment and feedback during this study.

Special thanks are due to all of authors' family members for their encouragement, support and patience throughout this work.

Finally, the authors are grateful to Amanda Costa for having devoted her competence and skills to finalising this report for publication.

TABLE OF CONTENTS

Foreword 3

List of figures 7

List of tables 9

List of abbreviations 11

Chapter 1 **INTRODUCTION** 13

Chapter 2 **DESCRIPTION OF EXERCISE 2** 15
2.1 General 15
2.2 Core and neutronics data 16
2.3 Core thermal-hydraulic boundary conditions model and its coupling with 3-D neutron kinetics model 43
2.4 Initial steady-state conditions 45
2.5 Transient calculations 47

Chapter 3 **METHODOLOGIES TO QUANTIFY THE ACCURACY OF THE CALCULATIONS** 49
3.1 Standard techniques for the comparison of results 49
3.1.1 Integral parameter values 50
3.1.2 One-dimensional (1-D) axial distributions 50
3.1.3 Two-dimensional (2-D) radial distributions 51
3.1.4 Time histories 51
3.2 ACAP analysis 52
3.3 Statistical analysis of normalised parameters 54
3.3.1 Two-dimensional (2-D) core-averaged radial power distribution 54
3.3.2 One-dimensional (1-D) core-averaged axial power distribution 56
3.3.3 One-dimensional (1-D) core-averaged axial power distribution for FAs 75 and 367 57
3.3.4 Multiple code dependencies 58

Chapter 4 **RESULTS AND DISCUSSION** 59
4.1 Steady-state results 60
4.1.1 Hot zero power (HZP) results 60
4.1.2 Hot power (HP) results 65
4.2 Transient results 74
4.2.1 Time histories 75
4.2.2 Snapshot at the time of maximum power before scram 86
4.2.3 Snapshot at the end of the transient (at 5 s) 94

Chapter 5 **CONCLUSIONS** 103

References 105

Appendix A Description of the computer codes used for analysis in Exercise 2 of the OECD/NRC BWR TT Benchmark 107
CRONOS2/FLICA4 (CEA, France) 109
DYN3D (FZR, Germany) 110
QUABOX/CUBBOX-ATHLET (GRS, Germany) 116
DNB/3D (NETCORP, USA) 116
TRAC-BF1/COS3D (NFI, Japan) 117
TRAC-BF1/SKETCH-INS (NUPEC, Japan) 118
RETRAN-3D and CORETRAN (PSI, Switzerland) 118
TRAC-BF1/NEM (PSU, USA) 121
TRAC-BF1/ENTRÉE (TEPSYS, Japan) 123
RELAP5/PARCS (U.PISA, Italy) 125
TRAC-BF1/NEM (UPV, Spain) 126
TRAB-3D (VTT, Finland) 127
POLCA-T (Westinghouse, Sweden) 128

Appendix B Questionnaire for Exercise 2 of the OECD/NRC BWR TT benchmarck 131
CRONOS2/FLICA4 (CEA, France) 134
DYN3D (FZR, Germany) 137
QUABOX/CUBBOX-ATHLET (GRS, Germany) 140
DNB-3D (NETCORP, USA) 143
TRAC-BF1/COS3D (NFI, Japan) 146
TRAC-BF1/SKETCH-INS (NUPEC, Japan) 149
RETRAN-3D (PSI, Switzerland) 152
CORETRAN-3D (PSI, Switzerland) 157
TRAC-BF1/NEM (PSU, USA) 163
TRAC-BF1/ENTRÉE (TEPSYS, Japan) 166
RELAP5/PARCS (U.PISA, Italy) 169
TRAC-BF1/NEM (UPV, Spain) 171
TRAB-3D (VTT, Finland) 177

Available on CD-ROM upon request

Appendix C Reference results

Appendix D1 Participant deviations in integral parameters

Appendix D2 Participant deviations axial parameters

Appendix D3 Participant deviations 2-D radial parameters

Appendix D4 Participant deviations time histories

List of figures

Figure 2-1. Reactor core cross-sectional view 33
Figure 2-2. PB2 initial fuel assembly lattice 34
Figure 2-3. PB2 reload fuel assembly lattice for 100 mil channels 35
Figure 2-4. PB2 reload fuel assembly lattice for 120 mil channels 36
Figure 2-5. PB2 reload fuel assembly lattice for LTA assemblies 37
Figure 2-6. PSU control rod grouping 38
Figure 2-7. Radial distribution of assembly types 39
Figure 2-8. Fuel assembly orientation for ADF assignment 40
Figure 2-9. Core orificing and TIP system arrangement 41
Figure 2-10. Elevation of core components 42
Figure 2-11. Exercise 2 vessel/core boundary condition model 44
Figure 2-12. Reactor core thermal-hydraulic channel radial map 45
Figure 2-13. PB2 HZP control rod pattern 46
Figure 2-14. PB2 HP control rod pattern 46
Figure 3-1. FOM configuration in ACAP 52
Figure 4-1. HZP k_{eff} 62
Figure 4-2. Core average relative axial power distribution at HZP 63
Figure 4-3. Relative power distribution for FA 75 at HZP 63
Figure 4-4. Relative power distribution for FA 367 at HZP 64
Figure 4-5. Mean radial power distribution at HZP (average of participants) 64
Figure 4-6. Standard deviation of radial power distribution at HZP 65
Figure 4-7. HP k_{eff} 66
Figure 4-8. Core average axial void fraction distribution at HP (Group 1) 67
Figure 4-9. Core average axial void fraction distribution at HP (Group 2) 68
Figure 4-10. Core average axial void fraction at HP (mean and deviation) 68
Figure 4-11. Core average relative axial power distribution at HP (Group 1) 69
Figure 4-12. Core average relative axial power distribution at HP (Group 2) 69
Figure 4-13. Core average relative axial power distribution at HP (mean and deviation) 70
Figure 4-14. Relative power distribution for FA 75 at HP (Group 1) 70
Figure 4-15. Relative power distribution for FA 75 at HP (Group 2) 71
Figure 4-16. Relative power distribution for FA 75 at HP (mean and deviation) 71
Figure 4-17. Relative power distribution for FA 367 at HP (Group 1) 72
Figure 4-18. Relative power distribution for FA 367 at HP (Group 2) 72
Figure 4-19. Relative power distribution for FA 367 at HP (mean and deviation) 73
Figure 4-20. Mean radial power distribution at HP (average of participants) 73
Figure 4-21. Standard deviation of radial power distribution at HP 74
Figure 4-22. Transient power (fission) 77
Figure 4-23. Transient power (fission – zoom) 77
Figure 4-24. Transient power (total) 78
Figure 4-25. Transient power (total – zoom) 78
Figure 4-26. Total reactivity 79
Figure 4-27. Total reactivity (zoom) 80
Figure 4-28. Total reactivity (mean and deviation) 80
Figure 4-29. Total reactivity (mean and deviation – zoom) 81
Figure 4-30. Doppler reactivity 82
Figure 4-31. Doppler reactivity (zoom) 82
Figure 4-32. Doppler reactivity (mean and deviation) 83
Figure 4-33. Doppler reactivity (mean and deviation – zoom) 83
Figure 4-34. Void reactivity 84

Figure 4-35. Void reactivity (zoom) 84
Figure 4-36. Void reactivity (mean and deviation) 85
Figure 4-37. Void reactivity (mean and deviation – zoom) 85
Figure 4-38. Time of maximum power before scram 86
Figure 4-39. Core axial power profile at maximum power before scram (fission power used) 87
Figure 4-40. Core axial power profile at maximum power before scram (total power used) 88
Figure 4-41. Core axial power profile at maximum power before scram (fission power used – mean and deviation) 88
Figure 4-42. Core axial power profile at maximum power before scram (total power used – mean and deviation) 89
Figure 4-43. Relative power of FA 75 at maximum power before scram (fission) 89
Figure 4-44. Relative power of FA 75 at maximum power before scram (total) 90
Figure 4-45. Relative power of FA 75 at maximum power before scram (mean and deviation – fission power used) 90
Figure 4-46. Relative power of FA 75 at maximum power before scram (mean and deviation – total power used) 91
Figure 4-47. Relative power of FA 367 at maximum power before scram (fission) 91
Figure 4-48. Relative power of FA 367 at maximum power before scram (total) 92
Figure 4-49. Relative power of FA 367 at maximum power before scram (mean and deviation – fission power used) 92
Figure 4-50. Relative power of FA 367 at maximum power before scram (mean and deviation – total power used) 93
Figure 4-51. Mean radial power distribution at maximum power before scram 93
Figure 4-52. Standard deviation of radial power distribution at maximum power before scram 94
Figure 4-53. Core axial power profile at end of transient (fission) 95
Figure 4-54. Core axial power profile at end of transient (total) 95
Figure 4-55. Core axial power profile at end of transient (mean and deviation – fission power used) 96
Figure 4-56. Core axial power profile at end of transient (mean and deviation – total power used) 96
Figure 4-57. Relative power of FA 75 at end of transient (fission) 97
Figure 4-58. Relative power of FA 75 at end of transient (total) 97
Figure 4-59. Relative power of FA 75 at end of transient (mean and deviation – fission power used) 98
Figure 4-60. Relative power of FA 75 at end of transient (mean and deviation – total power used) 98
Figure 4-61. Relative power of FA 367 at end of transient (fission) 99
Figure 4-62. Relative power of FA 367 at end of transient (total) 99
Figure 4-63. Relative power of FA 367 at end of transient (mean and deviation – fission power used) 100
Figure 4-64. Relative power of FA 367 at end of transient (mean and deviation – total power used) 100
Figure 4-65. Mean radial power distribution at end of transient 101
Figure 4-66. Standard deviation of radial power distribution at end of transient 101

List of tables

Table 1-1. List of participants in the Exercise 2 of the BWR TT benchmark 14
Table 2-1. PB2 fuel assembly data 18
Table 2-2. Assembly design 1 18
Table 2-3. Assembly design 2 19
Table 2-4. Assembly design 3 19
Table 2-5. Assembly design 4 19
Table 2-6. Assembly design 5 20
Table 2-7. Assembly design 6 20
Table 2-8. Decay constant and fractions of delayed neutrons 21
Table 2-9. Heavy-element decay heat constants 21
Table 2-10. Assembly design for Type 1 initial fuel 22
Table 2-11. Assembly design for Type 2 initial fuel 23
Table 2-12. Assembly design for Type 3 initial fuel 24
Table 2-13. Assembly design for Type 4 8×8 UO_2 reload 25
Table 2-14. Assembly design for Type 5 8×8 UO_2 reload 26
Table 2-15. Assembly design for Type 6 8×8 UO_2 reload, LTA 27
Table 2-16. Control rod data (movable control rods) 28
Table 2-17. Definition of assembly types 28
Table 2-18. Composition numbers in axial layer for each assembly type 29
Table 2-19. Range of variables 30
Table 2-20. Key to macroscopic cross-section tables 31
Table 2-21. Macroscopic cross-section table structure 31
Table 2-22. PB2 HZP initial conditions 45
Table 2-23. PB2 TT2 initial conditions from process computer P1 edit 46
Table 2-24. PB2 TT2 scram characteristics 47
Table 2-25. CRD position after scram vs. time 47
Table 3-1. Exercise 2 parameters for steady-state statistical comparisons 49
Table 3-2. Exercise 2 parameters for transient statistical comparisons 50
Table 4-1. Number of channels used and power submitted by the participants 61
Table 4-2. Models used at HZP 61
Table 4-3. HZP k_{eff} 62
Table 4-4. Models used at HP 66
Table 4-5. HP k_{eff} 67
Table 4-6. Models used in transient calculation 75
Table 4-7. Transient power, figure of merit 79
Table 4-8. Total reactivity, figure of merit 81
Table 4-9. Doppler reactivity, figure of merit 84
Table 4-10. Void reactivity, figure of merit 85
Table 4-11. Time of maximum power before scram 87

LIST OF ABBREVIATIONS

1-D	One-dimensional
2-D	Two-dimensional
3-D	Three-dimensional
ACAP	Automated Code Assessment Program
ADF	Assembly discontinuity factor
APRM	Average range power monitor
AVZ	Above vessel zero
BC	Boundary conditions
BE	British Energy
BOC	Beginning of cycle
BP	Burnable poison
BPV	Bypass valve
BVBO	Bypass valve begins opening
BVFO	Bypass valve full open
BWR	Boiling water reactor
CA	Control assembly
CEA	Commissariat à l'énergie atomique
CEPIR	Core exit pressure initial response
DPIR	Dome pressure initial response
EOC	End of cycle
EOT	End of transient
EPRI	Electric Power Research Institute
EXELON	Exelon Corporation
FA	Fuel assembly
FANP	Framatome ANP
FFT	Fast Fourier transform
FOM	Figure of merit
FZR	Forschungszentrum Rossendorf
GE	General Electric
GRS	Gesellschaft fur Anlagen- und Reaktorsicherheit mbH
HFP	Hot full power
HP	Hot power
HZP	Hot zero power
IBER	Iberdrola Ingenieria
LPRM	Local power range monitor
LWR	Light water reactor
ME	Mean error
MSIV	Main steam isolation valve
MSLB	Main steam line break
MVCEP	Maximum value per cent initial value of core exit pressure

NEA	Nuclear Energy Agency
NEM	Nodal expansion method
NETCORP	Nuclear Engineering Technology Corporation
NFI	Nuclear Fuel Industries, Ltd.
NP	Normalised power
NPP	Nuclear power plant
NRC	US Nuclear Regulatory Commission
NRS	Nuclear reactor systems
NSC	Nuclear Science Committee
NSSS	Nuclear steam supply system
NUPEC	Nuclear Power Engineering Corporation
OECD	Organisation for Economic Co-Operation and Development
PB	Peach Bottom Atomic Power Station
PB2	Peach Bottom Atomic Power Station Unit 2
PECo	Philadelphia Electric Company
PSI	Paul Scherrer Institute
PSU	Pennsylvania State University
PWR	Pressurised water reactor
SRV	Safety relief valve
TEPSYS	TEPCO Systems Corporation
T-H	Thermal-hydraulic
TSV	Turbine stop valve
TSVC	Turbine stop valve closing
TT	Turbine trip
TT2	Turbine trip test 2
UPI	University of Pisa
UPV	Universidad Politecnica de Valencia
VTT	Valtion Teknillinen Tutkimuskeskus
VBA	Visual basic for applications
WES	Westinghouse Electric Company

Chapter 1

INTRODUCTION

Prediction of a nuclear power plant's behaviour under both normal and abnormal conditions has an important effect on its safety and economic operation. Incorporation of full three-dimensional (3-D) models of the reactor core into system transient codes allows for a "best-estimate" calculation of interactions between the core behaviour and plant dynamics. Recent progress in computer technology has made the development of such coupled system thermal-hydraulic and neutron kinetics code systems feasible. Considerable efforts have been made in various countries and organisations in this direction. To verify the capability of the coupled codes to analyse complex transients with coupled core-plant interactions and to fully test thermal-hydraulic coupling, appropriate light water reactor (LWR) transient benchmarks need to be developed on a higher "best-estimate" level. The previous sets of transient benchmark problems separately addressed system transients (designed mainly for thermal-hydraulic system codes with point kinetics models) and core transients (designed for thermal-hydraulic core boundary conditions models coupled with a 3-D neutron kinetics model). The Nuclear Energy Agency (NEA) of the Organisation for Economic Co-operation and Development (OECD) has completed – under the auspices of the US Nuclear Regulatory Commission (NRC) – sponsorship of a pressurised water reactor (PWR) main steam line break (MSLB) benchmark [1] against coupled thermal-hydraulic and neutron kinetics codes. Similar benchmark against the coupled codes for a boiling water reactor (BWR) plant transient was also established as an OECD/NRC activity [2]. A turbine trip (TT) transient in a BWR is a pressurisation event in which the coupling between core phenomena and system dynamics plays an important role. In addition, the available real plant experimental data [4,5] makes the such benchmark problem very valuable. The NEA, OECD and US NRC have approved the BWR TT benchmark for the purpose of validating advanced system best-estimate analysis codes.

The established benchmark project was designed to test the coupled system thermal-hydraulic/ neutron kinetics codes for simulation of the Peach Bottom 2 (PB2 – a General Electric-designed BWR/4) turbine trip transient with a sudden closure of the turbine stop valve. Three turbine trip transients at different power levels were performed at the PB2 nuclear power plant (NPP) prior to shutdown for refuelling at the end of Cycle 2 in April 1977. The second test (TT2) is selected for the benchmark problem to investigate the effect of the pressurisation transient (following the sudden closure of the turbine stop valve) on the neutron flux in the reactor core. In a best-estimate manner the test conditions approached the design basis conditions as closely as possible. The actual data were collected, including a compilation of reactor design and operating data for Cycles 1 and 2 of PB2 and the plant transient experimental data. The transient was selected for this benchmark because it is a dynamically complex event and it constitutes a good problem to test the coupled codes on both levels: neutronics/thermal-hydraulics coupling, as well as core/plant system coupling. In the TT2 test, the thermal-hydraulic feedback alone limited the power peak and initiated the power reduction. The void feedback plays the major role while the Doppler feedback plays a subordinate role. The reactor scram then inserted additional negative reactivity and completed the power reduction and eventual core shutdown.

The purposes of this benchmark are met through the application of the three exercises, which are described in Volume 1 of the OECD/NRC *BWR TT Benchmark: Final Specifications* [2]. The purpose of the first exercise is to test the thermal-hydraulic system response and to initialise the participants' system models. Core power response is provided to reproduce the actual test results utilising either power or reactivity versus time data. The comprehensive analysis of the Exercise 1 was summarised in Volume II of the OECD/NRC *BWR TT Benchmark Volume II: Summary Results of Exercise 1* [3]. The purpose of Exercise 2 is to provide a clean initialisation of the coupled core models since the core thermal-hydraulic boundary conditions are provided. The second exercise has two steady-state conditions: hot zero power (HZP) conditions and the initial hot power (HP) conditions of TT2. The last exercise, Exercise 3, is the best-estimate coupled 3-D core/thermal-hydraulic system modelling. This exercise combines elements of the first two exercises of this benchmark and is an analysis of the transient in its entirety. Exercise 3 also has extreme scenarios that provide the opportunity to better test the code coupling and feedback modelling.

Comparative analysis of the submitted results for Exercise 2 has been performed and is summarised in this report. In total, 18 results have been submitted by the participants representing 16 different organisations from 9 different countries. A list of participants, who have submitted results to the PSU benchmark team for the second exercise, along with the code used to perform the analysis, is listed in Table 1-1. A more detailed description of each code is presented in Appendix A, and the modelling assumptions made by each participant are given in Appendix B.

Chapter 2 contains a description of Exercise 2 including the initial conditions. Chapter 3 discusses the utilised comprehensive statistical methodology for integral parameters, 1-D distributions, and time histories. Chapter 4 provides comparative analysis of the final results for the second exercise. Finally, Chapter 5 summarises the conclusions drawn from the analysis of Exercise 2.

Table 1-1. List of participants in the Exercise 2 of the BWR TT benchmark

No.	Participant*	Codes	Country
1	**CEA-33** (33-channel model)	CRONOS2/FLICA4	France
2	**CEA-764** (764-channel model)	CRONOS2/FLICA4	France
3	**FANP**	RAMONA5-2.1	Germany
4	**FZR** (3-D model with 764 core channels)	DYN3D	Germany
5	**GRS**	QUABOX/CUBBOX-ATHLET	Germany
6	**IBER**	RETRAN 3D–Mod 3.1	Spain
7	**NETCORP**	DNB-3D	USA
8	**NFI**	TRAC-BF1/COS3D	Japan
9	**NUPEC**	TRAC-BF1/SKETCH-INS	Japan
10	**PSI-A** (pressure BC at core inlet and outlet)	RETRAN-3D MOD 003.1	Switzerland
11	**PSI-B** (flow rate BC at core inlet and pressure BC at core outlet)	RETRAN-3D MOD 003.1	Switzerland
12	**PSI-C**	CORETRAN	Switzerland
13	**PSU**	TRAC-BF1/NEM	USA
14	**TEPSYS**	TRAC-BF1/ENTRÉE	Japan
15	**UPI**	RELAP5/ PARCS	Italy
16	**UPV**	TRAC-BF1/NEM	Spain
17	**VTT**	TRAB-3D	Finland
18	**WES**	POLCA-T	Sweden

* Participants' full names can be found in the List of Abbreviations.

Chapter 2

DESCRIPTION OF EXERCISE 2

2.1 General

After participants' system models are initialised and the thermal-hydraulic system responses of their codes are tested in the first exercise, studies are focused on the second exercise of PB2 TT2 benchmark. Exercise 2 consists of coupled reactor core calculations while the system thermal-hydraulics is modelled through imposed boundary conditions. The purpose of this exercise is to test the coupled core response and to initialise participant's core models.

Steady-state analyses are performed for two conditions in Exercise 2: hot zero power (HZP) conditions and the initial hot power (HP) conditions of TT2. The HZP state provides a clean initialisation of the core neutronics models since the thermal-hydraulic feedback is spatially uniform across the core.

The second exercise is to perform a coupled 3-D kinetics/thermal-hydraulic calculation for the reactor core using the PSU provided boundary conditions at core inlet and exit. The core boundary conditions are provided utilising a combination of the calculated PSU results and test data.

A TT transient in a BWR type reactor is considered one of the most complex events to be analysed because it involves the reactor core, the high pressure coolant boundary, associated valves and piping in highly complex interactions with variables changing very rapidly. The PB2 TT2 test starts with a sudden closure of the turbine stop valve (TSV) and then the turbine bypass valve begins to open. From a fluid flow phenomena point of view, pressure and flow waves play an important role during the early phase of the transient (of about 1.5 seconds) because rapid valve actions cause sonic waves, as well as secondary waves, generated in the pressure vessel. The pressure oscillation generated in the main steam piping propagates with relatively little attenuation into the reactor core. The induced core pressure oscillation results in changes of the core void distribution and fluid flow. The magnitude of the neutron flux transient taking place in the BWR core is affected by the initial rate of pressure rise caused by the pressure oscillation and has a spatial variation. The simulation of the power response to the pressure pulse and subsequent void collapse requires a 3-D core modelling supplemented by 1-D simulation of the remainder of the reactor coolant system. In Exercise 2 of the benchmark the later is modelled by the same boundary conditions imposed to the 3-D core models.

The reference design for the BWR is derived from real reactor, plant and operation data for the PB2 NPP and it is based on the information provided in EPRI reports [4-7] and some additional sources such as the PECo Energy Topical report [8]. Although complete set of core/neutronics and thermal-hydraulics input specifications are provided in Volume I [2], the data relevant to Exercise 2 are given in this section for the convenience of the reader.

In the following subsections of this chapter, descriptions of core and neutronics data, thermal-hydraulic core boundary conditions model and its coupling with the 3-D neutron kinetics model, initial steady-state conditions and transient calculations are provided.

2.2 Core and neutronics data

The reference design for the BWR is derived from real reactor, plant and operation data for the PB2 BWR/4 NPP and it is based on the information provided in EPRI reports and some additional sources such as the PECO Energy Topical Report. This chapter specifies the core and neutronic data to be used in the calculations of Exercise 2.

The radial geometry of the reactor core is shown in Figure 2-1. Radially, the core is divided into cells 15.24 cm wide, each corresponding to one fuel assembly (FA), plus a radial reflector (shaded area of Figure 2-1) of the same width. There are a total of 888 assemblies, 764 FAs and 124 reflector assemblies. Axially, the reactor core is divided into 26 layers (24 core layers plus top and bottom reflectors) with a constant height of 15.24 cm (including reflector nodes). The total active core height is 365.76 cm. The axial nodalisation accounts for material changes in the fuel design and for exposure and history variations. Geometric data for the FA and fuel rod is provided in Table 2-1. Data for different assembly designs is given in Tables 2-2 through 2-7. Fuel assembly lattice drawings, including detailed dimensions, for initial fuel, reload fuel with 100 and 120 mil channels and the lead test assemblies (LTA) are shown in Figures 2-2 through 2-5. The numbers 100 and 120 refer to the wall thickness of the channel (1 mil = 0.001 inches).

The core loading during the test was as follows: 576 fuel assemblies were the original 7×7 type from Cycle 1 (C1), and the remaining 188 were a reload of 8×8 fuel assemblies. One hundred and eighty-five control rods provided reactivity control. To build the participant's given neutronic model, these control rods can be grouped according to their initial insertion position. The control rod grouping used by PSU to perform reference calculations is presented in Figure 2-6.

Two neutron energy groups and six delayed neutron precursor families are modelled. The energy release per fission for the two prompt neutron groups is 0.3213×10^{-10} and 0.3206×10^{-10} W-s/fission, and this energy release is considered to be independent of time and space. It is assumed that 2% of fission power is released as direct gamma heating for the in-channel coolant flow and 1.7% for the bypass flow. Table 2-8 shows global core-wide decay time constants and fractions of delayed neutrons. In addition delayed parameters are provided in the cross-section library for each of the compositions. The prompt neutron lifetime is 0.45085×10^{-4}.

It is recommended that ANS-79 be used as a decay heat standard model. In total 71 decay heat groups are used: 69 groups are used for the three isotopes ^{235}U, ^{239}Pu and ^{238}U with the decay heat constants defined in the 1979 ANS standard; plus, the heavy-element decay heat groups for ^{239}U and ^{239}Np are used with constants given in Table 2-9. It is recommended that the participants also use the assumption of an infinite operation at a power of 3 293 MW_t. For participants who are not capable of using the ANS-79 decay heat standard, a file of the decay heat evolution throughout the transient is provided on CD-ROM and at the benchmark **ftp** site under the directory **Decay-Heat**. These predictions are obtained using the PSU coupled code results. The effective decay heat energy fraction of the total thermal power (the relative contribution in the steady state) is equal to 0.065583.

Nineteen assembly types are contained within the core geometry. There are 435 compositions. The corresponding sets of cross-sections are provided. Each composition is defined by material properties (due to changes in the fuel design) and burn-up. The burn-up dependence is a three-component vector of variables: exposure (GWd/t), spectral history (void fraction) and control rod history. Assembly designs are defined in Tables 2-10 through 2-15. Control rod geometry data is provided in Table 2-16. The definition of assembly types is shown in Table 2-17. The radial distribution of these assembly types within the reactor geometry is shown in Figure 2-7. The axial locations of compositions for each assembly type are shown in Table 2-18.

A complete set of diffusion coefficients, macroscopic cross-sections for scattering, absorption, and fission, assembly discontinuity factors (ADFs), as a function of the moderator density and fuel temperature is defined for each composition. The group inverse neutron velocities are also provided for each composition. Dependence of the cross-sections on the above variables is specified through a two-dimensional table look-up. Each composition is assigned to a cross-section set containing separate tables for the diffusion coefficients and cross-sections, with each point in the table representing a possible core state. The expected range of the transient is covered by the selection of an adequate range for the independent variables shown in Table 2-19. Specifically, Exercise 1 was used for selecting the range of thermal-hydraulic variables. A steady-state calculation was run using the TRAC-BF1 code and initial conditions of the second turbine trip for choosing discrete values of the thermal-hydraulic variables (pressure, void fraction and coolant/moderator temperature). A transient calculation was performed to determine the expected range of change of the above variables.

A modified linear interpolation scheme (which includes extrapolation outside the thermal-hydraulic range) is used to obtain the appropriate total cross-sections from the tabulated ones based on the reactor conditions being modelled. Table 2-20 shows the definition of a cross-section table associated with a composition. Table 2-21 shows the macroscopic cross-section table structure for one cross-section set. All cross-section sets are assembled into a cross-section library. The cross-sections are provided in separate libraries for rodded **(nemtabr)** and un-rodded compositions **(nemtab)**. The format of each library is as follows:

- The first line of data shows the number of data points used for the independent thermal-hydraulic parameters. The parameters used in this benchmark include fuel temperature and moderator density.
- Each cross-section set is in the order shown in Table 2-21. Each table is in the format described in Table 2-20. More detailed information on this format is presented in Appendix B. First, the values of the independent thermal-hydraulic parameters (fuel temperature and moderator density) used to specify that particular set of cross-sections are listed, followed by the values of the cross-sections* and ADFs. Since there is one-half symmetry for all the assembly designs, two ADFs per composition per energy group are provided – West (wide gap) and South (narrow gap). Because the fuel assembly designs employed in PB2 core design have one-half symmetry, it is assumed that North is equal to West and East is equal to South (e.g. Figure 2-8). Detector parameters† are included after the two-group cross-sections followed by the delayed neutron parameters for six groups. Finally, the group inverse neutron velocities complete the data for a given cross-section set.
- The dependence on fuel temperature in the reflector cross-section tables is also modelled. This is because the reflector cross-sections are generated by performing lattice physics transport calculations, including the next fuel region. In order to simplify the reflector feedback modelling the following assumptions are made for this benchmark: an average fuel temperature value equal to 550 K is used for the radial reflector cross-section modelling in both the initial steady-state and transient simulations, and the average coolant density for the radial reflector is equal to the inlet coolant density. For the axial reflector regions the following assumptions are made: for the bottom, the fuel temperature is equal to the inlet coolant temperature (per thermal-hydraulic channel or cell) and the coolant density is equal to the inlet coolant density (again per channel); for the top, the fuel temperature is equal to the outlet coolant temperature (per channel) and the coolant density is equal to the outlet coolant density (per channel).

* Please note that the provided absorption cross-sections already take the xenon thermal cross-sections into account; however, at the participants' request, the thermal macro and micro xenon cross-sections are listed in the cross-section sets.

† Detector parameters were described in Volume I, Section 2.6.

All cross-section data, along with a program for linear interpolation, are supplied on CD-ROM and at the benchmark **ftp** site under the directory **XS-Lib** in the format described above. Lattice physics calculations are performed by homogenising the fuel lattice and the bypass flow associated with it. When obtaining the average coolant density, a correction that accounts for the bypass channel conditions should be included since this is going to influence the feedback effect on the cross-section calculation through the average coolant density. The following approach should be applied:

$$\rho_{act}^{eff} = \frac{A_{act}\rho_{act} + A_{byp}\left(\rho_{byp} - \rho_{sat}\right)}{A_{act}} \qquad 2.1$$

where ρ_{act}^{eff} is the effective average coolant density for cross-section calculation, ρ_{byp} is the average moderator coolant density of the bypass channel, ρ_{sat} is the saturated moderator coolant density of the bypass channel, A_{act} is flow cross-sectional area of the active heated channel and A_{byp} is the flow cross-sectional area of the bypass channel. Bypass conditions should be obtained by adding a bypass channel to represent the core bypass region in the thermal-hydraulic model.

Table 2-1. PB2 fuel assembly data

	Initial load			**Reload**	**Reload**	**LTA special**
Assembly type	1	2	3	4	5	6
No. of assemblies, initial core	168	263	333	0	0	0
No. of assemblies, Cycle 2	0	261	315	68	116	4
Geometry	7 × 7	7 × 7	7 × 7	8 × 8	8 × 8	8 × 8
Assembly pitch, cm	15.24	15.24	15.24	15.24	15.24	15.24
Fuel rod pitch, cm	1.875	1.875	1.875	1.623	1.623	1.623
Fuel rods per assembly	49	49	49	63	63	62
Water rods per assembly	0	0	0	1	1	2
Burnable poison positions	0	4	5	5	5	5
No. of spacer grids	7	7	7	7	7	7
Inconel per grid, kg	0.225	0.225	0.225	0.225	0.225	0.225
Zr-4 per grid, kg	1.183	1.183	1.183	1.353	1.353	1.353
Spacer width, cm	4.128	4.128	4.128	4.128	4.128	4.128
Assembly average fuel composition:						
Gd_2O_3, g	0	441	547	490	328	313
UO_2, kg	222.44	212.21	212.06	207.78	208.0	207.14
Total fuel, kg	222.44	212.65	212.61	208.27	208.33	207.45

Table 2-2. Assembly design 1

Rod type	**No. of rods**	**Pellet density**		**Stack density**	**Gd_2O_3**	**UO_2**	**Stack length**
		UO_2 (g/cm^3)	**UO_2+Gd_2O_3 (g/cm^3)**	**(g/cm^3)**	**(g)**	**(g)**	**(cm)**
1	31	10.42	–	10.34	0	4 548	365.76
2	17	10.42	–	10.34	0	4 548	365.76
2s	1	10.42	–	10.34	0	4 140	330.2

Pellet outer diameter = 1.23698 cm.
Cladding = Zircaloy-2, 1.43002 cm outer diameter × .08128 cm wall thickness, all rods.
Gas plenum length = 40.64 cm.

Table 2-3. Assembly design 2

Rod type	No. of rods	Pellet density UO_2 (g/cm^3)	Pellet density $UO_2+Gd_2O_3$ (g/cm^3)	Stack density (g/cm^3)	Gd_2O_3 (g)	UO_2 (g)	Stack length (cm)
1	25	10.42	–	10.32	0	4 352	365.76
1s	1	10.42	–	10.32	0	3 935	330.20
2	12	10.42	–	10.32	0	4 352	365.76
3	6	10.42	–	10.32	0	4 352	365.76
4	1	10.42	–	10.32	0	4 352	365.76
5A	3	–	10.29	10.19	129	4 171	365.76
6B	1	10.42	10.29	10.27	54	4 277	365.76

Pellet outer diameter = 1.21158 cm.
Cladding = Zircaloy-2, 1.43002 cm outer diameter × .09398 cm wall thickness, all rods.
Gas plenum length = 40.132 cm.

Table 2-4. Assembly design 3

Rod type	No. of rods	Pellet density UO_2 (g/cm^3)	Pellet density $UO_2+Gd_2O_3$ (g/cm^3)	Stack density (g/cm^3)	Gd_2O_3 (g)	UO_2 (g)	Stack length (cm)
1	26	10.42	–	10.32	0	4 352	365.76
2	11	10.42	–	10.32	0	4 352	365.76
3	6	10.42	–	10.32	0	4 352	365.76
4	1	10.42	–	10.32	0	4 352	365.76
5A	2	–	10.29	10.19	129	4 171	365.76
6C	1	–	10.29	10.19	117	3 771	330.20
7E	1	10.42	10.25	10.28	43	4 292	365.76
8D	1	10.42	10.25	10.19	129	4 172	365.76

Pellet outer diameter = 1.21158 cm.
Cladding = Zircaloy-2, 1.43002 cm outer diameter × .09398 cm wall thickness, all rods.
Gas plenum length = 40.132 cm.

Table 2-5. Assembly design 4

Rod type	No. of rods	Pellet density UO_2 (g/cm^3)	Pellet density $UO_2+Gd_2O_3$ (g/cm^3)	Stack density (g/cm^3)	Gd_2O_3 (g)	UO_2 (g)	Stack length (cm)
1	39	10.42	–	10.32	0	3 309	365.76
2	14	10.42	–	10.32	0	3 309	365.76
3	4	10.42	–	10.32	0	3 309	365.76
4	1	10.42	–	10.32	0	3 309	365.76
5	5	–	10.29	10.19	98	3 172	365.76
WS	1	–	–	–	0	0	–

Pellet outer diameter = 1.05664 cm.
Cladding = Zircaloy-2, 1.25222 cm outer diameter × .08636 cm wall thickness, all rods.
Gas plenum length = 40.64 cm except water rod.
Gd_2O_3 in rod type 5 runs full 365.76 cm.
Water rod (WS) has holes drilled top and bottom to provide water flow and little or no boiling.
Water rod is also a spacer positioning rod.

Table 2-6. Assembly design 5

Rod type	No. of rods	Pellet density UO_2 (g/cm^3)	Pellet density $UO_2+Gd_2O_3$ (g/cm^3)	Stack density (g/cm^3)	Gd_2O_3 (g)	UO_2 (g)	Stack length (cm)
1	39	10.42	–	10.32	0	3 309	365.76
2	14	10.42	–	10.32	0	3 309	365.76
3	4	10.42	–	10.32	0	3 309	365.76
4	1	10.42	–	10.32	0	3 309	365.76
5	5	–	10.33	10.23	66	3 216	365.76
WS	1	–	–	–	0	0	–

Pellet outer diameter = 1.05664 cm.
Cladding = Zircaloy-2, 1.25222 cm outer diameter × .08636 cm wall thickness, all rods.
Gas plenum length = 40.64 cm, except water rod.
Gd_2O_3 in rod type 5 runs full 365.76 cm.
Water rod (WS) has holes drilled top and bottom to provide water flow and little or no boiling.
Water rod is also a spacer positioning rod.

Table 2-7. Assembly design 6

Rod type	No. of rods	Pellet density UO_2 (g/cm^3)	Pellet density $UO_2+Gd_2O_3$ (g/cm^3)	Stack density (g/cm^3)	Gd_2O_3 (g)	UO_2 (g)	Stack length (cm)
1	38	10.42	–	10.32	0	3 125	355.6
2	14	10.42	–	10.32	0	3 125	355.6
3	4	10.42	–	10.32	0	3 125	355.6
4	1	10.42	–	10.32	0	3 125	355.6
5	5	–	10.33	10.23	63	3 037	355.6
WR,WS	2	–	–	–	0	0	–
ENDS	62	10.42	–	10.32	0	223	25.4

Pellet outer diameter = 1.0414 cm.
Cladding = Zircaloy-2, 1.22682 cm outer diameter × .08128 cm wall thickness, all fuelled rods.
= Zircaloy-2, 1.50114 cm outer diameter × .07620 cm wall thickness, water rods.
Gas plenum length = 24.0792 cm.
Gd_2O_3 in rod type 5 runs full 355.60 cm.
Water rod (WS) has holes drilled top and bottom to provide water flow and little or no boiling.
Water rod is also a spacer positioning rod.

Table 2-8. Decay constant and fractions of delayed neutrons

Group	Decay constant (s^{-1})	Relative fraction of delayed neutrons in %
1	0.012813	0.0167
2	0.031536	0.1134
3	0.124703	0.1022
4	0.328273	0.2152
5	1.405280	0.0837
6	3.844728	0.0214

Total fraction of delayed neutrons: 0.5526%.

Table 2-9. Heavy-element decay heat constants

Group no. (isotope)	Decay constant (s^{-1})	Available energy from a single atom (MeV)
70 (^{239}U)	4.91×10^{-4}	0.474
71 (^{239}Np)	3.41×10^{-6}	0.419

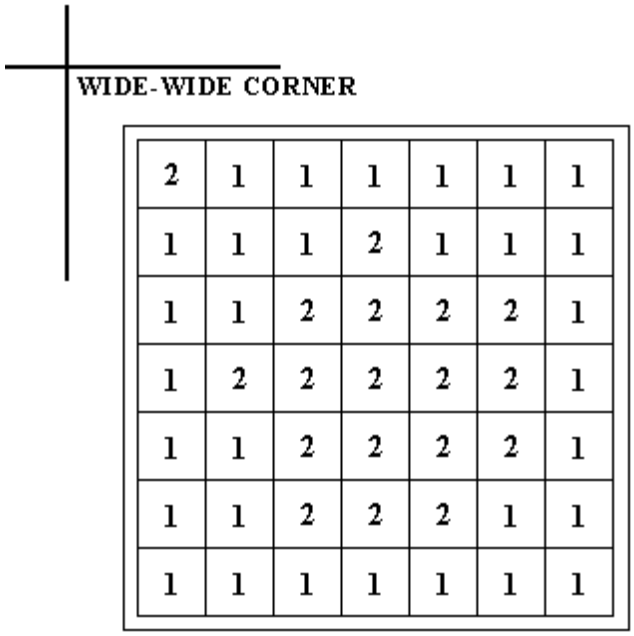

Table 2-10. Assembly design for Type 1 initial fuel

Rod type	^{23}U (wt.%)	Gd_2O_3 (wt.%)	No. of rods
1	1.33	0	31
2	0.71	0	18

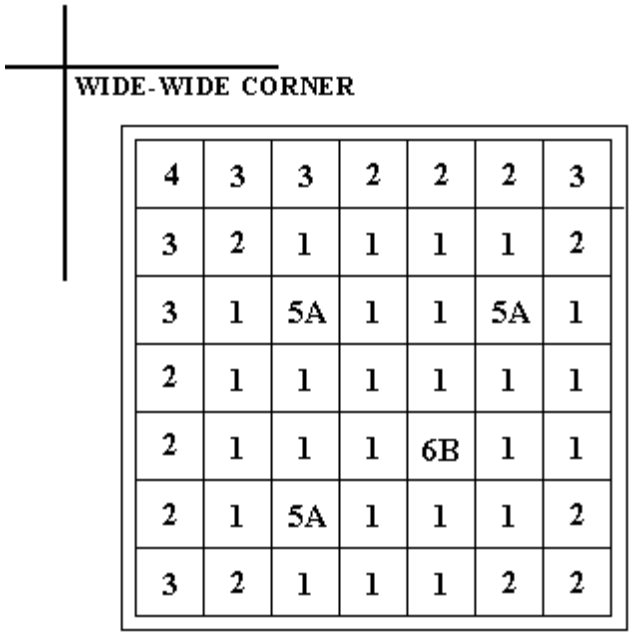

Table 2-11. Assembly design for Type 2 initial fuel

Rod type	^{235}U (wt.%)	Gd_2O_3 (wt.%)	No. of rods
1	2.93	0	26
2	1.94	0	12
3	1.69	0	6
4	1.33	0	1
5A	2.93	3.0	3
6B	2.93	3.0	1

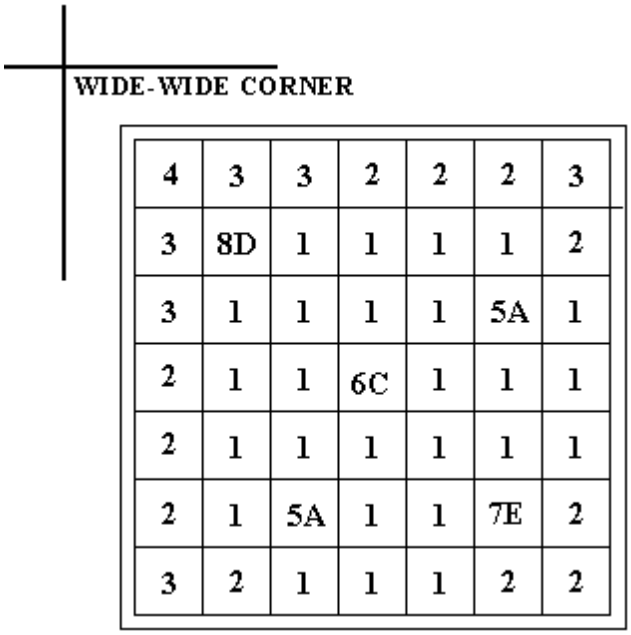

Table 2-12. Assembly design for Type 3 initial fuel

Rod type	^{235}U (wt.%)	Gd_2O_3 (wt.%)	No. of rods
1	2.93	0	26
2	1.94	0	11
3	1.69	0	6
4	1.33	0	1
5A	2.93	3.0	2
6C	2.93	3.0	1
7E	2.93	4.0	1
8D	1.94	4.0	1

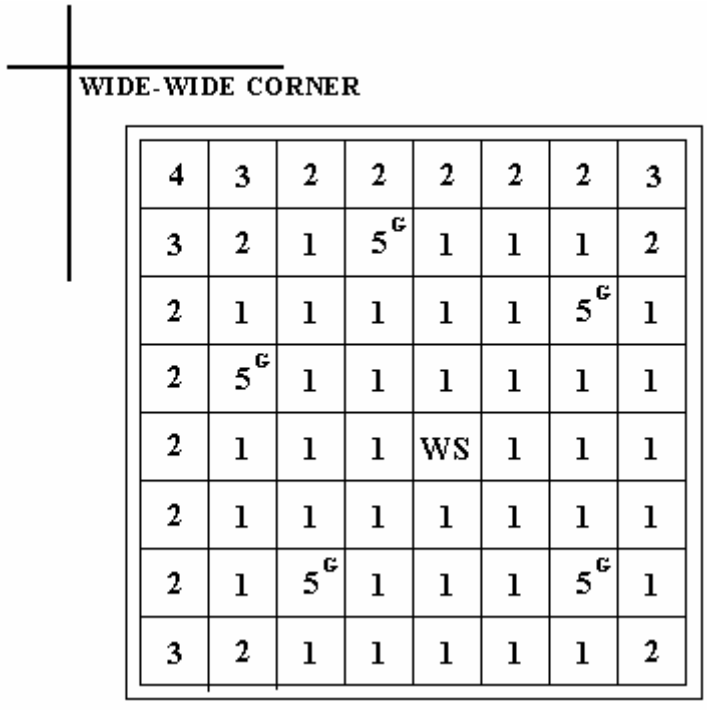

Table 2-13. Assembly design for Type 4 8 × 8 UO_2 reload

Rod type	^{235}U (wt.%)	Gd_2O_3 (wt.%)	No. of rods
1	3.01	0	39
2	2.22	0	14
3	1.87	0	4
4	1.45	0	1
5	3.01	3.0	5
WS	–	0	1

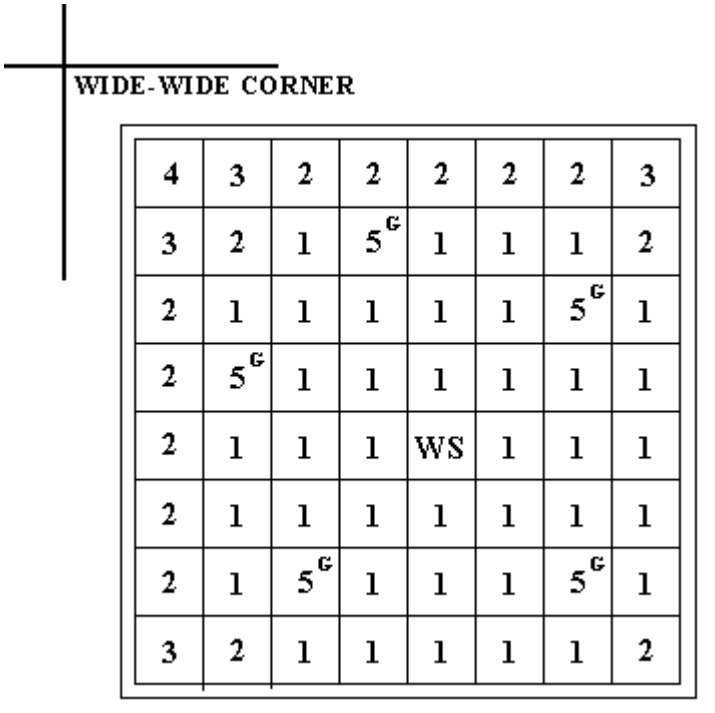

Table 2-14. Assembly design for Type 5 8 × 8 UO_2 reload

Rod type	^{235}U (wt.%)	Gd_2O_3 (wt.%)	No. of rods
1	3.01	0	39
2	2.22	0	14
3	1.87	0	4
4	1.45	0	1
5	3.01	2.0	5
WS	–	0	1

WS – Spacer positioning water rod.
G – Gadolinium rods.

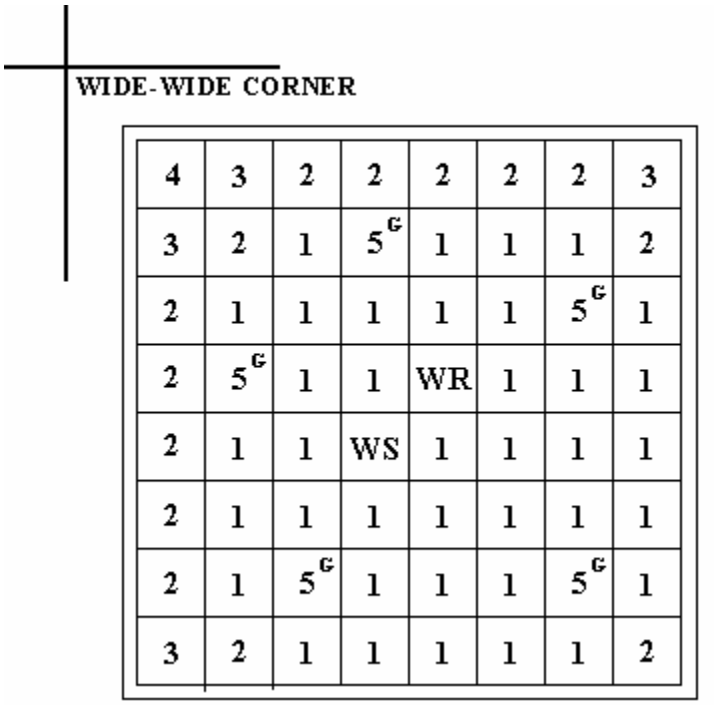

Table 2-15. Assembly design for Type 6 8 × 8 UO_2 reload, LTA

Rod type	^{235}U (wt.%)	Gd_2O_3 (wt.%)	No. of rods
1	3.01	0	38
2	2.22	0	14
3	1.87	0	4
4	1.45	0	1
5	3.01	2.0	5
WS	–	0	1
WR	–	0	1

WS – Spacer positioning water rod.
WR – Water rod.
G – Gadolinium rods.

Table 2-16. Control rod data (movable control rods)

Shape	Cruciform
Pitch, cm	30.48
Stroke, cm	365.76
Control length, cm	363.22
Control material	B_4C granules in Type-304, stainless steel tubes and sheath
Material density	70% of theoretical
Number of control material tubes per rod	84
Tube dimensions	.47752 cm outer diameter by .0635 cm wall
Control blade half span, cm	12.3825
Control blade full thickness, cm	.79248
Control blade tip radius, cm	.39624
Sheath thickness, cm	.14224
Central structure wing length, cm	1.98501
Blank tubes per wing	None

Table 2-17. Definition of assembly types

Assembly type	Assembly design (see Tables 2.10 through 2.15)
1	5
2	4
3	5
4	6
5	2
6	2
7	2
8	2
9	2
10	2
11	3
12	2
13	3
14	2
15	3
16	2
17	3
18	2
19	Reflector

Table 2-18. Composition numbers in axial layer for each assembly type

	1	2	3	4	5	6	7	8	9	10	11	12	13	14	15	16	17	18	19
1	433	433	433	433	433	433	433	433	433	433	433	433	433	433	433	433	433	433	433
2	1	25	49	73	97	121	145	169	193	217	241	265	289	313	337	361	385	409	435
3	2	26	50	74	98	122	146	170	194	218	242	266	290	314	338	362	386	410	435
4	3	27	51	75	99	123	147	171	195	219	243	267	291	315	339	363	387	411	435
5	4	28	52	76	100	124	148	172	196	220	244	268	292	316	340	364	388	412	435
6	5	29	53	77	101	125	149	173	197	221	245	269	293	317	341	365	389	413	435
7	6	30	54	78	102	126	150	174	198	222	246	270	294	318	342	366	390	414	435
8	7	31	55	79	103	127	151	175	199	223	247	271	295	319	343	367	391	415	435
9	8	32	56	80	104	128	152	176	200	224	248	272	296	320	344	368	392	416	435
10	9	33	57	81	105	129	153	177	201	225	249	273	297	321	345	369	393	417	435
11	10	34	58	82	106	130	154	178	202	226	250	274	298	322	346	370	394	418	435
12	11	35	59	83	107	131	155	179	203	227	251	275	299	323	347	371	395	419	435
13	12	36	60	84	108	132	156	180	204	228	252	276	300	324	348	372	396	420	435
14	13	37	61	85	109	133	157	181	205	229	253	277	301	325	349	373	397	421	435
15	14	38	62	86	110	134	158	182	206	230	254	278	302	326	350	374	398	422	435
16	15	39	63	87	111	135	159	183	207	231	255	279	303	327	351	375	399	423	435
17	16	40	64	88	112	136	160	184	208	232	256	280	304	328	352	376	400	424	435
18	17	41	65	89	113	137	161	185	209	233	257	281	305	329	353	377	401	425	435
19	18	42	66	90	114	138	162	186	210	234	258	282	306	330	354	378	402	426	435
20	19	43	67	91	115	139	163	187	211	235	259	283	307	331	355	379	403	427	435
21	20	44	68	92	116	140	164	188	212	236	260	284	308	332	356	380	404	428	435
22	21	45	69	93	117	141	165	189	213	237	261	285	309	333	357	381	405	429	435
23	22	46	70	94	118	142	166	190	214	238	262	286	310	334	358	382	406	430	435
24	23	47	71	95	119	143	167	191	215	239	263	287	311	335	359	383	407	431	435
25	24	48	72	96	120	144	168	192	216	240	264	288	312	336	360	384	408	432	435
26	434	434	434	434	434	434	434	434	434	434	434	434	434	434	434	434	434	434	434

Table 2-19. Range of variables

T Fuel (°K)	Rho M. (kg/m^3)
400.0	141.595
800.0	141.595
1 200.0	141.595
1 600.0	141.595
2 000.0	141.595
2 400.0	141.595
400.0	226.154
800.0	226.154
1 200.0	226.154
1 600.0	226.154
2 000.0	226.154
2 400.0	226.154
400.0	299.645
800.0	299.645
1 200.0	299.645
1 600.0	299.645
2 000.0	299.645
2 400.0	299.645
400.0	435.045
800.0	435.045
1 200.0	435.045
1 600.0	435.045
2 000.0	435.045
2 400.0	435.045
400.0	599.172
800.0	599.172
1 200.0	599.172
1 600.0	599.172
2 000.0	599.172
2 400.0	599.172
400.0	779.405
800.0	779.405
1 200.0	779.405
1 600.0	779.405
2 000.0	779.405
2 400.0	779.405

Table 2-20. Key to macroscopic cross-section tables

T_{f1}	T_{f2}	T_{f3}	T_{f4}	T_{f5}	T_{f6}
ρ_{m1}	ρ_{m2}	ρ_{m3}	ρ_{m4}	ρ_{m5}	ρ_{m6}
Σ_1	Σ_2	...			
		...	Σ_{34}	Σ_{35}	Σ_{36}

Where:
– T_f is the Doppler (fuel) temperature (°K)
– ρ_m is the moderator density (kg/m^3)
Macroscopic cross-sections are in units of cm^{-1}

Table 2-21. Macroscopic cross-section table structure

```
**************************************************************************
        Cross-Section Table Input
*
*       T Fuel          Rho Mod.
        6 6
*
**********  X-Section Set #
  #
**************************************************************************
        Group No. 1
*
**********  Diffusion Coefficient Table
*
**********  Absorption X-Section Table
*
**********  Fission X-Section Table
*
**********  Nu-Fission X-Section Table
*
**********  Scattering From Group 1 to 2 X-Section Table
*
**********  Assembly Disc. Factor Table - W
*
**********  Assembly Disc. Factor Table - S
*
**********  Detector Flux Ratio Table
*
**********  Detector Microscopic Fission X-Section Table
        *
```

```
*************************************************************************
        Group No. 2
*
**********   Diffusion Coefficient Table
*
**********   Absorption X-Section Table
*
**********   Fission X-Section Table
*
**********   Nu-Fission X-Section Table
*
**********   Xe Macroscopic X-Section Table
*
**********   Xe Microscopic X-Section Table
*
**********   Assembly Disc. Factor Table - W
*
**********   Assembly Disc. Factor Table - S
*
**********   Detector Flux Ratio Table
*
**********   Detector Microscopic Fission X-Section Table
*
**********   Detector Flux Ratio Table (not energy group dependent)
*
**********   Detector Microscopic Fission X-Section Table (not energy group dependent)
*
**********   Effective Delayed Neutron Yield in Six Groups
*
**********   Decay Constants for Delayed Neutron Groups
*
**********   Inv. Neutron Velocities
```

Figure 2-1. Reactor core cross-sectional view

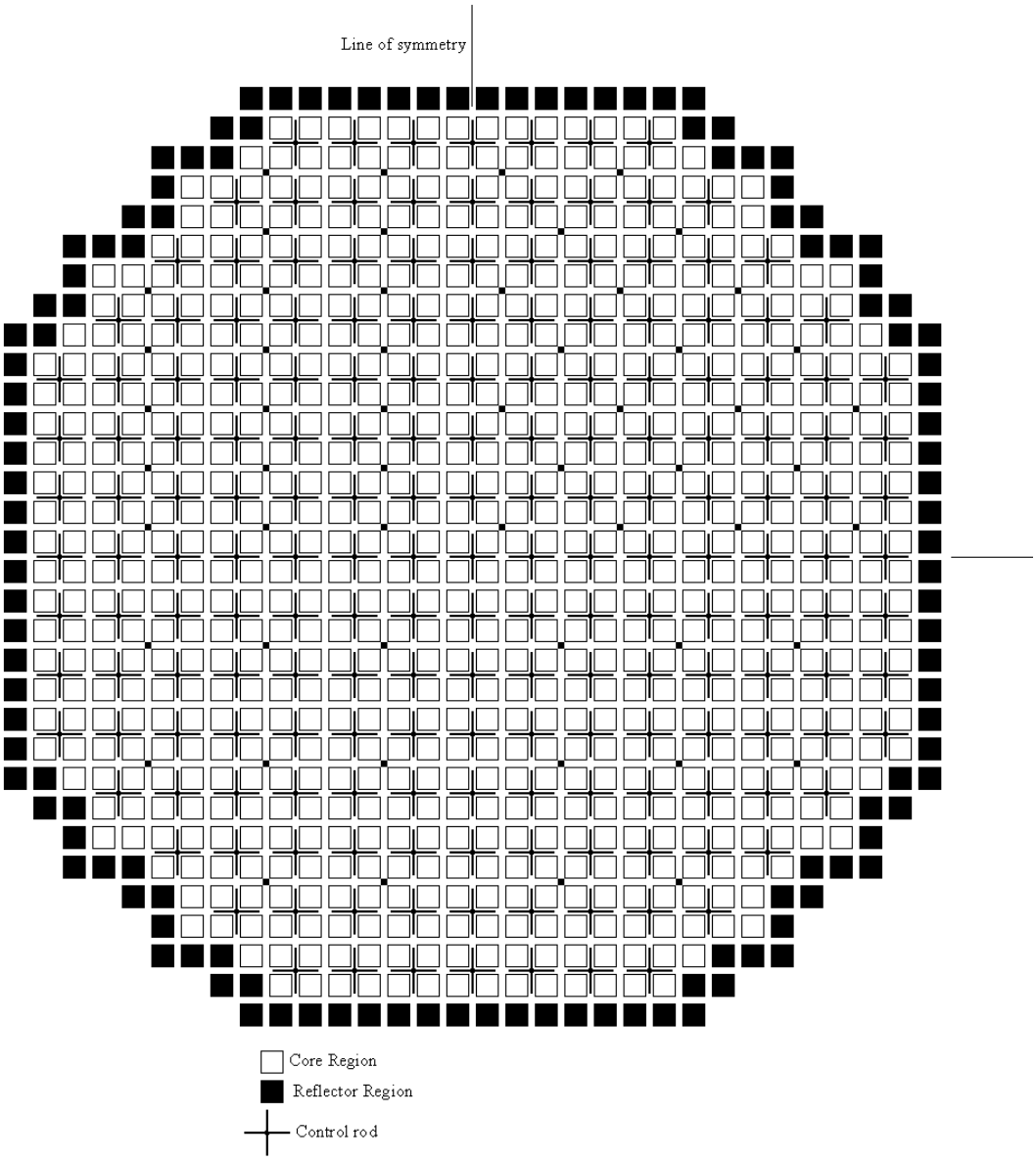

Figure 2-2. PB2 initial fuel assembly lattice

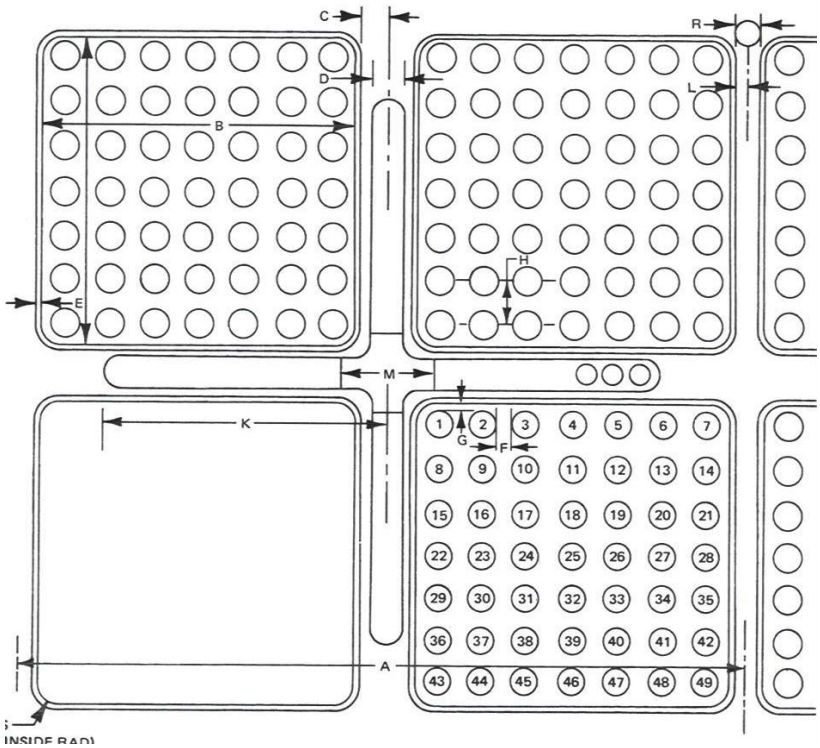

Dim. ID	A	B	C	D	E	F	G	H	I	J
Dim. (in)	12.0	5.278	0.375		0.080	0.175	0.1435	0.738		
Dim. (cm)	30.48	13.40612	.9525		.2032	.4445	.36449	1.87452		

Dim. ID	K	L	M	N	O	P	Q	R	S
Dim. (in)		0.187							0.38
Dim. (cm)		.47498							.9652

Figure 2-3. PB2 reload fuel assembly lattice for 100 mil channels

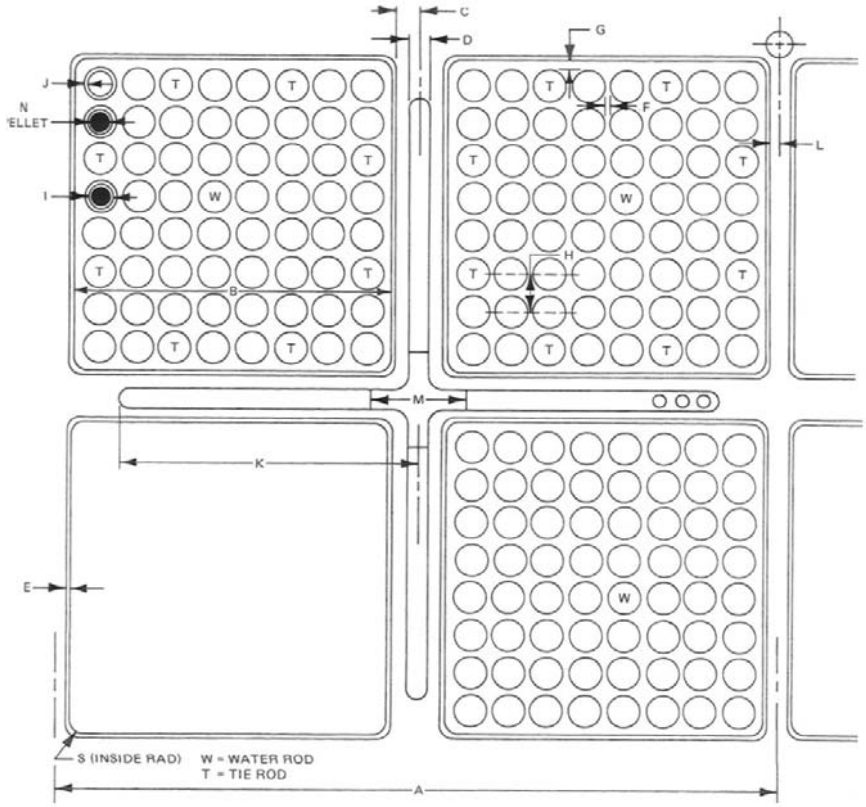

Dim. ID	A	B	C	D	E	F	G	H	I	J
Dim. (in)	12.0	5.278	0.355		0.100	0.147	0.153	0.64		
Dim. (cm)	30.48	13.40612	.9017		.254	.37338	.38862	1.6256		

Dim. ID	K	L	M	N	O	P	Q	R	S
Dim. (in)		0.167							0.38
Dim. (cm)		.42418							.9652

Figure 2-4. PB2 reload fuel assembly lattice for 120 mil channels

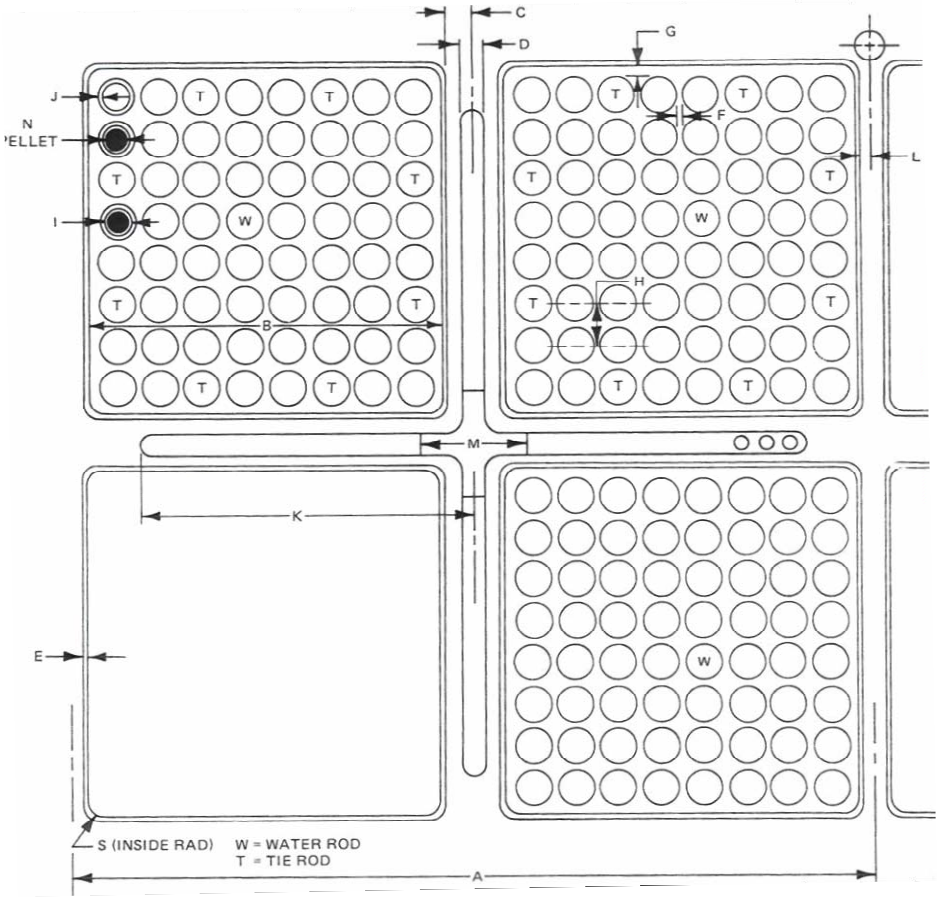

Dim. ID	A	B	C	D	E	F	G	H	I	J
Dim. (in)	12.0	5.278	0.355		0.120	0.147	0.153	0.64		
Dim. (cm)	30.48	13.40612	.8509		.3048	.37338	.38862	1.6256		

Dim. ID	K	L	M	N	O	P	Q	R	S
Dim. (in)		0.147							0.38
Dim. (cm)		.42418							.9652

Figure 2-5. PB2 reload fuel assembly lattice for LTA assemblies

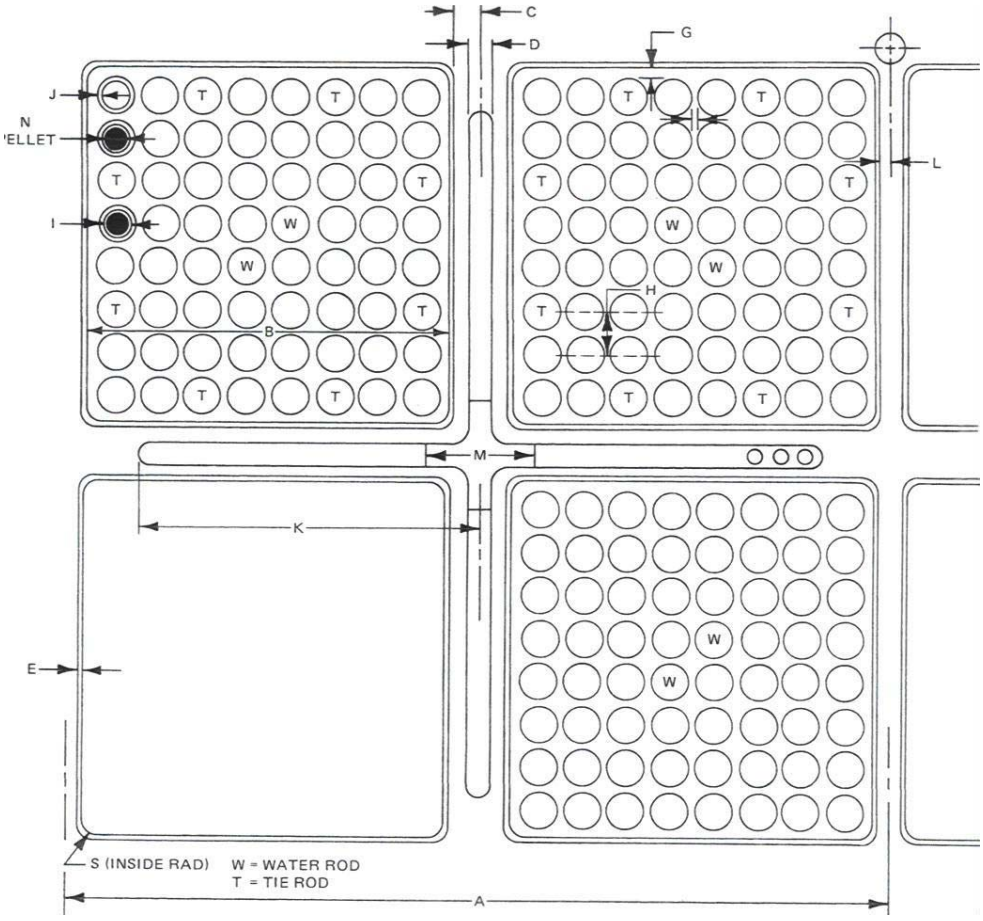

Dim. ID	A	B	C	D	E	F	G	H	I	J
Dim. (in)	12.0	5.278	0.355		0.100	0.157	0.158	0.64		
Dim. (cm)	30.48	13.40612	.9017		.254	.39878	.40132	1.6256		

Dim. ID	K	L	M	N	O	P	Q	R	S
Dim. (in)		0.167							0.38
Dim. (cm)		.42418							.9652

Figure 2-6. PSU control rod grouping

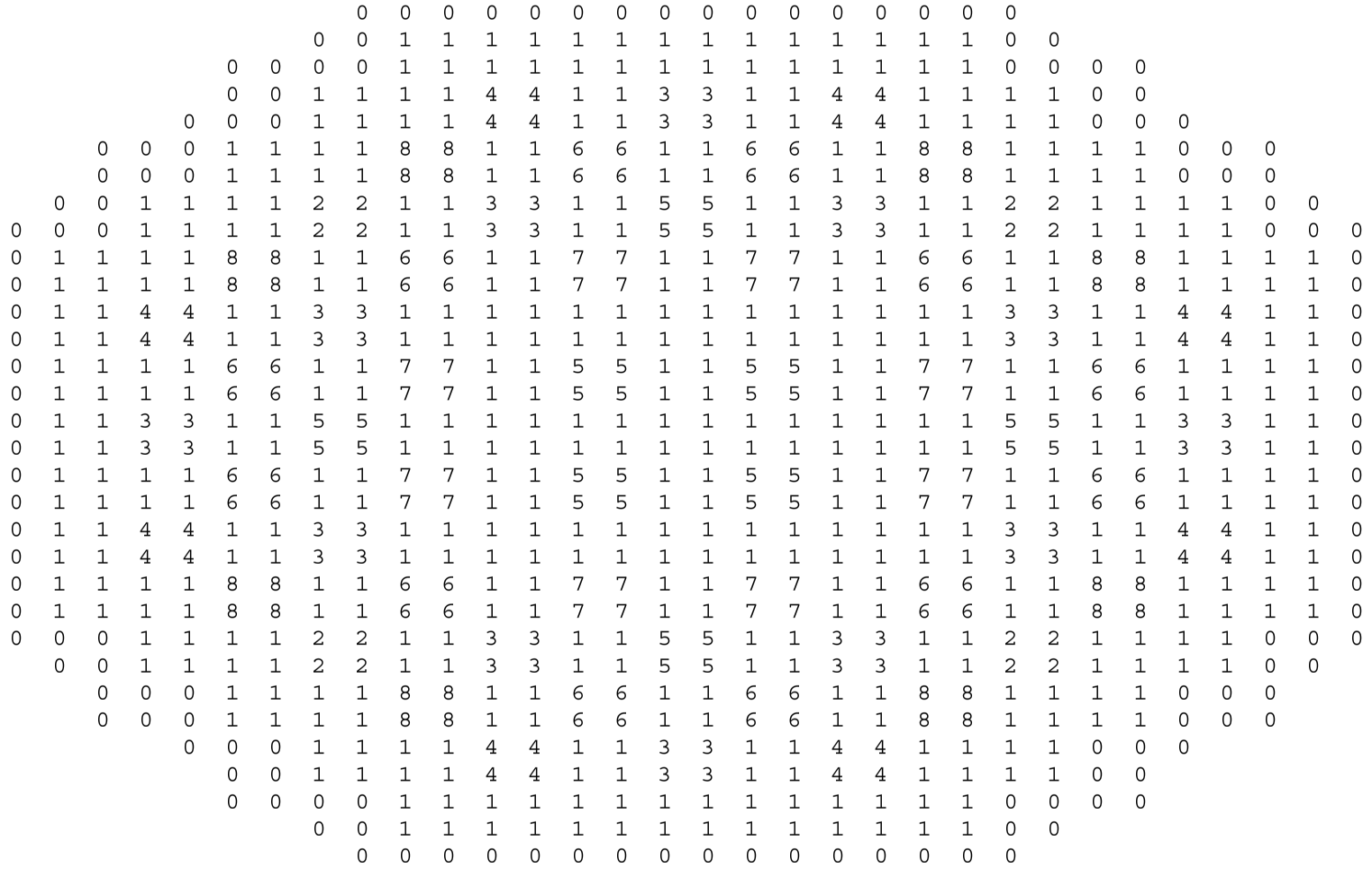

Figure 2-7. Radial distribution of assembly types

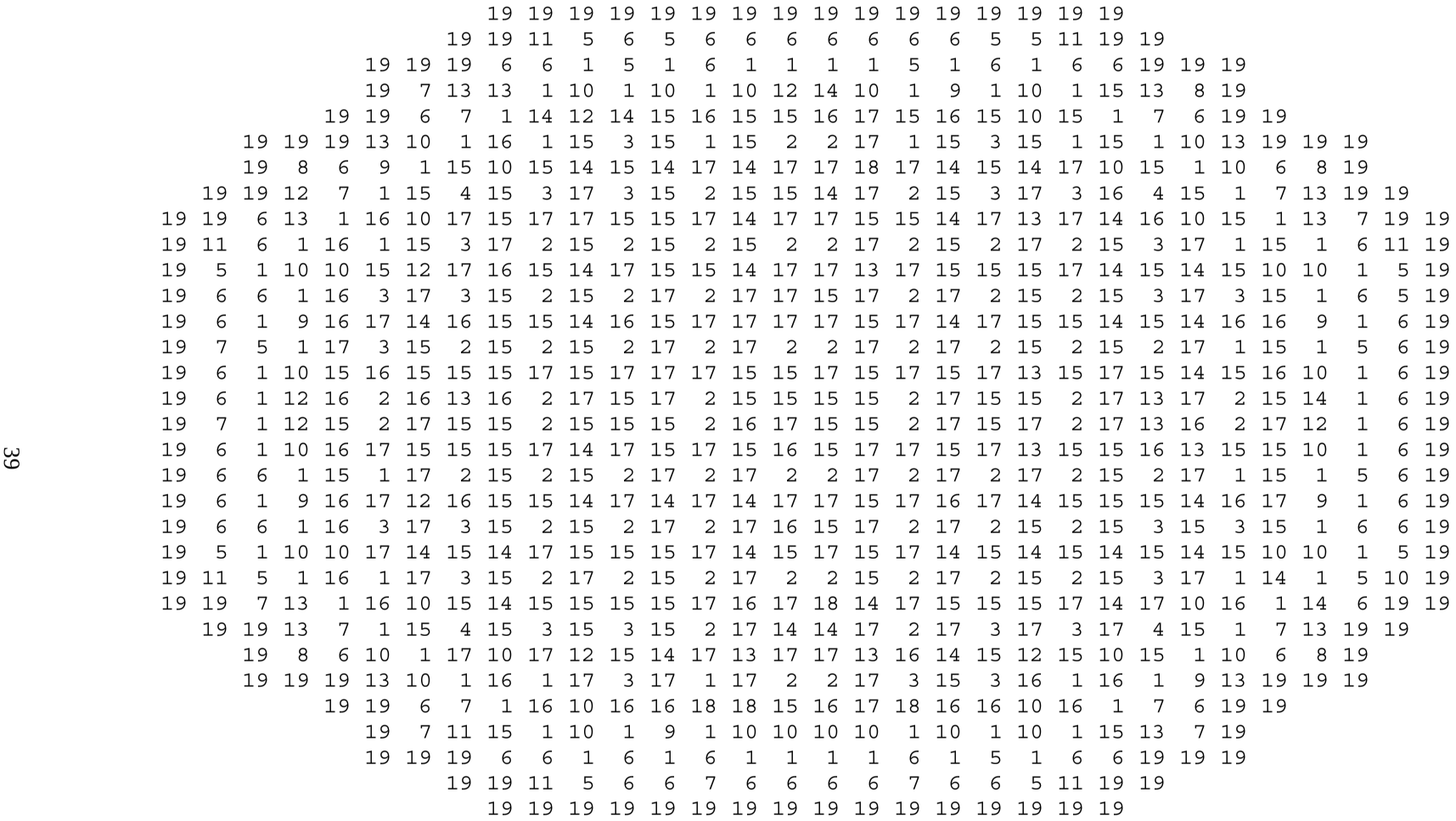

Figure 2-8. Fuel assembly orientation for ADF assignment

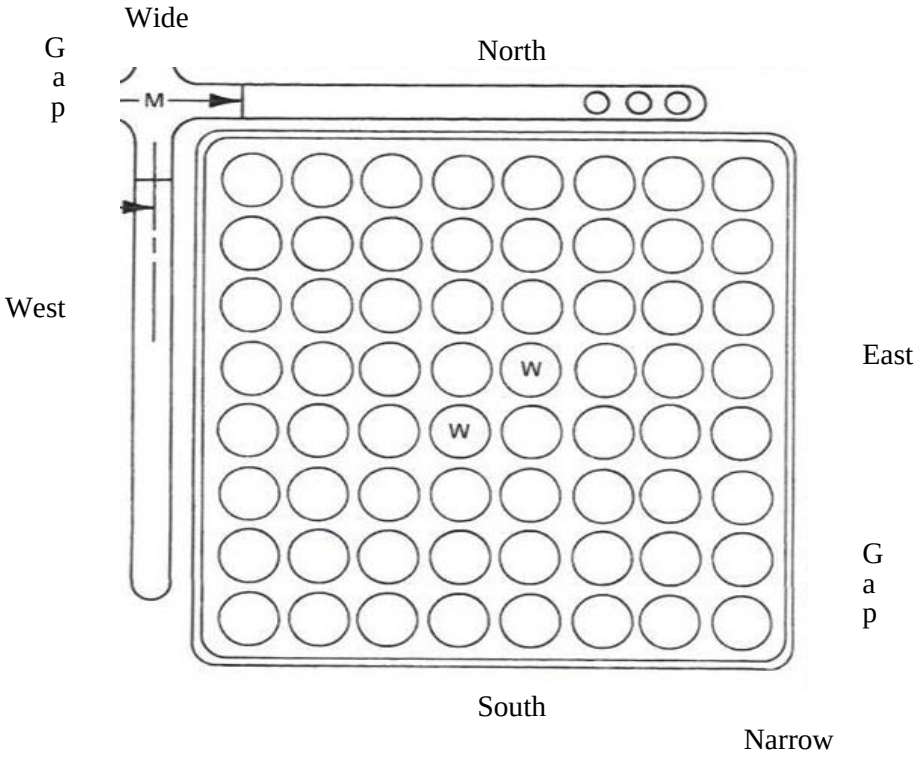

Figure 2-9. Core orificing and TIP system arrangement

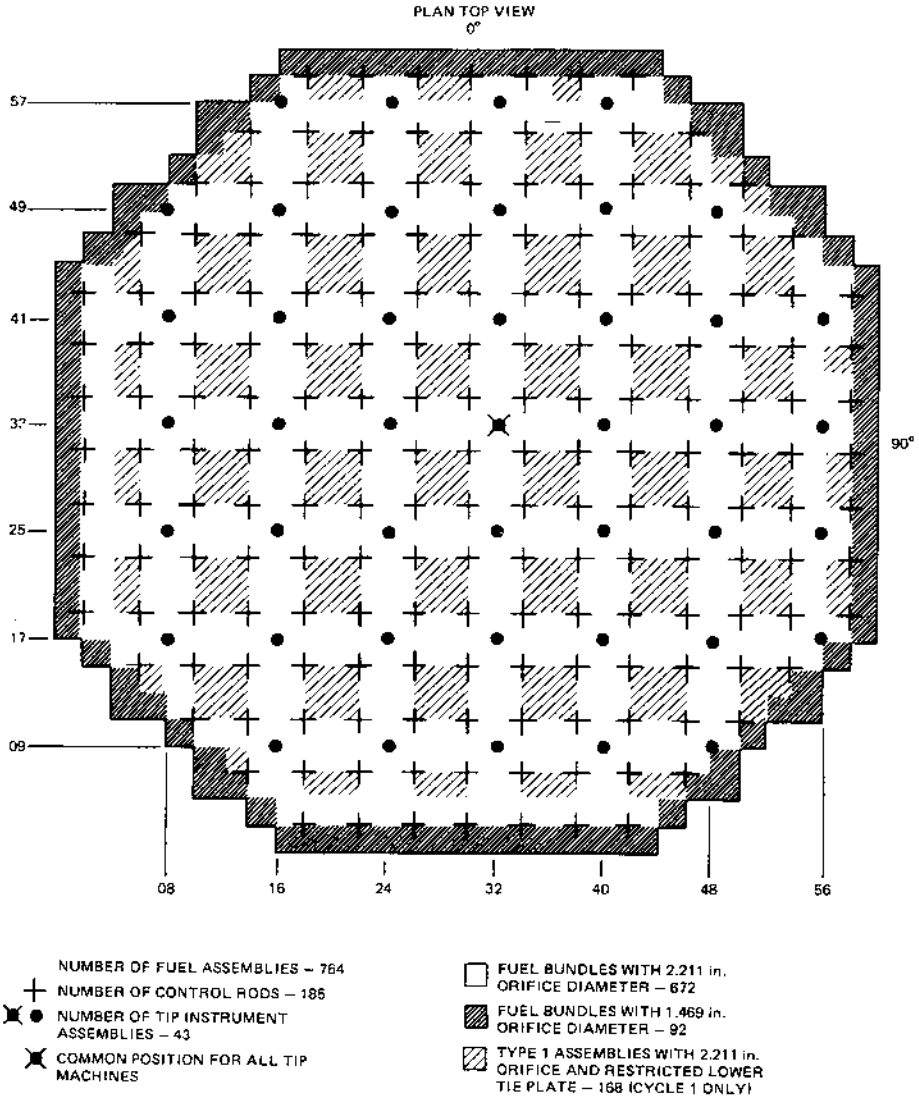

Figure 2-10. Elevation of core components

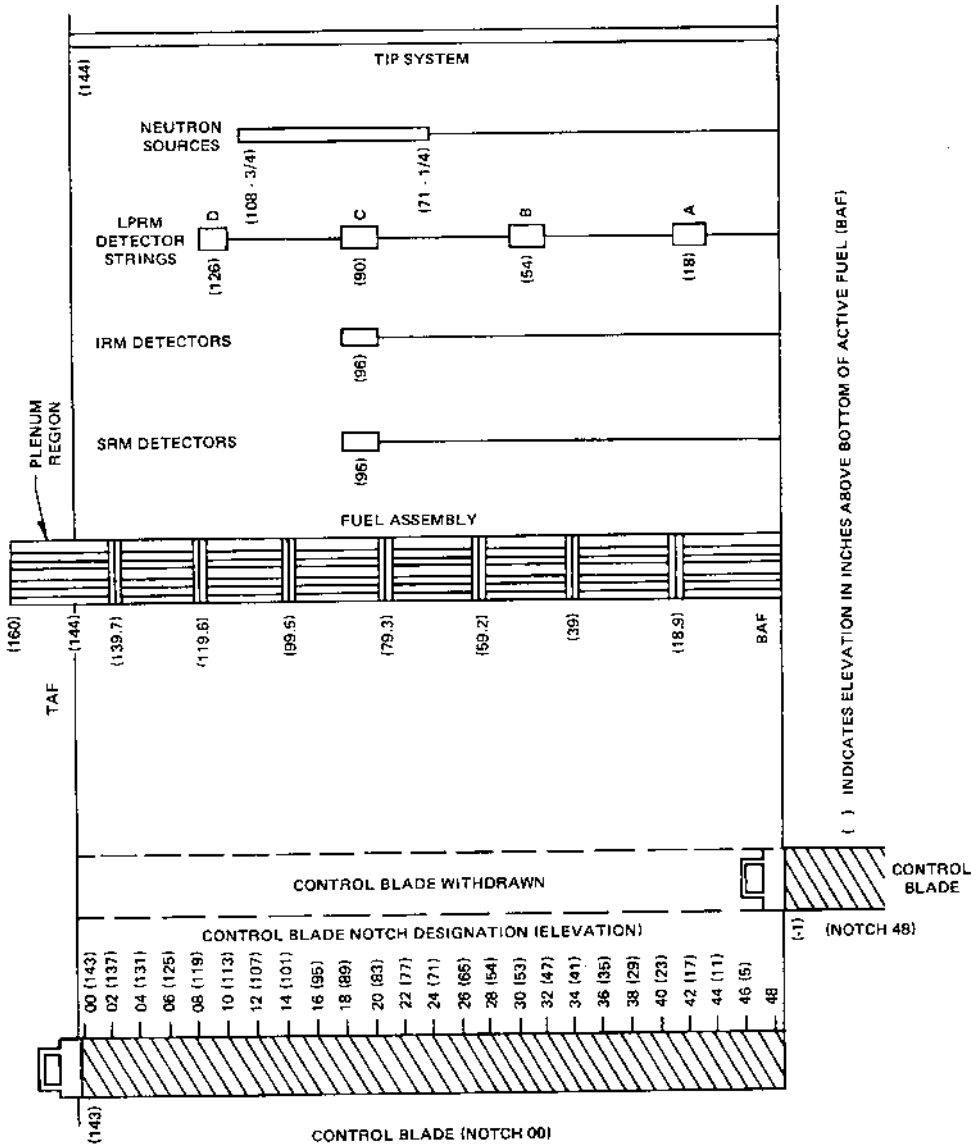

2.3 Core thermal-hydraulic boundary conditions model and its coupling with 3-D neutron kinetics model

PB2 is a GE designed BWR/4 with a rated thermal power of 3 293 MW, a rated core flow of 12 915 kg/s (102.5×10^6 lb/hr), a rated steam flow of 1 685 kg/s (13.37×10^6 lb/hr), and a turbine inlet pressure of 6.65 MPa (965 psia). Nuclear steam supply system (NSSS) has turbine-driven feed pumps and a two-loop M-G driven recirculation system feeding a total of 20 jet-pumps. There are totally four steam lines and each has a flow-limiting nozzle, main steam isolation valves (MSIVs), safety relief valves (SRVs), and a turbine stop valve (TSV). The steam bypass system consists of nine bypass valves (BPVs) mounted on a common header, which is connected to each of the four steam lines.

In Exercise 2 steady-state and transient analyses, core thermal-hydraulic boundary conditions model is used and it is coupled to the 3-D core neutron kinetics model. The full PB2 thermal-hydraulic model can be converted to a core thermal-hydraulic boundary condition model by defining inlet and outlet thermal-hydraulic boundary conditions. The developed model for performing the 3-D core thermal-hydraulic boundary condition calculation was built based on different TRAC-BF1 thermal-hydraulic components as follows.

A basic 33-channel thermal-hydraulic core boundary condition model was obtained from the PB2 TT2 TRAC-BF1 system model. Bottom and top boundary conditions are specified in this model using the FILL and BREAK TRAC-BF1 components. The developed model is illustrated in Figure 2-11. Figure 2-12 shows the thermal-hydraulic radial mapping scheme used to represent the PB2 reactor core. The feedback, or coupling, between neutronics and thermal-hydraulics can be characterised by choosing user supplied mapping schemes (spatial mesh overlays) in the radial and axial core planes.

Some of the inlet perturbations (inlet disturbances of both temperature and flow rate) are specified as a fraction of the position across the core inlet. This requires either a 3-D modelling of the vessel, or some type of a multi-channel model. The PSU developed core multi-channel model consists of 33 channels to represent the 764 fuel assemblies of the PB2 reactor core. The above core thermal-hydraulic model was built according to different criteria. The fuel assemblies are ranked according to the inlet orifice characteristics. The flow areas at channel inlet were adjusted in order to match the channel by channel flow rate distribution while preserving pressure drop across core support plate. Another criterion is the fuel assembly type (e.g. 7×7 or 8×8). The model is developed without lumping in a same core channel two or more fuel bundles of different types. This means that 8×8 fuel types are never lumped with 7×7 fuel types in a same core channel. Thermal-hydraulic conditions are also considered. For example, power peaking factors are re-normalised for the lumped channels and mass flows are taken into account during the lumping.

The 33 thermal-hydraulic channels shown in this figure are coupled to the neutronic code model in the radial plane shown in Figure 2-13. Thermal-hydraulic channels identified with zeroes are treated as reflector regions. This mapping scheme follows the spatial mesh overlays developed for the PB2 TRAC-BF1/NEM 3-D neutron kinetics/thermal-hydraulic model.

For the purposes of Exercise 2, it is recommended that an assembly flow area of 15.535 in^2 (1.0023×10^{-2} m^2) for fuel assemblies with 7×7 fuel rod arrays, and 15.5277 in^2 (1.0017×10^{-2} m^2) for fuel assemblies with 8×8 fuel rod arrays be used in the core thermal-hydraulic multi-channel models. There are 764 fuel assemblies in the PB2 reactor core. At EOC 2, there are 576 fuel assemblies of 7×7 type, and 188 of the 8×8 type. The radial distribution of assembly types is shown in Figure 2-7 in which the assembly types from 1 to 4 identify a fuel assembly with 8×8 fuel arrays and the assembly types from 5 to 18 identify a fuel assembly with 7×7 fuel rod arrays. The core hydraulic characteristics (e.g. core pressure drop) can be found in Ref. [5].

There are several files of data were provided to participants regarding the definition of the core thermal-hydraulic boundary condition model. These data are taken from a combination of the best-estimate core plant system code calculations performed and test data. The boundary conditions provided to the participants are both steady state and time dependent. They are provided for the bottom and top regions adjacent to the inlet and outlet region of the core region. These values are obtained from the lower and upper region of the vessel component of the TRAC-BF1 model [9-11]. The types of boundary conditions that are provided to the participants are:

- *At the inlet of the channels*: mass flows (kg/s) and temperatures (K) from 0 s to 5 s. Thirty-three files are provided since the model used to obtain these variables contains 33 thermal-hydraulic channels. Also, a single file containing core mass flow and core inlet temperature vs. time is provided to participants whose thermal-hydraulic models consist of a single average channel.

- *At the inlet and outlet of the thermal-hydraulic channels*: pressure (Pa) from 0 s to 5 s. Since all the channels have a common plenum, pressure is constant radially. Therefore, a single file containing pressure vs. time information is provided.

Figure 2-11. Exercise 2 vessel/core boundary condition model

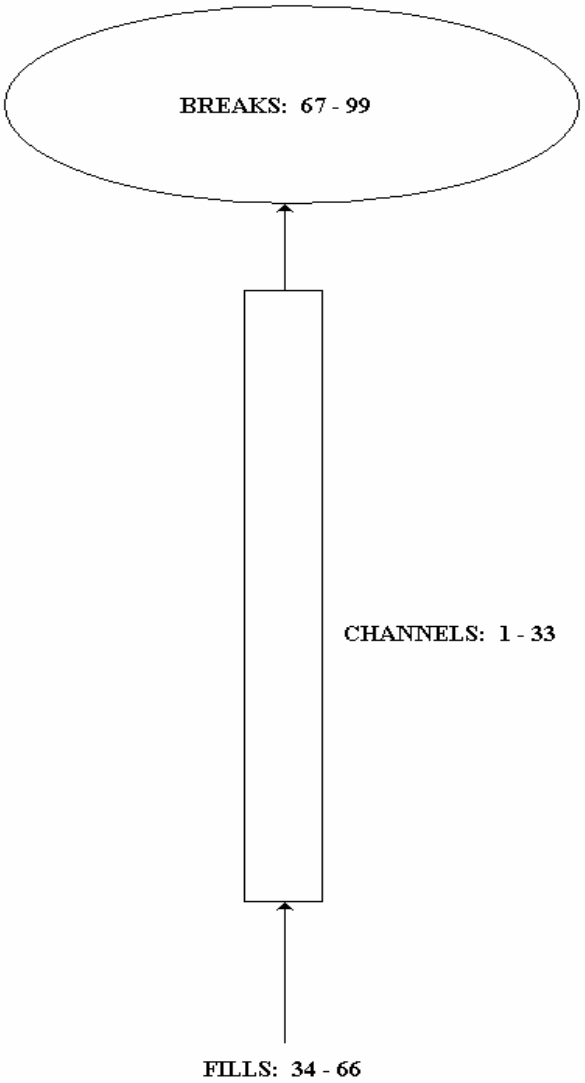

Figure 2-12. Reactor core thermal-hydraulic channel radial map

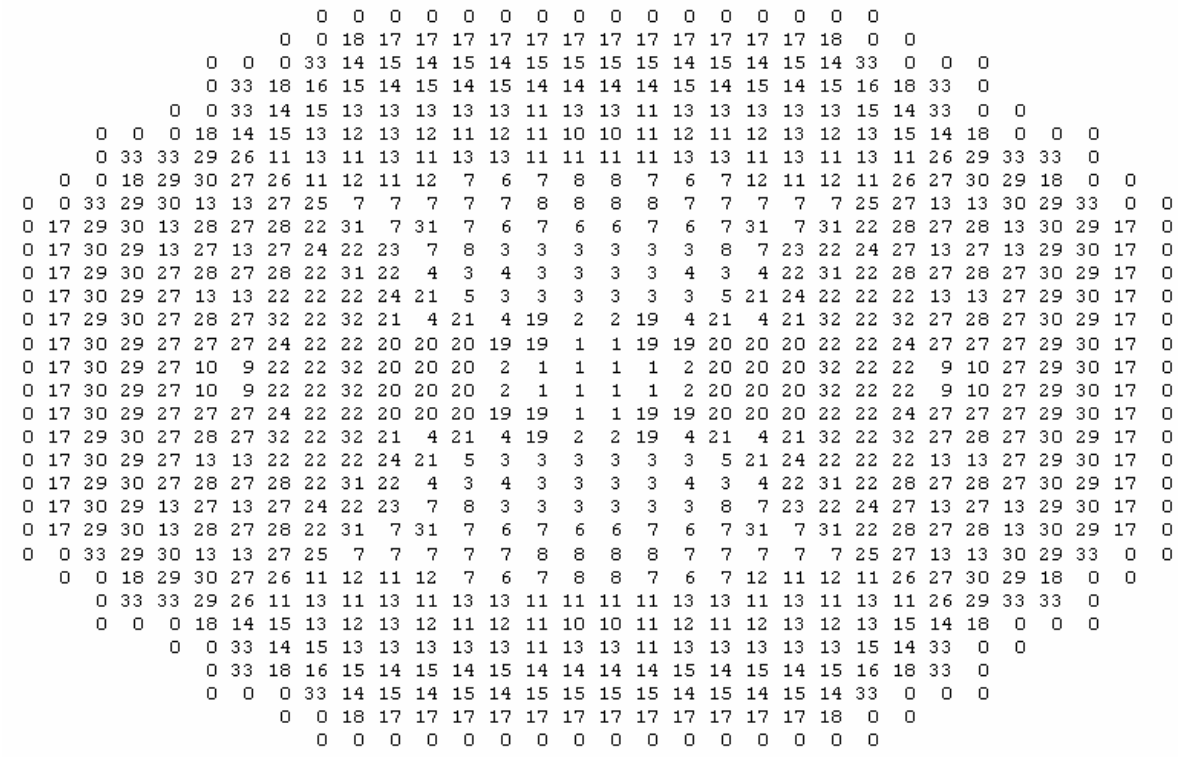

2.4 Initial steady-state conditions

The initial conditions for performing PB2 hot zero power (HZP) core calculations are chosen as 552.833 K for fuel temperature, 753.9777 kg/m^3 for average coolant density and 32.93 MW for the reactor power (see Table 2-22). The fixed thermal-hydraulic variables should be equally distributed through the whole core. The initial power corresponds to 1% of the PB2 nominal power. Figure 2-13 shows the HZP control rod pattern that should be used for the analysis of this calculation. The initial conditions along with the control rod pattern produce a critical or very near to critical reactor core. A similar control rod grouping approach as shown in Figure 2-13 could be useful to set up the control rod mapping scheme for just two control rod groups.

Table 2-22. PB2 HZP initial conditions

Fuel temperature, K	552.833
Average coolant density, kg/m^3	753.9777
Reactor power, MW	32.93

Turbine trip test 2 (TT2) was initiated from steady-state conditions after obtaining P1 edits from the process computer for nuclear and thermal-hydraulic conditions of the core. PB2 was chosen for the turbine trip tests because it is a large BWR/4 with relatively small turbine bypass capacity. During the test, the initial thermal power level was 61.6% rated 2 030 MW; core flow was 80.9% rated 10 445 kg/s (82.9 $\times$ 10^6 lb/hr); and average range power monitor (APRM) scram setting was 95% of nominal power. Table 2-23 provides the reactor initial conditions for performing steady-state calculations while Figure 2-14 shows the PB2 TT2 initial control rod pattern.

Figure 2-13. PB2 HZP control rod pattern

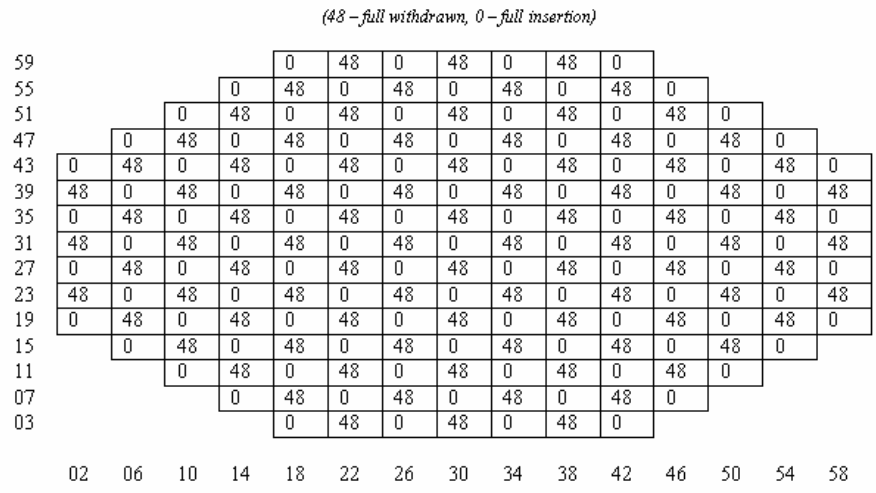

Table 2-23. PB2 TT2 initial conditions from process computer P1 edit

Core thermal power, MWt	2 030
Initial power level, % of rated	61.6
Gross power output, MWe	625.1
Feedwater flow, kg/s	980.26
Reactor pressure, Pa	6 798 470.0
Total core flow, kg/s	10 445.0
Core inlet subcooling, J/kg	48 005.291
Feedwater temperature, K	442.31
Core pressure drop, Pa	113 560.7
Jet-pump driving flow, kg/s	2 871.24
Core average exit quality, fraction	0.097
Core average void fraction, fraction	0.304
Core average power density, kW/l	31.28

Figure 2-14. PB2 HP control rod pattern

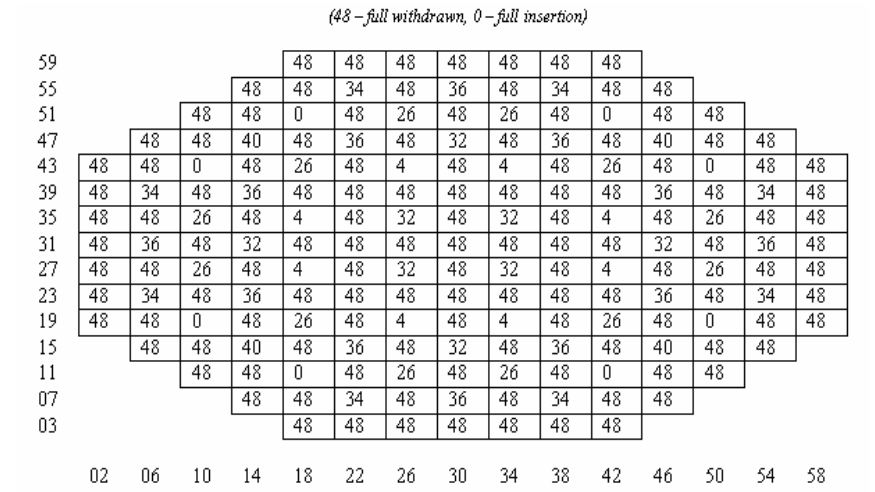

2.5 Transient calculations

Most of the important phenomena of interest during TT2 occurred in the first five seconds. Therefore, the transient will be simulated for this time period. The thermal-hydraulics system transient behaviour in Exercise 2 is modelled through boundary conditions imposed to the coupled core model. The only event, which needs to be modelled in this exercise, is the scram simulation. Table 2-24 shows the scram initiation time and the delay time that should be used for performing Exercise 2. Table 2-25 shows the average control rod density (CRD) position during reactor scram. An average velocity can be obtained from Table 2-24 for the scram modelling in the 3-D kinetics case. An approximate value obtained from the above table is 2.34 ft/s (0.713 m/s) for the first 0.04 seconds and 4.67 ft/s (1.423 m/s) thereafter.

Table 2-24. PB2 TT2 scram characteristics

APRM high flux scram set-point, % rated	95 (3 128.35 MWt)
Time delay prior to rod motion, msec	120
Time of scram initiation, sec	0.63
Initiates CR insertion, sec	0.75

Table 2-25. CRD position after scram vs. time

Time (sec)	Position (cm)
0.000	0.00
0.120	0.00
0.160	2.85
0.247	15.24
0.354	30.48
0.457	45.72
2.500	310.90
3.080	365.76
5.000	365.76

Chapter 3

METHODOLOGIES TO QUANTIFY THE ACCURACY OF THE CALCULATIONS

As mentioned briefly in Chapter 1, each of the 18 participants has submitted various results that were available for the statistical analysis. The submitted results for Exercise 2 can be classified in four types of data. These are integral parameter values, 1-D distribution, 2-D distributions and time histories. It was decided by the participants in the benchmark that the reference data used in the Exercise 2 comparative analysis is the so-called "averaged data". The reference solution for each requested parameter is based upon the statistical mean (averaged) value of all submitted results.

3.1 Standard techniques for the comparison of results

In Exercise 2, four types of data were analysed and the results of all participants were compared based on this classification. These data types were:

1) integral parameter values;
2) one-dimensional (1-D) axial distributions;
3) two-dimensional (2-D) radial distributions;
4) time history data.

It was necessary to develop a suite of statistical methods for each of these data types, which were applied in the comparative analysis. The statistical methods used in the comparative analysis of Exercise 2 are described in Subsections, 3.1.1, 3.1.2, 3.1.3 and 3.1.4.

Table 3-1 and Table 3-2 summarise the submitted data types for Exercise 2 problem conditions and the classifications of these data types.

Table 3-1. Exercise 2 parameters for steady-state statistical comparisons

Condition	Submitted data for statistical analysis	Classification
HZP	k_{eff}	Integral value
	Normalised axial power	1-D distribution
	Relative power for FA 75	1-D distribution
	Relative power for FA 367	1-D distribution
	Normalised radial power	2-D distribution
HP	k_{eff}	Integral value
	Core averaged axial void fraction	1-D distribution
	Normalised axial power	1-D distribution
	Relative power for FA 75	1-D distribution
	Relative power for FA 367	1-D distribution
	Normalised radial power	2-D distribution

Table 3-2. Exercise 2 parameters for transient statistical comparisons

Condition	Submitted data for statistical analysis	Classification
Transient	Core power	Time history
	Total reactivity	Time history
	Doppler reactivity	Time history
	Void reactivity	Time history
Snapshot at maximum power before scram	Time of maximum power before scram	Integral value
	Normalised axial power	1-D distribution
	Relative power for FA 75	1-D distribution
	Relative power for FA 367	1-D distribution
	Normalised radial power	2-D distribution
Snapshot at the end of transient	Normalised axial power	1-D distribution
	Relative power for FA 75	1-D distribution
	Relative power for FA 367	1-D distribution
	Normalised radial power	2-D distribution

3.1.1 Integral parameter values

These parameters include such values as k_{eff} for HZP and initial conditions of TT2 as well as time of maximum power before scram. In the analysis of integral values, there is no need to condition the data by isolating point of interest. Likewise, there are no curves to analyse. Thus, the mean value and standard deviation should be sufficient to facilitate a comparison of the results. Mean value, standard deviation, deviation and figure of merit (FOM) are calculated according to Eqs. (3.1), (3.2), (3.3) and (3.4), respectively.

$$x_{reference} = \frac{\sum_{i}^{N} x_i}{N} \tag{3.1}$$

$$\sigma = \pm\sqrt{\frac{\sum \left(x_i - x_{reference}\right)^2}{N-1}} \tag{3.2}$$

where σ is the standard deviation, x_i is the data submitted by each participant and N is the total number of received results.

The deviation and FOM can be computed as:

$$e_i = x_i - x_{reference} \tag{3.3}$$

$$\Phi_i = \frac{e_i}{\sigma} \tag{3.4}$$

where e_i is the difference between the participant's value and the mean value.

3.1.2 One-dimensional (1-D) axial distributions

Exercise 2 contains many steady-state and transient snapshots of the axial distributions of certain parameters through the core. The core average axial void fraction and power distributions are functions

of height or number of axial nodes. They can be displayed as an x-y plot. Similar methods of statistical analysis described in the previous section can be applied for each axial cell. One-dimensional axial distributions are compared with the average data submitted by the participants. Analyses are performed for each 1-D cell according to Eqs. (3.5), (3.6) and (3.7).

$$\sigma = \pm\sqrt{\frac{\sum\left(x_i - x_{reference}\right)^2}{N-1}} \tag{3.5}$$

where x_i is each participant's data and N is the total number of received results. FOM is computed as:

$$\Phi_i = \frac{e_i}{\sigma} \tag{3.6}$$

$$e_i = x_i - x_{reference} \tag{3.7}$$

For each participant, a single table is prepared that shows the deviations from mean and FOM at each axial position.

3.1.3 Two-dimensional (2-D) radial distributions

Exercise 2 also contains steady-state and transient snapshots of the radial distribution through the core for certain parameters. Due to the two-dimensional nature of such data, it is difficult to plot the results as with time history data and 1-D distributions. However, the same statistical methods can be used to generate mean values, standard deviations and participant deviations, and figures of merit.

Mean and standard deviation for each 2-D cell can be computed according to Eqs. (3.1) and (3.2). Such an analysis results in a 2-D map for mean values and standard deviations, rather than a single value for each parameter. Comparisons can thus be made for each cell, rather than only specific cells of interest.

The deviation and FOM can be computed according to Eqs. (3.3) and (3.4), respectively. For each participant, a map will be generated that shows deviations from the mean at each radial position. A second map will report the figures of merit.

3.1.4 Time histories

Participants were required to submit four different sets of time histories for Exercise 2. These are power (fission or total), total reactivity, Doppler reactivity and void reactivity histories for the five-second transient period. The averaged values were used as reference data for the statistical comparison purpose in the comparative analysis of the time histories. The averaged data are calculated according to the Eq. (3.8).

$$x_{reference} = \frac{\sum_i^N x_i}{N} \tag{3.8}$$

where x_i is each participant's data for the specified time interval and N is the total number of results received.

3.2 ACAP analysis

The comparative analysis was performed for code-to-code comparisons using the standard statistical methodology with the Automated Code Assessment Program (ACAP) [11]. ACAP is a tool developed to provide quantitative comparisons between nuclear reactor systems code results and experimental measurements. This software was developed under a contract with PSU and the NRC for use in PSU's code consolidation efforts. ACAP's capabilities are described as follows:

- draws upon a mathematical tool kit to compare experimental data and NRS code simulations;
- returns quantitative FOM associated with individual and suite comparisons;
- accommodates the multiple data types encountered in NRS environments;
- incorporates experimental uncertainty in the assessment;
- provides "event windowing" capability;
- accommodates inconsistencies between measured and computed independent variables (e.g. different time steps);
- provides a framework for automated, tunable weighting of component measures in the construction of overall FOM accuracy.

ACAP is a PC- and UNIX-station-based application that can be run interactively on PCs with Windows 95/98/NT, in batch mode on PCs as a WINDOWS console application, or in batch mode on UNIX stations as a command line executable. The D'Auria Fast Fourier Transformation (FFT) and mean error (ME) methods were used for the FOM calculations for time histories [12,13]. Figure 3-1 shows a snapshot of the FOM configuration for ACAP calculations in Exercise 2 of the benchmark. These methods are advanced techniques for analysis of time history data. Eqs. (3.9) to (3.14) represent the theory portion of the D'Auria FFT and ME methods [13].

Figure 3-1. FOM configuration in ACAP

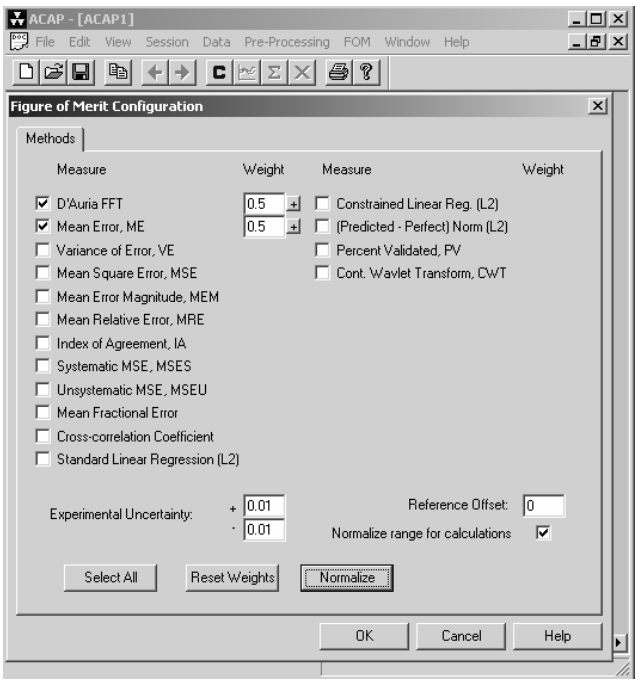

The Discrete Fourier Transform (DFT) can be calculated as:

$$\hat{\Phi}_m = \frac{1}{N}\sum_{i=1}^{N} \Phi_i e^{-2\pi \mathrm{Im} i/N} \tag{3.9}$$

The D'Auria measures are as follows:

- average amplitude (AA):

$$AA - \frac{\sum_{m=0}^{M} \left| \hat{P}_m - \hat{O}_m \right|}{\sum_{m=0}^{M} \left| \hat{O}_m \right|} \tag{3.10}$$

- weighted frequency (WF):

$$WF = \frac{\sum_{m=0}^{M} \left| \hat{P}_m - \hat{O}_m \right| \bullet f_m}{\sum_{m=0}^{M} \left| \hat{P}_m - \hat{O}_m \right|} \tag{3.11}$$

Mean error (ME) can be computed as:

$$ME = \frac{1}{N}\left\{ \sum_{i=1}^{N} \left(O_i - P_i \right) \right\} \tag{3.12}$$

where N is the number of data values, i is the sample index, Φ_i is the values spaced Δt apart, O_i is the i-th datum in experimental set P_i is the i-th datum in computed set, and f_m is the frequency of mode m.

The D'Auria and ME FOM equations are outlined below:

$$FOM_{D'AURIA} = \frac{1}{\left(\left[AA^2 + \left(\frac{K}{WF} \right)^2 \right]^{1/2} + 1 \right)} \tag{3.13}$$

where K is the constant used to weight the relative importance of the weighted frequency (WF) relative to the average amplitude (AA).

$$FOM_{ME} = \frac{1}{\left(\left| ME \right| + 1 \right)} \tag{3.14}$$

Note that the statistical FOM given by Eqs. (3.3) and (3.6) differs from the FOM calculated using Eqs. (3.13) and (3.14). FOM indicates that the participant results are closer to the reference solution if the former FOM [given by Eqs. (3.3) and (3.6)] is closer to zero, while the later FOM [given by Eqs. (3.13) and (3.14)] has to be closer to unity (1) to indicate better agreement.

The following procedure was applied during the ACAP calculation:

- *Step 1:* Data synchronisation was necessary due to the varying time steps of submitted participant data for the time histories. Regarding synchronisation, the cubic spline function was written in Visual Basic for Applications (VBA) and macro module inserted into the Microsoft Excel workbook file [14]. Then, all participants' results were set to a time interval of precisely 6 ms. The inserted module was outlined in the previous volume [3].

- *Step 2:* In order to avoid the effects of differing participant initialisation on the comparative analysis, actual values of the time history data were set to zero and they were called "delta changes". The delta changes were calculated by subtraction of initial value (at time zero) from the all other transient values (as shown below where *t* represents time in seconds).

  Delta Changes (t = 0.000) = Value (t = 0.000) – Value (t = 0.000)
  Delta Changes (t = 0.006) = Value (t = 0.006) – Value (t = 0.000)
  Delta Changes (t = 0.012) = Value (t = 0.012) – Value (t = 0.000)
  Delta Changes (t = 0.018) = Value (t = 0.018) – Value (t = 0.000)
  Delta Changes (t = 0.024) = Value (t = 0.024) – Value (t = 0.000)
  Delta Changes (t = 0.030) = Value (t = 0.030) – Value (t = 0.000)
  …

  and so on.

- *Step 3:* Using ACAP's user-friendly interactive options, a configuration must be selected and FOM calculation should be performed in accordance with the reference data.

3.3 Statistical analysis of normalised parameters

In the Exercise 2 comparative analysis, some parameters require special attention, because under certain circumstances the normalisation will become skewed. These parameters are:

- normalised axial power (snapshot) at the time of maximum power before scram;
- relative axial power for FAs 75 and 367 (snapshot) at the time of maximum power before scram;
- normalised radial power (snapshot) at the time of maximum power before scram;
- normalised axial power (snapshot) at the end of the transient (5 s);
- relative axial power for FAs 75 and 367 (snapshot) at the end of the transient (5 s);
- normalised radial power (snapshot) at the end of the transient (5 s).

Treating each of these parameters separately, the procedure for generating a comprehensive analysis that preserves the normalisation will be discussed.

3.3.1 Two-dimensional (2-D) core-averaged radial power distribution

This parameter is collected for the transient snapshots. The goal of the statistical analysis is to derive an average normalised power for each assembly:

$$\overline{NP_i} = \frac{\overline{p}_i}{\overline{p}_{FA}} \tag{3.15}$$

where, for N participants, $\overline{p}_i$, the average power density in radial assembly location i, is:

$$\overline{p}_i = \frac{1}{N}\sum_{j=1}^{N} p_{ij} \tag{3.16}$$

and $\overline{p}_{FA}$, the averaged assembly power density, is:

$$\overline{p}_{FA} = \frac{1}{N}\sum_{j=1}^{N} p_{FA,j} \tag{3.17}$$

Thus:

$$\overline{NP_i} = \frac{\sum_{j=1}^{N} p_{ij}}{\sum_{j=1}^{N} p_{FA,j}} \tag{3.18}$$

In the initial steady-state case the total core power is specified as Q = 2 030 MWt for the hot full power (HFP) conditions, so that the average power per fuel assembly is the same for all participants and:

$$\overline{NP_i} = \frac{1}{N}\frac{\sum_{j=1}^{N} p_{ij}}{p_{FA,c}} = \frac{1}{N}\sum_{j=1}^{N}\frac{p_{ij}}{p_{FA,c}} = \frac{1}{N}\sum_{j=1}^{N} NP_{ij} \tag{3.19}$$

where, given the total number of assemblies, M, is 764:

$$p_{FA,c} = \frac{Q}{M} \tag{3.20}$$

Thus, for the transient snapshots, where total power level and power per assembly vary among the participants, the following corrected procedure must be applied.

- *Step 1: Convert normalised values into absolute values.* Absolute values are achieved by multiplying the normalised value in each 2-D cell for each participant by the average power per assembly for the same participant, where the latter value is the total core power for that participant divided by 764 fuel assemblies.

- *Step 2: Calculate participant-averaged average power per assembly.* All participant values for total core power are averaged by the standard averaging technique to get the average core power. This value is divided by the number of fuel assemblies, 764, to get the average power per assembly, averaged over all participants. The same result can be obtained by averaging directly, with Eq. (3.1), all participants' values for average power per assembly.

- *Step 3: Generate mean solution using absolute values.* The map of absolute mean values is generated by the standard averaging procedure.

- *Step 4: Re-normalise mean solution.* Normalisation is attained by dividing each cell of the absolute map by the average power per assembly calculated in Step 2.

Unfortunately, the standard deviation and figure of merit can not be included in a normalised form, since the meaning of these statistical functions would be lost. Therefore, three maps must be provided instead of the usual two. Mean values and standard deviations are provided using absolute powers, and are accompanied by maps of the normalised mean values. Participant deviations and figures of merit are calculated relative to the absolute mean solution.

3.3.2 One-dimensional (1-D) core-averaged axial power distribution

This parameter is also collected for transient snapshots, and the final specifications require that all participants divide the core into 24 equal axial nodes. Where this is the case, the statistical analysis will be similar to that for the radial power distribution. The normalised mean axial power for a given axial node is given by:

$$\overline{NP}_{z,i} = \frac{\overline{p}_{z,i}}{\overline{p}_z} \tag{3.21}$$

where, $\overline{p}_{z,i}$, the average power density at axial layer *i*, is given by:

$$\overline{p}_{z,i} = \frac{1}{N}\sum_{j=1}^{N} p_{z,ij} \tag{3.22}$$

where $\overline{p}_z$, the core-averaged axial power density, is:

$$\overline{p}_z = \frac{1}{N}\sum_{j=1}^{N} p_{z,j} = \frac{1}{N}\sum_{j=1}^{N} \frac{p_{FA,j}}{24} \tag{3.23}$$

Thus:

$$\overline{NP}_{z,i} = \frac{\sum_{j=1}^{N} p_{z,ij}}{\sum_{j=1}^{N} \frac{p_{FA,j}}{24}} \tag{3.24}$$

For the steady-state cases, where the total core power level, *Q*, and average power per assembly are constant for all participants:

$$\overline{NP}_{z,i} = \frac{1}{N}\frac{1}{24}\sum_{j=1}^{N} \frac{p_{z,ij}}{p_{FA,j}} = \frac{1}{N}\sum_{j=1}^{N} NP_{z,ij} \tag{3.25}$$

As a result, the standard techniques for 1-D distribution can be applied for the steady-state cases; however, for the transient snapshots, where the average power per assembly will vary among the participants, the following procedure must be utilised:

- *Step 1: Convert normalised values into absolute values.* Absolute values are achieved by multiplying the normalised value in each axial node for each participant by the average power per node in the average assembly for the same participant, where the latter value is the total core power for that participant divided by 764 fuel assemblies and 24 axial nodes.

- *Step 2: Calculate participant-averaged average power per assembly*. All participant values for total core power are averaged by the standard averaging technique to get the average core power. This value is divided by the number of fuel assemblies, 764, to get the average power per assembly, which is finally divided by 24 to get the average power per axial node, averaged over all participants. The same result can be obtained by averaging directly all participants' values for average power per axial node, using Eq. (3.1).

- *Step 3: Generate mean solution using absolute values.* The table of absolute mean values is generated by the standard averaging procedure.

- *Step 4: Re-normalise mean solution.* Normalisation is attained by dividing each cell of the absolute map by the average power per node calculated in Step 2.

Once again, the standard deviation and figure of merit can not be included in a normalised form and two axial tables will be provided. Absolute mean values and standard deviations are provided along with re-normalised mean values in one table. Participant deviations and figures of merit, calculated relative to the absolute values, are presented in a second table. It should be noted that this procedure could be applied only where the participants have used 24 equal axial layers. Results from participants who do not adhere to this specification must first have their data converted to 24 equal nodes via a cell-volume weighting procedure.

3.3.3 One-dimensional (1-D) core-averaged axial power distribution for FAs 75 and 367

For maximum power before scram and at the end of transient snapshot cases, one-dimensional core-average power distribution is collected for FAs 75 and 367. It is treated in a similar manner as for the core-averaged axial power. Again, the specifications request that the fuel assembly be divided into 24 equal nodes. For the transient snapshots, the power in the assemblies 75 and 367 varies among the participants and the average normalised power per node is given by:

$$\overline{NP}_{z,i} = \frac{\sum_{j=1}^{N} p_{z,ij}}{\sum_{j=1}^{N} \frac{p_{FA,j}}{24}} \tag{3.26}$$

where the total power in FAs 75 and 367 can be extracted from each participant's 2-D core-averaged radial power distribution. The following method must be applied in every transient case:

- *Step 1: Convert normalised values into absolute values.* The absolute values are found by multiplying the normalised value in each axial node for each participant by the average power per 3-D node in the core for the same participant, where the latter value is the total core power divided by 764 assemblies and 24 axial nodes.

- *Step 2: Calculate participant-averaged average power per assembly*. All participant values for total core power are averaged by the standard averaging technique to get the average core power. This value is divided by the number of cells in the core – 764 assemblies times 24 axial layers – to get the average power per 3-D node, averaged over all participants.

- *Step 3: Generate mean solution using absolute values.* The map of absolute mean values is generated by the standard averaging procedure.

- *Step 4: Re-normalise mean solution.* Normalisation is attained by dividing each cell of the absolute map by the average power per node calculated in Step 2.

As with the previous two parameters, the results are reported in the form of mean values and standard deviations of the absolute values along with a re-normalised mean solution. Participant deviations and figures of merit are again calculated relative to the absolute mean solution.

3.3.4 Multiple code dependencies

It has been noted that some sets of results that have been submitted for this exercise are not fully independent of each other. That is, certain participants have submitted multiple sets from codes that differ from each other to varying degrees. In some cases, the differences are significant, and involve quite different kinetics models. In other cases, the differences are subtler. In the case of codes with only subtle differences, it may not be appropriate to treat the results as fully separate, and therefore subject to independent treatment in the averaging techniques described above.

To account for this circumstance, a two-step averaging process has been developed whereby sets of results that are determined to be "dependent" on each other are first averaged together, and the subsequent mean participant values are then included in the final averaging process. However, after examining the descriptions of each code that has been used in developing the submitted results, it was determined that such a two-step averaging process is not necessary in the present case, and it has not been applied.

Chapter 4

RESULTS AND DISCUSSION

The results, presented in this chapter, demonstrate the importance of the neutronic and coupled neutronic/thermal-hydraulics core modelling for analysis of pressure transients for BWRs. The tables and the figures of this chapter provide a comparison of the participants' results with the reference solutions as well as a discussion of observed agreement or disagreement.

It should be reminded that the second exercise consists of performing coupled-core boundary conditions calculations. The purpose of the second exercise is to test and initiate the participants' core models. Thermal-hydraulic boundary conditions are provided to the participants from the benchmark team. The thermal-hydraulic core boundary conditions provided are the core inlet pressure, core exit pressure, core inlet temperature and core inlet flow. In summary the second exercise is to perform a coupled 3-D kinetics/T-H calculation for the reactor core using the PSU-provided boundary conditions at core inlet and exit. Three-dimensional two-group macroscopic cross-section libraries are provided to the participants. The core inlet flow is provided in two formats: total core flow as a function of time and radially distributed flow as a function of time for 33 channels. In addition, the benchmark team provided the participants with normalised power vs. flow correlations for the different assembly types based on the detailed modelling in which each assembly represented by a thermal-hydraulic channel for the initial steady-state conditions. The studies performed by the benchmark team indicated that these correlations also apply reasonably well during the transient, which provided an opportunity for the participants to develop their own core coupled spatial mesh overlays.

The participants in Exercise 2 are required to provide steady-state results for two different conditions: hot zero power (HZP) and hot power (HP) conditions. For transient analysis, in addition to time histories, the participants are asked to submit results for two snapshots of the transient, one at the time of maximum power before scram and the other is at the end of transient.

The outline of this chapter is as follows:

- Steady-state results:
  - HZP results;
  - HP results.
- Transient results:
  - time histories;
  - results for the snapshot at the time of maximum power before scram;
  - results for the snapshot at the end of transient.

The comparison is made for the parameters that have important effects on the steady-state and transient scenarios. Statistical analysis was performed for each submitted parameter based on the

methodology extensively described in Chapter 3. The tables show values of the standard deviation and the figure of merit for each participant's result for a given parameter. The figures included in this chapter show the scatter of data about the reference solution.

The complete set of reference results with associated standard deviations are given in Appendix C while the complete set of the deviations of submitted results for all parameters from the reference solutions for each participant is given in Appendix D. This appendix is divided into four parts: D.1 (integral parameters), D.2 [one-dimensional (1-D) axial distributions], D.3 [two-dimensional (2-D) radial distributions] and D.4 (system and core averaged time histories). It should be noted that Appendix C and Appendix D are only available in electronic format in the CD-ROM (electronic) version of this report.

4.1 Steady-state results

Steady-state results consist of the results from HZP and HP conditions. For each condition, participants are asked to submit the following parameters:

- k_{eff};
- core averaged relative axial power distribution;
- relative power distributions for fuel assemblies 75 (rodded bundle) and 367 (un-rodded bundle) – numbering the core fuel region from top to bottom and from left to right;
- radial power distribution – two-dimensional assembly normalised power distribution (for the 3-D kinetics options).
- core averaged axial void fraction distribution (excluding the HZP state).

Table 4.1 presents the number of channels utilised in the thermal-hydraulics core models of the participants and the type of power model used in their calculations. This information should be taken into account during the discussion of the participants' deviations from the reference solutions. The term "total" in the table below refers to the total power, which includes power from decay heat and fission power together.

4.1.1 Hot zero power (HZP) results

An additional steady state was defined in the framework of the second exercise – HZP state with fixed thermal-hydraulic feedback. This allows for "clean" initialisation of the core neutronics models and cross-section modelling algorithms.

The results in this section should be considered together with Table 4.2. Important modelling issues were identified such as: the impact of using assembly discontinuity factors (ADF model), which are also provided to the participants in a similar table format as for the two group cross-sections; the xenon correction to account for the actual xenon concentration distribution at the initial steady-state conditions of the turbine trip test 2 (xenon model); the spatial distribution of the decay heat (decay model); and the bypass density correction (bypass model) in the cross-section feedback modelling to account for the deviations of bypass density from the saturated value used in the cross-section homogenisation since the cross-sections are generated by homogenising the bypass region associated with the lattice. Although the xenon, bypass and decay models are irrelevant for HZP conditions, the utilisation of BWR type ADF and ADF rotation modelling are important for the results especially for k_{eff} values and normalised radial power distributions.

Table 4-1. Number of channels used and power submitted by the participants

Participant	No. of channels	Power submitted
CEA-33	33	Fission
CEA-764	764	Fission
FANP	33	Fission
FZR	764	Total
GRS	764	Fission
IBER	1	Total
NFI	33	Fission
NUPEC	33	Fission
PSI-A	33	Fission
PSI-B	33	Fission
PSI-C	764	Fission
PSU	33	Total
TEPSYS	33	Total
UPI	33	Total
UPV	33	Total
VTT	764	Fission
WES	764	Fission

Table 4-2. Models used at HZP

Participant	Xenon	ADF	Bypass	Decay
CEA-33	No	No	No	No
CEA-764	No	No	No	No
FANP	No	Yes	Yes	Yes
FZR	No	Yes	No	No
GRS	No	No	No	No
IBER	No	Yes	No	No
NFI	Yes	No	No	No
NUPEC	No	Yes	No	No
PSI-B	No	Yes	Yes	No
PSI-C	No	Yes	Yes	No
PSU	No	Yes	No	Yes
TEPSYS	No	Yes	No	Yes
UPI	Yes	Yes	Yes	Yes
UPV	Yes	Yes	Yes	Yes
VTT	No	Yes	Yes	Yes
WES	No	Yes	Yes	No

Figure 4-1 presents a graphical comparison of participants' k_{eff} predictions with the mean value as a reference value while Table 4-3 provides k_{eff} values with the mean and standard deviation. The maximum deviated result is less than 2σ, showing that all participants' results agree well with the reference (mean) solution. The reason for discrepancies of CEA-33, CEA-764 and GRS results from the mean value can be attributed to the lack of ADF modelling.

Figure 4-2, Figure 4-3 and Figure 4-4 show a very good agreement of the participants' results for 1-D relative axial power distributions while Figures 4-5 and 4-6 show the mean of the radial power distribution and its standard deviation in a graphical format. The only significant deviation is observed

for UPI results in Figure 4-4. The latter plot gives an idea about the observed deviations in radial power distribution predictions. Since the participants use the same cross-section library and interpolation routine and the same radial nodalisation (one node per assembly) these deviations are coming from the different neutronics methods and utilisation or not of the ADFs. The mean values and standard deviations can be found in Appendix C and the deviations of each participant's solutions from the mean value can be found in Appendix D.

Figure 4-1. HZP k_{eff}

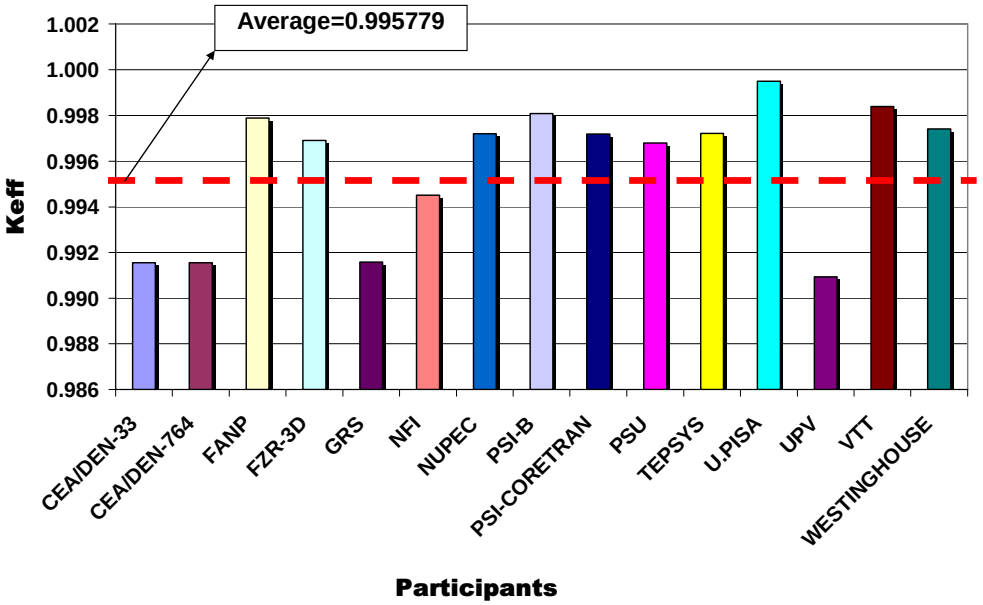

Table 4-3. HZP k_{eff}

Participant	HZP k_{eff}	Deviation (e_i)
CEA-33	0.991560	-0.004219
CEA-764	0.991560	-0.004219
FANP	0.997880	0.002101
FZR	0.996910	0.001131
GRS	0.991580	-0.004199
PSU	0.996788	0.001009
NFI	0.994500	-0.001279
NUPEC	0.997200	0.001421
PSI-B	0.998070	0.002291
PSI-C	0.997190	0.001411
TEPSYS	0.997210	0.001431
UPI	0.999500	0.003721
UPV	0.990940	-0.004839
VTT	0.998390	0.002611
WESTINGHOUSE	0.997410	0.001631
Average =	0.995779	
Standard deviation (σ) =	0.002923	

Figure 4-2. Core average relative axial power distribution at HZP

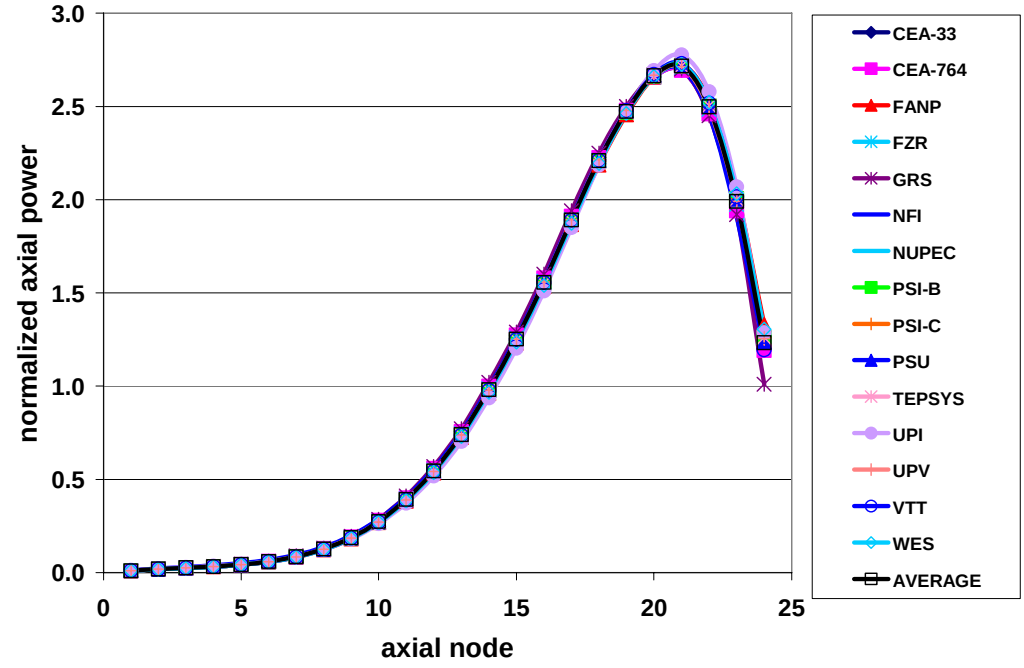

Figure 4-3. Relative power distribution for FA 75 at HZP

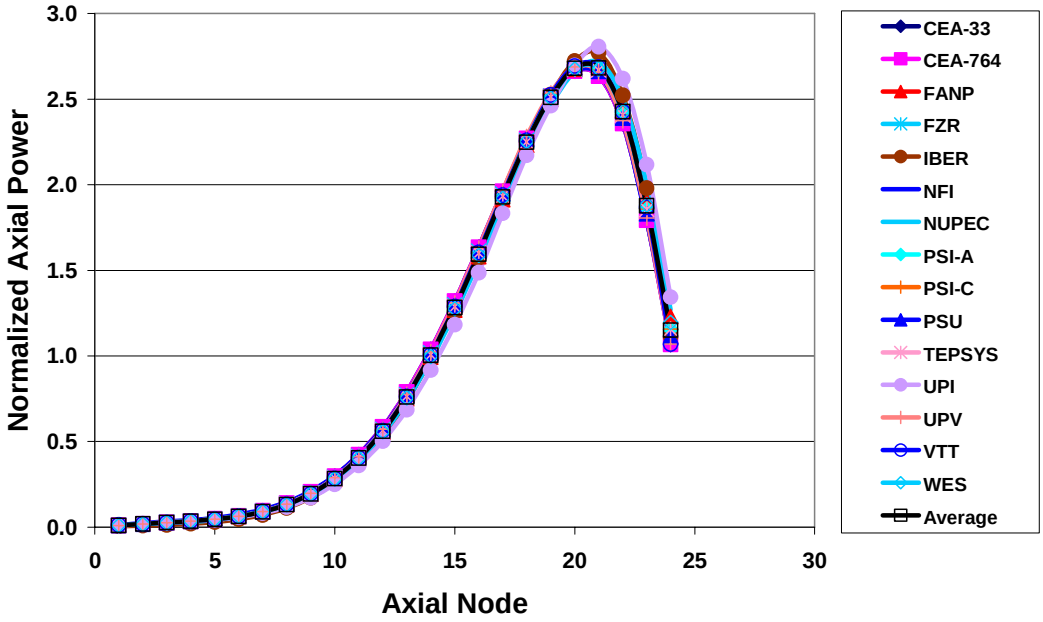

Figure 4-4. Relative power distribution for FA 367 at HZP

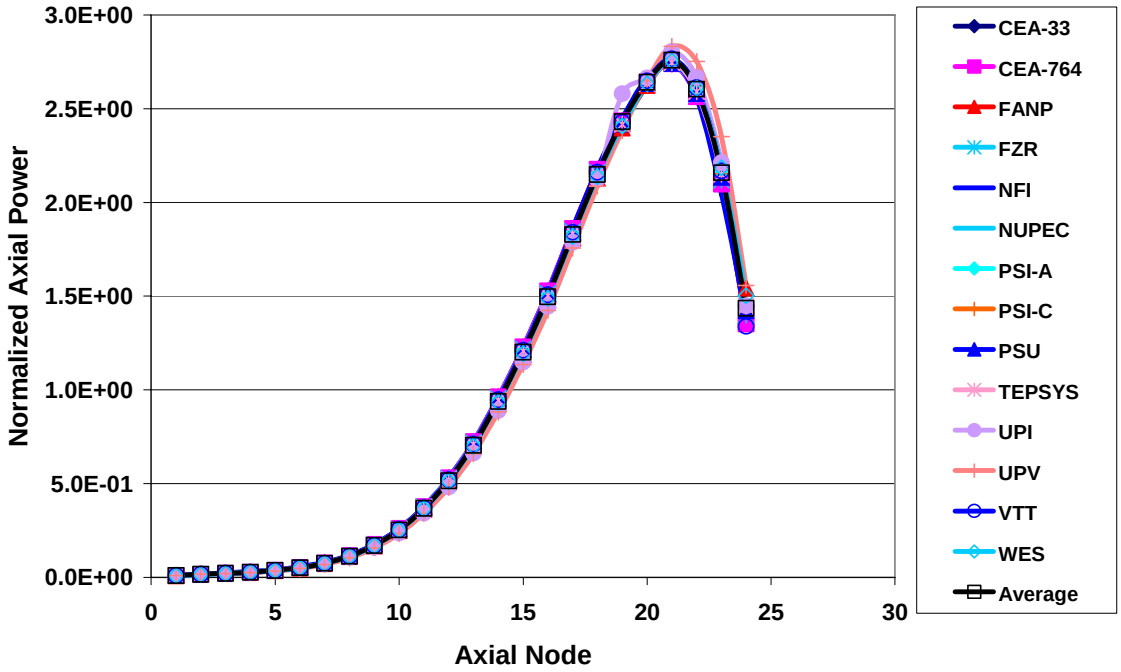

Figure 4-5. Mean radial power distribution at HZP (average of participants)

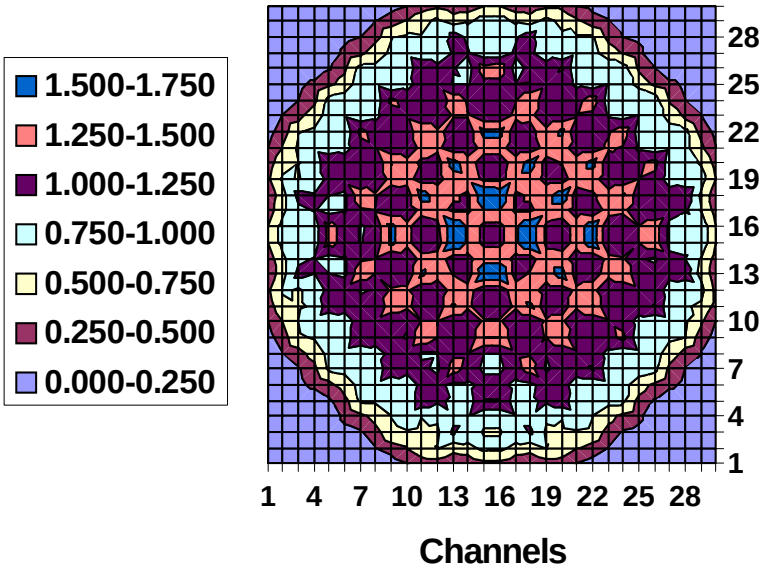

Figure 4-6. Standard deviation of radial power distribution at HZP

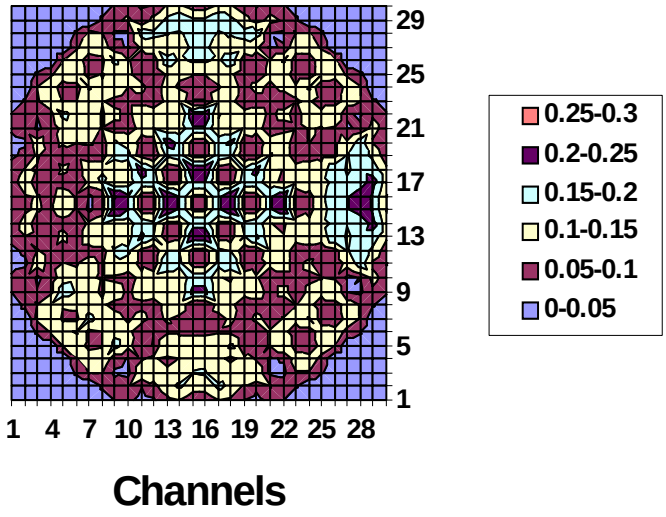

4.1.2 Hot power (HP) results

Hot power refers to the initial conditions of turbine-trip-test-at the EOC 2. Similar to the previous section, the results of this section should be considered together with Table 4-4. Core bypass flow density correction, xenon correction and BWR-type ADF and ADF rotation models are important for the HP results while the decay heat modelling is important for the transient. In particular, the utilisation of ADFs is important for k_{eff} values and radial power distribution predictions, and the core bypass flow density correction affects the axial power distributions.

Figure 4-7 presents a graphical comparison of participants' k_{eff} predictions with the mean value as a reference value, while Table 4-5 provides k_{eff} values with the mean and standard deviation. If the NETCORP solution is excluded as an outliner, the maximum deviated result can be found to be less then 2σ that also shows a good agreement of all of the rest of participants' results with the reference (mean) solution.

The most challenging part of the BWR steady-state analysis is the prediction of the void fraction distribution. Participants' core averaged axial void fraction distribution results are given in two figures, Figure 4-8 and Figure 4-9, while the mean and standard deviation are given in Figure 4-10. In principal the core averaged void fraction distribution results have a good agreement; however, PSI-A and PSI-B have noticeable deviation at the lower part of the core. From Figure 4-10 it can be seen that the standard deviation increases in the lower (bottom) part of the core which indicates differences in the void modelling in terms of sub-cooled boiling and vapour slip. Subsequently these deviations are propagated in the axial power profile predictions due to the void feedback mechanism (see Figures 4-11, 4-12 and Figure 4-13). The axial power profile predictions are also affected by utilisation or not of core bypass flow density correction

The comparisons of participants' relative axial power profile solutions for FAs 75 and 367 are given in Figures 4-14 through 4-19 and they show more pronounced deviations as compared to the core average axial power profile results. This is especially valid for the rodded bundle 75. The reason for such increased deviations are that at HP conditions the number of T-H channels and spatial mesh overlays with neutronics core model effect the local power predictions. The mean and standard deviation of radial power distribution at HP are given in Figures 4-20 and 4-21. In addition to utilisation

or not of ADFs the spatial mesh overlays also affect the radial power distribution predictions at HP. The utilisation or not of the xenon correction also contributes to observed deviations. The mean values and standard deviations of the submitted results can be found in Appendix C and the deviations of each participant's prediction from the mean solution can be found in Appendix D.

Table 4-4. Models used at HP

Participant	Xenon	ADF	Bypass	Decay
CEA-33	No	No	Yes	Yes
CEA-764	No	No	Yes	Yes
FANP	Yes	Yes	Yes	Yes
FZR	Yes	Yes	Yes	Yes
GRS	Yes	No	No	Yes
IBER	Yes	Yes	No	No
NFI	Yes	No	No	No
NUPEC	Yes	Yes	No	Yes
PSI-A	Yes	Yes	Yes	No
PSI-B	Yes	Yes	Yes	No
PSI-C	Yes	Yes	Yes	No
PSU	Yes	Yes	Yes	Yes
TEPSYS	Yes	Yes	Yes	Yes
UPI	Yes	Yes	Yes	Yes
UPV	Yes	Yes	Yes	Yes
VTT	Yes	Yes	Yes	Yes
WES	No	Yes	Yes	No

Figure 4-7. HP k_{eff}

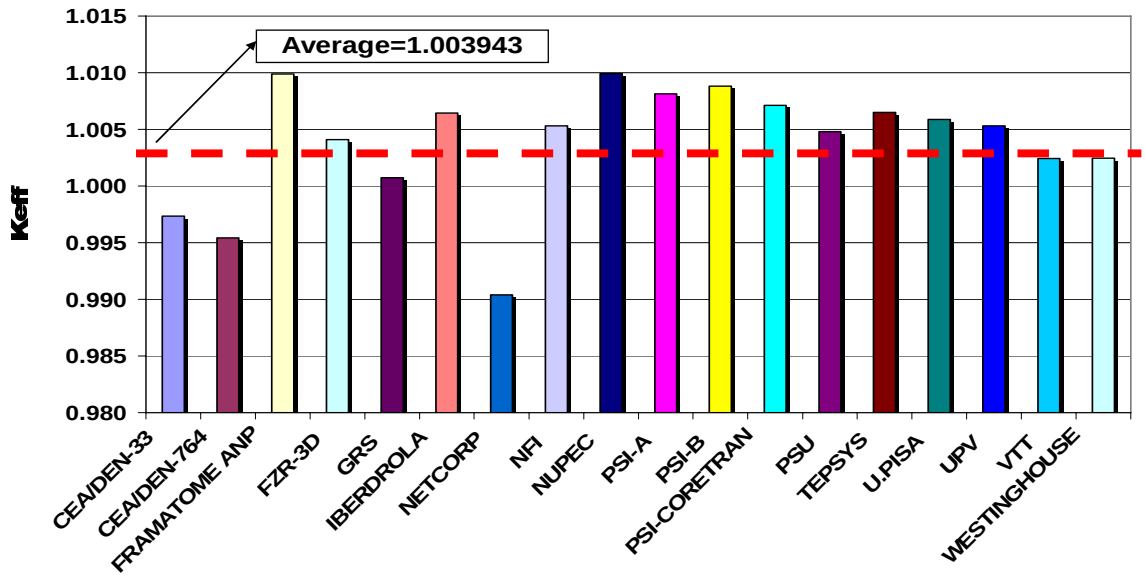

Table 4-5. HP k_{eff}

Participant	HP k_{eff}	Deviation (e_i)
CEA-33	0.997330	-0.006613
CEA-764	0.995440	-0.008503
FANP	1.009890	0.005947
FZR	1.004100	0.000157
GRS	1.000740	-0.003203
IBER	1.006437	0.002495
NETCORP	0.990400	-0.013543
NFI	1.005300	0.001357
NUPEC	1.009900	0.005957
PSI-A	1.008150	0.004207
PSI-B	1.008830	0.004887
PSI-C	1.007130	0.003187
PSU	1.004800	0.000857
TEPSYS	1.006500	0.002557
UPI	1.005860	0.001917
UPV	1.005300	0.001357
VTT	1.002410	-0.001533
WES	1.002450	-0.001493
Average =	1.003943	
Standard deviation (σ) =	0.005189	

Figure 4-8. Core average axial void fraction distribution at HP (Group 1)

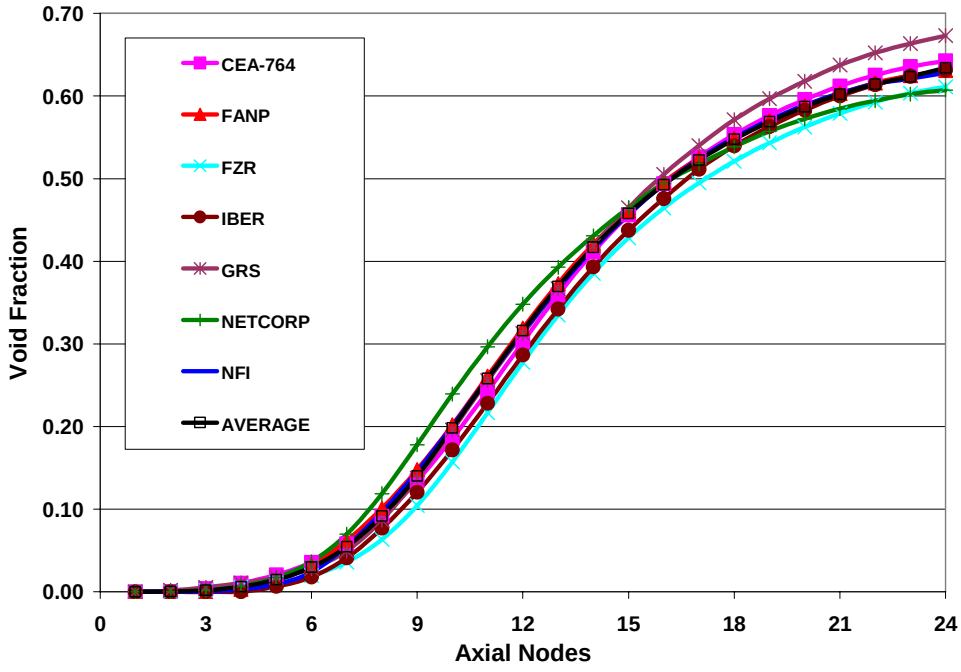

Figure 4-9. Core average axial void fraction distribution at HP (Group 2)

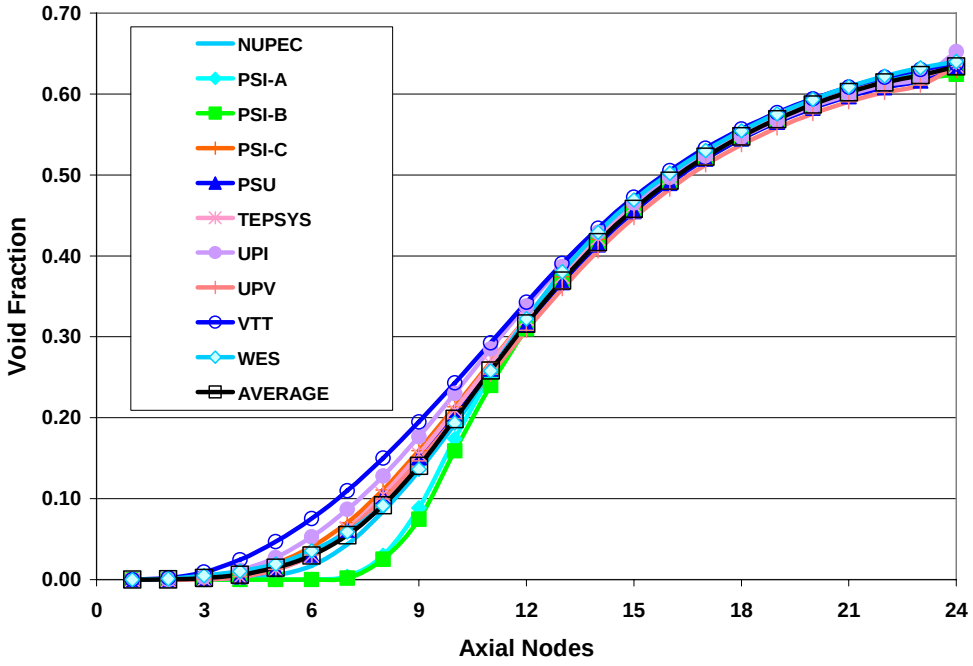

Figure 4-10. Core average axial void fraction at HP (mean and deviation)

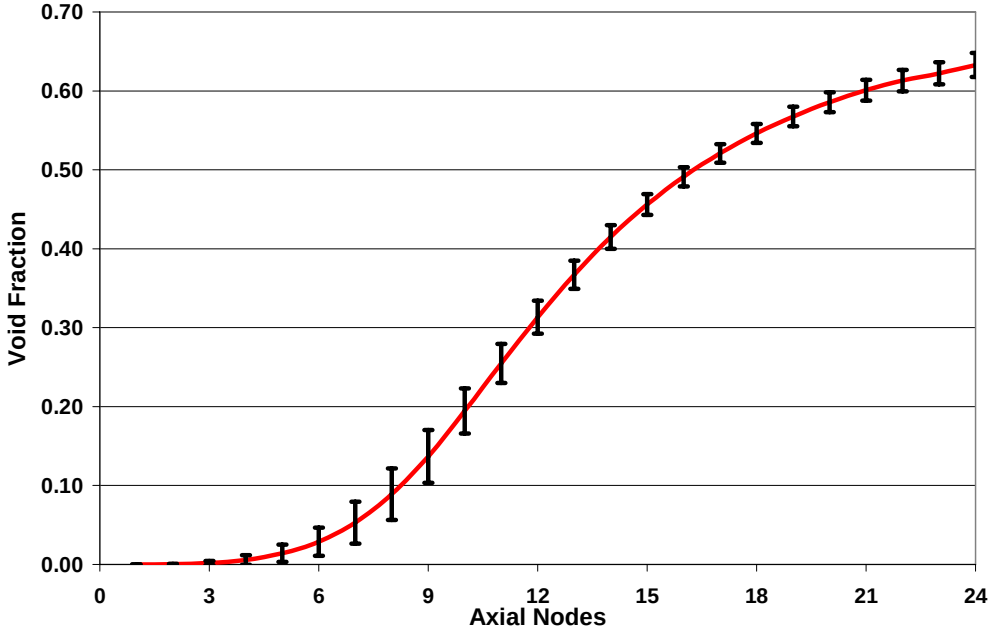

Figure 4-11. Core average relative axial power distribution at HP (Group 1)

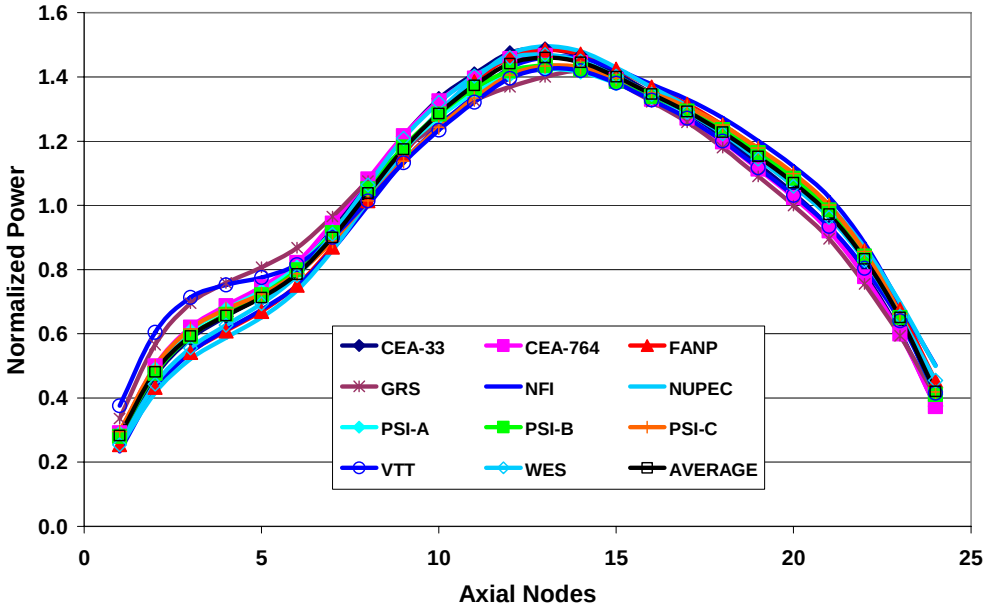

Figure 4-12. Core average relative axial power distribution at HP (Group 2)

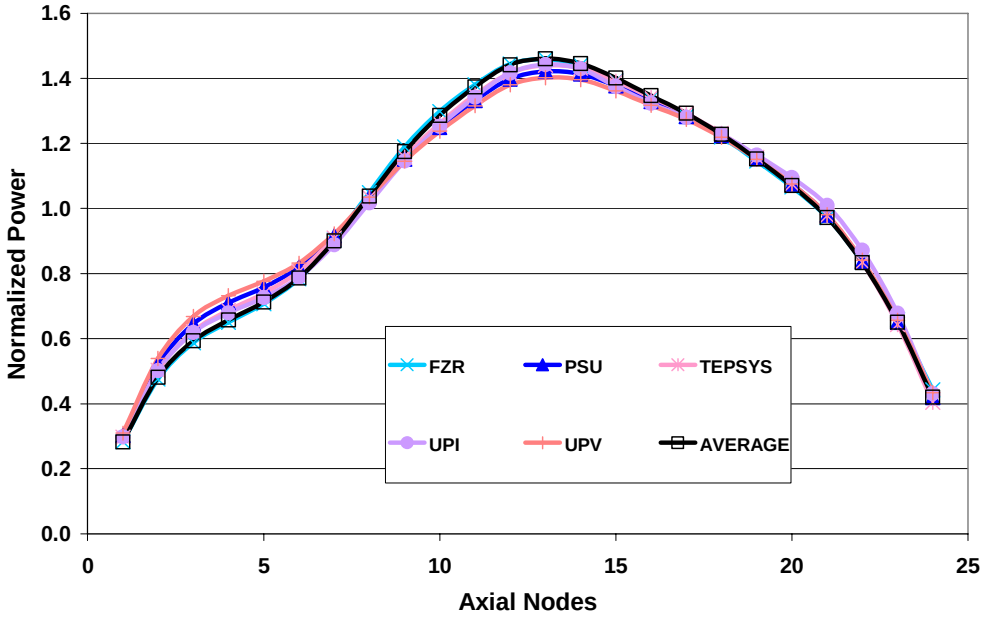

Figure 4-13. Core average relative axial power distribution at HP (mean and deviation)

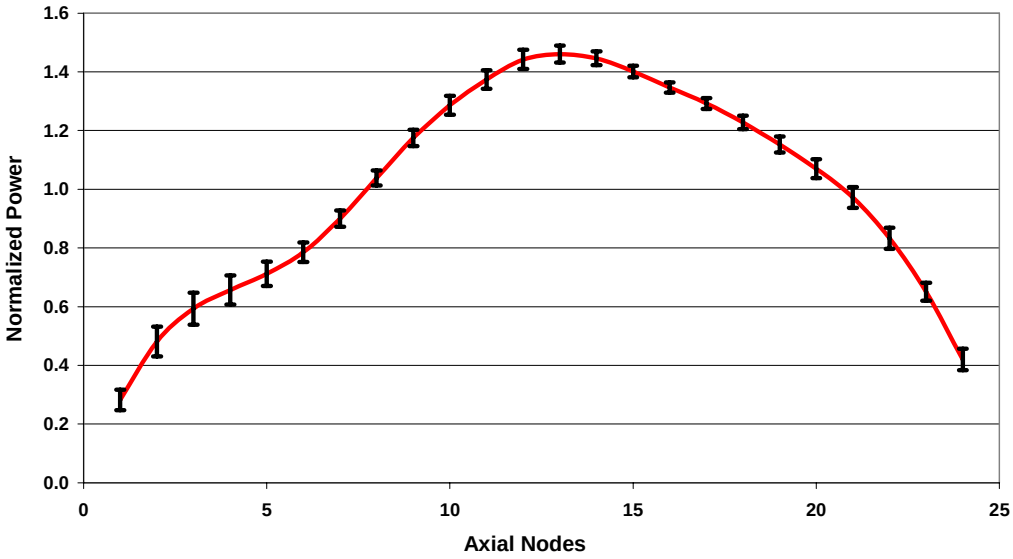

Figure 4-14. Relative power distribution for FA 75 at HP (Group 1)

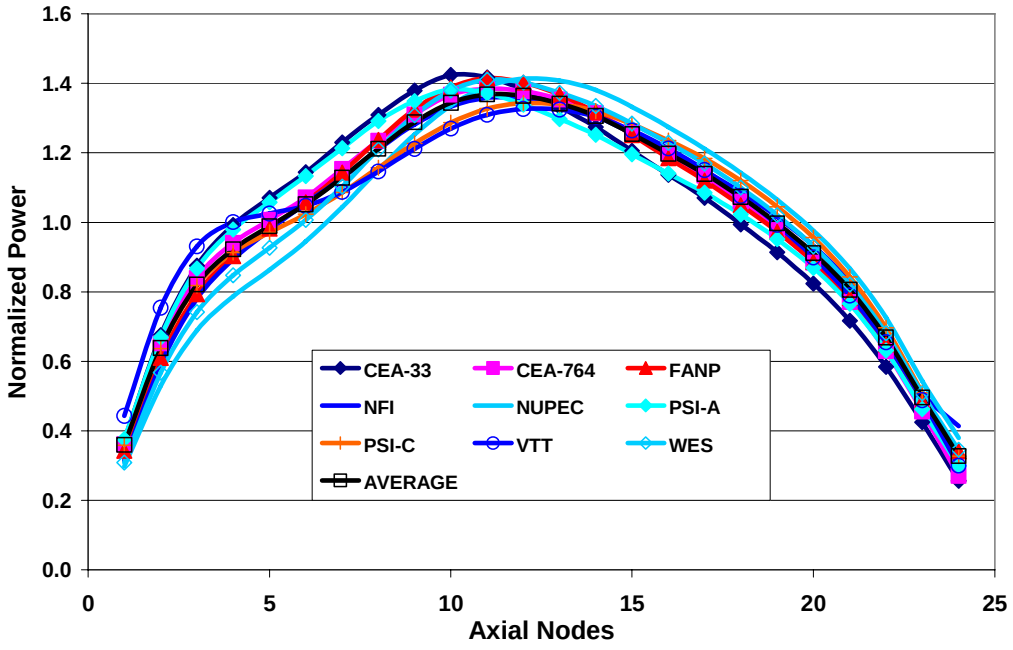

Figure 4-15. Relative power distribution for FA 75 at HP (Group 2)

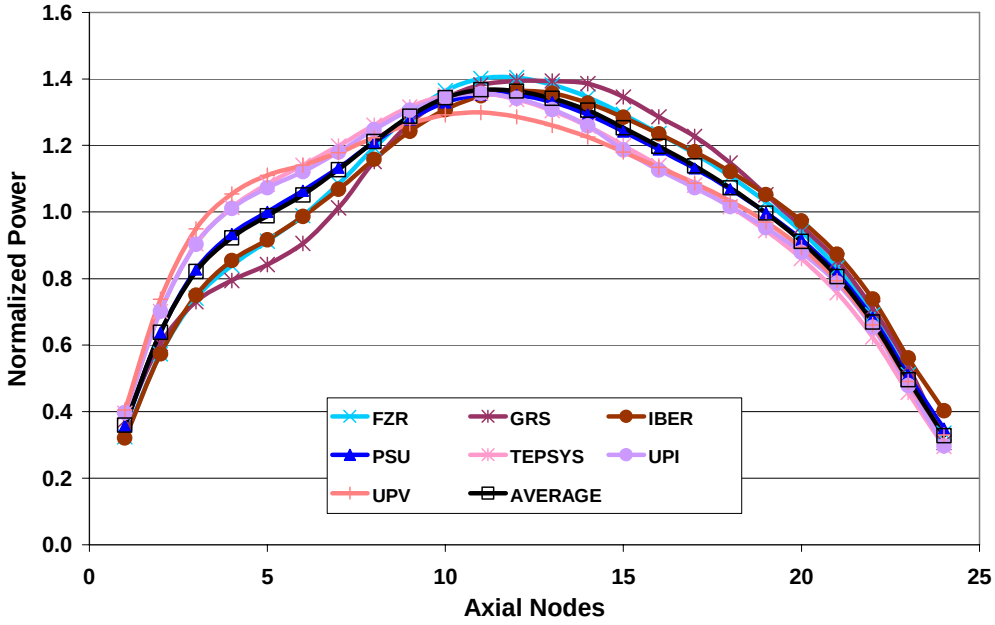

Figure 4-16. Relative power distribution for FA 75 at HP (mean and deviation)

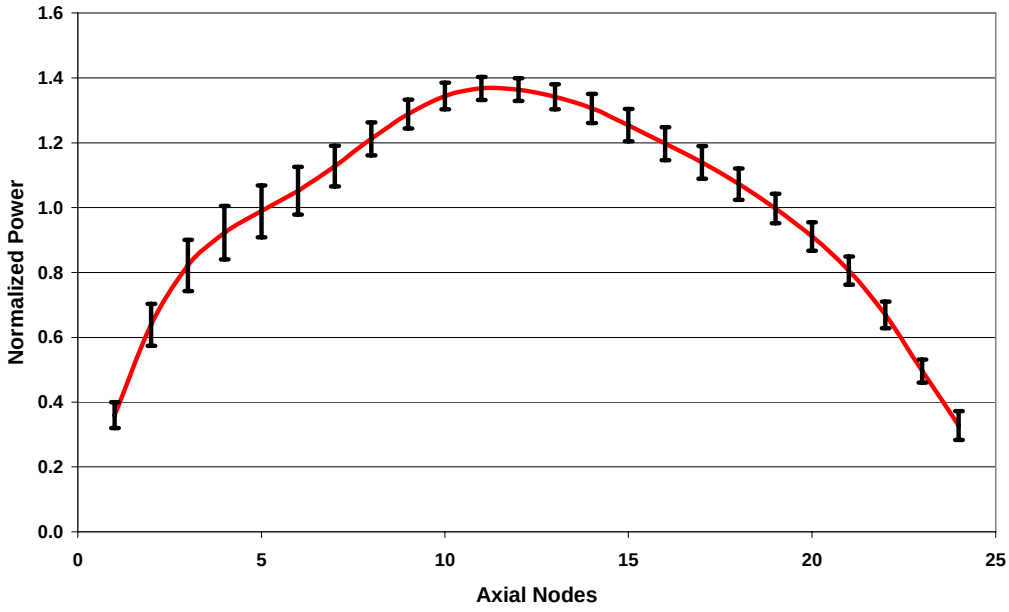

Figure 4-17. Relative power distribution for FA 367 at HP (Group 1)

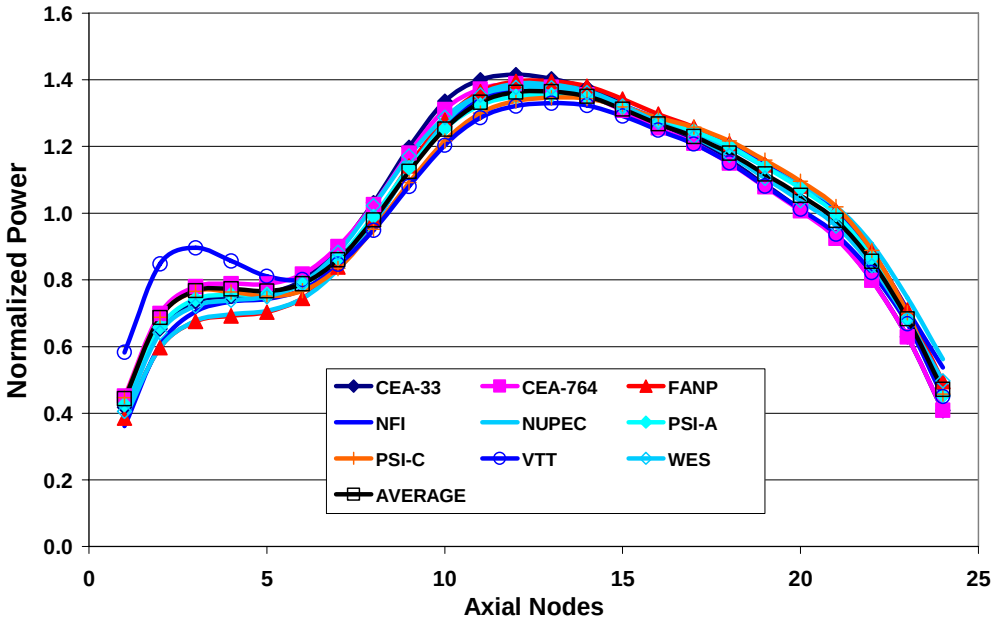

Figure 4-18. Relative power distribution for FA 367 at HP (Group 2)

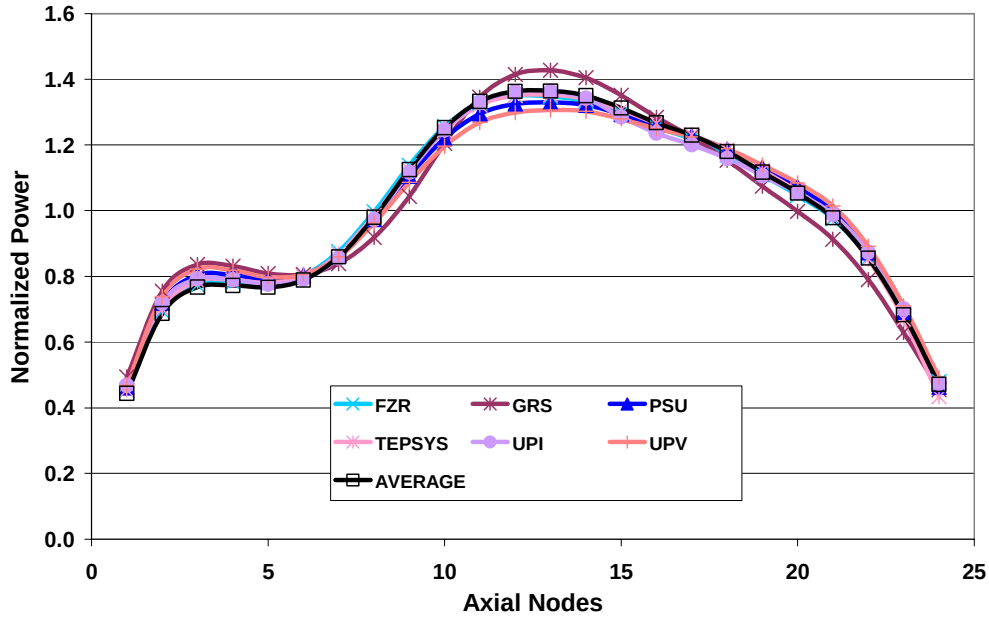

Figure 4-19. Relative power distribution for FA 367 at HP (mean and deviation)

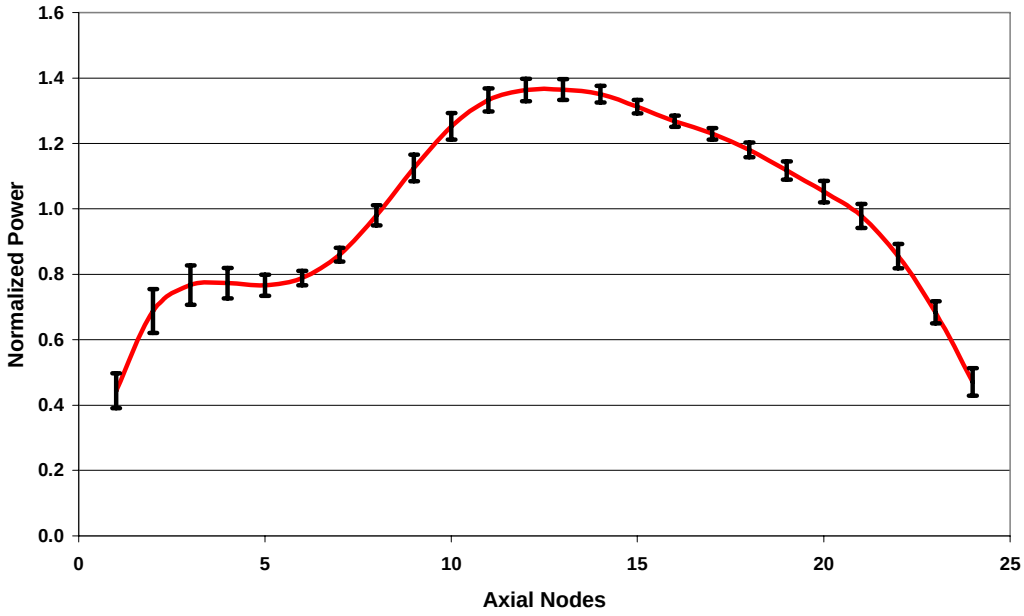

Figure 4-20. Mean radial power distribution at HP (average of participants)

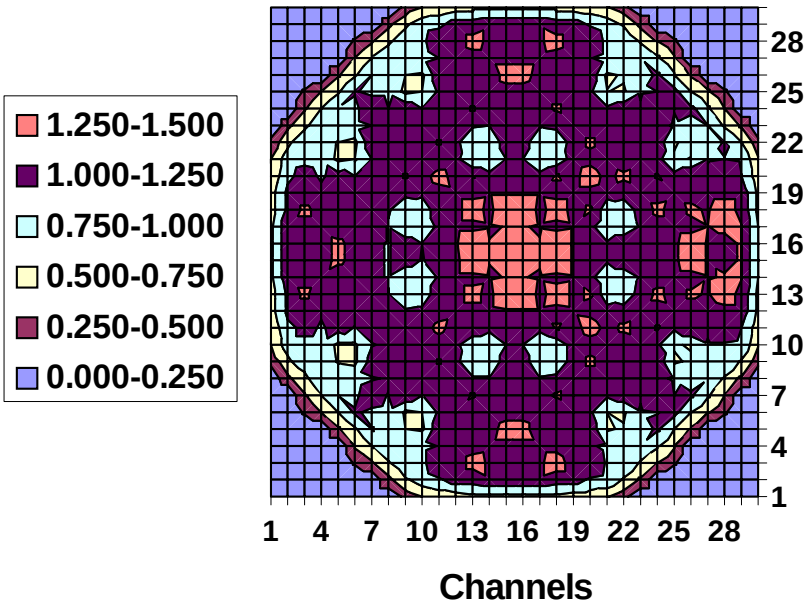

Figure 4-21. Standard deviation of radial power distribution at HP

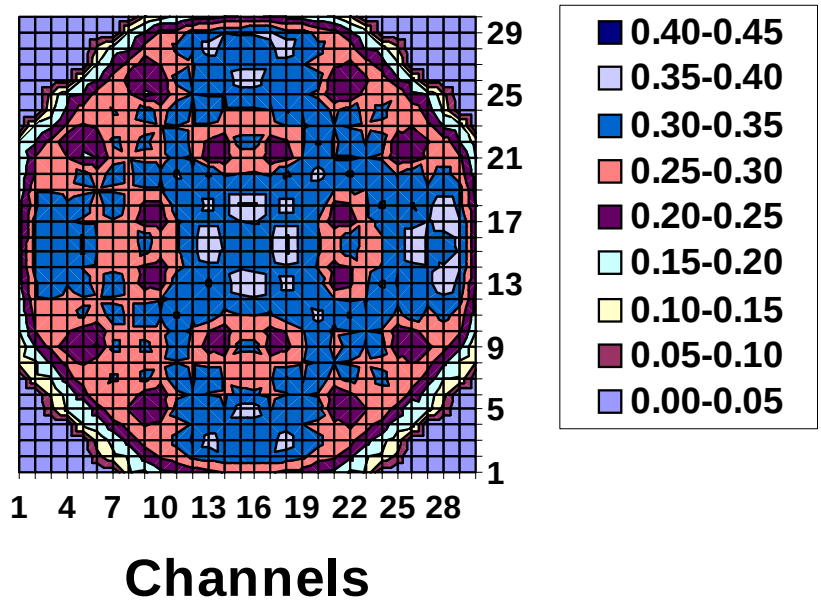

4.2 Transient results

The requested output in Exercise 2 in terms of transient results consists of core averaged time histories, snapshot at the time of maximum power before scram, and snapshot at the end of the 5 s transient. Participants are asked to submit the following parameters for each relevant case:

- Time histories:
  - core power;
  - total reactivity;
  - Doppler reactivity;
  - void reactivity.

- Snapshot at the time of maximum power before scram:
  - time of maximum power before scram;
  - core averaged relative axial power distribution;
  - relative power distribution for FA 75;
  - relative power distribution for FA 367;
  - radial power distribution.

- Snapshot at the end of the transient:
  - core averaged relative axial power distribution;
  - relative power distribution for FA 75;
  - relative power distribution for FA 367;
  - radial power distribution.

4.2.1 Time histories

In transient analyses of Exercise 2, core thermal-hydraulic boundary conditions model are utilised to test and initialise the coupled core response. The complete PB2 system thermal-hydraulic model is converted to a core thermal-hydraulic boundary condition model by defining inlet and outlet thermal-hydraulic boundary conditions. The simulated transient and the comparison of submitted results, presented in this section, not only provide an opportunity to understand the core reactivity feedback phenomena during a turbine trip transient but also allow for a comprehensive testing of the coupled neutronics/thermal-hydraulics core models.

The plots and tables given in this section provide a comparison of the participants' results for the parameters that have the greatest effect on the Exercise 2 analysis. For this reason only core averaged time histories were requested from the participants to be submitted. These histories are core power, total reactivity, Doppler reactivity and void reactivity.

Please note that the participants have preformed in advance sensitivity studies on temporal coupling schemes and time step sizes for obtaining converged solutions [16]. The results in this section should be considered together with the Table 4-6 since all of the models given in the table are important for the transient calculations.

Table 4-6. Models used in transient calculation

Participant	Xenon	ADF	Bypass	Decay
CEA-33	No	No	Yes	Yes
CEA-764	No	No	Yes	Yes
FANP	Yes	Yes	Yes	Yes
FZR	Yes	Yes	Yes	Yes
GRS	Yes	No	No	Yes
IBER	Yes	Yes	No	No
NFI	Yes	No	No	No
NUPEC	Yes	Yes	No	Yes
PSI-A	Yes	Yes	Yes	No
PSI-B	Yes	Yes	Yes	No
PSI-C	Yes	Yes	Yes	No
PSU	Yes	Yes	Yes	Yes
TEPSYS	Yes	Yes	Yes	Yes
UPI	Yes	Yes	Yes	Yes
UPV	Yes	Yes	Yes	Yes
VTT	Yes	Yes	Yes	Yes

The mean time histories are provided in this section as well as in Appendix C (supplied on the CD-ROM). The standard deviations are represented as error bounds for the time histories. The figures of merit are presented in the tables of this section. Additionally, the participant deviations and figures of merit are presented in Appendix D (also supplied on the CD-ROM), and are listed in the same order as the reference solutions.

In each case the figures (Figures 4-22 through 4-37) graphically illustrate the agreement or disagreement of participants' predictions. Statistical evaluation is employed to generate a mean solution, which is also shown in the plots.

Core power time evolutions are presented in two groups (fission or total) depending on the submitted core power type. Comparisons of the predictions of fission power evolution and the total power evolution calculated by each code throughout the transient (up to 5 seconds) are shown in Figures 4.22 and 4.24, while Figures 2.23 and 4.25 are zooming on the first one second of the transient where the power peak occurs. Table 4-7 provides figure of merit (FOM) for two different methods, D'Auria FFT and mean error.

When analysing the power history results it has to be taken into account that in the TT2 test, the thermal-hydraulic feedback alone limited the power peak and initiated the power reduction. The void feedback plays the mayor role while the Doppler feedback plays a subordinate role. The reactor scram then inserted additional negative reactivity and completed the power reduction and eventual core shutdown. The scram initiation time and the speed of the rod insertion were specified. The scram initiation time was specified since one of the objectives of the benchmark is to test coupled codes' capabilities to predict or not that the thermal-hydraulic feedback alone limits the power peak and initiates the power reduction. The power response to the pressure wave caused by the turbine trip (which is "seen" by the participants' core models through the provided core boundary conditions) in terms of timing and magnitude of power peak during the transient as predicted by different codes is a function of the total reactivity time evolution. In Figure 4-23 (the fission power group), the predicted power peak values of four participants, CEA-33, CEA/DEAN-764, PSI-B and NFI, are higher than the mean value. In total power group (Figure 4-24), only the TEPSYS solution differs from the others, which form a cluster. In reality, fission power (Figure 4-23) is slightly lower than total power which accounts decay heat. In general, the power history results are in a good agreement including TEPSYS results.

Figure 4.26 through Figure 4.37 show comparisons of the predictions of the total, Doppler and void reactivity throughout the transient. The total reactivity has three components – the negative tripped rod reactivity, moderator density (void) reactivity and Doppler feedback reactivity. The total reactivity behaviour before the scram is dominated by the void reactivity feedback mechanism. The fuel heat transfer parameters such as the UO_2 conductivity and gap conductivity and direct heating (2% to in-channel flow and 1.7% to bypass flow) were specified. The sources of modelling uncertainties in the void feedback model were identified in terms of sub-cooled boiling and vapour slip. Different density correlations and standards for water/steam property tables incorporated into the codes have also an important role on the void reactivity predictions by such codes (see Figures 4.34 and 4.37 and Table 4-10). As mentioned above the Doppler feedback plays a subordinate role. The discrepancies in the Doppler reactivity time history predictions (see Figures 4.30 and 4.33 and Table 4-9) come from the discrepancies in the results for core averaged Doppler temperature time evolution. The later are due to the different relations used for calculating the Doppler fuel temperature, and the radial and axial nodalisation of the heat structure used (fuel rod). Discrepancies at the end of the transient are due to different predictions of the tripped control rod reactivity by the participants' codes.

Figure 4-22. Transient power (fission)

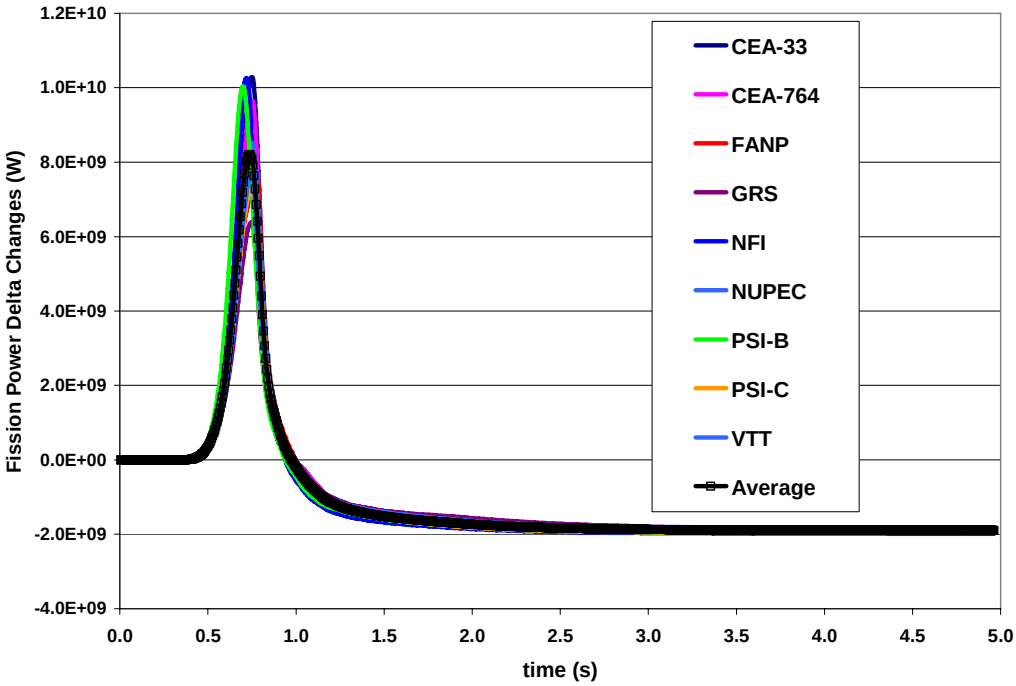

Figure 4-23. Transient power (fission – zoom)

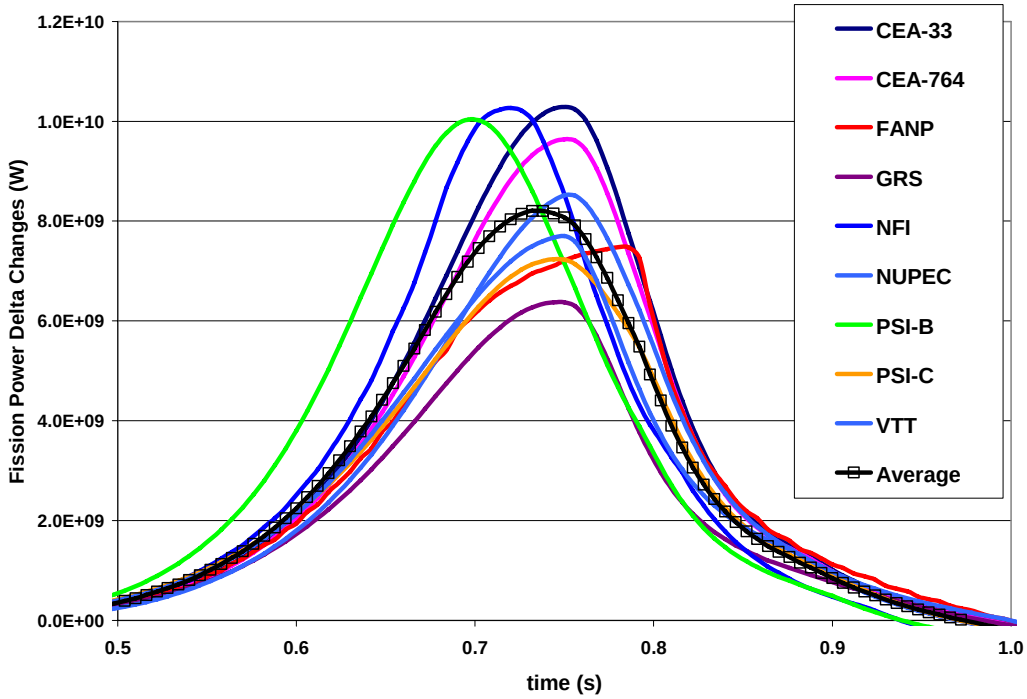

Figure 4-24. Transient power (total)

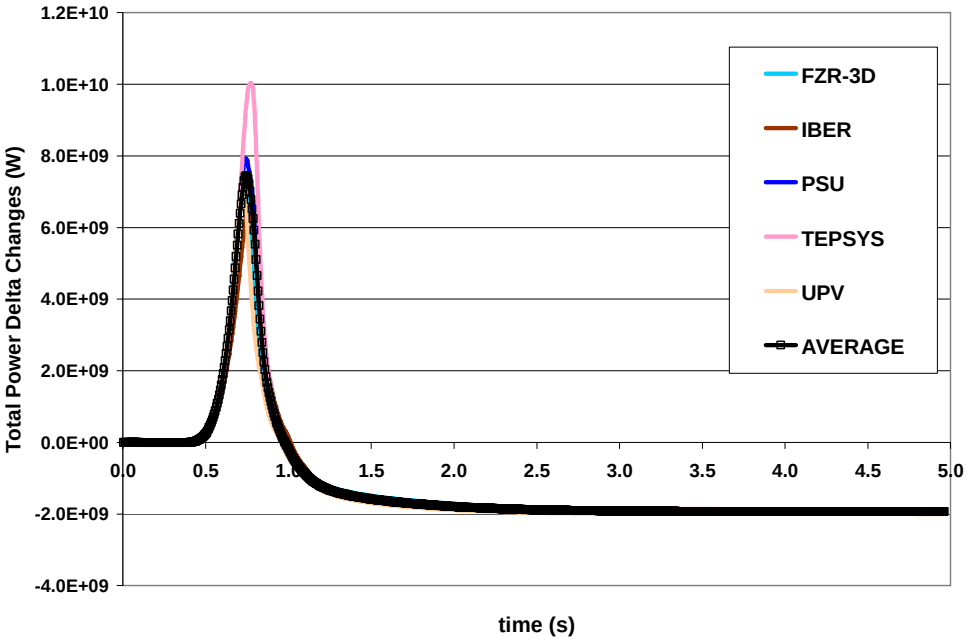

Figure 4-25. Transient power (total – zoom)

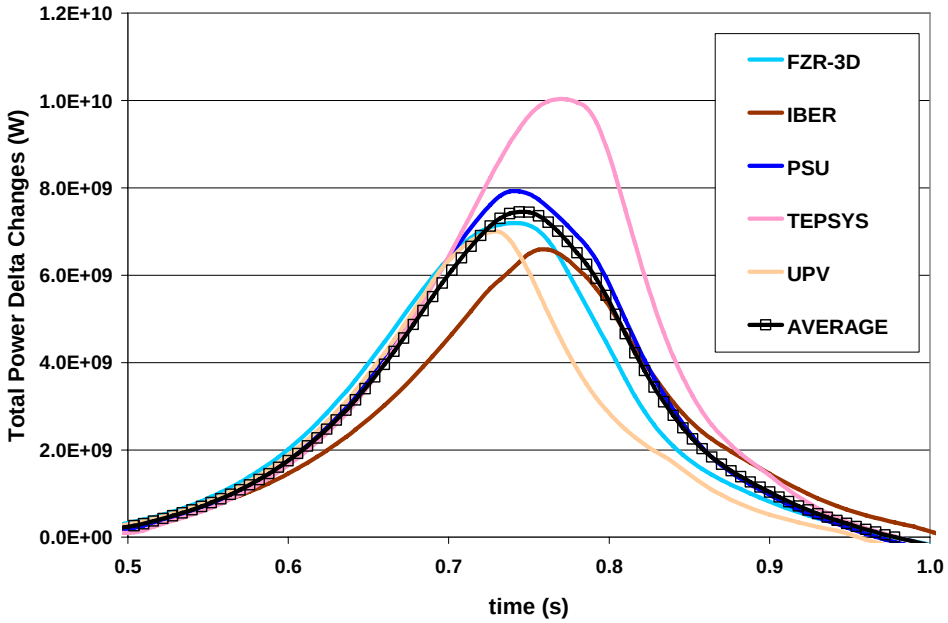

Table 4-7. Transient power, figure of merit

Fission power used			Total power used		
	D'Auria FFT	Mean error (ME)		D'Auria FFT	Mean error (ME)
CEA-33	0.7566	0.9964	**FZR**	0.7609	0.9922
CEA-764	0.7842	0.9984	**IBER**	0.7268	0.9974
FANP	0.7953	0.9994	**PSU**	0.7676	0.9976
GRS	0.7447	0.9974	**TEPSYS**	0.6963	0.9979
NFI	0.7602	0.9985	**UPV**	0.7852	0.9925
NUP	0.7914	0.9971			
PSI-A	0.6234	0.9894			
PSI-B	0.6968	0.9952			
PSI-C	0.8231	0.9982			
VTT	0.8390	0.9972			

Figure 4-26. Total reactivity

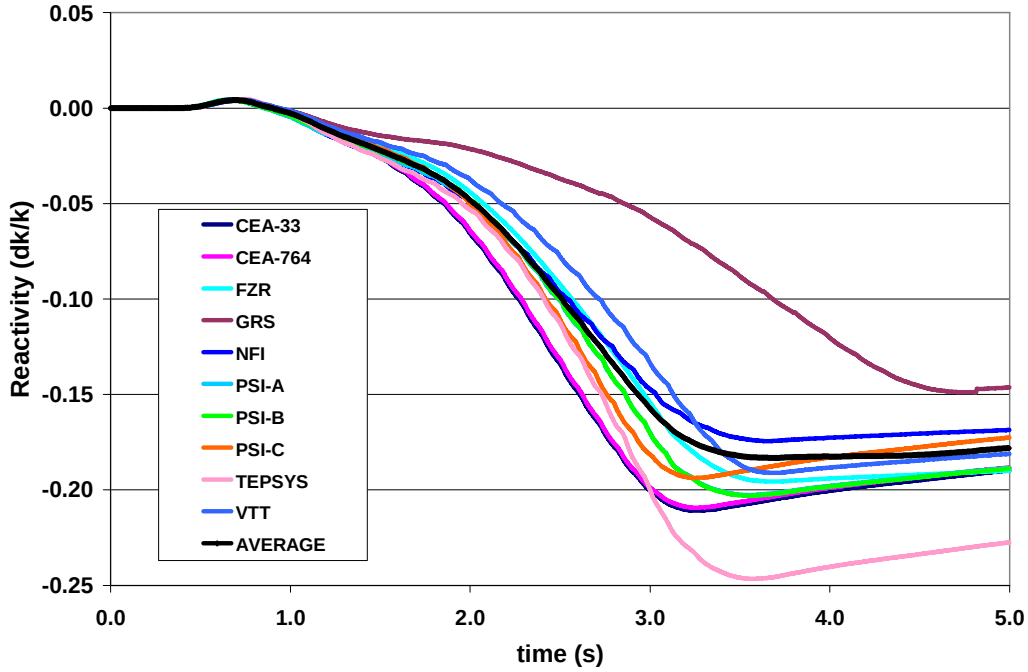

Figure 4-27. Total reactivity (zoom)

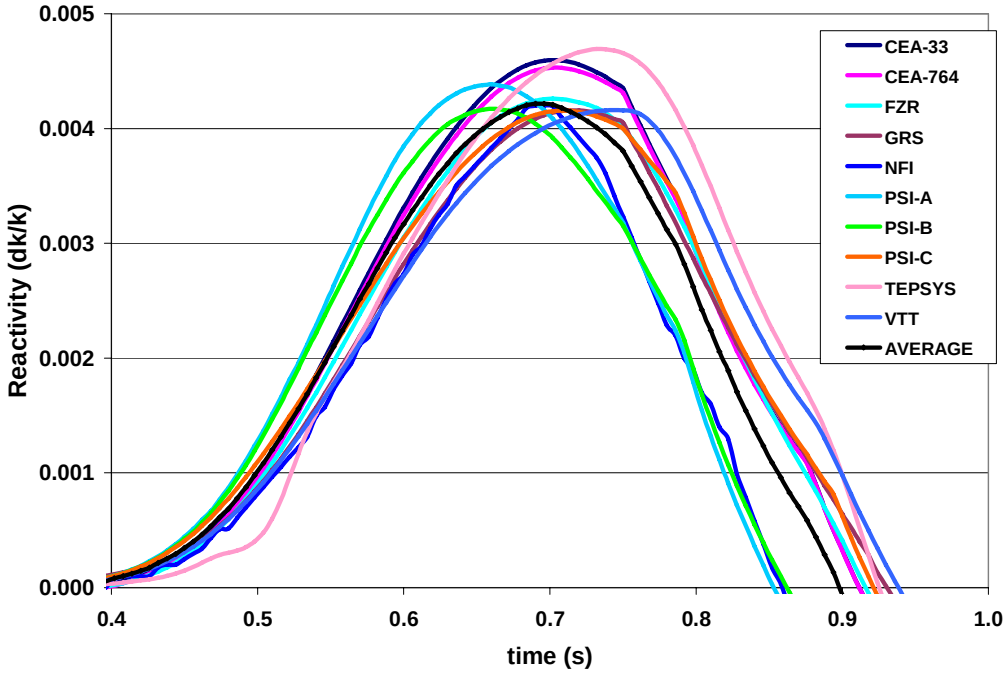

Figure 4-28. Total reactivity (mean and deviation)

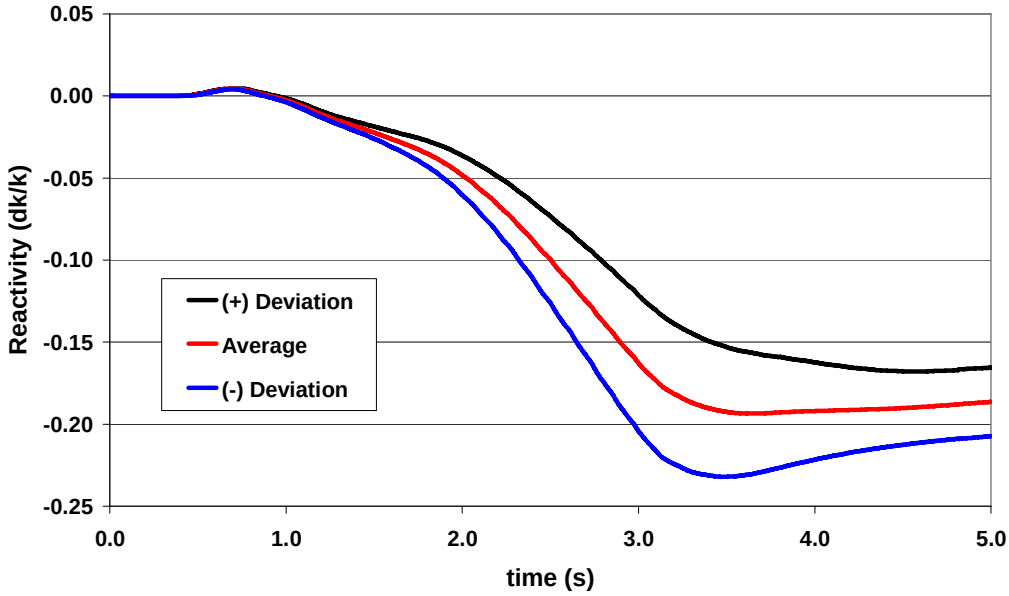

Figure 4-29. Total reactivity (mean and deviation – zoom)

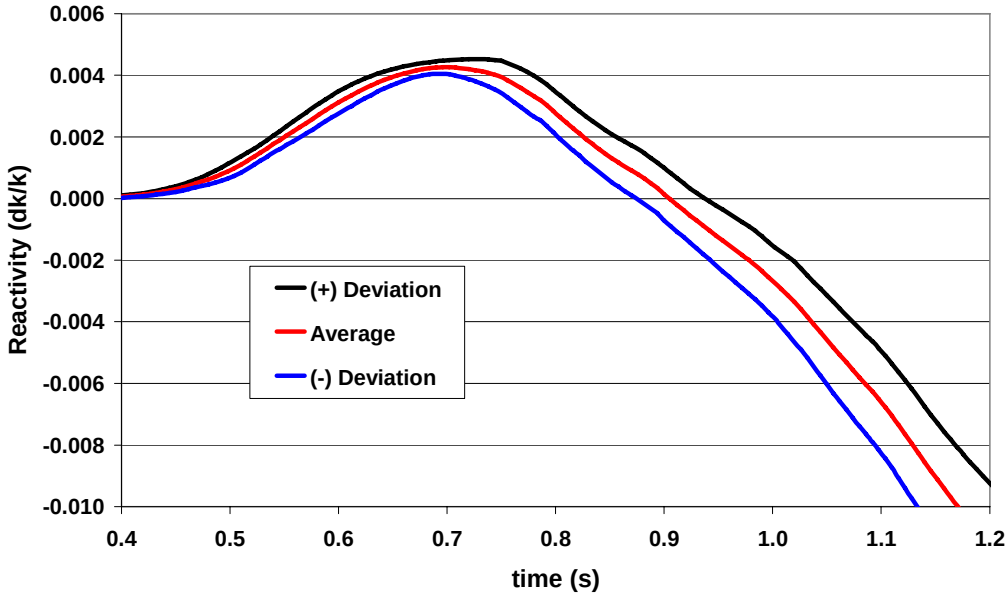

Table 4-8. Total reactivity, figure of merit

	D'Auria FFT	Mean error (ME)
CEA-33	0.8141	0.9413
CEA-764	0.8171	0.9465
GRS	0.6712	0.8127
NFI	0.8577	0.9592
PSI-A	0.8442	0.9838
PSI-B	0.8387	0.9849
PSI-C	0.8861	0.9988
VTT	0.8234	0.9574
FZR	0.8871	0.9910
TEPSYS	0.7670	0.8963

Figure 4-30. Doppler reactivity

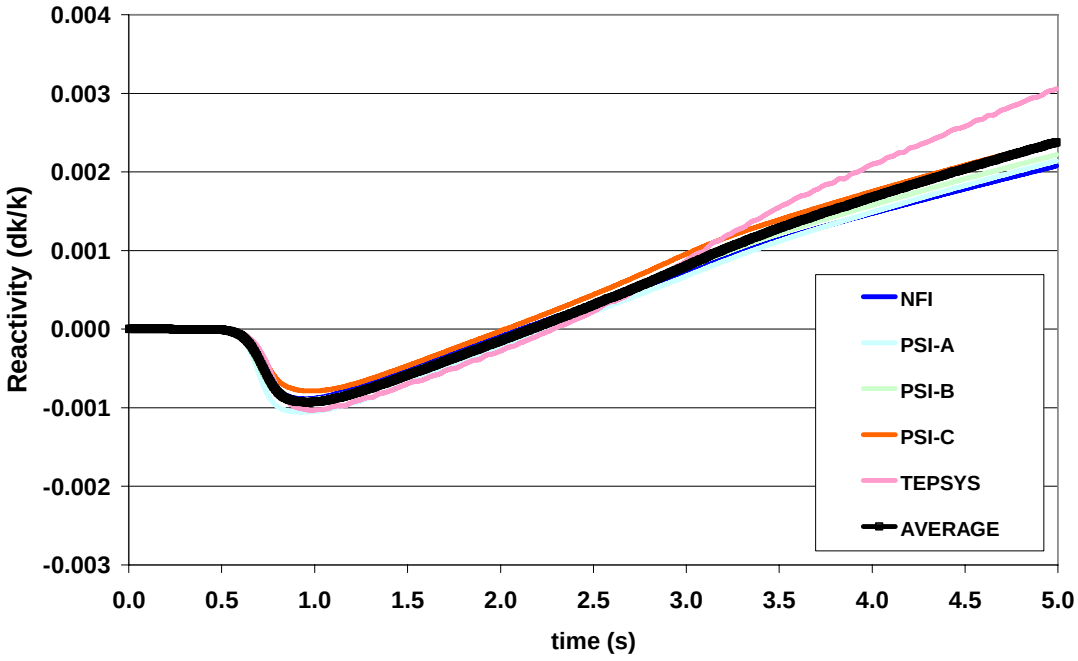

Figure 4-31. Doppler reactivity (zoom)

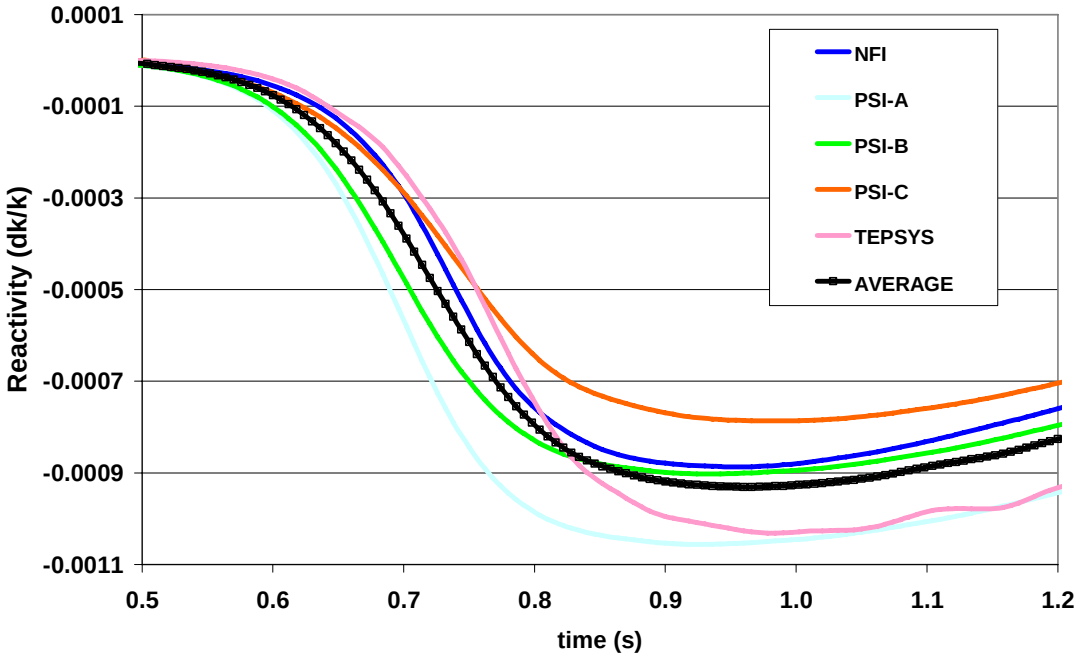

Figure 4-32. Doppler reactivity (mean and deviation)

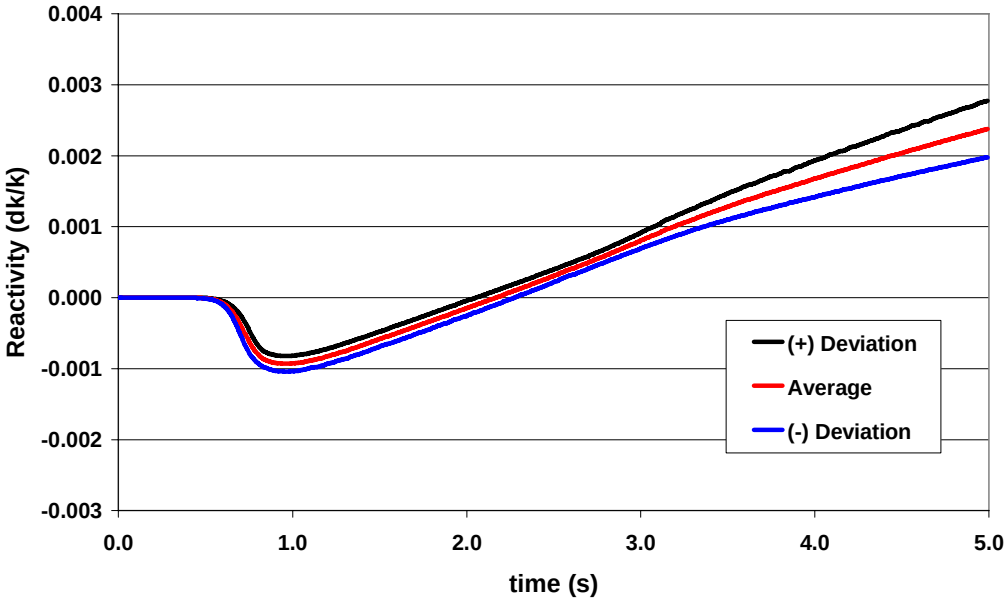

Figure 4-33. Doppler reactivity (mean and deviation – zoom)

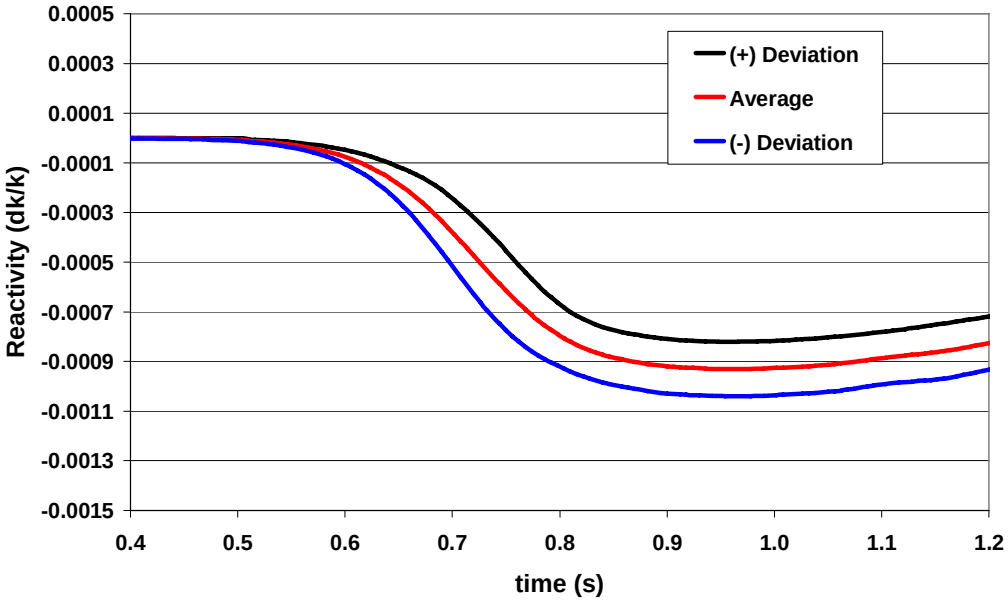

Table 4-9. Doppler reactivity, figure of merit

	D'Auria FFT	Mean error (ME)
NFI	0.8636	0.9827
PSI-A	0.8432	0.9628
PSI-B	0.8893	0.9901
PSI-C	0.8561	0.9727
TEPSYS	0.7693	0.9633

Figure 4-34. Void reactivity

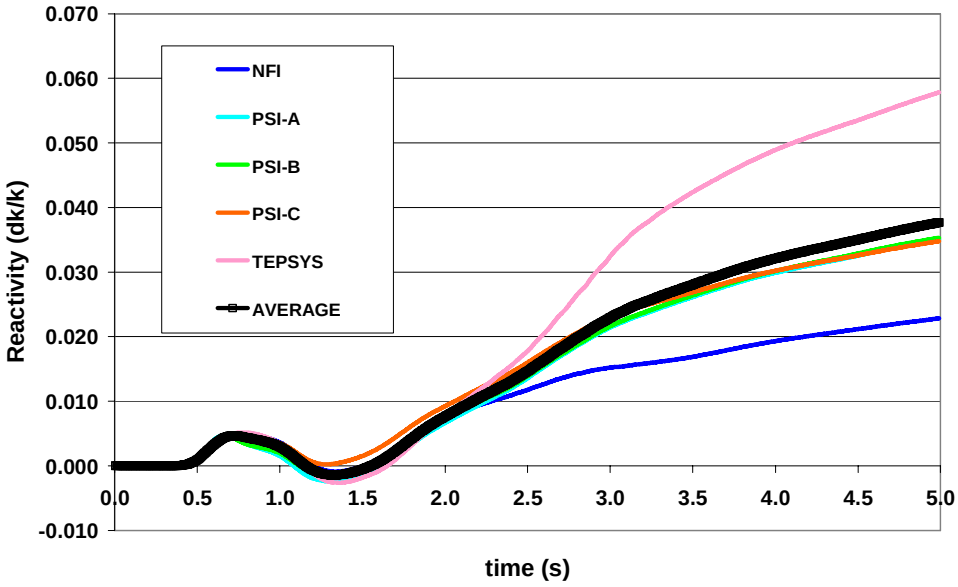

Figure 4-35. Void reactivity (zoom)

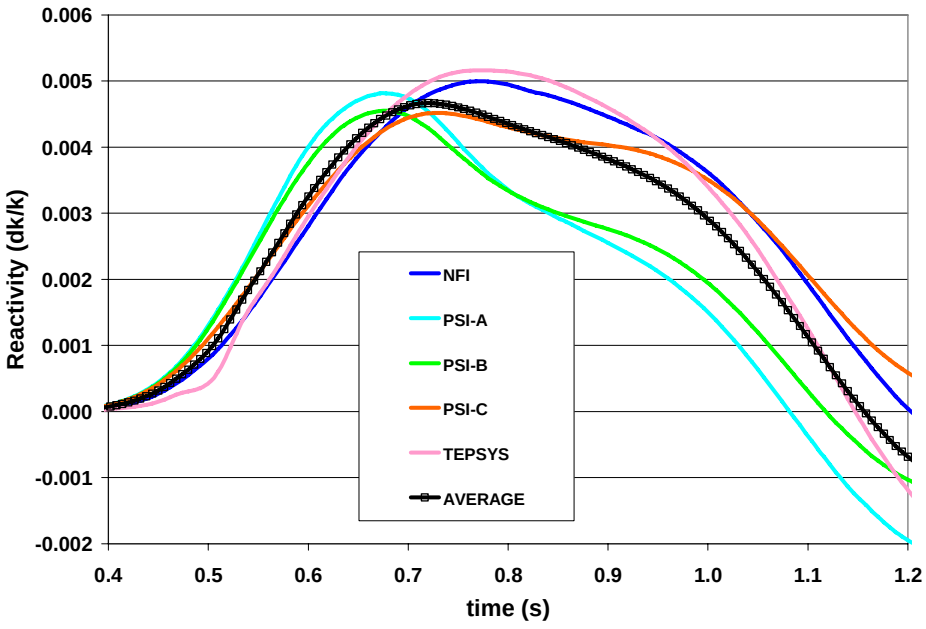

Figure 4-36. Void reactivity (mean and deviation)

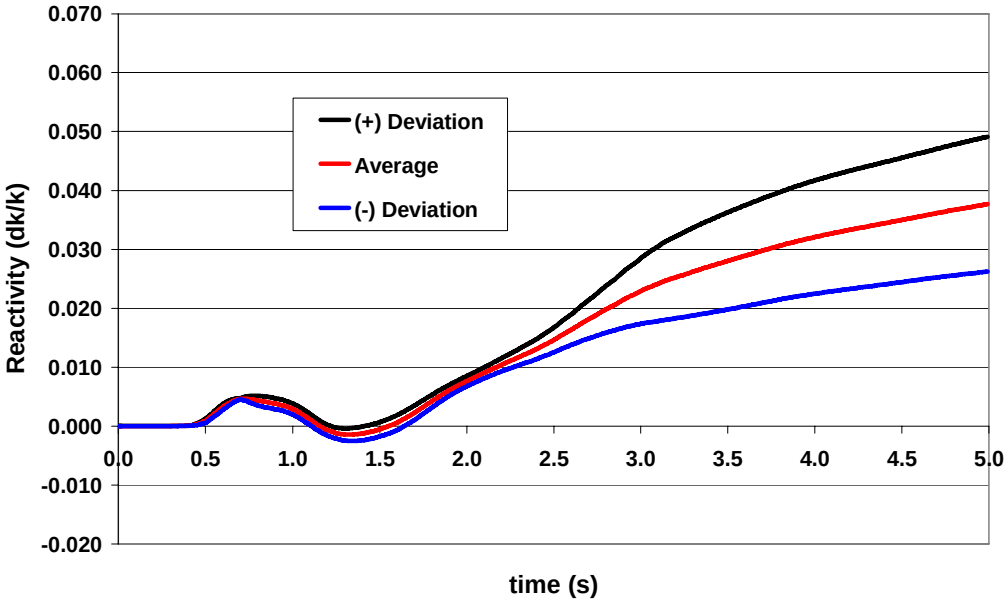

Figure 4-37. Void reactivity (mean and deviation – zoom)

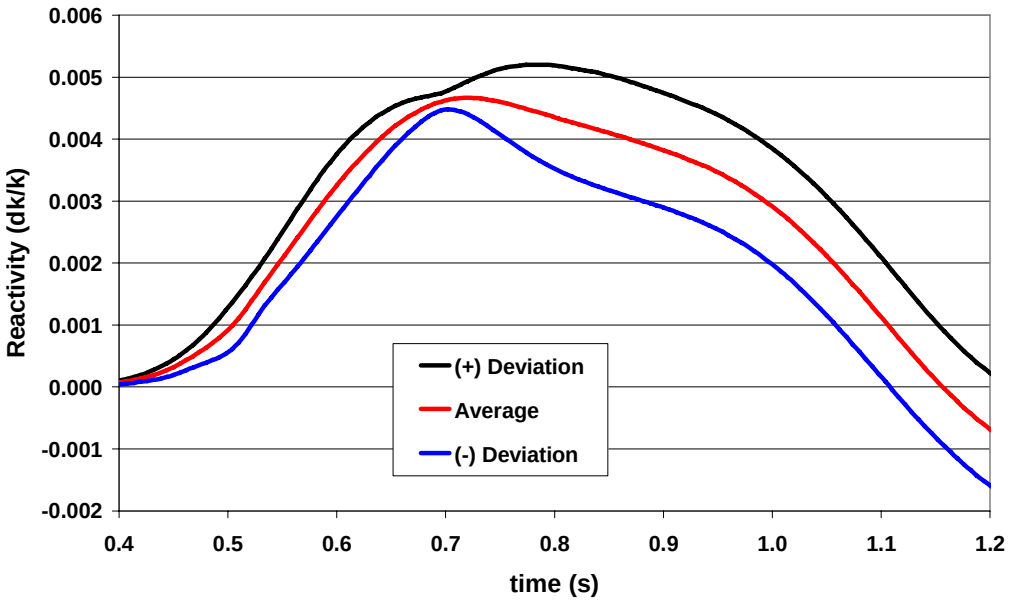

Table 4-10. Void reactivity, figure of merit

	D'Auria FFT	Mean error (ME)
NFI	0.7132	0.8787
PSI-A	0.8640	0.9703
PSI-B	0.8743	0.9791
PSI-C	0.8973	0.9987
TEPSYS	0.6396	0.8412

4.2.2 Snapshot at the time of maximum power before scram

Participants' results from snapshot at the time of maximum power before scram were analysed in order to investigate coupled neutronics/thermal-hydraulics modelling and the code capabilities of the participants at the conditions where the maximum power is reached and scram is still not activated.

Figure 4-38 presents a graphical comparison of participants' predictions of the time of maximum power before scram with the mean value as reference while Table 4-11 provides the values with the mean and standard deviation. In general results are in good agreement. If the PSI-A and PSI-B results are excluded, all deviations are within 2σ. The rest of the results in this section are presented in two groups – one for the participants that used fission power and the other for the participants that used total power. Small deviations are observed from the mean solution for the core average relative axial power distribution results given in Figures 4-39 and 4-40, while the mean and standard deviations are presented in Figures 4-41 and 4-42. In comparison to the HP results (Figure 4-13), the discrepancies are in average of the same magnitude but in the snapshot case they are more evenly distributed over the whole core height while in the HP case the maximum deviations are observed in the bottom part of the core. Good agreements are observed in the predictions of relative axial profiles for the selected rodded and un-rodded fuel assemblies, as shown in Figures 4-43 through 4-50. One observation from the presented comparisons for axial power distributions is that the results in the total power group agree better than the results fission power group. The major reason for this fact can be deducted in inspecting Table 4-6. It can be seen that all of the participants using total power utilise the bypass model (bypass density correction) while in the fission power group some participants utilise it and some do not. For the total power group results of axial distributions the differences in the decay heat models still do not impact the comparisons since at this snapshot the fission power is the dominating contributor to the total power and the radial fission power distribution in the snapshot is similar to the radial power distribution at the initial HP conditions. The mean solution for the radial power distribution and the standard deviation are given in Figures 4-51 and 4-52. If compared to the initial HP conditions the snapshot comparison of radial power distribution exhibits similar deviations since what really changed in the snapshot is the total power level and axial distribution but not the radial one since the scram is still not activated.

The complete list of the mean solutions and standard deviations can be found in Appendix C and the deviations of each participant's solutions from the mean value can be found in Appendix D. Both appendices are provided only in the electronic copy of this report distributed via a CD-ROM.

Figure 4-38. Time of maximum power before scram

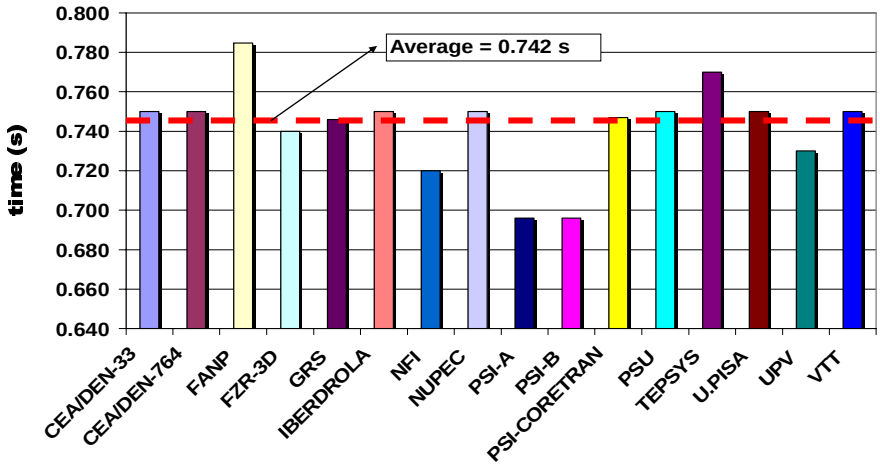

Table 4-11. Time of maximum power before scram

Participant	Time of max. power before scram (s)	Deviation (e_i)
CEA-33	0.750	0.008
CEA-764	0.750	0.008
FANP	0.785	0.042
FZR	0.740	-0.002
GRS	0.746	0.004
IBER	0.750	0.008
NFI	0.720	-0.022
NUPEC	0.750	0.008
PSI-A	0.696	-0.046
PSI-B	0.696	-0.046
PSI-C	0.747	0.005
PSU	0.750	0.008
TEPSYS	0.770	0.028
UPI	0.750	0.008
UPV	0.730	-0.012
VTT	0.750	0.008
Average =	0.742	
Standard deviation (σ) =	0.023	

Figure 4-39. Core axial power profile at maximum power before scram (fission power used)

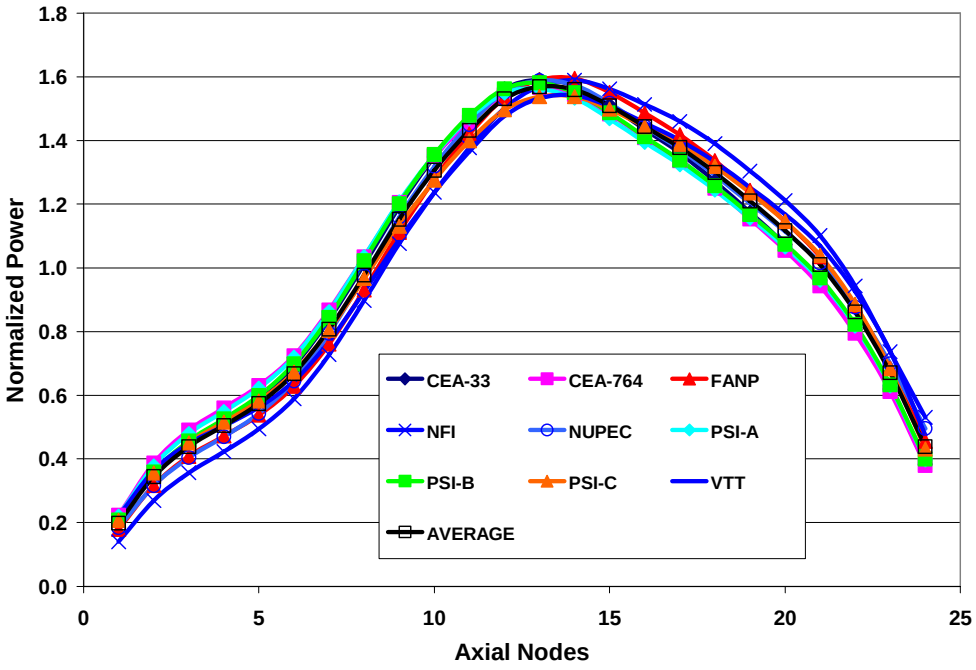

Figure 4-40. Core axial power profile at maximum power before scram (total power used)

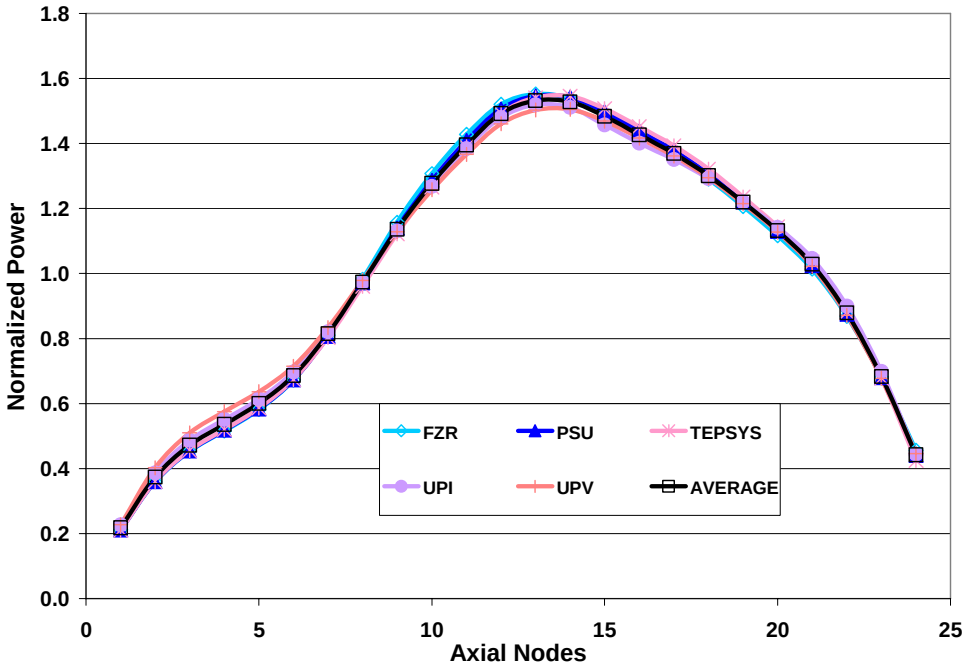

Figure 4-41. Core axial power profile at maximum power before scram (fission power used – mean and deviation)

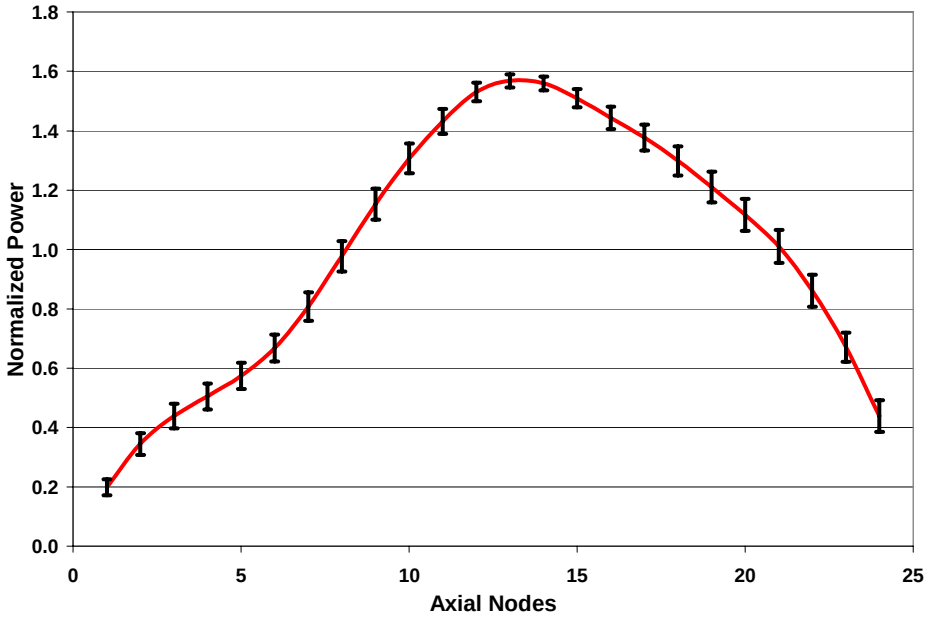

Figure 4-42. Core axial power profile at maximum power before scram (total power used – mean and deviation)

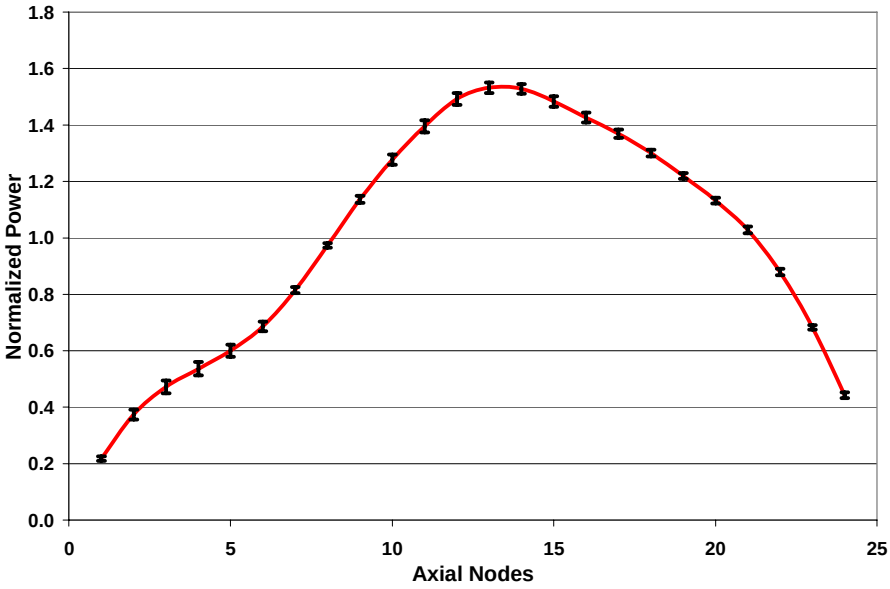

Figure 4-43. Relative power of FA 75 at maximum power before scram (fission)

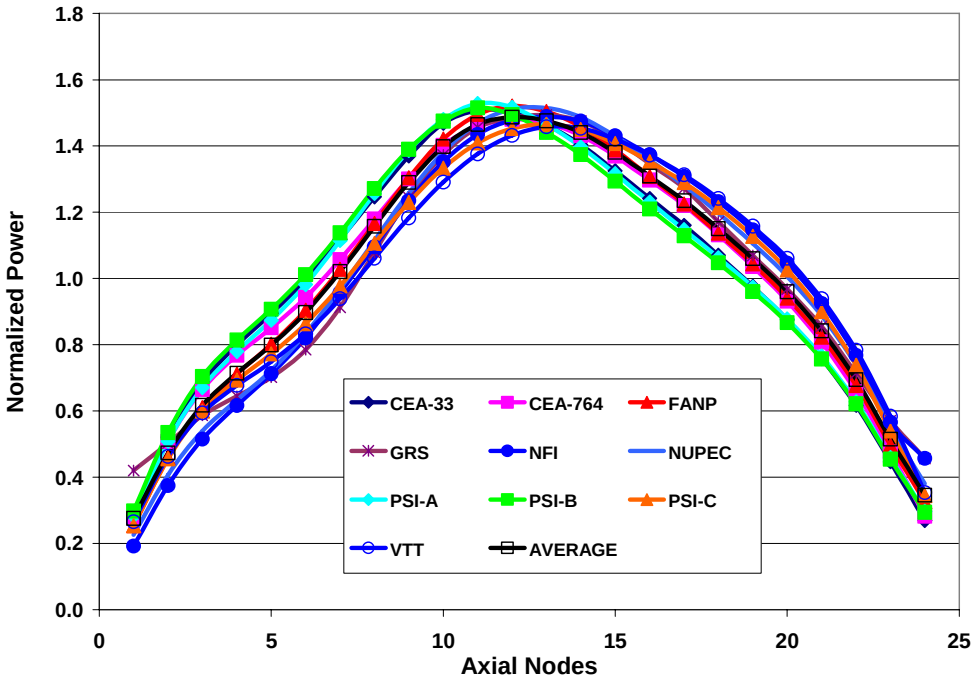

Figure 4-44. Relative power of FA 75 at maximum power before scram (total)

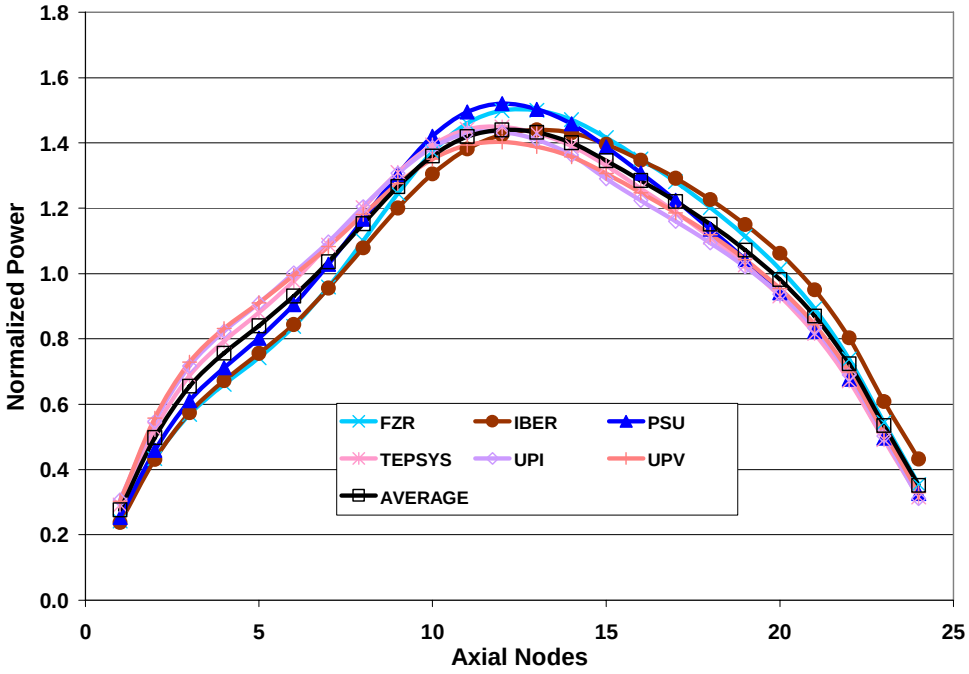

Figure 4-45. Relative power of FA 75 at maximum power before scram (mean and deviation – fission power used)

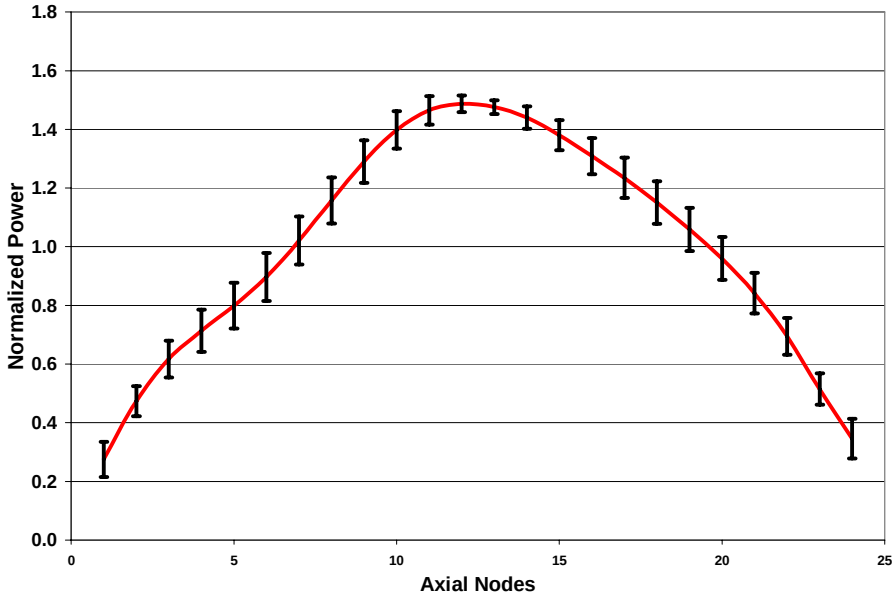

Figure 4-46. Relative power of FA 75 at maximum power before scram (mean and deviation – total power used)

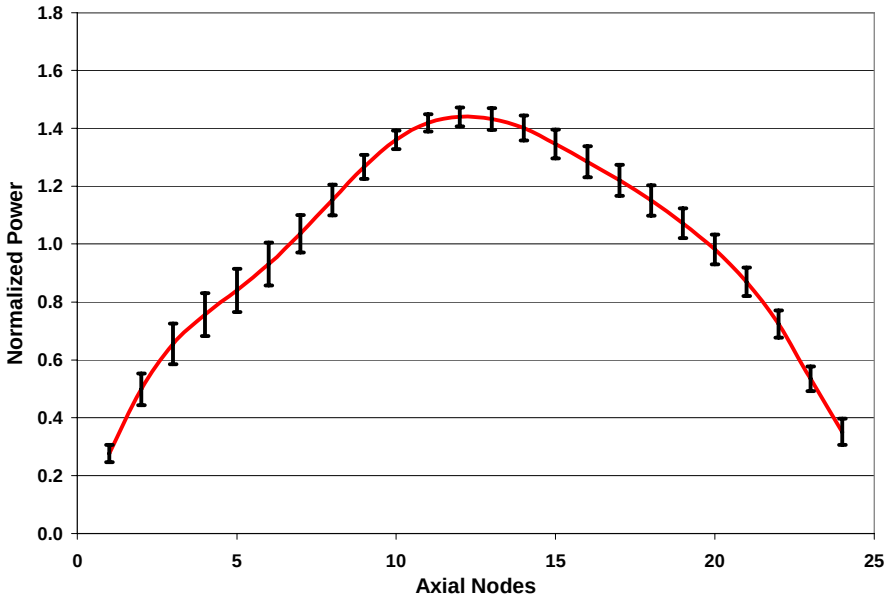

Figure 4-47. Relative power of FA 367 at maximum power before scram (fission)

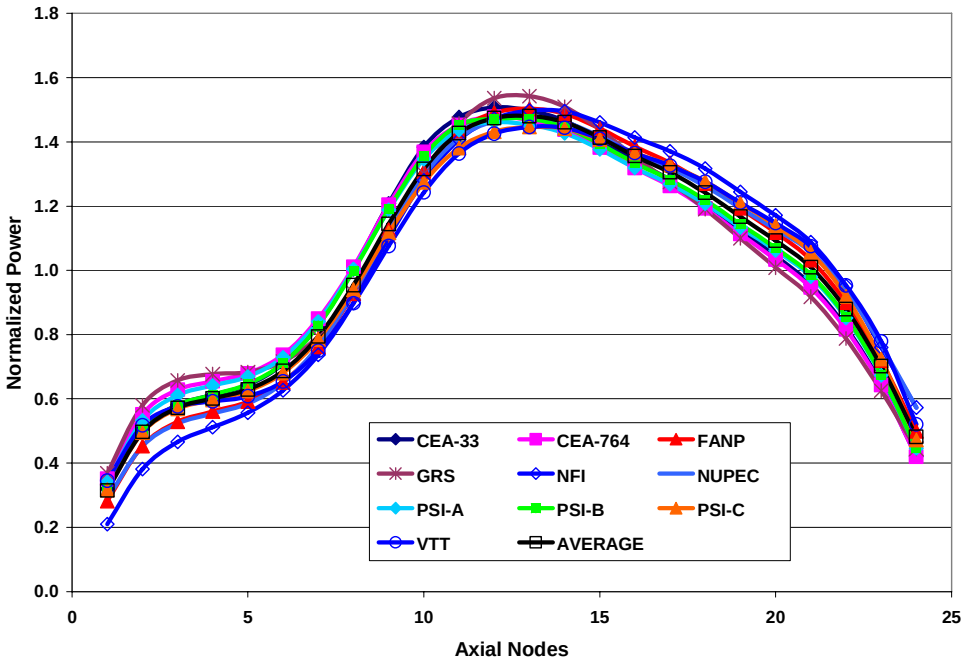

Figure 4-48. Relative power of FA 367 at maximum power before scram (total)

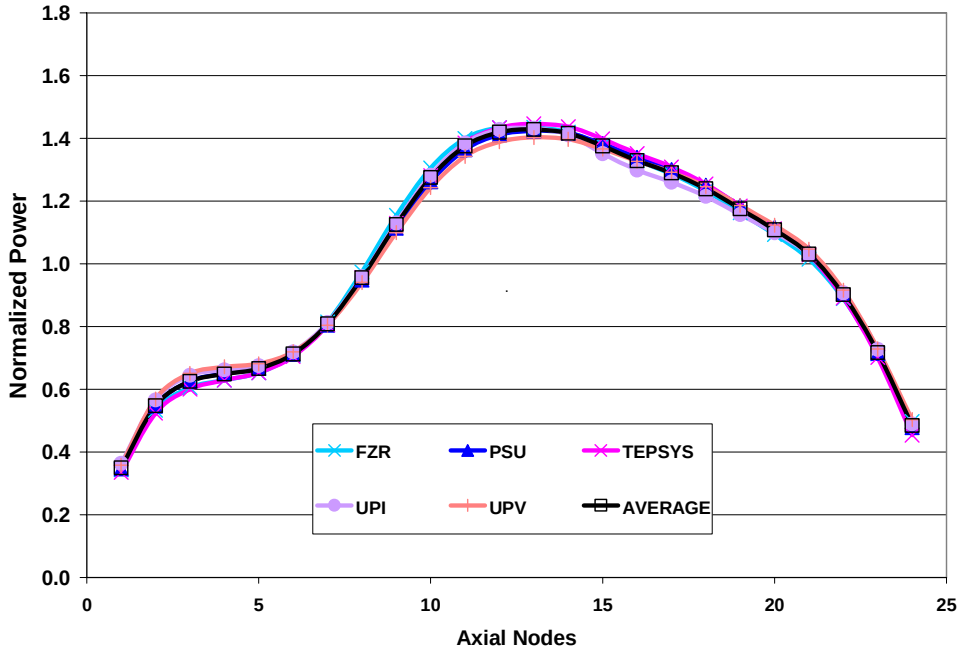

Figure 4-49. Relative power of FA 367 at maximum power before scram (mean and deviation – fission power used)

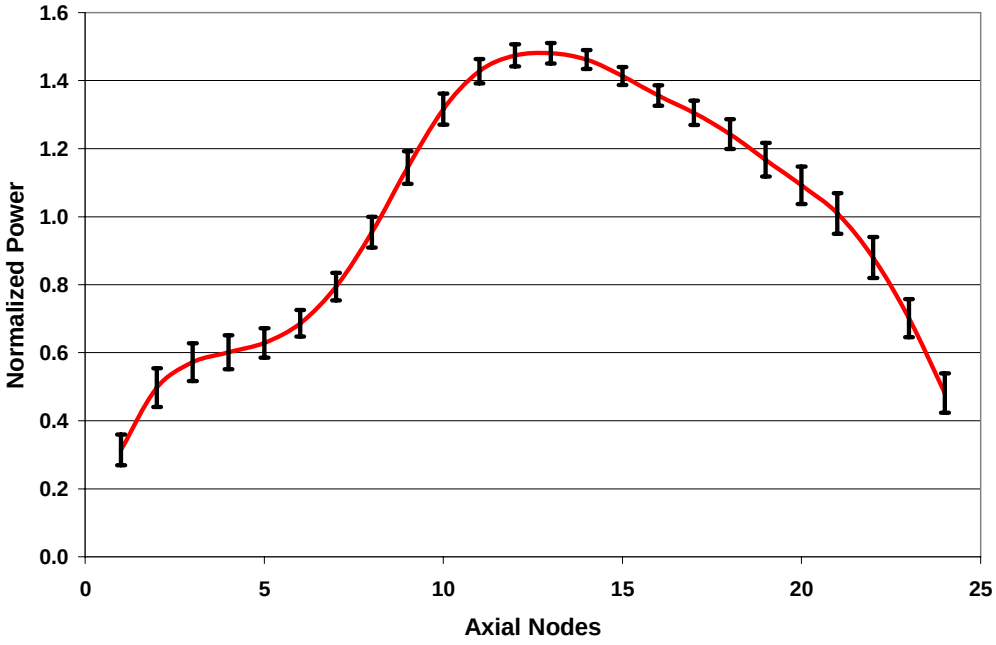

Figure 4-50. Relative power of FA 367 at maximum power before scram (mean and deviation – total power used)

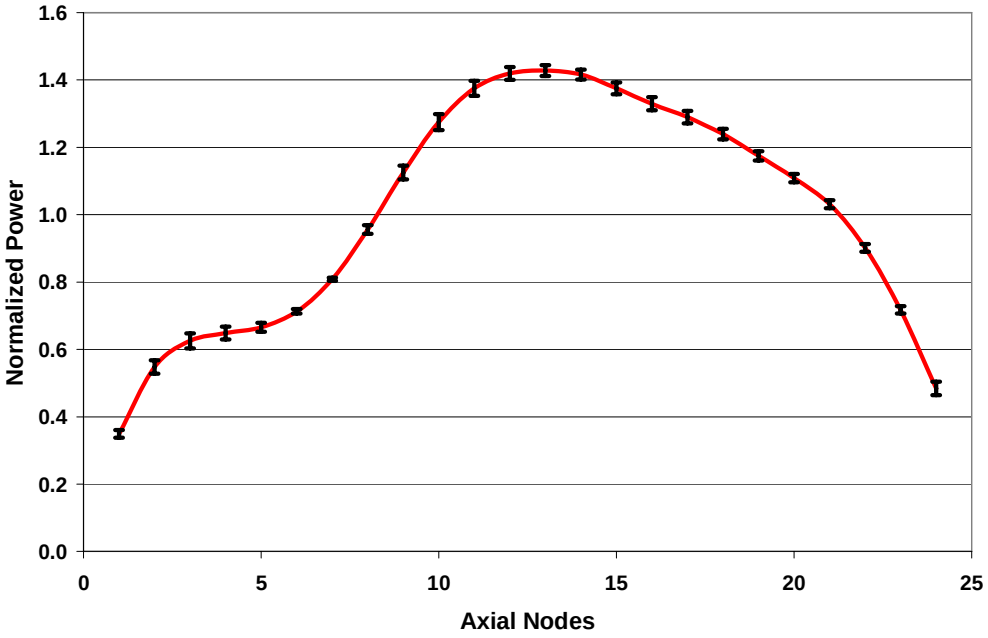

Figure 4-51. Mean radial power distribution at maximum power before scram

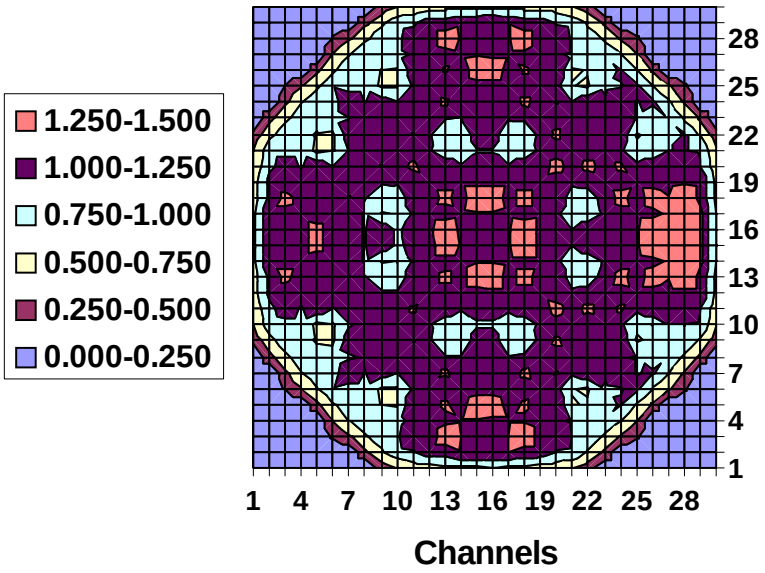

Figure 4-52. Standard deviation of radial power distribution at maximum power before scram

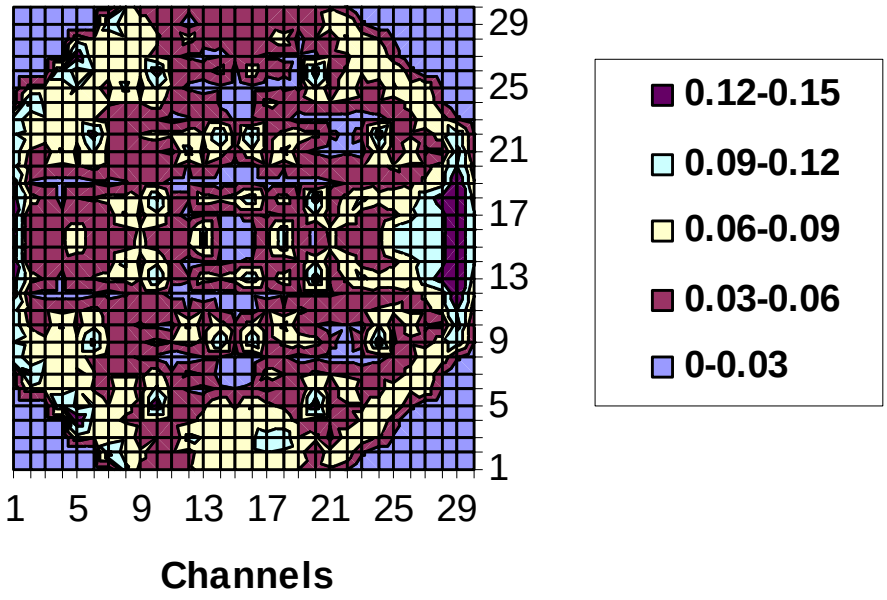

4.2.3 Snapshot at the end of the transient (at 5 s)

The conditions of the snapshot at the 5 s into the transient (the end of the simulated transient) are different from the conditions of the snapshot at the time of maximum power before scram. The bypass model still will play a role since the bypass density correction in the cross-section feedback modelling is to account for the deviations of bypass density from the saturated value used in the cross-section homogenisation (please note that the cross-sections are generated by homogenising the bypass region at saturated conditions associated with the lattice at actual conditions). The consistent utilisation of the ADF and xenon models is also relevant to the agreement (or disagreement) of participants' predictions for this snapshot. Since the control rods were tripped during the scram some of the differences are coming from the neutronics methods and control rod models. The decay modelling in total power group results for axial power distributions is very important because for this snapshot the decay heat is dominating contributor to the total power and it is very important how the spatial distribution of the decay heat is done – according to the fission power distribution at the initial HP conditions or according to the fission power distribution at this snapshot.

The core average relative axial power distribution results are compared and analysed in Figures 4-53 through 4-56. The relative power distribution results for selected un-rodded and rodded fuel assemblies is shown in Figures 4-57 through 4-64. The mean radial power distribution and standard deviation distribution are given in Figures 4-65 and 4-66. In summary, if compared to the comparisons of power distribution results for the snapshot at the time of maximum time before scram case, the discrepancies in the participants' results are higher for the snapshot at the end of transient. It should also be noted that there is a significant deviation in lower part of axial power profile for NUPEC results in Figure 4-53.

The complete list of the mean solutions and standard deviations can be found in Appendix C and the deviations of each participant's solutions from the mean value can be found in Appendix D. Both appendices are provided only in the electronic copy of this report distributed via CD-ROM.

Figure 4-53. Core axial power profile at the end of transient (fission)

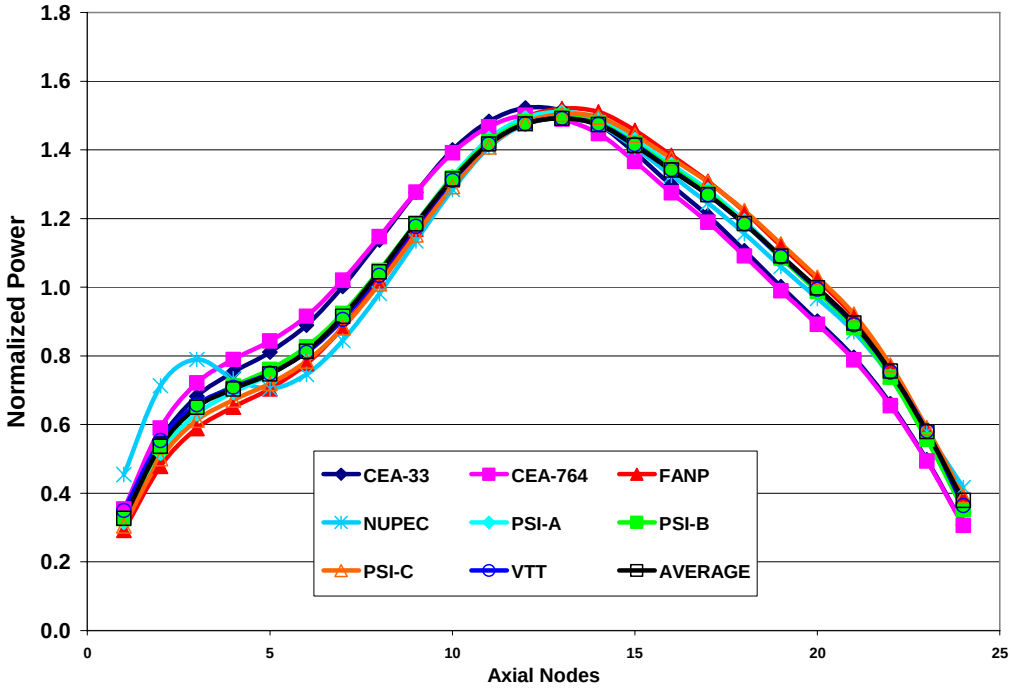

Figure 4-54. Core axial power profile at the end of transient (total)

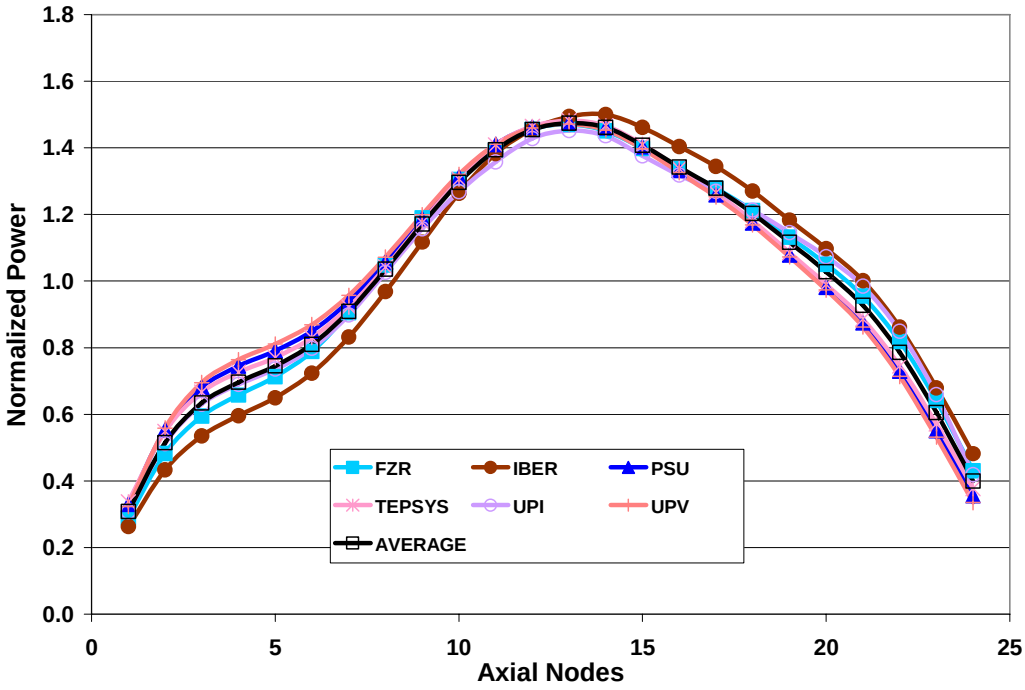

Figure 4-55. Core axial power profile at the end of transient (mean and deviation – fission power used)

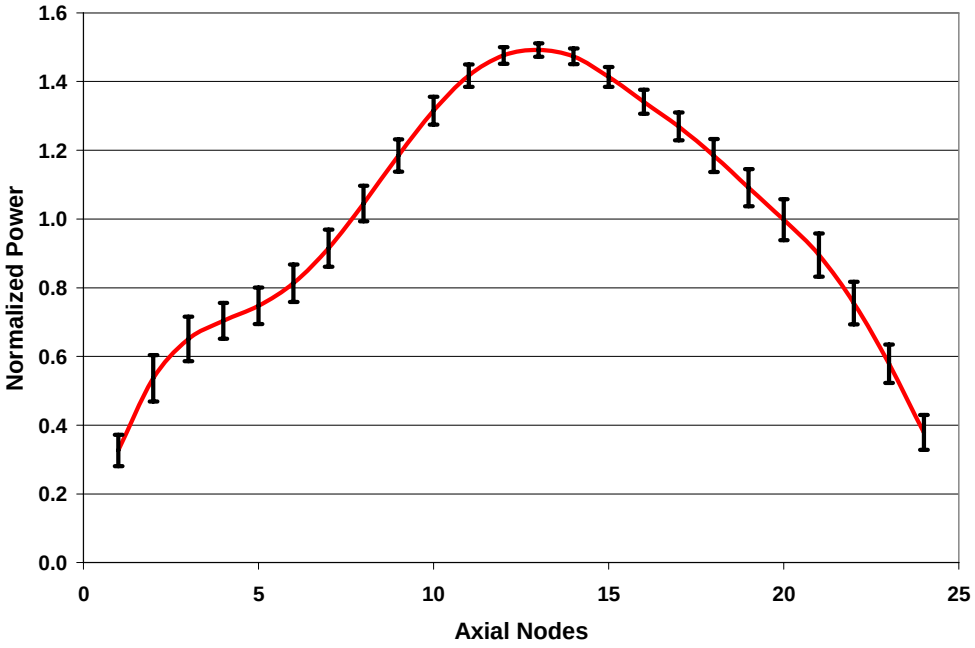

Figure 4-56. Core axial power profile at the end of transient (mean and deviation – total power used)

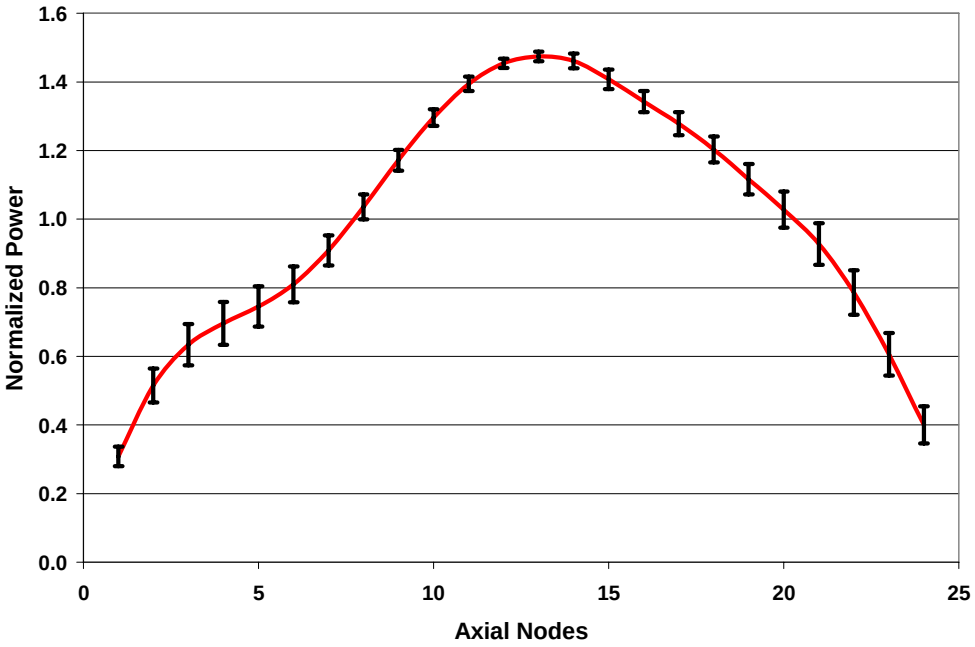

Figure 4-57. Relative power of FA 75 at end of transient (fission)

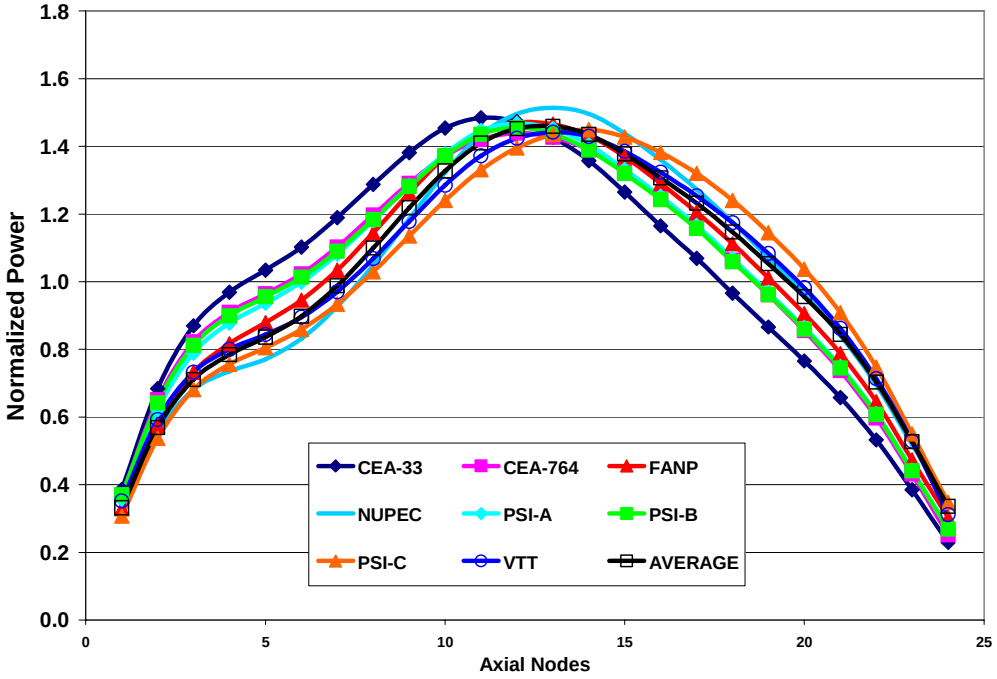

Figure 4-58. Relative power of FA 75 at end of transient (total)

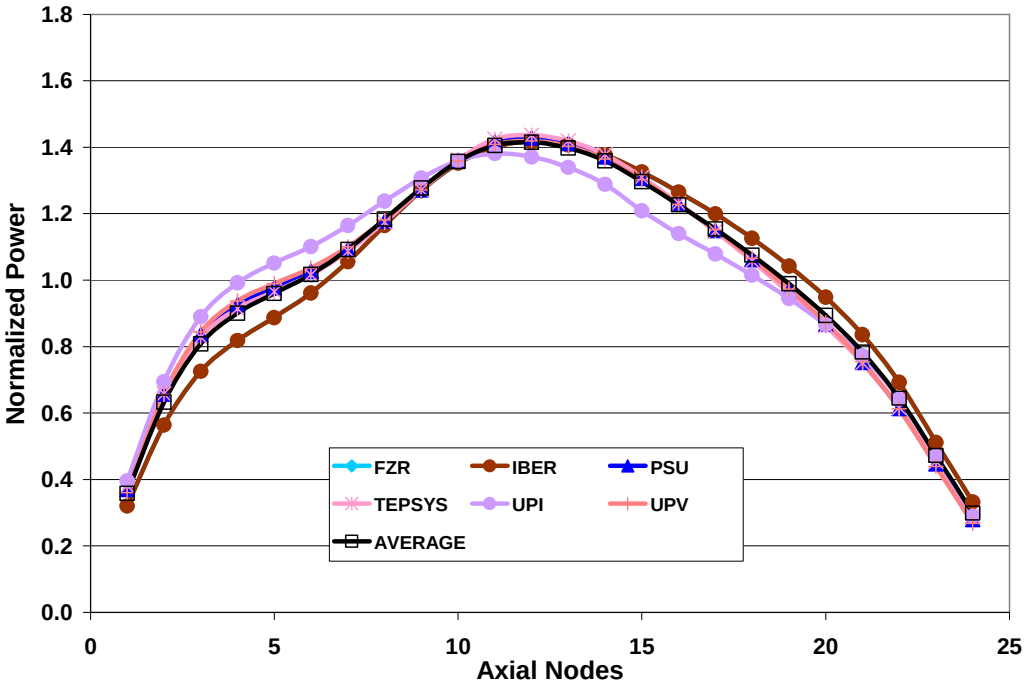

Figure 4-59. Relative power of FA 75 at end of transient (mean and deviation – fission power used)

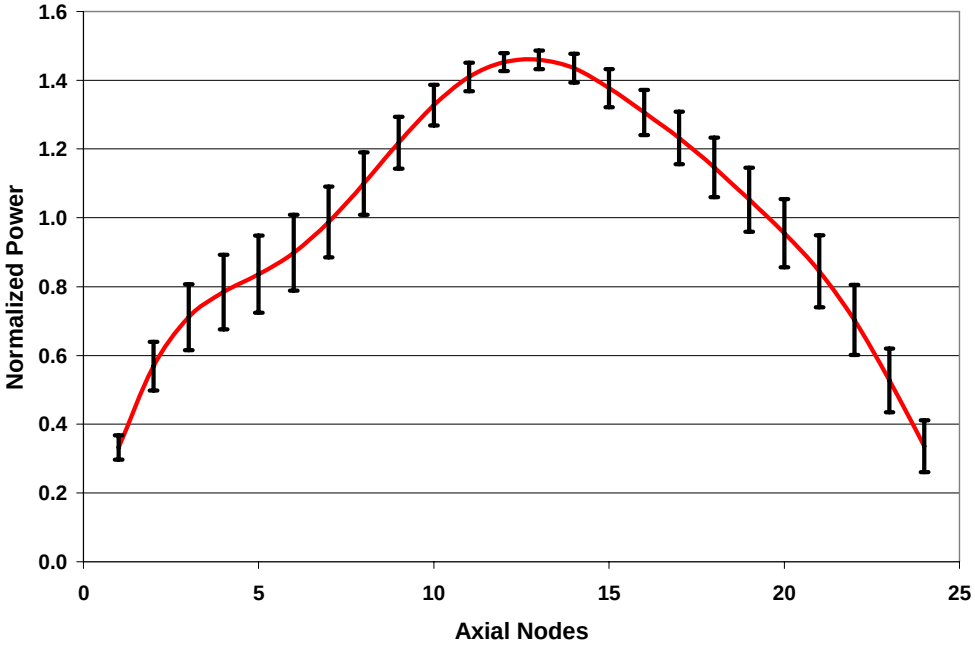

Figure 4-60. Relative power of FA 75 at end of transient (mean and deviation – total power used)

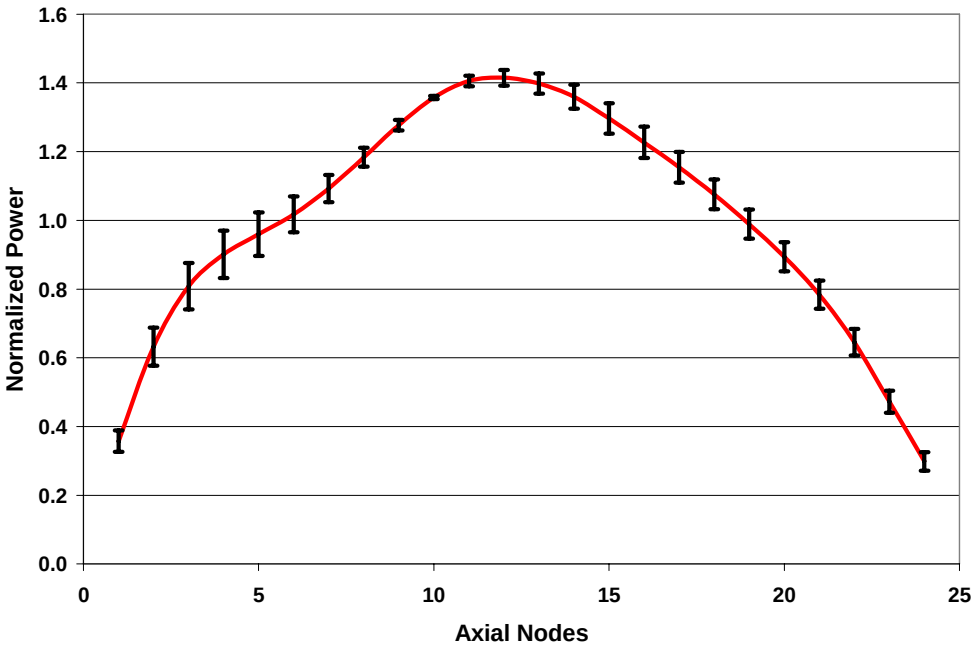

Figure 4-61. Relative power of FA 367 at end of transient (fission)

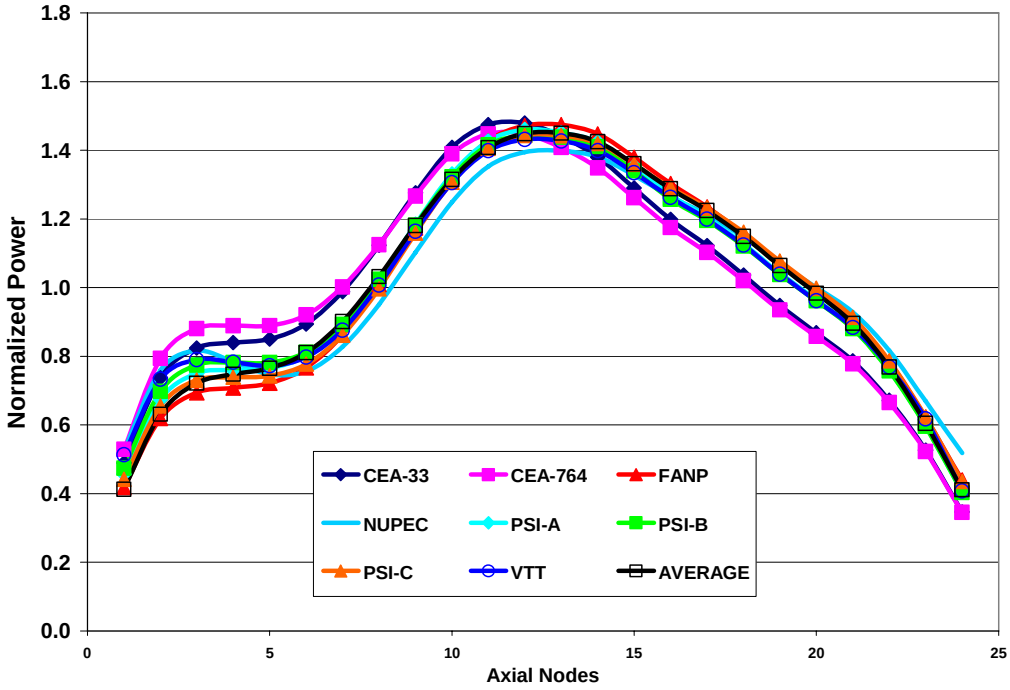

Figure 4-62. Relative power of FA 367 at end of transient (total)

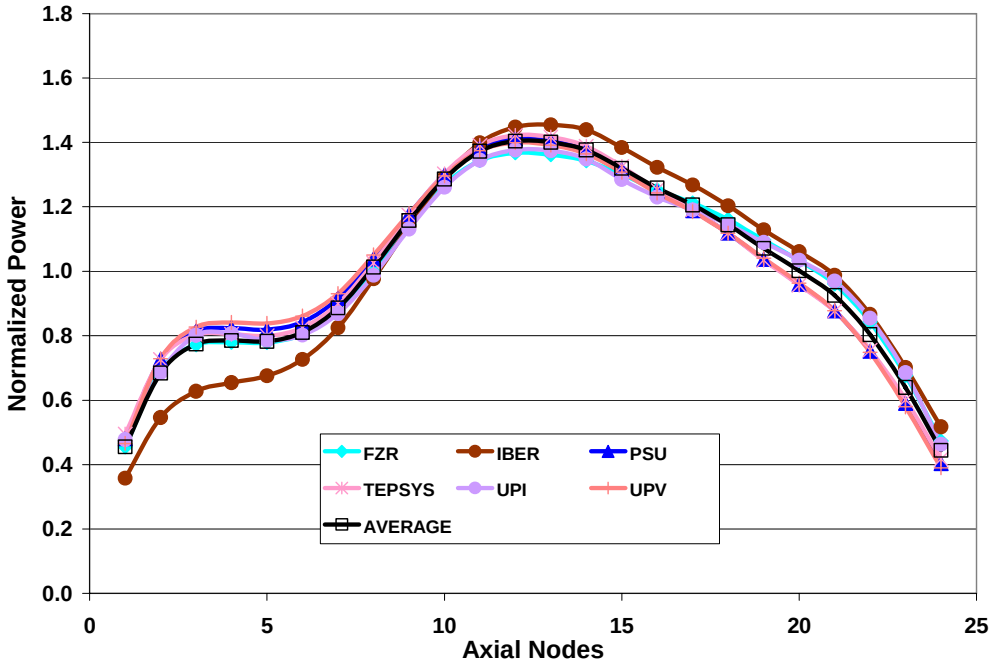

Figure 4-63. Relative power of FA 367 at end of transient (mean and deviation – fission power used)

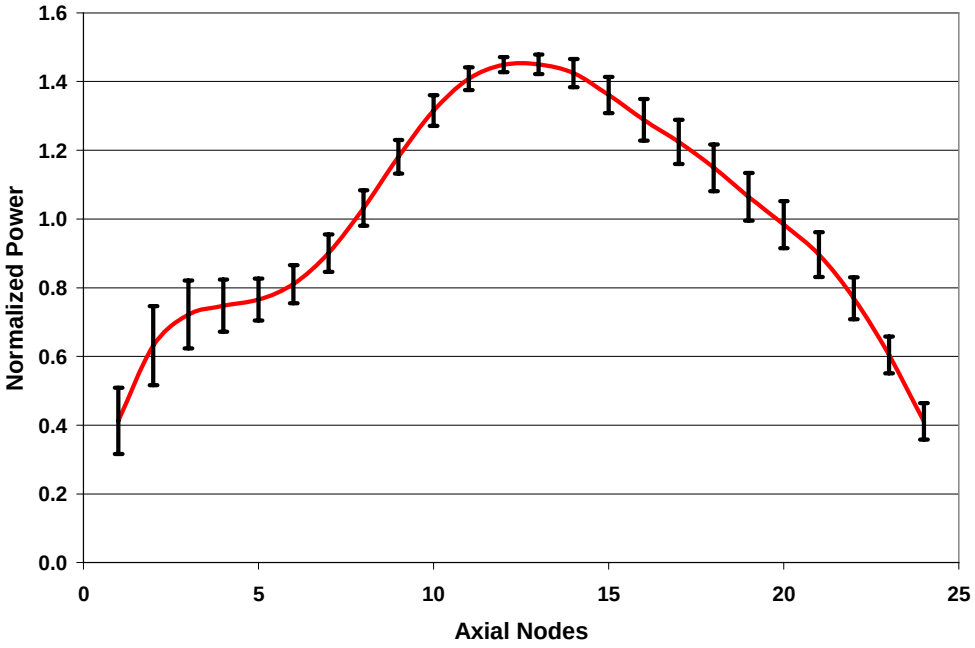

Figure 4-64. Relative power of FA 367 at end of transient (mean and deviation – total power used)

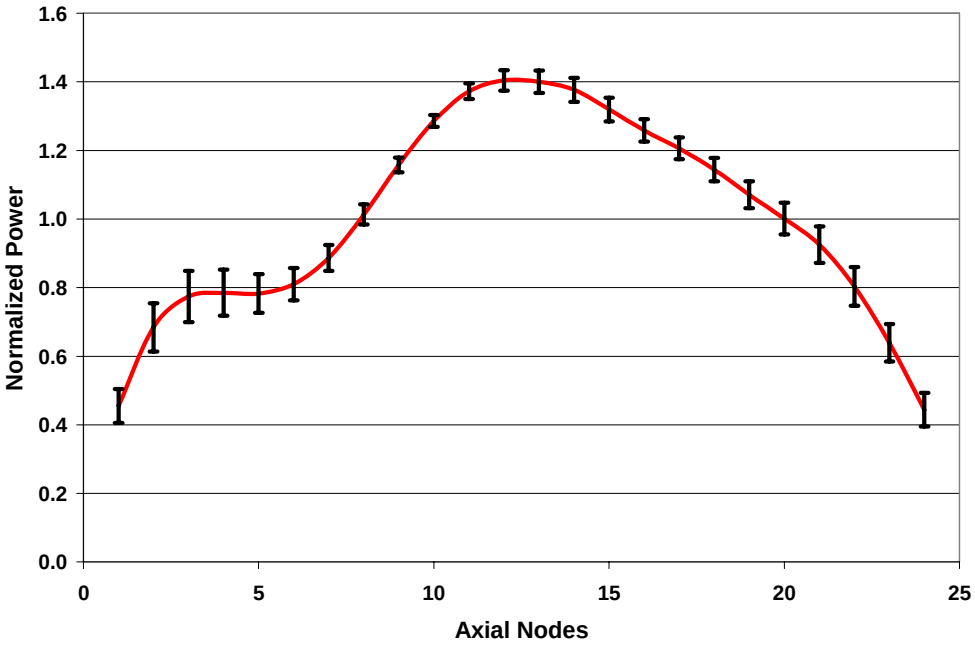

Figure 4-65. Mean radial power distribution at end of transient

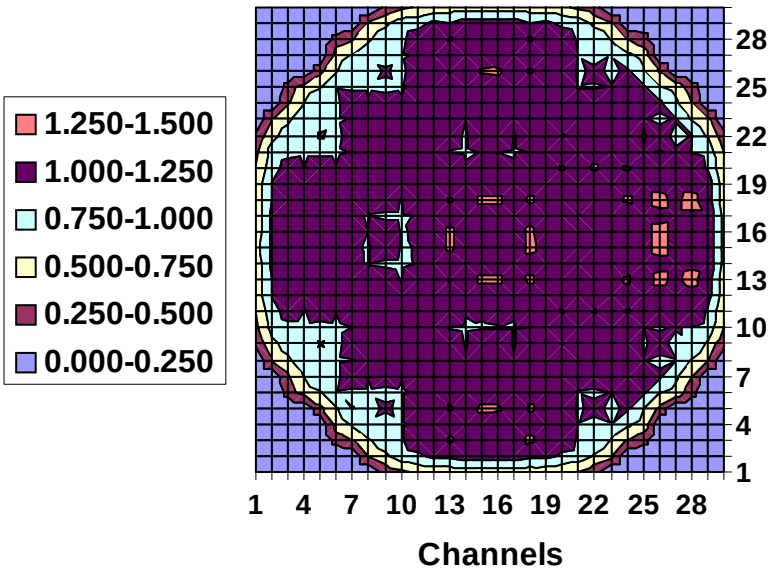

Figure 4-66. Standard deviation of radial power distribution at end of transient

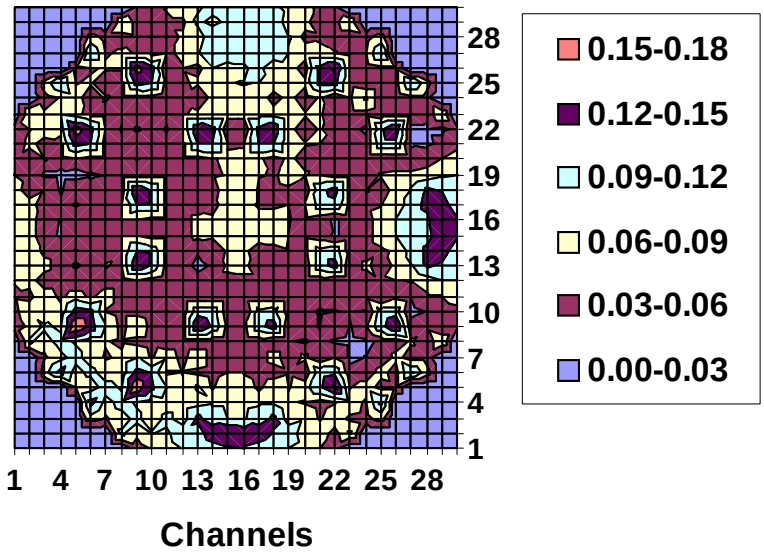

Chapter 5

CONCLUSIONS

The developed multi-level methodology is employed to perform a validation of coupled codes for BWR transient analysis. For this purpose, the application of three exercises was performed in the BWR TT benchmark. These exercises include the evaluation of different steady states, and simulation of different transient scenarios. In this volume, Exercise 2 of the OECD/NRC BWR TT benchmark was discussed in detail in order to meet the objectives of the validation of best-estimate coupled codes.

The second exercise consists of performing coupled-core boundary conditions calculations, the purpose being to test and initiate the participants' core models. Thermal-hydraulic boundary conditions are provided to the participants from the benchmark team. The thermal-hydraulic core boundary conditions provided are the core inlet pressure, core exit pressure, core inlet temperature and core inlet flow. In summary the second exercise is to perform a coupled 3-D kinetics/T-H calculation for the reactor core using the PSU-provided boundary conditions at core inlet and exit. Three-dimensional two-group macroscopic cross-section libraries are provided to the participants. The core inlet flow is provided in two formats: total core flow as a function of time and radially distributed flow as a function of time for 33 channels. In addition, the benchmark team provided the participants with normalised power vs. flow correlations for the different assembly types based on the detailed modelling in which each assembly represented by a thermal-hydraulic channel for the initial steady-state conditions. The studies performed by the benchmark team indicated that these correlations also apply reasonably well during the transient, which provided an opportunity for the participants to develop their own core coupled spatial mesh overlays. An additional steady state was defined in the framework of the second exercise – hot zero power (HZP) state with fixed thermal-hydraulic feedback. This allows for "clean" initialisation of the core neutronics models and cross-section modelling algorithms.

This benchmark problem has been well-accepted internationally, with 18 participants representing 9 countries. CEA submitted two sets of results using coarse core T-H nodalisation with 33 channels and fine core T-H nodalisation with 764 core channels – one T-H channel per neutronics assembly. PSI submitted two sets of results with RETRAN-3D using different sets of core boundary conditions and one set of results using CORETRAN. The results submitted by the participants are used to make code-to-code comparisons and a subsequent statistical analysis. The results encompass several types of data for both thermal-hydraulic and neutronics parameters at the initial steady-state conditions and throughout the TT transient, including integral parameters, 1-D axial distributions, 2-D radial distributions and time histories.

Detailed assessments of the differences between the calculated results submitted by the participants for this exercise were presented in Chapter 4 of this volume. Overall, the participants' results for integral parameters, core-averaged axial distributions, and core-averaged time histories are in good agreement, considering some of the shortcomings in participants' current models, uncertainties of some system parameters, and difficulties in interpreting some of the measured responses.

During the comparative analysis of the participants' results for the second exercise the following sources of modelling uncertainties were identified: core pressure drop in terms of local losses and friction models, core bypass modelling, void feedback model in terms of sub-cooled boiling and

vapour slip and time step size which is a user optional parameter. The fuel heat transfer parameters as the UO_2 conductivity and gap conductivity and direct heating (2% to in-channel flow and 1.7% to bypass flow) were specified. The scram initiation time and the speed of the rod insertion were also specified. The scram initiation time was specified since one of the objectives of the benchmark is to test coupled codes' capabilities to predict for TT2 that the thermal-hydraulic feedback alone limits the power peak and initiates the power reduction. Other important modelling issues were identified such as the impact of using assembly discontinuity factors, which are also provided to the participants in a similar table format as for the two group cross-sections; xenon correction to account for the actual xenon concentration distribution at the initial steady-state conditions of the turbine trip test 2; number of thermal-hydraulic channels and spatial mapping schemes with the neutronics core model; decay heat modelling; and bypass density correction in the cross-section feedback modelling to account for the deviations of bypass density from the saturated value used in the cross-section homogenisation since the cross-sections are generated by homogenising the bypass region associated with the lattice. Different code formulations/correlations for Doppler temperature and moderator density, affected both core-averaged power and reactivity time histories and local distributions throughout the transient since these two parameters are the major feedback parameters for the cross-section modelling impacting in this way the neutronics predictions.

While the purpose of the first exercise is to initialise and test the primary and secondary system model responses, the purpose of the second exercise is to initialise and test the coupled-core thermal-hydraulic/3-D neutronics response. Both exercises prepare the foundation of conducting Exercise 3 in a consistent and systematic way. Exercise 3 is defined as a best-estimate coupled-core plant transient modelling.

The PB TT2 test has previously been analysed elsewhere with different codes and models [6,7]. These analyses involved not only point kinetics and 1-D kinetics system simulations, but also 3-D kinetics/core thermal-hydraulics boundary conditions calculations. Each of the organisations performing these separate analyses generated their own point kinetics parameters, 1-D cross-sections and 3-D cross-section libraries. It is thus not possible to directly compare the results of different organisations, especially for the parameters where the measured data is not available. In most of the 3-D core boundary conditions analyses the cross-section functionalisation for instantaneous dependencies was done either by using polynomial fitting procedure or the procedure using multi-level tables with base and partial cross-sections. In both cases the instantaneous cross-term effects (which are important for the transient analysis) are not modelled completely, which led to different degree of underestimation of the void feedback (void coefficient) depending on the procedure used.

The current OECD/NRC BWR TT benchmark is designed to provide a validation basis for the new generation best-estimate codes – coupled 3-D kinetics system thermal-hydraulic codes. Based on previous experience, three benchmark exercises were defined in order to develop and verify, in a consistent way, the thermal-hydraulic system model, the coupled-core model, and the coupled-core/ system modelling. The three exercises defined also helped to identify the key parameters for modelling a turbine trip transient. This in turn allowed the evaluation of these key parameters, through the performance of sensitivity studies, which allowed the benchmark team to assist the participants in the most efficient way. The participants use the cross-section library generated by the benchmark team, which removes the uncertainties introduced with using different cross-section generation and modelling procedures. The defined benchmark cross-section modelling approach is a direct interpolation in multi-dimensional tables with complete representation of the instantaneous cross-section cross-term dependencies. Developing a more in-depth knowledge of the coupled computer code systems is important because 3-D kinetic/thermal-hydraulic codes will play a critical role in the future of nuclear analysis. It is anticipated that the results of this benchmark problem will assist in the understanding of the behaviour of the next generation of coupled computer codes.

REFERENCES

[1] Ivanov, K., T. Beam, A. Baratta, A. Irani, N. Trikouros, *PWR MSLB Benchmark – Final Specifications*, NEA/NSC/DOC(97)15, Nuclear Energy Agency, October 1997.

[2] Solis, J., K. Ivanov, B. Sarikaya, A. Olson, K. Hunt, *Boiling Water Reactor Turbine Trip (TT) Benchmark – Volume I: Final Specifications*, NEA/NSC/DOC(2001)1, Nuclear Energy Agency.

[3] Akdeniz, B., K. Ivanov, A. Olson, *BWR TT Benchmark – Volume II: Summary Results of Exercise*, NEA/NSC/DOC(2004)21, Nuclear Energy Agency.

[4] Larsen, N., *Core Design and Operating Data for Cycles 1 and 2 of Peach Bottom 2*, EPRI NP-563, June 1978.

[5] Carmichael, L., R. Niemi, *Transient and Stability Tests at Peach Bottom Atomic Power Station Unit 2 at End of Cycle 2*, EPRI NP-564, June 1978.

[6] Hornyik, K., J. Naser, *RETRAN Analysis of the Turbine Trip Tests at Peach Bottom Atomic Power Station Unit 2 at the End of Cycle 2*, EPRI NP-1076-SR Special Report, April 1979.

[7] Moberg, L., J. Rasmussen, T. Sauar and O. Oye, *RAMONA Analysis of the Peach Bottom-2 Turbine Trip Transients*, EPRI NP-1869, June 1981.

[8] Olson, A.M., *Methods for Performing BWR System Transient Analysis*, Topical Report PECo-FMS-0004-A, Philadelphia Electric Company (1988).

[9] Borkowski, J., N. Wade, *TRAC-BF1/MOD1 – Model Description*, NUREG/CR-4356 EGG-2626, Vol. 1, Idaho National Engineering Laboratory, EG&G Idaho, Inc., August 1992.

[10] Steinke, R., V. Martinez, N. Schnurr, J. Spore, J. Valdez, *TRAC-M/FORTRAN 90 (Version 3.0) User's Manual*, NUREG/CR-6722, pp. 2-1 to 2-2, May 2001.

[11] Ivanov, K., M. Vela Garcia, J. Solis, Andy M. Olson, *OECD/NRC BWR TT Benchmark: A Core Boundary Condition Model Approach*, TANSAO 85, 275-277 (2001).

[12] Kuntz, R., G. Kasmala, J. Mahaffy, *Automated Code Assessment Program: Technique Selection and Mathematical Prescription*, Letter Report 3, Applied Research Laboratory, The Pennsylvania State University, April 1998.

[13] Ambrosini, W., R. Bovalini, F. D'Auria, "Evaluation of Accuracy of Thermal-hydraulics Code Calculations", *Energia Nucleare*, Vol. 7, No. 2 (1990).

[14] *Cubic Spline for Excel Workbook*, SRS1 Software, February 2003, available on-line as follows: http://www.srs1software.com.

[15] "OECD/NRC BWR Turbine Trip Benchmark Special Issue", *Nuclear Science and Engineering*, Vol. 148, No. 2, October 2004.

Appendix A

DESCRIPTION OF THE COMPUTER CODES USED FOR ANALYSIS IN EXERCISE 2 OF THE OECD/NRC BWR TT BENCHMARK

CRONOS2/FLICA4 (CEA, France)

CRONOS2

CRONOS is the computer tool devoted to neutronic core computation in the SAPHYR system, which also includes APOLLO2 for neutronic assembly calculation and FLICA4 for thermal-hydraulic core calculation. CRONOS has been designed to provide all the computational means necessary for nuclear reactor core calculations, including design, fuel management, follow-up and accidents. CRONOS allows steady-state, kinetic, transient, perturbation and burn-up calculations. The power calculation takes into account the thermal-hydraulic feedback effects. All of this can be done without any limitation on any parameter (angular discretisation, energy groups and spatial meshes). CRONOS was written with the objective of optimising its performance and its portability. It is based on a modular structure that allows a great flexibility of use. A special user-oriented language, named GIBIANE, and a shared numerical toolbox have been developed to chain the various computation modules. The code solves either the diffusion equation or the even parity transport equation with anisotropic scattering and sources. Different geometries are available such as 1-, 2- or 3-D Cartesian, 2- or 3-D hexagonal and cylindrical geometries. Four different solvers are available: PRIAM, MINOS, CDIF and VNM. The PRIAM solver uses the second-order form of the transport equation and is based on S_N angular discretisation and a finite element approximation on the even flux (primal approximation). This solver is mainly devoted to accurate reference calculation for either Cartesian or hexagonal geometry. The MINOS nodal solver is based on mixed dual finite element for diffusion or simplified P_N equations. This solver performs very fast kinetic and static calculations. The CDIF solver uses finite difference approximation for the diffusion equation, and is devoted to pin-by-pin rectangular calculation. The VNM solver based on the VARIANT method will be soon connected to CRONOS. It is based on a mixed primal method and P_N approximation and will be mainly devoted to computation of fast breeder reactors.

References

Fedon-Magnaud, C., "Pin-by-pin Transport Calculation with CRONOS Reactor Code", *M&C Madrid*, 27-30 September 1999.

Lautard, J., D. Schneider, A.M. Baudron, "Mixed Dual Methods for Neutronic Reactor Core Calculations in the CRONOS System", *M&C Madrid*, 27-30 September 1999.

Lautard, J., *et al*., "CRONOS – A Modular Computational System for Neutronic Core Calculation", IAEA Meeting, Cadarache, France (1990).

FLICA4

FLICA4 is the thermal-hydraulics code of the SAPHYR system, which also includes CRONOS2 for neutronic core calculations and APOLLO2 for neutronic assembly calculations. SAPHYR codes are based on a modular structure that allows a great flexibility of use. A special user-oriented language, named GIBIANE, and a shared numerical toolbox have been developed to chain the various computation modules. FLICA4 is a 3-D two-phase compressible flow code, especially devoted to reactor core analysis. The fluid is modelled by a set of four equations: mass, momentum, and energy conservation for the two-phase mixture, and mass conservation for the vapour. The velocity disequilibrium is taken into account by a drift flux correlation. A 1-D thermal module is used to solve the conduction in solids (fuel). Thanks to the modular design of the SAPHYR codes, numerous closure laws are available for wall friction, drift flux, heat transfer and critical heat flux (CHF), and many fluids can be calculated

(liquids like lead or freons, gases like hydrogen or carbon dioxide). A specific set of correlations has been qualified in FLICA3 for PWR applications. An extensive qualification program for FLICA4 is underway, based on recent experimental data, in order to cover a wider range of flow conditions.

FLICA4 includes an object-oriented pre-processor to define the geometry and the boundary conditions. Radial unstructured meshes are available, without any limitation on the number of cells. Zooming on a specific radial zone can be performed by a second calculation using a finer mesh (for instance a sub-channel calculation of the hot assembly). The fully implicit numerical scheme is based on the finite volumes and a Roe solver. This kind of method is particularly accurate, with a low numerical diffusion.

References

Toumi, I., A. Bergeron, D. Gallo, E. Royer, D. Caruge, "FLICA4: A Three-dimensional Two-phase Flow Computer Code with Advanced Numerical Methods for Nuclear Applications", *Nuclear Engineering and Design*, 200, 139-155 (2000).

Bergeron, A., D. Caruge, P. Clément, "Assessment of the 3-D Thermal-hydraulic Nuclear Computer Code FLICA4 on Rod Bundle Experiments", *NURETH-6*, San Francisco, 3-8 October 1999.

Toumi, I., D. Caruge, "An Implicit Second Order Method for 3-D Two-phase Flow Calculations", *Nuclear Science Engineering*, 130, 213-225 (1998).

DYN3D (FZR, Germany)

Capabilities

DYN3D is a three-dimensional core model for dynamic and depletion calculations in light water reactor cores with quadratic or hexagonal fuel assembly geometry. The two-group neutron diffusion equation is solved by nodal methods. A thermal-hydraulic model of the reactor core and a fuel rod model are implemented in DYN3D. The reactor core is modelled by parallel coolant channels which can describe one or more fuel elements. Starting from the critical state (k_{eff}-value, critical boron concentration or critical power) the code allows to simulate the neutronic and thermal-hydraulic core response to reactivity changes caused by control rod movements and/or changes of the coolant core inlet conditions. Depletion calculations can be performed to determine the starting point of the transient. Steady state concentrations of the reactor poisons can be calculated. The transient behaviour of Xe and Sm can be analysed. The decay heat is taken into account based on power history and during the transient. Hot channels can be investigated by using the nodal flux reconstruction in assemblies and the pin powers of the cell calculations. Cross-section libraries generated by different cell codes for different reactor types are linked with DYN3D. Macroscopic cross-section libraries created within the common software platform can easily be linked to DYN3D.

Methods of solution

Neutron kinetics

The neutron kinetic model is based on the solution of the three-dimensional two-group neutron diffusion equation by nodal expansion methods. Different methods are used for quadratic and hexagonal fuel assembly geometry. It is assumed that the macroscopic cross-sections are spatially

constant in a node being the part of a fuel assembly. With Cartesian geometry, the three-dimensional diffusion equation of each node is transformed into one-dimensional equations in each direction x, y, z by transversal integrations. The equations are coupled by the transversal leakage term. In each energy group, the one-dimensional equations are solved with the help of flux expansions in polynomials up to the second order and exponential functions being the solutions of the homogeneous equation. The fission source in the fast group and the scattering source in the thermal group as well as the leakage terms are approximated by the polynomials. In the case of hexagonal fuel assemblies, the diffusion equation in the node is transformed into a two-dimensional equation in the hexagonal plane and a one-dimensional equation in the axial direction. The two equations are coupled by the transverse leakage terms which are approximated by polynomials up to the second order. Considering the two-dimensional equation in the hexagonal plane, the side-averaged values (HEXNEM1) or the side-averaged and the corner point values (HEXNEM2) of flux and current are used for the approximate solution of the diffusion equation. The method used for the one-dimensional equations of the Cartesian geometry is applied for the axial direction. It is extended to two dimensions in the HEXNEM1 and HEXNEM2 methods. In the steady state, the homogeneous eigenvalue problem or the heterogeneous problem with given source is solved. An inner and outer iteration strategy is applied. The outer iteration (fission source iteration) is accelerated by Chebychev extrapolation.

The steady-state iteration technique is applied for the calculation of the initial critical state, the depletion calculations and the Xe and Sm dynamics. Concerning reactivity transients an implicit difference scheme with exponential transformation is used for the time integration over the neutronic time step. The exponents in each node are calculated from the previous time step or during the iteration process. The precursor equations are analytically solved, assuming the fission rate behaves exponentially over the time step. The heterogeneous equations obtained for each time step are solved by an inner and outer iteration technique similar to the steady state.

Thermal-hydraulics

The parallel channels are coupled hydraulically by the condition of equal pressure drop over all core channels. Additionally, the so-called hot channels can be considered for the investigation of hot spots and uncertainties in power density, coolant temperature or mass flow rate. Thermo-hydraulic boundary conditions for the core like coolant inlet temperature, pressure, and coolant mass flow rate or pressure drop must be given as input for DYN3D. The module FLOCAL comprises a one- or two-phase coolant flow model on the basis of four differential balance equations for mass, energy and momentum of the two-phase mixture and the mass balance for the vapour phase allowing the description of thermodynamic non-equilibrium between the phases, a heat transfer regime map from one-phase liquid up to post-critical heat transfer regimes and superheated steam. A fuel rod model for the calculation of fuel and cladding temperatures is implemented. A thermo-mechanical fuel rod model allows the estimation of the relevant heat transfer behaviour of the gas gap during transients and the determination of some parameters for fuel rod failure estimation.

The two-phase flow model is closed by constitutive laws for heat mass and momentum transfer, e.g. vapour generation at heated walls, condensation in the sub-cooled liquid, phase slip ratio, pressure drop at single flow resistances and due to friction along the flow channels as well as heat transfer correlations. Different packages of water and steam thermo-physical properties presentation can be used.

Coupling neutron kinetics/thermal-hydraulics

A two-time-step scheme consisting of thermal-hydraulic and neutron kinetic time steps is used for the transient integration. One or several neutron kinetic steps are used within a thermal-hydraulic step.

Iterations between neutron kinetics and thermal-hydraulics are carried out in the steady state as well as for each thermal-hydraulic time step. Based on the changes of the main physical parameters of the transient process the time step size is controlled during the calculation.

Programming language

FORTRAN90 on Windows, Unix and Linux platforms.

Outstanding features

Special models

The assembly discontinuity factors (ADF) can be considered in the two geometries, Cartesian and hexagonal. The pin-wise flux reconstruction can be used for hot channel calculation during the DYN3D run. A decay heat model based on the power history or the initial power distribution can be taken into account during the transient. The decay heat model integrated in the code is based on the four fissionable isotopes ^{235}U, ^{238}U, ^{239}Pu and ^{241}Pu, the contributions from the decay of actinides resulting from the neutron capture and the contributions from the decay of nuclides formed by neutron capture in fission products. Based on perturbation theory, the reactivity contributions due to control rod motions, changes of moderator properties and fuel temperatures are calculated.

A model for description of the mixing of coolant from different primary loops in the downcomer and lower plenum of VVER-440 type reactors is implemented. It is based on the special feature of VVER-440 type reactors, that the coolant flow in the downcomer is nearly parallel without large re-circulation vortexes as they are known from Western-type PWRs. Thus the flow can be well described in the potential flow approximation, where the Navier-Stokes equations can be solved analytically for the 2-D flow in the downcomer. The velocity gradient in the radial direction was neglected. In the lower control rod chamber a parallel flow with constant velocity was assumed. With this approximation of the velocity field the diffusion equation for the temperature is solved. The solution is presented as a closed analytical expression based on series of orthogonal eigenfunctions. The turbulence was taken into account by constant scalar turbulent Peclet numbers defined individually for the downcomer and the lower control rod chamber. The turbulent Peclet numbers describe the intensity of turbulent diffusion and were adapted to experimental data. For the validation of the model, measured values from an air operated 1:5 scaled VVER-440 model were used. Temperature measurements were taken at the end of the downcomer and at the inlet of the reactor core. Further, the model was validated against measured operational data from NPP with VVER-440 and CFD calculations.

Concerning the transport of boron gradients into the core at low velocities a particle-in-cell model for avoiding the numerical diffusion can be applied in DYN3D. Integrated fuel rod model allows considering dynamic changes in heat transfer conditions (gap behaviour) and fuel rod failure limits estimation on-line during transient calculations.

Coupling with system codes and CFD

DYN3D is coupled with the system code ATHLET to analyse a wide range of transients. Regarding the thermal-hydraulics of the core three different types of coupling are implemented:

- internal coupling;
- external coupling;
- parallel coupling.

In the internal coupling, the neutron kinetics is described by DYN3D and ATHLET models the whole thermal-hydraulics. Data exchange is performed via internal interfaces. In the external coupling, the core, including neutron kinetics and thermal-hydraulics, is simulated by DYN3D, and the remaining system is simulated by ATHLET. Boundary conditions at the core inlet and outlet are exchanged during the calculation. The thermal-hydraulics of the core are analysed by the two codes DYN3D and ATHLET in the parallel coupling. The code structure of DYN3D (data modules within FORTRAN90) allows relatively easy coupling to other thermal-hydraulic system codes. Internal and external couplings between DYN3D and RELAP5 realised by international partners (IPPE Obninsk, VUJE Trnava) also exist. Off-line coupling with CFD for providing realistic boundary conditions at the core inlet with respect to coolant mixing in the downcomer and lower plenum has been realised. A module based on semi-analytical perturbation reconstruction (SAPR) has been developed and coupled to DYN3D allowing the determination of boron concentration and coolant temperature distributions at the core inlet from response functions obtained by CFD calculations or experimentally. Coupling of DYN3D neutron kinetics module or DYN3D core model (including thermal-hydraulics) with other -D or 3-D thermal-hydraulic modules (including CFD for open and porous media) is feasible based on common software platform (SALOME).

Validation

DYN3D has been validated by numerous benchmarks (including experimental results) for both Cartesian and hexagonal fuel element geometry.

Steady-state problems

- 3-D IAEA benchmark (Cartesian);
- 2-D IAEA benchmarks modified for hexagonal geometry;
- 2-D and 3-D Seidel benchmark for VVER-440 (hexagonal);
- 3-D Schulz benchmark for VVER-1000 (hexagonal);
- Atomic Energy Research (AER) benchmark problem concerning control rod worth of VVER-440 reactor (hexagonal);
- comparison of calculated reactor parameters (critical boron concentration, reactivity coefficients, control rod efficiency) with measured data for different VVER-reactors;
- comparison of assembly-averaged and pin-wise neutron flux distribution measured at V-1000 zero power test facility (hexagonal).

Transient problems

- kinetic experiments at the zero power reactor LR-0 (hexagonal);
- 1st through 3rd kinetic benchmarks of AER with ejection of asymmetrical control rods in a VVER-440 (hexagonal);
- 4th kinetic benchmark of AER of a boron dilution transient in a VVER-440 (hexagonal);
- NEACRP benchmarks on control rod ejections in PWR (Cartesian);
- NEA-NSC benchmarks on uncontrolled withdrawal of control rods at hot zero power in PWR (Cartesian);

- OECD/NRC main steam line break benchmark – Exercise 2 (Cartesian);
- OECD/NRC main steam line break benchmark – Exercise 3 analysed with DYN3D/ATHLET (Cartesian);
- 5^{th} kinetic benchmarks of AER on main steam header break in a VVER-440 with DYN3D/ ATHLET (hexagonal);
- comparison of DYN3D/ATHLET results with measured data for operational transients in nuclear power plants with VVER type reactors;
- DYN3D/ATHLET calculations of the turning-off of one feedwater pump from working two in the Balakovo-4 VVER-1000 (hexagonal);
- DYN3D/ATHLET calculations for the load drop down to house load level in one of the two working turbines in Loviisa-1 VVER-440 (hexagonal);
- OECD BWR turbine trip benchmark in the reactor Peach Bottom-2 – Exercise 2 analysed with DYN3D (Cartesian);
- OECD BWR turbine trip benchmark in the reactor Peach Bottom-2 – Exercise 3 analysed with DYN3D/ATHLET (Cartesian);
- DYN3D/ATHLET calculations for drop of a single control rod and power control action in the VVER 440/213 of NPP Bohunice 3 (hexagonal);
- DYN3D/ATHLET calculations for the coast-down of a second main coolant pump (start-up test) in the VVER-1000/V-320 of Kozloduy 6 (hexagonal);
- DYN3D Calculations for the V-1000 test facility and comparisons with the measurements (hexagonal).

References

Grundmann U., U. Rohde, *DYN3D/M2 – A Code for Calculation of Reactivity Transients in Cores with Hexagonal Geometry*, IAEA Technical Committee Meeting on Reactivity Initiated Accidents, Vienna (1989), Report ZfK-690, Rossendorf (1989) or Report FZR 93-01, Rossendorf (1993).

Grundmann, U., J. Hádek, "Calculations of Neutron Kinetics Experiments on the LR-0 Reactor with the Three-dimensional Code DYN3D/M1", *Kernenergie*, 34, 12 (1991).

Grundmann, U., U. Rohde, "Investigations on a Boron Dilution Accident for a VVER-440 Type Reactor by the Help of the Code DYN3D", *Proceedings of the 1994 Topical Meeting on Advances in Reactor Physics*, Vol. III, pp. 464-471, Knoxville, TN (USA), 11-15 April 1994.

Grundmann, U., *The Code DYN3DR for Steady-state and Transient Analyses of Light Water Reactor Cores with Cartesian Geometry*, Report FZR-114, Rossendorf, November 1995.

Grundmann, U., U. Rohde, "DYN3D – A Three-dimensional Core Model for Steady State and Transient Analysis in Thermal Reactors", *Proceedings of the International Conference on the Physics of Reactors (PHYSOR 96)*, Mito, Japan, 16-20 Sept. 1996.

Grundmann, U., U. Rohde, "The Reactor Code DYN3DR – Transient Calculations of NEACRP Benchmarks for PWR and BWR", *Proceedings Jahrestagung Kerntechnik '96*, Mannheim (1996).

Selected Safety Aspects of WWER-440 Model 213 Nuclear Power Plants: Final Report of the IAEA Project on Evaluation of Safety Aspects for WWER-440 Model 213 NPP, Vienna, International Atomic Energy Agency, ISBN 92-0-101196-2 (1996).

Kyrki-Rajamäki, R., U. Grundmann, A. Kereszturi, "Results of Three-dimensional Hexagonal Dynamic Benchmark Problems for VVER Type Reactors", *Proceedings of the Int. Conf. on the Physics of Reactors (PHYSOR'96)*, Mito, Japan, ,16-20 Sept. 1996, pp. J229-J238.

Grundmann, U., U. Rohde, *Verification of the Code DYN3DR with the Help of International Benchmarks*, Report FZR-195, Rossendorf (1997).

Grundmann U., F. Hollstein, "A Two-dimensional Intranodal Flux Expansion Method for Hexagonal Geometry", *Nuclear Science and Engineering*, 133, 201-212 (1999).

Grundmann, U., "HEXNEM – A Nodal Method for the Solution of the Neutron Diffusion Equation in Hexagonal Geometry", *Proceedings of the Conference on Mathematics and Computations in Nuclear Applications (M&C'99)*, Madrid, 27-30 September 1999, pp. 1086-1095.

Grundmann, U., S. Kliem, U. Rohde, "Analysis of the Exercise 2 of the OECD – MSLB Benchmark with the Code DYN3D/R", *Proceedings of the Conference on Mathematics and Computations in Nuclear Applications (M&C'99)*, Madrid, 27-30 September 1999.

Kliem, S., U. Grundmann, U. Rohde, "Analysis of the OECD MSLB Benchmark Using the Coupled Code DYN3D/ATHLET", *Proceedings of the 8th International Conference on Nuclear Engineering (ICONE 8)*, Baltimore (USA), 2-6 April 2000.

Grundmann, U., S. Kliem, "Analyses of the OECD MSLB Benchmark with the Codes DYN3D and DYN3D/ATHLET", *Transactions of the American Nuclear Society*, Volume 84, pp. 23-25, June 2001.

Mittag, S., S. Kliem, F-P. Weiß, R. Kyrki-Rajamäki, A. Hämäläinen, S. Langenbuch, S. Danilin, J. Hadek, G. Hegyi, A. Kuchin, D. Panayotov, "Validation of Coupled Neutron Kinetic/Thermal-Hydraulic Codes. Part 1: Analysis of a VVER-1000 Transient (Balakovo-4)", *Annals of Nuclear Energy*, 28, pp. 857-873 (2001).

Kozmenkov, Y., Y. Orekhov, U. Grundmann, S. Kliem, U. Rohde, A. Seidel, "Development and Benchmarking of the DYN3D/RELAP5 Code System", *Proceedings of Jahrestagung Kerntechnik 2001*, Dresden, 15-17 Mai 2001, pp. 15-18.

Grundmann, U., U. Rohde, "Analysis of the Boiling Water Reactor Turbine Trip Benchmark with the Code DYN3D", *Proc. Int. Conference on the New Frontiers of Nuclear Technology: Reactor Physics, Safety and High-performance Computing (PHYSOR 2002)*, Seoul, Korea, 7-10 Oct. 2002.

Grundmann, U., S. Kliem, "Analyses of the OECD Main Steam Line Break Benchmark with the Codes DYN3D and ATHLET", *Nucl. Technol*., 142, 146 (2003).

Grundmann, U., U. Rohde, "Different Simulations of Phase II of the OECD/NRC BWR Turbine Trip Benchmark with the Code DYN3D", *Annual Meeting on Nuclear Technology*, Berlin, 20-22 May 2003.

Mittag, S., P. Petkov, U. Grundmann, "Discontinuity Factors for Non-multiplying Material in Two-dimensional Hexagonal Reactor Geometry", *Annals of Nucl. Energy*, 30/13, pp. 1347-1364 (2003).

Grundmann, U., S. Kliem, U. Rohde, "Analysis of the Boiling Water Reactor Turbine Trip Benchmark with the Codes DYN3D and ATHLET/DYN3D", *Nuclear Science and Engineering*, forthcoming.

QUABOX/CUBBOX-ATHLET (GRS, Germany)

The code system QUABOX/CUBBOX-ATHLET is developed at GRS on the base of thermo-fluid dynamic system cede ATHLET for analysis of the whole plant behaviour under accident conditions and the core model code QUABOX/CUBBOX for the analysis of the 3-D reactor core behaviour.

The ATHLET code is a thermo-fluid dynamic system code for a wide range of applications comprising anticipated and abnormal plant transients, small and intermediate leaks as well as large breaks in PWRs and BWRs. The code offers the possibility of choosing between different models of fluid dynamics. The two-phase flow is described either by a five-equation model or a full six-equation model for mass, energy and momentum of both phases including models for non-condensables. The code structure is highly modular, and allows an easy implementation of different physical models. The basic modules are: thermo-fluid dynamics, neutron kinetics, general control simulation and numerical integration method FEBE. ATHLET provides a modular network approach for the representation of a thermal-hydraulic system. The analyses presented in the current work are made with the version of ATHLET release 1.2E.

The 3-D reactor core behaviour is described by QUABOX/CUBBOX. This code solves the neutron diffusion equations with two energy neutron groups and six groups of delayed neutron precursors. The coarse mesh method is based on a polynomial expansion of neutron flux in each energy group. The time integration is performed by a matrix-splitting method, which decomposes the solution into implicit one-dimensional step for each spatial direction. The reactivity feedback is taken into account by dependence of homogenised cross-section on feedback parameters, the functional dependence can be defined in a very general and flexible manner.

The coupling approach for 3-D neutronics models implemented in ATHLET is based on a general interface, which separates data structures from neutronics and thermo-fluid dynamic code and performs the data exchange in both directions. The approach has been successfully applied to couple other 3-D neutronics codes. The internal coupling method has the following features: the fluid dynamic equations for the primary circuit and the flow channels in the reactor core region are completely modelled and numerically solved by ATHLET methods. The time integration in the neutronics code QUABOX/ CUBBOX is performed separately. Therefore, both codes maintain their capabilities. The time step size is synchronised during the transient, whereby the accuracy control is preferably done by the fluid dynamic code. The coupling allows a flexible mapping defined by input between fuel assemblies of the core loading and the thermo-fluid dynamic channels. Also, the axial meshes for neutronics and fluid dynamics can be defined independently. The coupled code ATHLET-QUABOX/CUBBOX has already been applied to study complex plant transient conditions.

DNB/3D (NETCORP, USA)

DNB/3D is a FORTRAN 77 computer program that simulates the nuclear steam supply system of a boiling water reactor under transient conditions. Geometry and system component options are provided to represent any of the current BWR designs. The major features of DNB/3D are:

- Point, 1-D and 3-D neutronic kinetics models including Doppler, moderator density and control rod feedback along with standard decay heat models. Initially subcritical cores can be represented. A power forced option is also provided.
- Multi-node radial and axial coolant channels and fuel rods.
- Fixed nodalisation in the reactor vessel and steam lines.

- One-dimensional homogeneous equilibrium conservation of mass, energy and momentum.
- Mechanistic non-equilibrium flow quality or profile fit model option to represent slip with the coolant channels.
- Steam line includes representation of the MSIV, turbine control and stop valves, RSV and steam bypass valves.
- Method of characteristics used to solve conservation equations in the steam lines.
- Turbine representation
- Structural metal components represented. Reactor protection and safety systems represented.
- Control systems represented. Complete self-initialisation of all components and models.
- Provisions to represent a wide variety of transient and accident scenarios. Flexible restart capability. British or Sl input/output option.

TRAC-BF1/COS3D (NFI, Japan)

NFI's code system used for this benchmark is TRAC-BF1/COS3D. COS3D based on modified one-group neutronics model is a three-dimensional core simulator. TRAC-BF1 is a plant simulator based on two-fluid model. TRAC-BF1/COS3D is a coupled system of both codes, which are connected using a parallel computing tool.

COS3D is a 3-D BWR core simulator used for designing and licensing analyses and core managements of commercial BWR plants in Japan. The neutronics model deals with three-dimensional geometry of rectangular co-ordinates. The characteristics of COS3D neutron kinetics model are as follows:

- modified one-group time-dependent diffusion equation derived from three-group diffusion equation;
- six delayed neutron precursor groups;
- direct consideration of feedback effect due to changes of moderator density, fuel temperature and control rod movement.

TRAC-BF1 includes a full non-homogeneous, non-equilibrium, two-fluid thermal-hydraulic model of two-phase flow. This also includes detailed modelling of a fuel bundle, thermal equilibrium critical flow model and so on. RPV is treated as three-dimensional nodalisation, and the other components are one-dimensional. The fundamental equations of thermal-hydraulics consist of mass, energy and momentum for each phase.

Instantaneous variables, namely, moderator density and fuel temperature are calculated at each *CHAN* component of TRAC-BF1. Those variables are transferred from TRAC-BF1 to COS3D via Parallel Virtual Machine (PVM). After COS3D calculates the neutronic condition according to those variables, it returns the power distribution data to TRAC-BF1. Then TRAC-BF1 calculates the thermal-hydraulic condition in the plant based on the power distribution. Such a data transfer is executed by turns at every time step on Unix or Linux environments.

TRAC-BF1/SKETCH-INS (NUPEC, Japan)

NUPEC used the SKETCH-INS/TRAC-BF1 coupled-code system in Exercise 2. The coupled-code system was originally developed at the Japan Atomic Energy Research Institute (JAERI) by a coupling of the best-estimate BWR transient analysis code TRAC-BF1 with the three-dimensional neutron kinetics code SKETCH-N. The coupling between the codes is organised using an interface module based on the massage-passing library called Parallel Virtual Machine (PVM).

TRAC-BF1 is the latest public domain BWR version of TRAC, which concerns thermal-hydraulics, fuel heat transfer and plant systems. Thermal-hydraulics utilises the two-fluid model that solves six balance equations of mass, momentum and energy for liquid and vapour phases. Two-phase flow in the core region is treated as one-dimensional parallel vertical flows. The heat transfer model solves 1-D radial heat conduction equations. Standard finite differential method with staggered mesh is used for space integration of both fluid flow and heat conduction. Time integration of the fluid flow equations is performed by the semi-implicit scheme with the stability enhanced two-step (SETS) method.

The SKETCH-INS code is a modification of the SKETCH-N code that was originally developed at JAERI. The SKETCH-INS code deals with neutron kinetics, which solves time-dependent diffusion equations in three-dimensional Cartesian co-ordinates. The code treats two neutron energy groups and six groups of delayed neutron precursors. In order to improve the spatial resolution accuracy, an assembly discontinuity factor (ADF) was implemented in the code upon the original one. Reactivity feedback is taken into account with moderator density, fuel temperature, and control rod motion and reactor scram. The ANS-1979 standard decay heat model has been implemented in the code. Direct gamma heating is taken into account for the in-channel active coolant flow. Numerical methods for the neutronic calculations are as follows. Polynomial and semi-analytical nodal method based on the nonlinear iteration procedure is used for spatial integration of diffusion equations. Time integration of the neutron kinetics equations is performed by the fully implicit scheme.

RETRAN-3D and CORETRAN (PSI, Switzerland)

RETRAN-3D

Within the STARS project at PSI, the code environment for the coupled 3-D reactor kinetics/ thermal-hydraulics transient analyses of the Swiss light water reactors (LWRs) is based principally on RETRAN-3D and CORETRAN, both for PWR and BWR systems. (It should be noted that the TRACE code since recently gets more and more importance within and without the project and that other codes are used for specific applications: e.g. RAMONA for BWR stability.) Both codes play distinct roles in this environment; RETRAN-3D is used for the analysis of coupled 3-D core/plant system transients, while CORETRAN is used for core-only dynamic analysis. An important aspect is that both codes are based on an identical neutronics algorithm, allowing the use of CORETRAN as an interface code to help prepare the 3-D core model for RETRAN-3D. This approach forms the basis of the PSI 3-D transient analysis methodology.

Participation in the OECD/NRC Peach Bottom 2 (PB2) turbine trip (TT) benchmark was prompted by the following considerations. First, the PSI methodology has so far only been assessed for neutronically-driven transients, and for a PWR system transient. As the benchmark addresses a BWR transient driven by system thermal-hydraulic perturbations, it extends the range of the codes' assessment. Secondly, the benchmark incorporates three different phases, which are, from the PSI point of view, well suited to a comprehensive assessment of all the participating codes. Consequently, PSI participated in all three phases of the benchmark.

RETRAN-3D MOD003.1, which is used in all three phases of the benchmark, is developed by EPRI to perform licensing and best-estimate transient thermal-hydraulic analyses of LWRs and it is maintained by CSA/USA. RETRAN-3D is used to analyse thermal-hydraulic transients and requires numerical input data that completely describe the components and geometry of the system being analysed. The input data include fluid volume sizes, initial flow, pump features, power generation, heat exchanger properties, and material compositions.

RETRAN-3D can calculate a steady-state initialisation from a minimal amount of information. The steady-state option computes volume enthalpies from a steady-state energy balance, with the restriction that generally only one enthalpy may be supplied per flow system. The range of applications of RETRAN-3D contains also the spatial kinetics behaviour of multi-dimensional reactor cores. RETRAN-3D also permits the analysis of systems with non-equilibrium thermodynamic conditions and allows for the presence of non-condensable gases in the fluid stream.

CORETRAN

CORETRAN-01 [1] is a three-dimensional core simulation program developed by EPRI, aimed at performing both core depletion and core transient analyses for LWRs. The code principally consists of an explicit coupling between a neutronic module and a thermal-hydraulic module, both "internally" built-in as part of the code. In both modules, the core is represented using a full representation, i.e. one neutronic channel per fuel assembly coupled to one single thermal-hydraulic channel. In the neutronic module reflectors are treated explicitly, while in the thermal-hydraulic module, one or several bypass channels can be added. Moreover, because the neutronic model has also been implemented in the RETRAN-3D program [2], CORETRAN can be used as an interface code to prepare the 3-D core model for RETRAN-3D, which is the methodology applied at PSI [2]. To summarise, CORETRAN can be seen as a plenum-to-plenum full core analysis tool making it very suitable not only for an accurate steady-state core follow analysis [3] but also for the 3-D simulation of reactivity-initiated accidents [4-5] as well as for the detailed analysis of the dynamical core response to "external" perturbations (i.e. specified by means of appropriate plenum-to-plenum boundary conditions).

Neutronics

The neutronic module solves in Cartesian 3-D geometry the steady-state and transient two-group neutron diffusion equations and the delayed neutron precursor equations for six groups. Two distinct nodal kinetic models are available. The first model is provided by means of the ARROTTA module implemented as part of the code and based on the Analytical Nodalisation Method (ANM). The second neutronic model uses a Coarse Mesh Finite Difference (CMFD) non-linear iteration procedure where the local two-node problems are solved using a hybrid ANM/Nodal Expansion Method (NEM) kernel. For both models, a dynamic frequency transformation of both the neutron fluxes and the delayed neutron precursor concentrations is employed and fully implicit or semi-implicit schemes can be used for the temporal discretisation. The cross-section model is based on a multi-dimensional interpolation from a set of 1-D, 2-D and 3-D tables produced with an assembly lattice code and containing cross-sections for base depletion calculations (i.e. as function of burn-up and historical variables) and for branch calculations (i.e. to model instantaneous feedback effects). A macroscopic depletion model can be applied to perform steady-state core follow analyses and an explicit model for the treatment of the time-dependent variation of four fission products (xenon, iodine, promethium and samarium) is also available. A pin power reconstruction module for both steady-state and transient applications is available and based on polynomial expansions for the fast intra-nodal flux and hyperbolic functions for the thermal flux, combined with several options for the corner-fluxes estimates. Finally, the assembly spatial discretisation allows for heterogeneous axial nodalisation while a 1×1 mesh is normally applied for the radial assembly representation, although a 2×2 mesh can be used for PWR applications.

Thermal-hydraulics

The thermal-hydraulic (T-H) module is principally based on the VIPRE code with the following three main options to solve the channel hydraulics. The first option is based on a four-equation model with forced flow along with a drift flux formulation and solved using a semi-implicit method. The second option is originally from the VIPRE-01 code and consists of a three-equation homogeneous equilibrium model (HEM) along with void and slip correlation profiles and solved using a fully implicit method. The third option is taken from the VIPRE-02 code and is based on a two-fluid six-equation model solved using a fully implicit scheme. Any of these options can be applied to a full core analysis with explicit coupling to the neutronic module so that a single separate T-H flow channel is assigned to each (neutronic) fuel assembly. A heterogeneous axial nodalisation of the T-H channels can be applied in order to allow for axial variations of the fuel assembly design (flow area, wetted/heated perimeters) and to allow for a detailed specification of pressure loss coefficients (inlet, spacers, outlet). Leakage flows from the lower plenum and from the fuel assemblies to the bypass channel can be modelled as well as water tube flows within fuel assemblies.

The boundary conditions can be specified for both steady-state and transient applications and include, among others, inlet enthalpy, total core flow (alternatively individual channel flow) and core outlet pressure (alternatively core pressure drop). When the total core flow and core outlet pressure are specified, a flow split calculation is performed to determine the individual channel flows including bypass with the condition for a uniform core pressure drop. A broad range of critical heat flux (CHF), critical power ratio (CPR), two-phase and heat transfer correlations are available, as is the possibility to enter “user” correlations. Additionally, PWR cross-flows can be taken into account when using the HEM or the two-fluid options. With these two options, detailed sub-channel analysis can also be performed where a fuel assembly is divided into a number of channels that communicate laterally and where the (time-varying) axial power shape can be defined. (i.e. no coupling to neutronics). Concerning the solution of the fuel heat conduction equation, an implicit finite-difference method is employed. A non-linear iterative procedure with the channel hydraulic solution is used to ensure convergence with regards to the wall heat fluxes, the rod temperatures and the channel flows. The heat conduction model can treat nuclear fuel rods but also electric heater rods, hollow tubes and walls. Fuel properties are based on the MATPRO code but can alternatively be specified by the user. A dynamic conductance model for the (fuel-cladding) gap, aimed at taking into account changes in fuel rod dimensions and fill gas pressure, is also available.

References

[1] Eisenhart, L.D., A.F. Dias, J.L. Westacott, T.J. Downar, H.G. Joo. *CORETRAN-01: A Three-dimensional Program for Reactor Core Physics and Thermal-hydraulics Analysis. Volume 1: Theory and Numerical Analysis*, EPRI Report WO-3574, Revision 3, November 2000 (2000).

[2] Paulsen, M.P., C.E. Peterson, G.C. Gose, J.H. McFadden, J.G. Shatford, J.L. Westacott, P.P. Cebull, J.Y. Wu, P.J. Jensen, *RETRAN-3D – A Program for Transient Thermal-hydraulic Analysis of Complex Fluid Flow Systems. Volume 1: Theory and Numerics*, EPRI Report NP-7450 (A), Volume 1, Revision 5, July 2001 (2001).

[3] Ferroukhi, H., F. Holzgrewe, P. Coddington, ”Towards a Best-estimates Steady-state and Transient Analysis Using the CORETRAN Code”, *Proc. Int. Mtg. Best-estimate Methods in Nuclear Safety Installation Analysis (BE2000)*, Washington, DC, USA, 12-16 November 2000 (2000).

[4] Ferroukhi, H., P. Coddington, "Uncontrolled Rod Bank Withdrawal Benchmark Analyses with CORETRAN and RETRAN-3D", *Proc. Int. Mtg. Mathematical Methods for Nuclear Applications (M&C 2001),* Salt Lake City, Utah, USA, 9-13 September 2001 (2001).

[5] Ferroukhi, H., P. Coddington. "The Analysis of Pressurised Water Reactor and Boling Water Reactor Reactivity Transients with CORETRAN and RETRAN-3D", *Nuclear Technology*, Vol. 142, No. 1, pp. 19-34, April 2003 (2003).

TRAC-BF1/NEM (PSU, USA)

TRAC-BF1

TRAC-BF1 is an advanced best-estimate computer program for boiling water reactor accident analysis [1]. The TRAC-BWR Code Development Program at the Idaho National Engineering Laboratory (INEL) was a program developing versions of the Transient Reactor Analysis Code (TRAC) to provide the US Nuclear Regulatory Commission (NRC) and the public with a best-estimate capability for the analysis of accidents and transients in boiling water reactor (BWR) systems and related experimental facilities. This effort began in October 1979 and resulted in the first publicly released version of the code, TRAC-BD1, 1-1 which was sent to the National Energy Software Center in February 1981. The mission of this first version of the code was to provide a best-estimate capability for the analysis of design basis loss-of-coolant accidents (LOCAs) in BWRs. The code provided a unified and consistent treatment of the design basis LOCAs sequence beginning with the blowdown phase, through heat-up, then re-flood with quenching, and finally ending with the refill phase of the LOCA scenario. New models developed for TRAC-BD1 in order to accomplish its mission included (a) a full two-fluid non-equilibrium, non-homogeneous thermal-hydraulic model of two-phase flow in all parts of the BWR system, including a three-dimensional treatment of the BWR pressure vessel; (b) a detailed model of a BWR fuel bundle, which includes the following models: a radiation heat transfer model for thermal radiation between multiple fuel rod groups, the inner surface of the channel wall, and the liquid and steam phases in the channel; a leakage path model; and a quench front tracking capability for both falling films and bottom flooding quench fronts on all rod groups and the inner surface of the channel wall; (c) simplified models of BWR hardware components, such as the jet pump and separator-dryer; (d) a counter-current flow limiting model for BWR geometries; (e) a non-homogeneous critical flow model; and (f) flow regime-dependent constitutive relations for the transfer of mass, energy, and momentum between the liquid and steam phases in two-phase flow and between each phase and structure.

The mission of the second publicly released version of the code, TRAC-BD1/MOD1, was expanded to include not only large- and small-break LOCAs but also operational transients and anticipated transients without scram (ATWS) for which point reactor kinetics is applicable. Models developed to support the broadening of the scope of the mission of the TRAC-BWR codes included:

- balance of plant models, such as turbine, feedwater heaters and condenser;
- a simple lumped parameter containment model;
- reactivity feedback model for use in the point reactor kinetics model;
- soluble boron transport model;
- non-condensable gas transport model;
- two-phase level tracking model;

- control systems model;
- generalised component-to-component heat and mass transfer models;
- improved constitutive models for the transfer of mass, energy and momentum between the two phases and between the phases and structure.

User convenience features, such as free-format input and extensive error checking of the input data, were also included in TRAC-BD1/MOD1.

The mission of TRAC-BF1/MOD1 was the same as for TRAC-BD1/MOD1, however the new capabilities built into this code make it more suitable for that mission. The new models and capabilities in TRAC-BF1/MOD1 include:

- material Courant-limit-violating numerical solution for all one-dimensional hydraulic components;
- implicit steam separator/dryer model;
- implicit turbine model;
- improved interfacial heat transfer;
- improved interfacial shear model;
- a condensation model for stratified vertical flow;
- one-dimensional neutron kinetics model;
- improved control system logic and solution method.

In addition to these code improvements, a preload processor was written for TRAC-BF1, its graphic routines were improved for adaptation to the Nuclear Plant Analyser (NPA) at the INEL, and more than 95% of the coding has been converted to ANSI Standard FORTRAN 77.

TRAC-BF1/MOD1 can be applied to any BWR accident analysis or thermal-hydraulic test facility, including those requiring reactivity feedback effects, control system simulation, and/or a balance-of-plant model. TRAC-BF1/MOD1 was applied to experimental facilities ranging from simple pipe blowdowns, such as the Edwards pipe tests, to integral LOCA tests, such as the two-loop test apparatus (TLTA) facility, and even to multi-dimensional test facilities such as the slab core test facility (SCTF). BWR small-break LOCAs have also been simulated with TRAC-BD1. The BWR fuel bundle model is quite versatile and was used to simulate not only BWR fuel bundles within a BWR reactor vessel but also stand-alone, single-bundle experiments in which advanced bundle hydraulics and heat transfer models are required.

NEM-3D

The Nodal Expansion Method (NEM) is a 3-D multi-group nodal code developed and used at the Pennsylvania State University (PSU) for modelling both steady-state and transient core conditions [2]. The code has options for modelling 3-D Cartesian, cylindrical and hexagonal geometry. This code is based on the nodal expansion method for solving the nodal equations in three dimensions. It utilises a transverse integration procedure and is based on the partial current formulation of the nodal balance equations. The leakage term in the one-dimensional transverse integrated equations is approximated using a standard parabolic expansion by using the transverse leakages in three neighbour nodes. The

nodal coupling relationships are expressed in partial current formulation and the time dependence of the neutron flux is approximated by a first order, fully explicit, finite difference scheme. This method has been shown to very efficient although it lacked the precision of the advanced nodal codes. An upgrade of the method has recently been completed, replacing the fourth-order polynomial expansion with a semi-analytical expression utilising a more accurate approximation of the transverse leakage. This code has been benchmarked for Cartesian, cylindrical and hexagonal geometry. NEM is coupled with the Penn State versions of TRAC-PF1 and TRAC-BF1.

The NEM spatial model is based on the transverse integrated procedure. Two levels of approximation are used: fourth-degree transverse integrated flux representation and the quadratic leakage approximation. The nodal coupling relationships are expressed in a partial current formulation. The time dependence of the neutron flux is approximated by a first order, fully implicit, finite-difference scheme, whereas the time dependence of the neutron precursor distributions is modelled by a linear time-integrated approximation. The coarse-mesh-rebalance and asymptotic extrapolation methods are used to accelerate convergence of the iterative solution process. Several benchmark problems were used to assess the NEM model in both steady-state and transient conditions. Very good agreement was obtained among the reference results and those from NEM.

TRAC-BF1 and NEM are coupled using parallel virtual machine (PVM) environment [3]. The numerical scheme of the PVM coupling is a semi-implicit scheme for the calculated power [4]. In most cases (especially during steady state calculation), the number of times the three-dimensional (3-D) kinetics calculations performed can be optimised to speedup the calculation. For this purpose, a multiple time step marching scheme is implemented in TRAC-BF1/NEM calculation. This scheme allows TRAC-BF1 solution to march several steps while NEM only marched one large time step.

References

[1] Giles, M., *et al.*, TRAC-*BF1/MOD1: An Advanced Best Estimate Computer Program for Boiling Water Reactor Accident Analysis Volume 1: Model Description*, NUREG/CR-4356 EGG-2626, pp. 1-1 to 1-2, May 1992.

[2] Bandini, R., "A Three-dimensional Transient Neutronics Routine for the TRAC-PF1 Reactor Thermal Hydraulic Computer Code", PhD Thesis, The Pennsylvania State University (1990).

[3] Geist, A., *et. al*., "PVM: Parallel Virtual Machine – A Users Guide and Tutorial for Networked Parallel Computing", The MIT Press, Cambridge, Massachusetts, London, England (1994).

[4] Lu, S., "GE Simplified Boiling Water Reactor Stability Analysis in Time Domain", PhD Thesis, The Pennsylvania State University (1997).

TRAC-BF1/ENTRÉE (TEPSYS, Japan)

This system is composed of the 3-D nodal kinetic code ENTRÉE and the state-of-the-art two-fluid thermal-hydraulic plant simulator TRAC/BF1. Numerical methodologies of ENTRÉE and the parallel coupling techniques of these two codes were described in detail in a different paper written by the authors (see the reference below). Figure A-1 depicts the linkage of two codes applied in this benchmark.

Neutronic constants consist of macroscopic and microscopic cross-sections, discontinuity factors, detector response parameters and so on. They are evaluated by the detailed two-dimensional assembly

transport code and are transformed into a binary library based on the multiple-table function of historical and instantaneous variables. Exposure weighted moderator density, fuel temperature and control rod density are classified as historical variables together with exposure. They are evaluated by the 3-D steady-state core simulator. On the other hand, instantaneous variables consist of moderator density and fuel temperature evaluated at test points. They are solved as state variables of CHAN components in TRAC/BF1 and are updated at every time step. The control rod density is normally controlled by ENTRÉE itself or it is transferred from TRAC/BF1 together with arbitrary trip signals.

Reference

Hotta, A., H. Ninokata A.J. Baratta, "Development of Parallel Coupling System Between Three Dimensional Nodal Kinetic Code ENTRÉE and Two-fluid Plant Simulator TRAC/BF1", *J. Nucl. Sci. Technol*., 37 (10), 840 (2000).

Figure A-1. TRAC-BF1/ENTRÉE coupling scheme

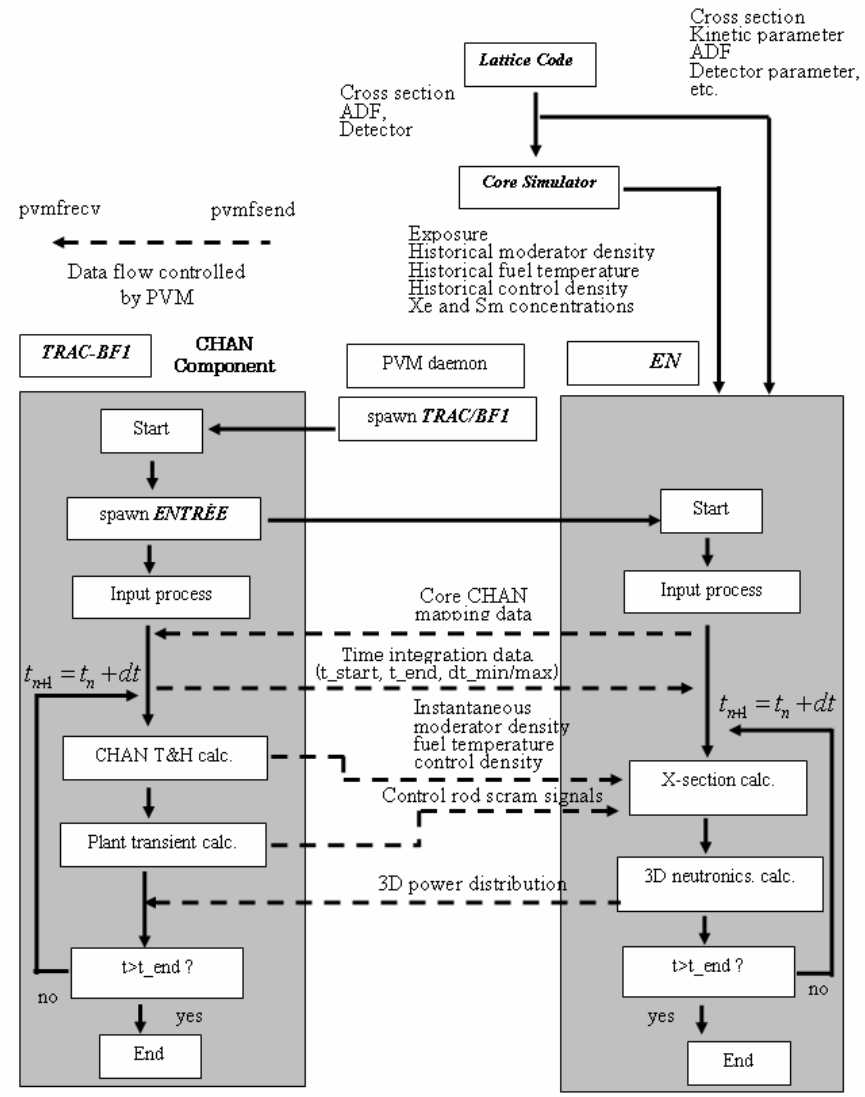

RELAP5/PARCS (U.PISA, Italy)

RELAP5

The light water reactor (LWR) transient analysis code, RELAP5, was developed at the Idaho National Engineering Laboratory (INEL) for the US Nuclear Regulatory Commission (NRC). Code uses include analyses required to support rule-making, licensing audit calculations, evaluation of accident mitigation strategies, evaluation of operator guidelines and experiment planning analysis. RELAP5 has also been used as the basis for a nuclear plant analyser. Specific applications have included simulations of transients in LWR systems such as loss of coolant, anticipated transients without scram (ATWS), and operational transients such as loss of feedwater, loss of off-site power, station blackout and turbine trip. RELAP5 is a highly generic code that, in addition to calculating the behaviour of a reactor coolant system during a transient, can be used for simulation of a wide variety of hydraulic and thermal transients in both nuclear and non-nuclear systems involving mixtures of steam, water, non-condensable and solute.

The RELAP5/MOD3 code is based on a non-homogeneous and non-equilibrium model for the two-phase system that is solved by a fast, partially implicit numerical scheme to permit economical calculation of system transients. The objective of the RELAP5 development effort from the outset was to produce a code that included important first-order effects necessary for accurate prediction of system transients but that was sufficiently simple and cost effective so that parametric or sensitivity studies were possible.

The code includes many generic component models from which general systems can be simulated. The component models include pumps, valves, pipes, heat releasing or absorbing structures, reactor point kinetics, electric heaters, jet pumps, turbines, separators, accumulators and control system components. In addition, special process models are included for effects such as form loss, flow at an abrupt area change, branching, choked flow, boron tracking and non-condensable gas transport.

The system mathematical models are coupled into an efficient code structure. The code includes extensive input checking capability to help the user discover input errors and inconsistencies. Also included are free-format input, re-start, re-nodalisation and variable output edit features. These user conveniences were developed in recognition that generally the major cost associated with the use of a system transient code is in the engineering labour and time involved in accumulating system data and developing system models, while the computer cost associated with generation of the final result is usually small.

The code development has benefited from extensive application and comparison to experimental data in the LOFT, PBF, Semiscale, ACRR, NRU and other experimental programs.

The numerical solution is obtained with a semi-implicit scheme based on replacing the system of differential equations with a system of finite-difference equations partially implicit in time. The method has a material Courant time step stability limit. However, this limit is implemented in such a way that the single-node Courant violations are permitted without adverse stability effects.

PARCS

PARCS is a three-dimensional (3-D) reactor core simulator which solves the steady-state and time-dependent neutron diffusion equation to predict the dynamic response of the reactor to reactivity perturbations such as control rod movements or changes in the temperature/fluid conditions in the reactor core. The code is applicable to both PWR and BWR cores loaded with either rectangular or

hexagonal fuel assemblies. The neutron diffusion equation is solved with two energy groups for the rectangular geometry option, whereas any number of energy groups can be used for the hexagonal geometry option. PARCS is coupled directly to the thermal-hydraulics systems codes TRAC-M and RELAP5 which provide the temperature and flow field information to PARCS during the transient. The thermal-hydraulic solution is incorporated into PARCS as feedback into the few-group cross-sections. Neutronically, the coarse mesh finite difference (CMFD) formulation is employed in PARCS to solve for the neutron fluxes in the homogenised nodes. In rectangular geometry, the analytic nodal method (ANM) is used to solve the two-node problems for accurate resolution of coupling between nodes in the core, whereas the triangle-based polynomial expansion nodal (TPEN) method is used for the same purpose in hexagonal geometry.

Numerous sophisticated spatial kinetics calculation methods have been incorporated into PARCS in order to accomplish the various tasks with high accuracy and efficiency. For example, the CMFD formulation provides a means of performing a fast transient calculation by avoiding expensive nodal calculations at times in the transient when there is no strong variation in the neutron flux spatial distribution. Specifically, a conditional update scheme is employed in PARCS so that the higher order nodal update is performed only when there are substantial changes in the core condition to require such an update. The temporal discretisation is performed using the theta method with an exponential transformation of the group fluxes. A transient fixed source problem is formed and solved at each time point in the transient. For spatial discretisation, the stabilised ANM two-node kernel or the multi-group TPEN kernel is used to obtain the nodal coupling relation that represents the interface current as a linear combination of the node average fluxes of the two nodes contacting the interface.

TRAC-BF1/NEM (UPV, Spain)

The coupled code used by the UPV for the Exercise 2 was the TRAC-BF1/NEM code.

TRAC-BF1

The TRAC code is an advanced, best-estimate computer program for BWR transient and accident analysis. It belongs to the TRAC series of codes that are six-equation, non-equilibrium two-fluid codes. The TRAC mathematical models are intended to solve a coupled set of field equations which is set up to describe the T-H behaviour of the coolant flow in a BWR system as well as the flow of energy in the fuel elements and the structural components of the reactor. The two-fluid models for the fluid flow in the BWR system are solved in TRAC in the one- and three-dimensional components. This code is modular in nature. The above feature makes it easier to add or modify the code models.

NEM

The NEM code is a three-dimensional neutron kinetics model for performing steady-state and transient simulations, based on the Nodal Expansion Method (NEM). Two levels of approximation have been used: fourth-degree transverse-integrated flux representation and the quadratic leakage approximation. The nodal coupling relationships are expressed in a partial current formulation. The time dependence of the neutron flux is approximated by a first order, fully implicit, finite-difference scheme, whereas the time dependence of the neutron precursor distributions is modelled by a linear time-integrated approximation. The coarse-mesh-rebalance and asymptotic extrapolation methods are used to accelerate convergence of the iterative solution process. Several benchmark problems have been used to assess the NEM model in both steady-state and transient conditions.

The NEM models are based on two-energy-group diffusion theory equations with an option to choose between Cartesian and hexagonal geometry. Calculations include six delayed neutron precursor groups with definition for the delayed neutron precursor parameters in each spatial node. The NEM solution has incorporated assembly discontinuity factors. The solution method also accounts for the direct treatment of time dependence with an implicit integration scheme. To reproduce initial steady-state conditions, a core-modelling methodology was developed. Some of the NEM code's advanced features include the selection of up to six energy groups, 1-D decay heat model, and an efficient and flexible cross-section generation algorithm.

TRAB-3D (VTT, Finland)

TRAB-3D [1] is the latest member of the code system developed at VTT Energy for LWR reactor dynamics calculations. The neutron kinetics model of the new code is based on the three-dimensional VVER dynamics code HEXTRAN [2,3], but the nodal equations are solved in rectangular fuel assembly geometry, instead of hexagonal. In the neutronics solution the two-group nodal fluxes are constructed from two spatial modes, the asymptotic or fundamental mode and the transient mode. The former mode is approximated by polynomials and the latter by exponential functions. Also, flux discontinuity factors can be specified on the transverse interfaces of nodes. The nodal flux model of TRAB-3D contains eight degrees of freedom per group in a transverse cross-section and they are adjusted by continuity conditions for group fluxes and currents and for their first moments at nodal interfaces.

Thermal-hydraulics and fuel heat transfer models are the same as in the axially 1-D dynamics code TRAB [4], which includes descriptions of both the reactor core and the BWR cooling circuit. Thus the dynamic behaviour of the whole primary circuit of a reactor can be analysed with TRAB-3D. For PWR dynamics the core model of TRAB-3D is coupled with the SMABRE PWR circuit model.

Comparisons with fine-mesh finite difference calculations have shown that TRAB-3D solves the diffusion equations for homogeneous fuel assemblies of a two-dimensional reactor core with an accuracy of better than 1% in assembly powers. The validation history of TRAB-3D, so far, includes the calculation of OECD/NEACRP 3-D light water reactor benchmark problems and verification against measurements from real BWR plant transients. Much of the validation, however, has already been done by various calculations with HEXTRAN and TRAB since the same models for neutron kinetics and thermal-hydraulics description are used in TRAB-3D.

References

[1] Kaloinen, E., R. Kyrki-Rajamäki, "TRAB-3D a New Code for Three-dimensional Reactor Dynamics", *CD-ROM Proceedings of ICONE-5, 5th International Conference on Nuclear Engineering*, Nice, France, paper ICONE5-2197 (1997).

[2] Kyrki-Rajamäki, R., "HEXTRAN: Three-dimensional Reactor Dynamics Code for VVER-reactor Cores", *Proc. of the Int. Topical Meeting on Advances in Mathematics, Computations and Reactor Physics*, Pittsburgh, USA, American Nuclear Society, pp. 30.2 4-1 to 30.2 4-5 (1990).

[3] Kyrki-Rajamäki, R., "Three-dimensional Reactor Dynamics Code for VVER-type Nuclear Reactors", VTT Publications 246, Technical Research Centre of Finland, Espoo, Finland (Thesis for DrTech) (1995).

[4] Rajamäki, M., *TRAB. A Transient Analysis Program for BWR, Part 1. Principles*, Report 45, Technical Research Centre of Finland, Nuclear Engineering Laboratory, Helsinki, Finland (1980).

POLCA-T (Westinghouse, Sweden)

POLCA-T is a coupled 3-D core neutron-kinetics and system thermal-hydraulics computer code. The code is able to perform steady-state and transient analysis of BWR. The code is based to different extend on models and tools for BWR and PWR analysis used in POLCA7, BISON and RIGEL codes. The code utilises new advanced methods and models in neutron kinetics, thermal-hydraulics and numerics. The main features of the code can be summarised as follows:

- Full 3-D model of the reactor core: The neutronics models in the code are the same as those in the well-known static core analyser POLCA7 with addition of proper 3-D kinetics model.
- Advanced five-equation thermal-hydraulic model with thermal non-equilibrium description of the steam-water mixture and its coupling to the heat structures. Separate mass and energy balances of the phases. Drift flux model that can handle all flow regimes.
- Heat transfer model that works also in post-dry-out.
- The gas phase can consist of steam and non-condensable gases. The liquid phase can contain dissolved non-condensable gas.
- Boron transport model.
- Use of the same thermal-hydraulics model for core and plant systems.
- 2-D fuel rod heat transfer model, gas gap model consistent with design code and complete range of heat transfer regimes. Code is also able to model all plant heat structures.
- Dry-out and DNB correlations (using pin power distributions model).
- Full geometrical flexibility of the code: volume cells, flow paths, heat structures, materials, pumps, measurements, controls, etc. are all input data. Code is able to analyse different power plants and test facilities.
- Balance of plant, control and safety systems: The reactor pressure vessel, external pump loops, steam system and feedwater system, ECC systems and steam relief system are modelled to the desired details. Large and valuable set of input models that already exists can be used.
- Stable numerical method that allows long time steps, which is used also for steady-state solution. The low dependence on the size of the time step is due to the implicit numerical integration, which is close to second order by means of θ-weighting.

Due to the above-mentioned features POLCA-T code makes possible a comprehensive approach to plant analysis with full consistency in steady-state and transient calculations. The consistency in BWR core and system modelling, when transient analyses are performed, is also achieved by using the same basic model and the same design database for core data (cross-section data, burn-up, xenon and other 3-D distributions obtained from depletion calculations), fuel thermal-mechanical behaviour (properties) and system data. Thus full consistency is also possible between predicted core and system parameters and their behaviour over a very wide range of phenomena and processes important both for design and safety analyses.

The application areas of the POLCA-T code consist of three groups: BWR steady-state core design, BWR stability, transients and accident analyses and modelling of experimental test facilities.

Applications for BWR steady-state core design are covered by the POLCA7 wide-range capabilities regarding:

- evaluation of reactivity and power distribution at cold and hot core conditions;
- detailed thermal-hydraulic analysis;
- control operations (reactivity search modes: boron, power, flow, control rod, axial offset and minimum boron control);
- detectors simulation;
- evaluation of fuel pin and pellet powers and burn-up;
- evaluation of peaking factors based on pin results;
- dry-out and DNB margin calculations (based on pin power distributions);
- fission heat load parameters (margins) calculations;
- pellet cladding interaction calculations;
- depletion calculation with tracking of the most important fissile isotopes and fission products;
- fuel bundle, control rod, fuel channel and fixed in-core detectors depletion;
- shutdown margins evaluation;
- shutdown cooling;
- xenon transients;
- reactivity coefficients (void, burn-up, moderator temperature).

Applications to BWR safety analysis include operational transient, stability, RIA, ATWS, ATWC and LOCA as follows:

- feedwater flow increase/feedwater temperature decrease transients;
- loss of feedwater flow transients;
- pressure increase transients – analysis with regard to the cladding;
- pressure increase transients – analysis with regards to the reactor coolant pressure boundary;
- pressure decrease transients;
- re-circulation flow increase transients;
- re-circulation flow decrease transients;
- control rod withdrawal error;
- inadvertent loading transients;
- control rod drop accident;
- stability analysis;
- anticipated transients without scram (ATWS);
- anticipated transients without control rods (ATWC).

The POLCA-T code is well adapted to analyse the type of scenarios with a number of failing control rods. Boron transport model makes it possible also to analyse different types of boron shutdown scenarios. Applications to modelling of separate test facilities (such as FRIGG) are foreseen not only for code validation but also for pre-test analysis and experiments planning and optimisation.

References

Panayotov, D., U. Bredolt, P. Jerfsten, "POLCA-T – Consistent BWR Core and Systems Modelling", *ANS/AESJ/ENS Int. Conf. Top Fuel 2003*, Paper 410, Wurzburg (G), 16-19 March 2003.

Lindahl, S-Ö., E. Müller, "Status of ABB Atom's Core Simulator POLCA", *Int. Conf. PHYSOR96*, Mito, Japan, 16-20 September 1996.

Wijkström, H., "ABB Atom's New Code for 3-D Static and Transient Analysis", *Proceedings of the German Nuclear Society Workshop on Thermal and Fluid Dynamics, Reactor Physics and Computing Methods*, Rossendorf, Germany, 31 January-1 February 2000.

Panayotov, D., "OECD/NRC BWR Turbine Trip Benchmark: Simulation by POLCA-T Code", *PHYSOR2002 International Conference on the New Frontiers of Nuclear Technology: Reactor Physics, Safety and High-performance Computing*, Track H-2, Paper 3C-02, Seoul, Korea.

Appendix B

QUESTIONNAIRE FOR EXERCISE 2 OF THE OECD/NRC BWR TT BENCHMARK

QUESTIONNAIRE FOR EXERCISE 2

I. Thermal-hydraulic core model

a) Core thermal-hydraulic (T-H) model and nodalisation (1-D, 3-D and number of channels or cells) – how are channels/T-H cells chosen?
b) Bypass channel modelling?
c) Number of heat structures (fuel rods) modelled?
d) Which core thermal-hydraulic initial and transient boundary conditions are used and how?
e) Radial and axial heat structure (fuel rod) nodalisation?
f) Used correlations for fuel properties vs. temperature?

II. Core neutronics model

a) Number of radial nodes per assembly?
b) Axial nodalisation?
c) Radial and axial reflector modelling?
d) Cross-section interpolation procedure used?
e) Used method to get a critical reactor at the beginning of transient?
f) How xenon effect is modelled?
g) How Assembly Discontinuity Factor (ADF) is modelled?
h) Is bypass density correction used? If it is used, how it is modelled?
i) How decay heat modelling is modelled?

III. Coupling schemes

a) Hydraulics/heat structure spatial mesh overlays (mapping schemes in radial and axial plane)?
b) Hydraulics/neutronics spatial mesh overlays (mapping schemes in radial and axial plane)?
c) Heat structure/neutronics spatial mesh overlays mapping schemes in radial and axial plane)?
d) Temporal coupling scheme?
e) Coupling numerics – explicit, semi-implicit or implicit?
f) Coupling method – external or internal?
g) Coupling design – serial integration or parallel processing?

IV. General

a) User assumptions?
b) Specific features of the used codes?
c) Number of solutions submitted per participant and how they differ?

CRONOS2/FLICA4 (CEA, France)

I. Thermal-hydraulic core model

a) Core thermal-hydraulic (T-H) model and nodalisation (1-D, 3-D, and number of channels or cells) – how are channels/T-H cells chosen?

Two models were used (two sets of results): 33 channels, 1-D, as proposed by the benchmark specifications and 764 channels, 3-D, i.e. one channel per fuel assembly. In both cases, there are 37 axial nodes.

b) Bypass channel modelling?

One average bypass channel for the whole core.

c) Number of heat structures (fuel rods) modelled?

As many as channels, i.e. 33 and 764 heat structures.

d) Which core thermal-hydraulic initial and transient boundary conditions are used and how?

We have used the specified boundary conditions, mass flow and temperature at core inlet, pressure at core outlet. Temperature is actually converted into enthalpy, using the specified pressure at core inlet.

e) Radial and axial heat structure (fuel rod) nodalisation?

There are 10 radial nodes (6 in the fuel, 4 in the cladding) in each fuel rod, and 37 axial nodes.

f) Used correlations for fuel properties vs. temperature?

We have used the specified correlations for heat capacity, conductivity. Volumetric mass is constant versus temperature (cf. specifications).

II. Core neutronics model

a) Number of radial nodes per assembly?

764 radial nodes.

b) Axial nodalisation?

26 axial nodes.

c) Radial and axial reflector modelling?

The reflector has the same nodalisation as the fuel assemblies.

d) Cross-section interpolation procedure used?

CRONOS2 internal procedure, based on the same linear interpolation algorithm as specified.

e) Used method to get a critical reactor at the beginning of transient?

The fission is normalised by the steady-state eigenvalue.

f) How xenon effect is modelled?

Xenon is not modelled, that means we do not correct the cross-sections for xenon effect.

g) How Assembly Discontinuity Factor (ADF) is modelled?

ADF are not taken into account.

h) Is bypass density correction used? If it is used, how it is modelled?

Density is corrected for bypass as specified.

i) How decay heat modelling is modelled?

Decay heat is modelled as specified: total decay heat versus time from the specifications, and constant 3-D distribution (same as initial fission power).

III. Coupling schemes

a) Hydraulics/heat structure spatial mesh overlays (mapping schemes in radial and axial plane)?

There is one heat structure per hydraulic channel. The axial nodalisation is the same for hydraulic channels and heat structures.

b) Hydraulics/neutronics spatial mesh overlays (mapping schemes in radial and axial plane)?

For axial direction, we use a standard linear projection algorithm implemented in FLICA4. For radial direction, either the nodalisation is the same (764 channels), or (33 channels) a specific method was developed to lump the fuel assemblies.

c) Heat structure/neutronics spatial mesh overlays mapping schemes in radial and axial plane)?

Same as b).

d) Temporal coupling scheme?

The time step is the same for neutronics and thermal-hydraulics.

e) Coupling numerics – explicit, semi-implicit or implicit?

Semi-implicit.

f) Coupling method – external or internal?

External, using ISAS software.

g) Coupling design – serial integration or parallel processing?

Parallel processing.

IV. General

a) User assumptions?

None.

b) Specific features of the used codes?

?

c) Number of solutions submitted per participant and how they differ?

Two solutions were submitted. They differ only by thermal-hydraulics: 33 or 764 channels [cf. I.a)].

DYN3D (FZR, Germany)

I. Thermal-hydraulic core model

a) Core thermal-hydraulic (T-H) model and nodalisation (1-D, 3-D, and number of channels or cells) – how are channels/T-H cells chosen?

One T-H channel/fuel assembly.

b) Bypass channel modelling?

One average T-H channel for bypass in the core.

c) Number of heat structures (fuel rods) modeled?

One fuel rod/T-H channel.

d) Which core thermal-hydraulic initial and transient boundary conditions are used and how?

Total mass flow through the core and core bypass, inlet temperatures, core exit pressure.

e) Radial and axial heat structure (fuel rod) nodalisation?

10 radial and 24 equal axial nodes.

f) Used correlations for fuel properties vs. temperature?

Specified.

II. Core neutronics model

a) Number of radial nodes per assembly?

One node/assembly.

b) Axial nodalisation?

24 equal axial layers for the core and 2 layers for axial reflectors =26 layers.

c) Radial and axial reflector modelling?

Radial reflector modelled by assemblies, each of axial reflectors were modelled by one layer of 15.24 cm

d) Cross-section interpolation procedure used?

Yes.

e) Used method to get a critical reactor at the beginning of transient?

Eigenvalue k_{eff}.

f) How xenon effect is modelled?

Given Xe concentration.

g) How Assembly Discontinuity Factor (ADF) is modelled?

Explicitly.

f) Is bypass density correction used? If it is used, how it is modelled?

Bypass densities were taken into account by using the specified formula of cross-section calculation.

g) How decay heat modelling is modelled?

The own decay heat model of DYN3D was used by assuming a very long fuel cycle with the initial power distribution.

III. Coupling schemes

a) Hydraulics/heat structure spatial mesh overlays (mapping schemes in radial and axial plane)?

One fuel rod/T-H channel, 24 equal axial core layers.

b) Hydraulics/neutronics spatial mesh overlays (mapping schemes in radial and axial plane)?

One T-H channel/fuel assembly, 24 equal axial core layers.

c) Heat structure/neutronics spatial mesh overlays mapping schemes in radial and axial plane)?

One fuel rod/fuel assembly, 24 equal axial core layers.

d) Temporal coupling scheme?

Several neutronic time steps/T-H time step.

e) Coupling numerics – explicit, semi-implicit or implicit?

Explicit with iterations between neutronics and thermal-hydraulics.

f) Coupling method – external or internal?

Internal.

g) Coupling design – serial integration or parallel processing?

Serial integration.

IV. General

a) User assumptions?

Use of the implemented boiling model of Molochnikov.

b) Specific features of the used codes?

See code description.

c) Number of solutions submitted per participant and how they differ?

In addition to the three-dimensional solution a one-dimensional solution with cross-sections condensed from several steady-state calculations were submitted.

QUABOX/CUBBOX-ATHLET (GRS, Germany)

I. Thermal-hydraulic core model

a) Core thermal-hydraulic (T-H) model and nodalisation (1-D, 3-D, and number of channels or cells) – how are channels/T-H cells chosen?

33 T-H channels, as specified, and 765 T-H channels (764 fuel assemblies + 1 reflector assembly).

b) Bypass channel modelling?

One bypass channel.

c) Number of heat structures (fuel rods) modelled?

33 (one average fuel rod for each T-H channel), 764 (one average fuel rod for each T-H channel).

d) Which core thermal-hydraulic initial and transient boundary conditions are used and how?

As specified.

e) Radial and axial heat structure (fuel rod) nodalisation?

Axial: 24 nodes in active core and one node per upper and lower reflector, radial: one per assembly.

f) Used correlations for fuel properties vs. temperature?

Built-in ATHLET correlations (very similar to the specified).

II. Core neutronics model

a) Number of radial nodes per assembly?

1:1 modelling.

b) Axial nodalisation?

24+2 nodes.

c) Radial and axial reflector modelling?

Yes.

d) Cross-section interpolation procedure used?

Subr. lin4d.f – as specified.

e) Used method to get a critical reactor at the beginning of transient?

K_{eff} search, adjustment of fission cross-sections.

f) How xenon effect is modelled?

As specified (additional cross-section in the XS libraries).

g) How Assembly Discontinuity Factor (ADF) is modelled?

ADF is not modelled.

h) Is bypass density correction used? If it is used, how it is modelled?

Yes. Simplified model is developed based on non-boiling of the coolant in the bypass channels.

i) How decay heat modelling is modelled?

The specified table values are implemented.

III. Coupling schemes

a) Hydraulics/heat structure spatial mesh overlays (mapping schemes in radial and axial plane)?

1:1 scheme and as specified (33 T-H channels).

b) Hydraulics/neutronics spatial mesh overlays (mapping schemes in radial and axial plane)?

1:1 scheme.

c) Heat structure/neutronics spatial mesh overlays mapping schemes in radial and axial plane)?

1:1 scheme and as specified (33 T-H channels).

d) Temporal coupling scheme?

Specific synchronisation of time-step.

e) Coupling numerics – explicit, semi-implicit or implicit?

Serial, semi-implicit.

f) Coupling method – external or internal?

Internal.

g) Coupling design – serial integration or parallel processing?

Serial.

IV. General

a) User assumptions?

No.

b) Specific features of the used codes?

No.

c) Number of solutions submitted per participant and how they differ?

Only one solution with 764 T-H channels.

DNB-3D (NETCORP, USA)

I. Thermal-hydraulic core model

a) Core thermal-hydraulic (T-H) model and nodalisation (1-D, 3-D, and number of channels or cells) – how are channels/T-H cells chosen?

The core T-H model is a 1-D homogeneous equilibrium model that consists of 185 channels with each channel essentially representing 4 fuel bundles. Each T-H channel has 24 equal length axial nodes. The void distribution that is used in the neutronic calculations uses a profile fit model to obtain the effects of slip.

b) Bypass channel modelling?

The core bypass is represented by 1 channel that has a single axial node.

c) Number of heat structures (fuel rods) modelled?

There is 1 average fuel rod per T-H channel. Each fuel rod has 24 axial nodes that correspond to the T-H nodes. Each fuel node is modelled by 7 concentric rings (5 in the oxide and 2 in the cladding).

d) Which core thermal-hydraulic initial and transient boundary conditions are used and how?

The initial and transient boundary conditions that were used corresponded to those provided in the final specification and/or on the ftp site. The core inlet temperature and core inlet and outlet pressures were used as input to calculate the core inlet enthalpy and core average pressure. The flow distribution amongst the T-H channels was calculated based on the channel flow distribution provided in the final specification and/or on the ftp site.

e) Radial and axial heat structure (fuel rod) nodalisation?

See I.c) above.

f) Used correlations for fuel properties vs. temperature?

The fuel properties as contained in the final specification were used.

II. Core neutronics model

a) Number of radial nodes per assembly?

The core neutronic nodalisation was identical to the core T-H nodalisation, i.e. there were 185 radial nodes and 24 axial nodes per radial node.

b) Axial nodalisation?

See II.a) above.

c) Radial and axial reflector modelling?

The radial and axial reflector modelling used albedo boundary conditions for the core nodes at the reflector interfaces.

d) Cross-section interpolation procedure used?

The cross-section interpolation procedure was the one provided with the cross-sections; i.e. lint4d.f.

e) Used method to get a critical reactor at the beginning of transient?

The initial criticality was established by an iterative eigenvalue calculation using a source over-relation method.

f) How xenon effect is modelled?

Xenon was modelled directly through the cross-sections provided in the final specification.

g) How Assembly Discontinuity Factor (ADF) is modelled?

ADF was not modelled. Cross-sections provided in the final specification were used without applying these factors.

h) Is bypass density correction used? If it is used, how it is modelled?

The core bypass density correction was not applied.

i) How decay heat modelling is modelled?

The decay heat was modelled using the core average value provided by the final specifications and distributing it throughout the core based on the initial relative power distribution.

III. Coupling schemes

a) Hydraulics/heat structure spatial mesh overlays (mapping schemes in radial and axial plane)?

There is a direct one-to-one relationship between the T-H and heat structure nodes, so that there are no spatial overlays per se.

b) Hydraulics/neutronics spatial mesh overlays (mapping schemes in radial and axial plane)?

There is a direct one-to-one relationship between the T-H and neutronic nodes, so that there are no spatial overlays per se.

c) Heat structure/neutronics spatial mesh overlays mapping schemes in radial and axial plane)?

There is a direct one-to-one relationship between the heat structure and neutronic nodes, so that there are no spatial overlays per se.

d) Temporal coupling scheme?

The temporal coupling scheme consists of solving the T-H, heat structure and neutronic models for a user-specified fixed time step. Each model is solved independently, and feedback effects are updated at the beginning of the next time step. The T-H and heat structure calculations utilise a Runge-Kutta 5th-order solution technique, while the neutronic calculations employ a semi-implicit technique.

e) Coupling numerics – explicit, semi-implicit or implicit?

The coupling numeric calculations are explicit as indicated in III.d) above.

f) Coupling method – external or internal?

The coupling calculations are performed internally.

g) Coupling design – serial integration or parallel processing?

The coupling calculations are performed using serial integration.

IV. General

a) User assumptions?

The model utilises 1 channel to represent essentially 4 fuel bundles. Thus, each channel is used to compute the average power for the 4 fuel bundles it represents. That average power is distributed over the 4 bundles based on the initial relative power distribution provided in the final specification and/or on the ftp site.

b) Specific features of the used codes?

The T-H calculations are based on a 1-D homogeneous equilibrium model; however the void distribution that is used in the neutronic calculations uses a profile fit model to obtain the effects of slip.

c) Number of solutions submitted per participant and how they differ?

Not applicable, since only one solution was submitted.

TRAC-BF1/COS3D (NFI, Japan)

I. Thermal-hydraulic core model

a) Core thermal-hydraulic (T-H) model and nodalisation (1-D, 3-D, and number of channels or cells) – how are channels/T-H cells chosen?

1-D, 33 channels, 24 nodes per active fuel length. Radial T-H nodalisation is the same as the radial map shown in Figure 3.2.2 of BWRTT specifications.

b) Bypass channel modelling?

No.

c) Number of heat structures (fuel rods) modelled?

Answer: 4 types of fuel assembly are modelled based on Figures 2.2.2, 2.2.3, 2.2.4 and 2.2.5 of BWRTT specifications.

7×7	49 fuel rods
8×8-100mil channel	63 fuel rods and 1 water rod
8×8-120mil channel	63 fuel rods and 1 water rod
8×8 LTA	62 fuel rods and 2 water rods

d) Which core thermal-hydraulic initial and transient boundary conditions are used and how?

Core thermal-hydraulic initial and transient boundary conditions are provided as specifications, that is, initial and transient channel inlet flow rate and outlet pressure. We use these specifications directly to conditions of 33 channels like Figure 3.2.1 of BWRTT specification.

e) Radial and axial heat structure (fuel rod) nodalisation?

Radial direction: 5-mesh for fuel pellet, 1 for gap region and 2 for fuel rod, axial direction: 24 node.

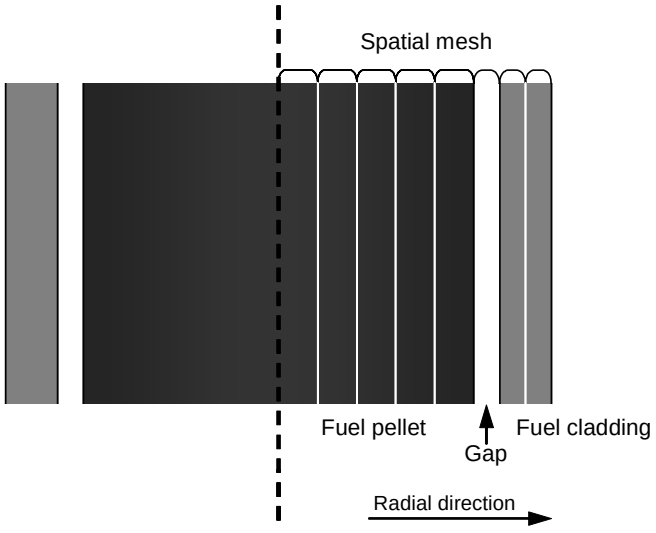

f) Used correlations for fuel properties vs. temperature?

Fuel properties are used based on Section 3.3 of BWRTT specifications.

II. Core neutronics model

a) Number of radial nodes per assembly?

One.

b) Axial nodalisation?

24 nodes per active fuel length.

c) Radial and axial reflector modelling?

We assume that the neutron flux at the reflector centre is equal to 0.0.

d) Cross-section interpolation procedure used?

Provided cross-section interpolation procedure is used.

e) Used method to get a critical reactor at the beginning of transient?

We get the initial steady state by null transient calculation.

f) How xenon effect is modelled?

Provided xenon density is used. We assume that xenon density is constant during the transient.

g) How Assembly Discontinuity Factor (ADF) is modelled?

ADF is not used.

h) Is bypass density correction used? If it is used, how it is modelled?

No.

i) How decay heat modelling is modelled?

Decay heat model is not included in Exercise2.

III. Coupling schemes

a) Hydraulics/heat structure spatial mesh overlays (mapping schemes in radial and axial plane)?

Hydraulics/heat structure (fuel rod) spatial mesh (fuel rod group) is one. Radial peaking is not considered.

b) Hydraulics/neutronics spatial mesh overlays (mapping schemes in radial and axial plane)?

The spatial mesh is the same as the radial map shown in Figure 3.2.2 of the BWRTT specifications.

c) Heat structure/neutronics spatial mesh overlays mapping schemes in radial and axial plane)?

Number of radial neutronics spatial mesh is 1 per assembly, therefore with regard to neutronics calculation the heat structure inner assembly is not considered.

d) Temporal coupling scheme?

e) Coupling numerics – explicit, semi-implicit or implicit?

Explicit.

f) Coupling method – external or internal?

External.

g) Coupling design – serial integration or parallel processing?

Serial integration.

IV. General

a) User assumptions?

Nothing special.

b) Specific features of the used codes?

NFI's code system used for this benchmark is TRAC-BF1/COS3D, which is a coupled system of TRAC-BF1 and 3-D core simulator, COS3D. COS3D adopts the modified one-group neutronics model. Therefore, we use one-group cross-sections which are collapsed from two-group macroscopic cross-sections provided for this benchmark. The adequacy of this method has been verified by means of the comparison between one-group and two-group model analyses.

c) Number of solutions submitted per participant and how they differ?

One solution submitted.

TRAC-BF1/SKETCH-INS (NUPEC, Japan)

I. Thermal-hydraulic core model

a) Core thermal-hydraulic (T-H) model and nodalisation (1-D, 3-D, and number of channels or cells) – how are channels/T-H cells chosen?

The reactor pressure vessel is modelled in 1-D cylindrical coordinates with one radial ring and three axial levels. Thermal-hydraulic channels were treated as 1-D, 33 parallel channels according to Figure 3.2.2 in the final specifications.

b) Bypass channel modelling?

The reactor vessel simulated core bypass region. The core bypass flow was simulated with a leak path model from T-H channel to the vessel (core bypass) region. Gamma heating in the bypass region was neglected.

c) Number of heat structures (fuel rods) modelled?

33 heat structures, i.e. one heat structure for one T-H channel.

d) Which core thermal-hydraulic initial and transient boundary conditions are used and how?

Table 5.2.1 in the final specifications was used for the initial condition. During the transient, the following boundary conditions are used, the data for which were obtained from CD-ROM: core inlet total flow rate, core inlet flow temperature, core exit pressure.

e) Radial and axial heat structure (fuel rod) nodalisation?

Radial: pellet 10 rings, gap 1 ring, crud 2 rings, axial: 24 nodes.

f) Used correlations for fuel properties vs. temperature?

MATPRO in TRAC-BF1, which is consistent with the final specifications.

II. Core neutronics model

a) Number of radial nodes per assembly?

One node.

b) Axial nodalisation?

24 nodes.

c) Radial and axial reflector modelling?

Radial: 1 node (Figure 2.4.2), axial: bottom 2 nodes, top one node.

d) Cross-section interpolation procedure used?

Cross-section was fitted as a pronominal function of coolant density and fuel temperature.

e) Used method to get a critical reactor at the beginning of transient?

k_{eff} was set 1 at the beginning of transient.

f) How xenon effect is modelled?

Xenon absorption is excluded at HZP. Absorption cross-section with xenon absorption is used at HP and transient.

g) How Assembly Discontinuity Factor (ADF) is modelled?

Same as the Code Smith model.

h) Is bypass density correction used? If it is used, how it is modelled?

Not used.

i) How decay heat modelling is modelled?

Same as the ANS-1979.

III. Coupling schemes

a) Hydraulics/heat structure spatial mesh overlays (mapping schemes in radial and axial plane)?

Radial: One heat structure per one T-H channel, axial: same noding.

b) Hydraulics/neutronics spatial mesh overlays (mapping schemes in radial and axial plane)?

Radial: 33 T-H channels/764 neutronic channels, axial: same noding.

c) Heat structure/neutronics spatial mesh overlays mapping schemes in radial and axial plane)?

Radial: 33 heat structure/764 neutronic channels, axial: same noding.

d) Temporal coupling scheme?

PVM coupling scheme.

e) Coupling numerics – explicit, semi-implicit or implicit?

Explicit.

f) Coupling method – external or internal?

External.

g) Coupling design – serial integration or parallel processing?

Parallel processing.

IV. General

a) User assumptions?

None.

b) Specific features of the used codes?

Polynomial and semi-analytical nodal method based on the non-linear iteration procedure (Zimin, *et al*., 1998) is used for spatial integration of diffusion equations. Time integration of the neutron kinetics equations is performed by the fully implicit scheme.

Zimin, V.G., H. Ninokata, L. Pogosbekyan, "Polynomial and Semi-analytic Nodal Methods for Non-linear Iteration Procedure", *Proc. ANS Int. Conf. on the Physics of Nuclear Science and Technology (PHYSOR)*, Long Island, New York, 5-8 October 1998, Vol. 2, pp. 994-1002 (1998).

c) Number of solutions submitted per participant and how they differ?

One solution submitted.

RETRAN-3D (PSI, Switzerland)

I. Thermal-hydraulic core model

a) Core thermal-hydraulic (T-H) model and nodalisation (1-D, 3-D, and number of channels or cells) – how are channels/T-H cells chosen?

In the core region, the flow from the lower plenum is mainly to the core inlet volume, with a small fraction of the total core flow flowing through the core bypass volume. From the core inlet volume, most of the coolant flows into the core, while again a small amount enters the core bypass volume. The core region is represented by 34 thermal-hydraulic channels, each with 24 axial nodes, and the flow through each channel corresponds to the combined flow through a certain number of fuel assemblies. The steam/water mixture flowing out of the top of the core channels flows into a single core exit volume and from there into the upper plenum, where it mixes with the core bypass flow.

Figure 1. Nodalisation of the core region

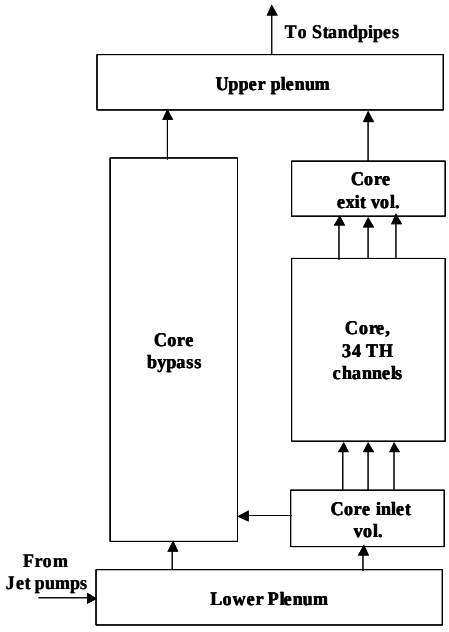

It consists of the core, the core inlet volume, the core exit volume and the core bypass volume. 34 thermal-hydraulic channels represent the core itself, where each channel consists of 24 axially stacked volumes levels. In the PSI methodology, the input required for RETRAN-3D to perform a 3-D core calculation consists of three separate input files, two of which are prepared by CORETRAN, and the remaining one forms part of the normal RETRAN-3D input structure. The two files prepared by CORETRAN consist of a transient cross-section (tcs) file, and a file containing geometric information for all the individual fuel assemblies (cdi or CORETRAN Data Interface file). The additional information contained within the standard RETRAN input includes a “map” which allocates each reactor fuel assembly to a given RETRAN core hydraulic channel (a total of 34 such channels were used in the present analysis, see below). Thus, prior to the RETRAN-3D calculation, a CORETRAN static calculation of Phase 2 (see above) was performed to provide well-founded parameters for the 3-D core. Accordingly, in the benchmark Phase II and III calculations, the neutronics

parameters of each of the 764 fuel assemblies have been entered at 24 axial levels. The combining, or “lumping”, of the flow through these assemblies into the 34 thermal-hydraulic channels is that suggested in the benchmark specification (Figure 3.2.2 in Solis, *et al*., 2001), except that since RETRAN-3D will not combine assembly types with different numbers of fuel rods within the same hydraulic channel, Channel 26 in [Solis, *et al*., Figure 3.2.2] was subdivided into two separate channels: Number 26 (for the 4 outermost fuel assemblies with Assembly Design 5 [Solis, *et al*., Figure 2.4.2]), and Number 34 (for the 4 innermost fuel assemblies with Assembly Design 4).

Figure 2. Thermal-hydraulic channel radial map, with Channels 10, 34 highlighted

The + symbols represent differently inserted control rods

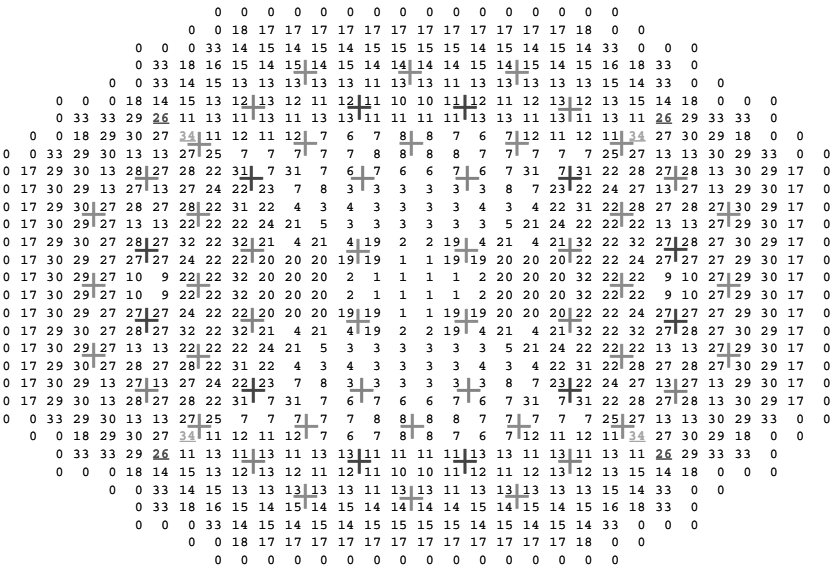

b) Bypass channel modelling?

The core bypass (as in the Phase I calculation) is modelled as a RETRAN-3D volume, which is connected to the lower plenum, core inlet and upper plenum volumes. For the coupling of the thermal-hydraulics with the neutronics calculations in the core, the RETRAN-3D code separates the core bypass volume into 24 axially stacked volumes.

c) Number of heat structures (fuel rods) modelled?

The flow in the core is lumped into 34 thermal-hydraulic channels at 24 axial levels and an additional bypass channel and the same number heat structures (34*24) are modelled by RETRAN-3D. Bypass heating is taken into account.

d) Which core thermal-hydraulic initial and transient boundary conditions are used and how?

We have submitted two solutions using RETRAN-3D, called PSI-A and PSI-B. The RETRAN-3D solutions described in this section read initial conditions from CORETRAN, including the flow distributions in the thermal-hydraulics channels. From the initial flow distributions the loss coefficients are also calculated and used for the transient calculation in RETRAN-3D.

For both RETRAN-3D calculations the upper plenum pressure is used as (outlet) boundary condition and the same lower plenum fluid enthalpy is used. In the PSI-A calculation the pressure in the lower plenum is used as the inlet boundary condition. In a second option, PSI-B, the total flow rate through the lower plenum into the core region, i.e. the sum of the core and bypass flows, is used as the inlet boundary condition into the lower plenum.

e) Radial and axial heat structure (fuel rod) nodalisation?

The flow in the core is lumped into 34 thermal-hydraulic channels at 24 axial levels and an additional bypass channel and the same number heat structures (34*24) are modelled by RETRAN-3D. Each of these heat structures is defined to consist of fuel, gap and cladding.

f) Used correlations for fuel properties vs. temperature?

All specified correlations for fuel and cladding properties have been used.

II. Core neutronics model

a) Number of radial nodes per assembly?

Same radial nodalisation as in CORETRAN, see PSI CORETRAN questionnaire.

b) Axial nodalisation?

Same axial nodalisation as in CORETRAN, see PSI CORETRAN questionnaire.

c) Radial and axial reflector modelling?

Same procedure as in CORETRAN, see PSI CORETRAN questionnaire.

d) Cross-section interpolation procedure used?

Same procedure as in CORETRAN, see PSI CORETRAN questionnaire.

e) Used method to get a critical reactor at the beginning of transient?

Same procedure as in CORETRAN, see PSI CORETRAN questionnaire.

f) How xenon effect is modelled?

Same procedure as in CORETRAN, see PSI CORETRAN questionnaire, except that xenon number distributions are read from an additional RETRAN-3D input file.

g) How Assembly Discontinuity Factor (ADF) is modelled?

Same procedure as in CORETRAN, see PSI CORETRAN questionnaire.

h) Is bypass density correction used? If it is used, how it is modelled?

Same procedure and assumptions as applied for the PSI CORETRAN calculation, except that bypass heating is taken into account and noting that the actual nodal moderator density is obtained from the RETRAN-3D channel hydraulic solution and that the bypass conditions are calculated using the non-conducting heat exchanger option.

i) How decay heat modelling is modelled?

The RETRAN-3D decay heat model used is based on the 1979 ANS standard.

III. Coupling schemes

a) Hydraulics/heat structure spatial mesh overlays (mapping schemes in radial and axial plane)?

A total of 34 heat structures are used to model an average fuel pin in each of the 34 heated thermal-hydraulic channels (see next question). The radial distribution of the fuel pins hence corresponds to the thermal-hydraulic channel representation. For the axial nodalisation, each fuel pin is discretised in a similar manner as the corresponding thermal-hydraulic channel, i.e. 24 axial volumes.

b) Hydraulics/neutronics spatial mesh overlays (mapping schemes in radial and axial plane)?

All of the 764 fuel assemblies are modelled as single neutronic channels mapped on 34 thermal-hydraulic channels. For the axial nodalisation, 24 uniform volumes nodes are consistently used in the neutronic and thermal-hydraulic representation of the active fuel part.

c) Heat structure/neutronics spatial mesh overlays mapping schemes in radial and axial plane)?

Same as above, see a) and b).

d) Temporal coupling scheme?

The complete mathematical model used in RETRAN-3D consists of a very large system of differential and algebraic equations that describe the numerous physical phenomena that occur in complex thermal-hydraulic systems. A variety of numerical methods are required due to the nature of the equations that make up the complete RETRAN-3D model and the wide range of analyses for which the code is used. The differential equation models in RETRAN-3D include:

- mass, momentum, and energy equations for the coolant fluid;
- conduction equation for heat transfer in solids;
- multi-dimensional (3-D) kinetics for power generation in the core;
- model equations for some equipment components and special physical processes.

In general, these equations are coupled in the following manner. The neutron kinetics equations give the power generated in the fuel rods, which provides the internal volumetric heat generation rate for the conduction equations for the fuel rods. In this application the Coarse Mesh Finite Difference (CMFD) non-linear iteration procedure is used, where the local two-node problems are solved using a Nodal Expansion Method (NEM). The coupling between the kinetics and the heat conduction equations is explicit. The heat conduction solution uses implicit coupling between the heat transfer correlations and the source term for the energy equations. Feedback between the thermal-hydraulic equations and the kinetics equations is also treated explicitly in this application.

e) Coupling numerics – explicit, semi-implicit or implicit?

Explicit coupling, see also answer to d).

f) Coupling method – external or internal?

Internal coupling.

g) Coupling design – serial integration or parallel processing?

Serial integration.

IV. General

a) User assumptions?

For the benchmark calculation the same bypass density correction has been implemented in RETRAN-3D as for the PSI CORETRAN calculation and consequently also a uniform flow area ratio is assumed.

b) Specific features of the used codes?

For the core bypass heating the non-conducting heat exchanger option in RETRAN-3D is used. An effective core bypass density correction is implemented according to the benchmark specifications in RETRAN-3D as in CORETRAN, which is non-standard for both codes. The same thermal fuel and cladding properties as before in CORETRAN have been entered in RETRAN-3D using tables. An algebraic slip equation based on drift flux model of Chexal-Lellouche (recommended option) is used for the thermal-hydraulic calculation. The neutron void reactivity is calculated from profile fit equation.

c) Number of solutions submitted per participant and how they differ?

We submitted two solutions using RETRAN-3D, called PSI-A and PSI-B. Both RETRAN-3D calculations differ in the inlet boundary condition only. (Thus in particular the hot zero power (HZP) calculation is identical for cases.) In the PSI-A calculation the pressure in the lower plenum is used as the inlet boundary condition. In a second option, PSI-B, the total flow rate through the lower plenum into the core region, i.e. the sum of the core and bypass flows, is used as the inlet boundary condition into the lower plenum. Both calculations use the same lower plenum fluid enthalpy provided in the benchmark specifications for the inlet boundary condition. The inlet pressure boundary condition case PSI-A results in a slightly smaller inlet flow rate for the core (relative to the flow boundary condition case PSI-B). In addition, the core exit flow rate is also reduced. Together, this results in a slightly reduced net flow of water into the core region before the time of the power maximum, which in turn means a smaller increase in the (void) reactivity. These slight differences in the flow behaviour lead to a power peak for the pressure boundary condition case about 20% lower than that for the flow boundary condition case. This illustrates the sensitivity of the power peak to small changes in the system parameters; namely, in the lower plenum flow rate and pressure.

CORETRAN-3D (PSI, Switzerland)

I. Thermal-hydraulic core model

a) Core thermal-hydraulic (T-H) model and nodalisation (1-D, 3-D, and number of channels or cells) – how are channels/T-H cells chosen?

The CORETRAN code consists of the ARROTTA module for the neutronics calculations and the VIPRE-02 module for the thermal-hydraulic (T-H) solution. For Peach Bottom 2, a full core T-H representation is used through VIPRE-02, i.e. 764 parallel channels are modelled. Each of these channels corresponds to one unique neutronic channel, i.e. fuel assembly modelled in ARROTTA. However, to take into account the unheated zones at the assembly inlet and outlet, the axial nodalisation for the T-H channels differ slightly from the neutronic one as shown in the figure below. It is important to emphasise that in the active fuel axial zone, the same nodalisation is used for a neutronic channel and its corresponding T-H channel. Moreover, an additional T-H channel is modelled in VIPRE-02 to represent the bypass region (see answer to question b). Parallel (1-D) flow is assumed in each channel.

Figure 1. CORETRAN neutronic and T-H full core representation

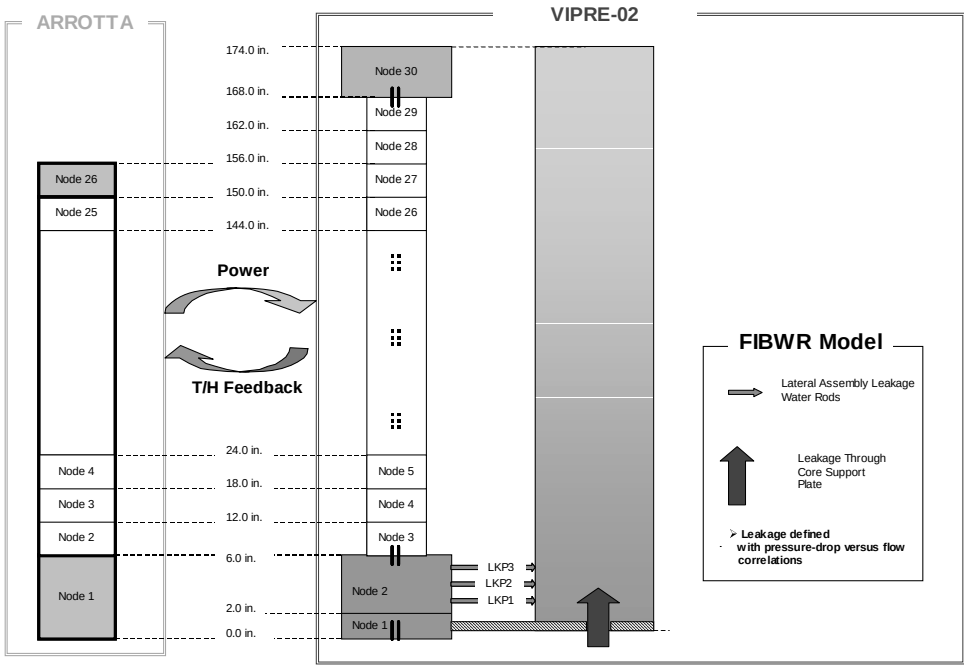

b) Bypass channel modelling?

The bypass channel is in CORETRAN only implemented in the T-H model (i.e. VIPRE-02). This is done by modelling, in addition to the 764 individual flow channels, an extra T-H channel to represent the bypass region. The geometry required for this extra channel is the flow area and the wetted perimeter. This data is derived by lumping the following unheated coolant regions in the core:

- between fuel assemblies;
- between the peripheral fuel assemblies and the core shroud.

The intra-assembly bypass, i.e. the water rods are not taken into account for this bypass channel. To derive the geometry of the bypass channel, the diameter of the core shroud D_{CS} was estimated from Figure 25 in the EPRI Report NP-563 (Larsen, N.H., *Core Design and Operating Data for Cycle 1 and 2 of Peach Bottom 2*) as follows:

$$D_{CS} \approx 220.47 \text{ in.} = 5.6 \text{ m}$$

Thereafter, the assembly outer pitch was estimated, assuming it uniform for all channels, as:

$$P_{OUT} \approx 5.374. \text{ in.} = 0.1365 \text{ m}$$

The bypass area was thereafter calculated, without including the area for water rods, as:

$$A_{BYP} = \pi \cdot \left(\frac{D_{CS}}{2} \right)^2 - \left(764 \cdot P_{OUT}^2 \right) \approx 21.7 - 14.235 \approx 7.464 \text{ m}^2 = 11569.22 \text{ in.}$$

Similarly, the wetted perimeter was calculated as:

$$WP_{BYP} = \left[2 \cdot \pi \cdot \left(\frac{D_{CS}}{2} \right) \right] + \left[764 \times 4 \times P_{OUT} \right] \approx 433.67 \text{ m}$$

c) Number of heat structures (fuel rods) modelled?

For each T-H flow channel (except the bypass), the geometry and the number of fuel pins are explicitly defined for each T-H axial node, based on the benchmark specifications [1] for the fuel design type of the T-H given channel. However, in the active zone, VIPRE-02 uses an average-pin when solving the fuel heat conduction equations. Hence for the 764 T-H channels, a single "average" fuel pin is used yielding a total of 764 heat structures.

d) Which core thermal-hydraulic initial and transient boundary conditions are used and how?

For the steady-state results, a flow split option is used to determine the coolant flow in each T-H channel including the bypass channel. The boundary conditions are the uniform core inlet temperature, the total core inlet mass flow and the uniform core exit pressure.

For the transient analysis, the specified time-dependant functions for the uniform core inlet temperature, the channel inlet mass flow for all 764 plus bypass channel ("reconstructed" from the specified flow for 33 channel groups) and the uniform core exit pressure are used.

e) Radial and axial heat structure (fuel rod) nodalisation?

Axial heat conduction is neglected and only radial conduction is taken into account. The pellet is discretised in 6 concentric mesh rings, 2 rings are used for the gap and the cladding. Axially, each fuel pin is discretised in 24 equal-sized nodes.

f) Used correlations for fuel properties vs. temperature?

All specified correlations for fuel and cladding properties have been used.

II. Core neutronics model

a) Number of radial nodes per assembly?

A 1 × 1 radial assembly mesh is used (i.e. 1 radial node per assembly).

b) Axial nodalisation?

The neutronics model contains 24 active nodes and two reflector nodes (bottom and top). All nodes have equal size.

c) Radial and axial reflector modelling?

Both radial reflectors and axial reflectors are explicitly modelled. The geometry and nodalisation for the radial reflectors is identical to the one used for the active fuel assemblies and contains hence 26 axial nodes (i.e. 24 + 2 reflector nodes).

d) Cross-section interpolation procedure used?

The specified cross-section tables and the provided interpolation routine have been implemented and used.

e) Used method to get a critical reactor at the beginning of transient?

Normalisation of the fission cross-section with the initial (steady-state) K_{eff} value.

f) How xenon effect is modelled?

A SIMULATE summary file containing the nodal xenon number density distributions was provided by the benchmark organisers and used to define a CORETRAN restart file containing only the xenon nodal distributions (i.e. all other distributions set to zero). Then, a two-step procedure was used for the xenon correction during the cross-section evaluation.

Step 1: Evaluate the thermal macroscopic absorption cross-section with no xenon as:

$$\Sigma_{a,2}^{NoXe} = \Sigma_{a,2} - \Sigma_{Xe}$$

where $\Sigma_{a,2}$ is the thermal absorption cross-section (interpolated from the specified cross-section data tables) and Σ_{Xe} is the macroscopic xenon cross-section (interpolated from the specified cross-section data tables).

Step 2: Compute the corrected thermal absorption macroscopic cross-section as:

$$\Sigma_{a,2}^{Corr} = \Sigma_{a,2}^{NoXe} + n_{Xe} \cdot \sigma_{Xe}$$

where n_{Xe} is the (nodal) xenon number density read from the restart file, σ_{Xe} is the xenon microscopic cross-section (interpolated from the specified cross-section data tables) and $\Sigma_{a,2}^{NoXe}$ is the nodal macroscopic thermal absorption cross-section with no xenon (obtained from Step 1).

g) How Assembly Discontinuity Factor (ADF) is modelled?

The ADFs are modelled to correct for heterogeneous flux condition at the interfaces. They are treated as all other specified cross-sections (i.e. tables and interpolation procedure).

h) Is bypass density correction used? If it is used, how it is modelled?

The bypass density correction is applied with a two-step procedure.

Step 1: First, the nodal moderator density (for an active fuel node) obtained from the T-H solution is corrected to take into account bypass density changes as follows:

$$\rho_{act}^{eff} = \rho_{act} + \frac{A_{Byp}}{A_{act}} \cdot \left(\rho_{byp} - \rho_{sat}\right)$$

where ρ_{act} is the nodal density calculated by VIPRE-02, ρ_{byp} and ρ_{sat} are the bypass actual and saturation density respectively and $\frac{A_{Byp}}{A_{act}}$ is the ratio of the bypass flow are to the active flow area.

Step 2. The corrected moderator density of step 1 is then used by the neutronic module to evaluate the cross-sections (i.e. by interpolation from specified tables).

Note 1. An approximation is made by using a uniform bypass-to-active area ratio $\frac{A_{Byp}}{A_{act}}$ for all active nodes based on the observation that fuel type design 2 and 3 were the predominant assembly types. Hence, the geometry of these bundles was considered significantly representative for all fuel channels. The geometry for the fuel design type 2 is shown in figure below.

Figure 2. Geometry of fuel type 2 with surrounding bypass water

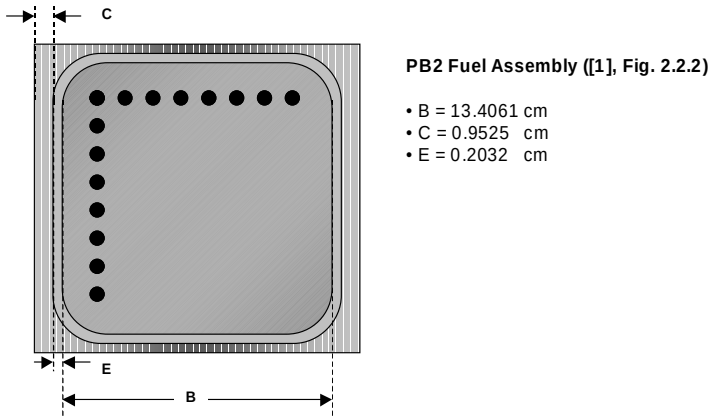

To derive the ratio based on the geometry above, a constant gap between fuel channels was assumed and the eventual presence of control rod blades was neglected. The assumed gap was chosen as D = 2*C. Thereafter, the ratio used for all fuel nodes is evaluated as:

$$A_{Ratio} = \frac{A_{byp}}{A_{act}} = \frac{\left(B + 2 \cdot C + 2. \cdot E\right)^2 - \left(B + 2E\right)^2}{FA} \approx 0.56141$$

where *FA* is the active fuel channel area which for simplicity was defined as constant for all channels with the value *FA*= 100 cm^2.

Note 2. The bypass heating (1.7%) is not applied.

i) How decay heat modelling is modelled?

The decay heat model is not used.

III. Coupling schemes

a) Hydraulics/heat structure spatial mesh overlays (mapping schemes in radial and axial plane)?

There are 764 thermal-hydraulic channels (one for each fuel assembly) and corresponding 764 heat structures (an average fuel pin is computed from the intra-nodal pin layout description and geometry). The heat structures are only modelled in the active part of the core where the same axial nodalisation as for the T-H channel representation is used.

b) Hydraulics/neutronics spatial mesh overlays (mapping schemes in radial and axial plane)?

Neutronically, 764 active "channels" are used for the fuel assemblies (plus additional radial reflectors). Thermal-hydraulically, there are 764 "channels" plus an additional bypass channel. Each of the 764 neutronic channels is coupled to a single T-H channel. The neutronic reflectors channels and the T-H bypass channel are not coupled. The axial nodalisation for the active zone of each channel is identical in the neutronics and the T-H representation (see further details provided with answer to Question I).

c) Heat structure/neutronics spatial mesh overlays mapping schemes in radial and axial plane)?

Same as above [answers a) and b)]

d) Temporal coupling scheme?

The neutronics are solved by the ARROTTA module using the Analytical Nodalisation Method and an implicit (Crank-Nicholson) temporal discretisation scheme. The VIPRE-02 module handles the thermal-hydraulics, in solving both of the fuel heat conduction equations and the channel hydraulics. Fuel heat conduction equations are solved using a semi-implicit method. The channel hydraulics solution scheme is based on a 6-equation, 2-fluid formulation solved using a fully implicit procedure.

e) Coupling numerics – explicit, semi-implicit or implicit?

Explicit coupling between the T-H module (VIPRE-02) and the neutronic module (ARROTTA). Within the T-H solution scheme, an iterative procedure is used between the fuel heat conduction and the channel hydraulic solutions until temperatures, heat fluxes and flows are converged.

f) Coupling method – external or internal?

CORETRAN uses an internal coupling between ARROTTA and VIPRE-02. CORETRAN is used as a stand-alone, i.e. not coupled with an external code. The specified thermal-hydraulic boundary conditions are applied to the core inlet and the core outlet via the VIPRE-02 module.

g) Coupling design – serial integration or parallel processing?

CORETRAN uses a serial integration procedure.

IV. General

a) User assumptions?

The following assumptions were made:

- approximate reactor and assembly data to derive the bypass channel geometry [see answer to Question I.b)];
- uniform flow area ratio (i.e. applied to all active core nodes) for the bypass density correction [see answer to Question II.h)].
- bypass heating of 1.7% was neglected [see answer to Question II.h)].

b) Specific features of the used codes?

The nominal CORETRAN version used is CORETRAN-01 MOD001 (Nov. 2000). However, several modifications were implemented to comply with the benchmark specification:

- VIPRE-02 internal fuel and cladding property tables have been replaced by specified correlations [see answer to Question I.f)].
- The CORETRAN nominal cross-section model was replaced by using specified cross-section tables and interpolation routine [see answer to Question II.d)].
- The bypass density correction is not normally used in CORETRAN and was only implemented for this benchmark [see answer to Question II.h)].

c) Number of solutions submitted per participant and how they differ?

One CORETRAN solution for the steady-state analysis and one solution for the transient analysis were submitted.

TRAC-BF1/NEM (PSU, USA)

I. Thermal-hydraulic core model

a) Core thermal-hydraulic (T-H) model and nodalisation (1-D, 3-D, and number of channels or cells) – how are channels/T-H cells chosen?

Based on 1-D TRAC-BF1 model 33 core channels were connected 33 BREAK components at the core inlet and 33 BREAK components at the core outlet. In addition to the core channels two bypass channels were modelled in order to simulate core bypass flow phenomena

b) Bypass channel modelling?

Two bypass channels one for centre orifice and another for peripheral orifice.

c) Number of heat structures (fuel rods) modelled?

One per channel.

d) Which core thermal-hydraulic initial and transient boundary conditions are used and how?

Core inlet and outlet pressure boundary conditions were applied.

e) Radial and axial heat structure (fuel rod) nodalisation?

Radial: 5 pellet + 1 gap + 2 cladding, axial: 24 active + 1 lower ref. + 1 upper ref.

f) Used correlations for fuel properties vs. temperature?

PBTT benchmark specifications.

II. Core neutronics model

a) Number of radial nodes per assembly?

One per assembly.

b) Axial nodalisation?

24 active + 1 lower ref. + 1 upper ref.

c) Radial and axial reflector modelling?

One reflector at radial boundaries and axially, one node for upper and one node for lower boundaries of the channels.

d) Cross-section interpolation procedure used?

Linear interpolation.

e) Used method to get a critical reactor at the beginning of transient?

Eigenvalue solution and fixed source solution are used.

f) How xenon effect is modelled?

Microscobic cross-sections and number densities provided by benchmark team were used.

g) How Assembly Discontinuity Factor (ADF) is modelled?

Values from cross-section libraries were used. Those libraries were provided by benchmark team.

h) Is bypass density correction used? If it is used, how it is modelled?

Yes. Methodology is consistent with the final specification.

i) How decay heat modelling is modelled?

Answer: ANS-1979 Std.

III. Coupling schemes

a) Hydraulics/heat structure spatial mesh overlays (mapping schemes in radial and axial plane)?

One-by-one mapping.

b) Hydraulics/neutronics spatial mesh overlays (mapping schemes in radial and axial plane)?

According to methodology specified in the final specification.

c) Heat structure/neutronics spatial mesh overlays mapping schemes in radial and axial plane)?

Same as one applied for hydraulics/neutronics spatial mesh overlays.

d) Temporal coupling scheme?

T-H state variables of previous step were fixed.

e) Coupling numerics – explicit, semi-implicit or implicit?

Explicit coupling.

f) Coupling method – external or internal?

External.

g) Coupling design serial integration or parallel processing?

Parallel Virtual Machine (PVM).

IV. General

a) User assumptions?

Assumptions are based on the specifications.

b) Specific features of the used codes?

N/A

c) Number of solutions submitted per participant and how they differ?

One solution was submitted.

TRAC-BF1/ENTRÉE (TEPSYS, Japan)

I. Thermal-hydraulic core model

a) Core thermal-hydraulic (T-H) model and nodalisation (1-D, 3-D, and number of channels or cells) – how are channels/T-H cells chosen?

1-D channel model by TRAC/BF1: 35 regions (33 active + 2 bypass).

b) Bypass channel modelling?

Two regions (one for centre orifice and another for peripheral orifice).

c) Number of heat structures (fuel rods) modelled?

One for each channel.

d) Which core thermal-hydraulic initial and transient boundary conditions are used and how?

Transient boundary conditions were applied.

e) Radial and axial heat structure (fuel rod) nodalisation?

Radial: 5 pellet + 1 gap + 2 cladding, axial: 24 active + 1 lower ref. + 1 upper ref.

f) Used correlations for fuel properties vs. temperature?

As specified in Final Specification (default of TRAC/BF1).

II. Core neutronics model

a) Number of radial nodes per assembly?

One per assembly.

b) Axial nodalisation?

24 active + 1 lower ref. + 1 upper ref.

c) Radial and axial reflector modelling?

Radial: one per reflector, axial: one for lower and another for upper reflector.

d) Cross-section interpolation procedure used?

Linear interpolation regarding to independent instantaneous variables.

e) Used method to get a critical reactor at the beginning of transient?

Eigenvalue solution + fixed source solution.

f) How xenon effect is modelled?

Production of Xe micro cross-section (given by OECD/NEA) and Xe number density (also given by OECD/NEA).

g) How Assembly Discontinuity Factor (ADF) is modelled?

General Equivalence Theory (same as SIMULATE3).

h) Is bypass density correction used? If it is used, how it is modelled?

Yes. According to methodology specified in the final specification.

i) How decay heat modelling is modelled?

ANS-1979 Std.

III. Coupling schemes

a) Hydraulics/heat structure spatial mesh overlays (mapping schemes in radial and axial plane)?

One-by-one mapping.

b) Hydraulics/neutronics spatial mesh overlays (mapping schemes in radial and axial plane)?

According to methodology specified in the final specification.

c) Heat structure/neutronics spatial mesh overlays mapping schemes in radial and axial plane)?

Same as one applied for hydraulics/neutronics spatial mesh overlays.

d) Temporal coupling scheme?

T-H state variables of previous step were fixed.

e) Coupling numerics – explicit, semi-implicit or implicit?

Explicit coupling.

f) Coupling method – external or internal?

External.

g) Coupling design serial integration or parallel processing?

PVM.

IV. General

a) User assumptions?

N/A

b) Specific features of the used codes?

Automatic time-step-control method introduced considering changing rate of state variables.

c) Number of solutions submitted per participant and how they differ?

N/A

RELAP5/PARCS (U.PISA, Italy)

I. Thermal-hydraulic core model

a) Core thermal-hydraulic (T-H) model and nodalisation (1-D, 3-D, and number of channels or cells) – How are channels/T-H cells chosen?

3-D, 33 channels according to the benchmark specification core mapping.

b) Bypass channel modelling?

Yes. One bypass channel is modelled.

c) Number of heat structures (fuel rods) modelled?

33 heat structures.

d) Which core thermal-hydraulic initial and transient boundary conditions are used and how?

The considered boundary conditions are those provided in the NEA/BWRTT CD-ROM (core inlet mass flow rate, core inlet temperature, core outlet pressure).

e) Radial and axial heat structure (fuel rod) nodalisation?

24 axial nodes and 33 radial nodes.

f) Used correlations for fuel properties vs. temperature?

Tables are used (fuel properties variation with temperature).

II. Core neutronics model

a) Number of radial nodes per assembly?

1

b) Axial nodalisation?

24

c) Radial and axial reflector modelling?

888

d) Cross-section interpolation procedure used?

Bi-linear.

e) Used method to get a critical reactor at the beginning of transient?

The convergence of the schema calculating Keff.

f) How xenon effect is modelled?

Yes.

g) How Assembly Discontinuity Factor (ADF) is modelled?

ADFs are read from the cross-section tables.

h) Is bypass density correction used? If it is used, how it is modelled?

No.

i) How decay heat modelling is modelled?

The ANS-79 is considered.

III. Coupling schemes

a) Hydraulics/heat structure spatial mesh overlays (mapping schemes in radial and axial plane)?

33/33 radial per 24/24 axial nodes.

b) Hydraulics/neutronics spatial mesh overlays (mapping schemes in radial and axial plane)?

34/19 radial per 24/24 axial nodes.

c) Heat structure/neutronics spatial mesh overlays mapping schemes in radial and axial plane)?

34/19 radial per 24/24 axial nodes.

d) Temporal coupling scheme?

Contemporary in parallel process.

e) Coupling numerics – explicit, semi-implicit or implicit?

Semi-implicit.

f) Coupling method – external or internal?

Internal.

g) Coupling design – serial integration or parallel processing?

Parallel processing.

IV. General

h) User assumptions?

i) Specific features of the used codes?

RELAP5 is a largely validated system code, PARCS allows simulating the whole core (taking into account all the fuel assemblies) and allows pin-to-pin flux reconstruction.

j) Number of solutions submitted per participant and how they differ?

One solution submitted.

TRAC-BF1/NEM (UPV, Spain)

I. Thermal-hydraulic core model

a) Core thermal-hydraulic (T-H) model and nodalisation (1-D, 3-D, and number of channels or cells) – how are channels/T-H cells chosen?

The nodalisation, which was the proposed in specifications, has 33 thermal-hydraulic channels and 26 axial levels (24 core layers plus top and bottom reflectors).

Core thermal-hydraulic channel radial map

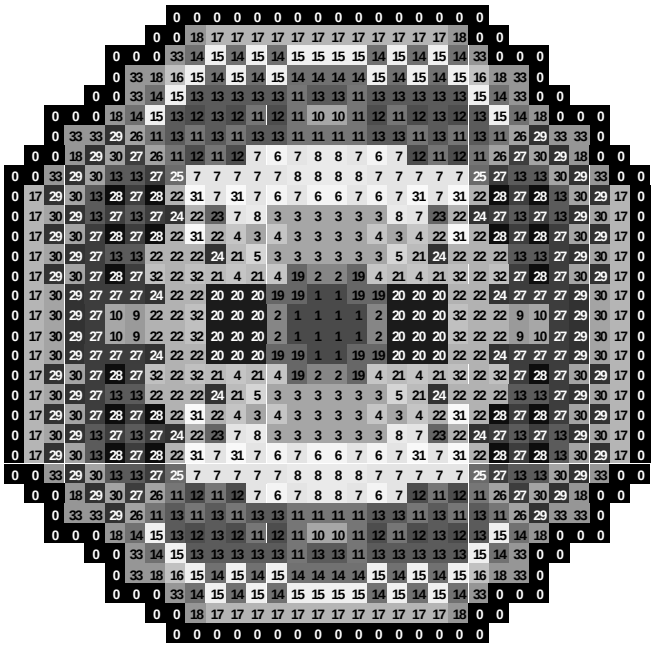

Axial nodalisation

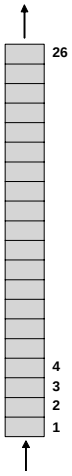

b) Bypass channel modelling?

The bypass is modelled by a TRAC channel component.

c) Number of heat structures (fuel rods) modelled?

There are a total of 888 assemblies, 764 fuel assemblies and 124 reflector assemblies. 576 fuel assemblies are 7×7 type and the remaining 188 are 8×8 type.

d) Which core thermal-hydraulic initial and transient boundary conditions are used and how?

The boundary conditions are imposed by the FILL and BREAK components of TRAC-BF1. The boundary conditions are the proposed in the specifications. See figure below.

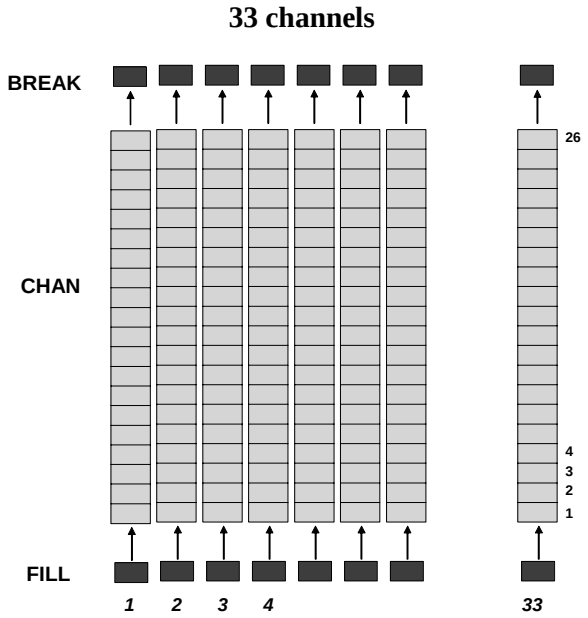

e) Radial and axial heat structure (fuel rod) nodalisation?

The thermal power is calculated for each node by the neutronic code, and this power is allocated in the correspondent axial and radial node of the heat structure.

f) Used correlations for fuel properties vs. temperature?

No.

II. Core neutronics model

a) Number of radial nodes per assembly?

We have used 1 radial node per assembly.

b) Axial nodalisation?

There are 26 axial levels, 24 core layers plus top and bottom reflectors.

c) Radial and axial reflector modelling?

The radial and axial reflector are modelled. The distribution of reflector is the proposed in specifications.

d) Cross-section interpolation procedure used?

The cross-sections are interpolated linearly with a subroutine that uses four-point linear interpolation to calculate t real cross-section based on two-group total eight cross-section data.

e) Used method to get a critical reactor at the beginning of transient?

We have calculated the steady state and we assure that the eigenvalue k_{eff} is approximately 1. After that, we normalised dividing Nu fission by $k_{eff.,}$ and then, we start the transient.

f) How xenon effect is modelled?

The effect of xenon is introduced in the absorption cross-section coefficients for the 764 fuel assemblies and for the 24 core levels by means of the following equation:

$$\Sigma_{a,2}^{i*} = \Sigma_{a,2}^{i} - \Sigma_{Xe,2}^{i} + N_{Xe}^{i}\sigma_{Xe,2}^{i}$$

where $\Sigma_{a,2}^{i*}$ is the modified absorption cross-section coefficient for node i and group 2, $\Sigma_{a,2}^{i}$ is the absorption cross-section coefficient for node i and group 2, $\Sigma_{Xe,2}^{i}$ is the xenon macroscopic cross-section coefficient for node i and group 2, $\sigma_{Xe,2}^{i}$ is the xenon microscopic cross-section coefficient for node i and group 2, and N_{Xe}^{i} is the xenon concentration for node i.

g) How Assembly Discontinuity Factor (ADF) is modelled?

The values of ADF obtained from the files *nemtab* and *nemtabr* are taken by the neutronic code and used in the calculations integrated in the code.

h) Is bypass density correction used? If it is used, how it is modelled?

When obtaining the average coolant density, a correction that accounts for the bypass channels conditions are included by the following equation:

$$\rho_{act}^{eff} = \frac{A_{act}\rho_{act} + A_{byp}(\rho_{byp} - \rho_{sat})}{A_{act}}$$

where ρ_{act}^{eff} is the effective average coolant density for cross-section calculation, ρ_{byp} is the average coolant density for cross-section calculation, ρ_{sat} is the saturated moderator coolant density of the bypass channel, A_{act} is the flow cross-sectional area of active heated channel and A_{byp} is the flow cross-sectional area of the bypass channel

i) How decay heat modelling is modelled?

With subroutines of TRAC-BF1 with 1-D neutron kinetics.

III. Coupling schemes

a) Hydraulics/heat structure spatial mesh overlays (mapping schemes in radial and axial plane)?

There are 33 TRAC-BF1 channel components with 26 channel hydraulic cells.

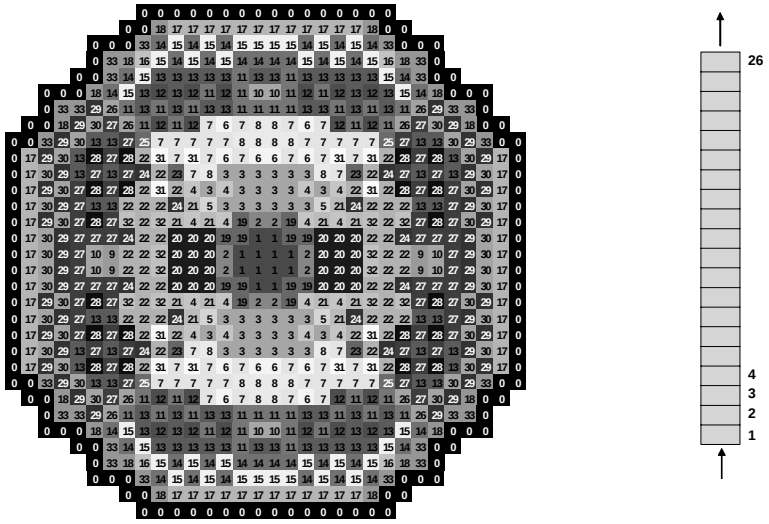

b) Hydraulics/neutronics spatial mesh overlays (mapping schemes in radial and axial plane)?

The core is divided into 888 assemblies. 764 fuel assemblies and 124 reflector assemblies. There are 19 different types of fuel assemblies distributed as it is in the figure with the characteristics described in the specifications.

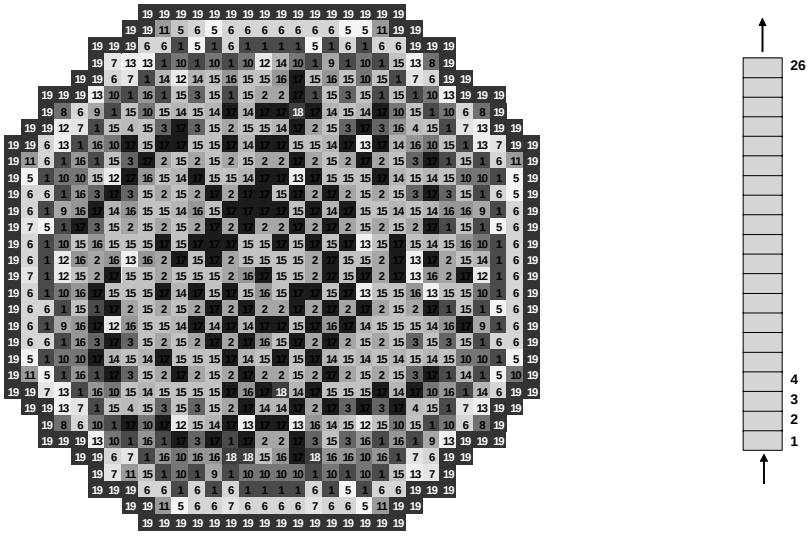

c) Heat structure/neutronics spatial mesh overlays mapping schemes in radial and axial plane)?

See figure below.

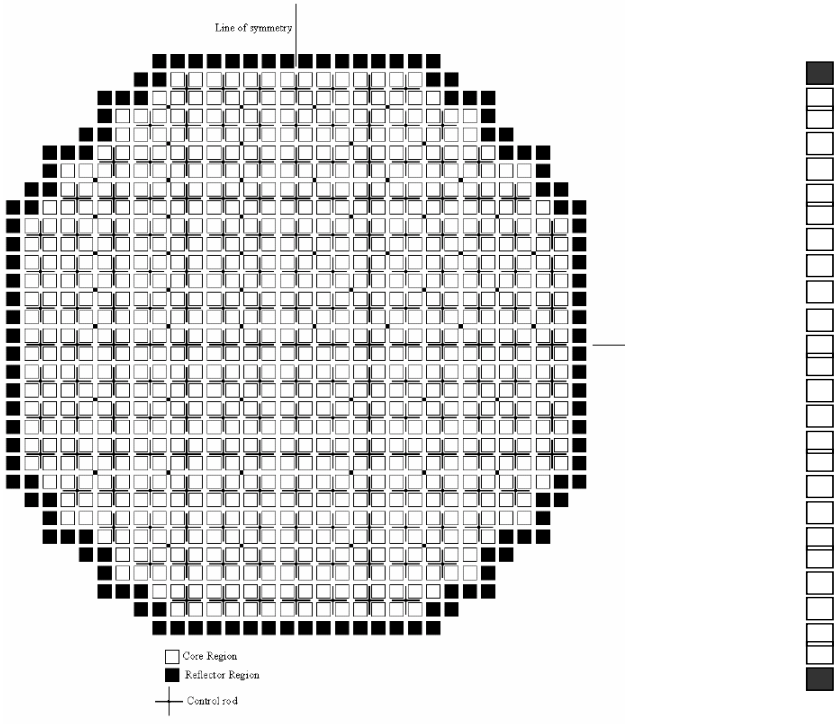

d) Temporal coupling scheme?

See figure below.

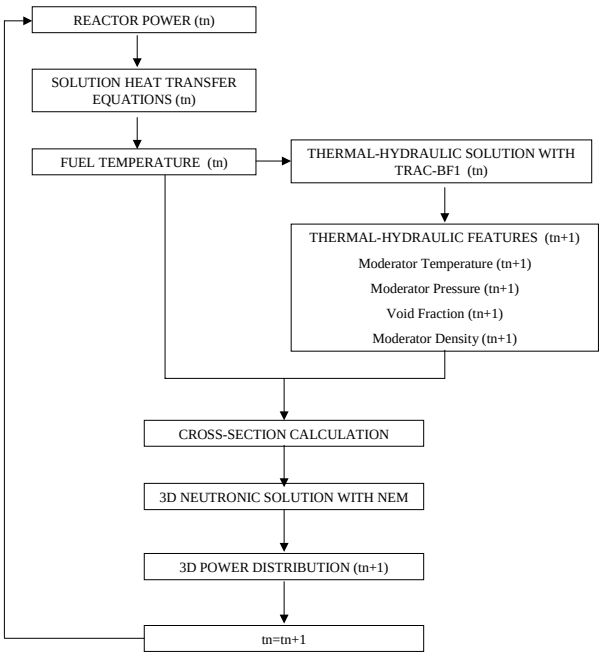

e) Coupling numerics – explicit, semi-implicit or implicit?

Semi-implicit.

f) Coupling method – external or internal?

Internal.

g) Coupling design – serial integration or parallel processing?

Serial integration.

IV. General

a) User assumptions?

b) Specific features of the used codes?

c) Number of solutions submitted per participant and how they differ?

TRAB-3D (VTT, Finland)

I. Thermal-hydraulic core model

a) Core thermal-hydraulic (T-H) model and nodalisation (1-D, 3-D, and number of channels or cells) – how are channels/T-H cells chosen?

1-D channels, one channel per fuel assembly, 764 active core channel, 24 axial mesh intervals of equal height.

b) Bypass channel modelling?

Two core bypass channels with 24 axial mesh intervals of equal height. The first channel corresponds to the flow between central core assemblies with direct heating and feedback to neutronics. Second channel corresponds to the peripheral bypass, and is not coupled to the neutronics calculation.

c) Number of heat structures (fuel rods) modelled?

One fuel rod per fuel assembly, 764 fuel rods.

d) Which core thermal-hydraulic initial and transient boundary conditions are used and how?

Outlet pressure and total mass flow, as well as inlet temperature, used as steady-state and transient boundary conditions. Inlet pressure and flow distribution checked to be adequately correct in steady state.

e) Radial and axial heat structure (fuel rod) nodalisation?

Five radial points for fuel rods, two more radial mesh points for the cladding, 24 axial layers of equal height.

f) Used correlations for fuel properties vs. temperature?

As specified in Section 3.3 of the final specifications.

II. Core neutronics model

a) Number of radial nodes per assembly?

One node per assembly.

b) Axial nodalisation?

24 axial nodes of equal height.

c) Radial and axial reflector modelling?

Reflector nodes not modelled. Albedo boundary conditions calculated from the reflector cross-sections given in the specifications.

d) Cross-section interpolation procedure used?

Linear interpolation.

e) Used method to get a critical reactor at the beginning of transient?

Number of neutrons from fission divided by calculated k_{eff}.

f) How xenon effect is modelled?

The suggested xenon correction used for the full power steady state and the transient with the xenon number density kept constant during the transient. No correction for the HZP calculation.

g) How Assembly Discontinuity Factor (ADF) is modelled?

ADFs interpolated from tables similarly as the cross-sections.

h) Is bypass density correction used? If it is used, how it is modelled?

Yes, as specified, from the first bypass channel [cf. question b)].

i) How decay heat modelling is modelled?

Time evolution of decay heat (ANSI-79 standard) followed dynamically in each assembly. For axial distribution the initial steady-state fission power distribution is used through the transient.

III. Coupling schemes

a) Hydraulics/heat structure spatial mesh overlays (mapping schemes in radial and axial plane)?

One-to-one mapping. Each hydraulics channel corresponds to one heat structure with the same axial nodalisation.

b) Hydraulics/neutronics spatial mesh overlays (mapping schemes in radial and axial plane)?

One-to-one mapping. Each neutronics node corresponds to one hydraulics mesh interval radially and axially.

c) Heat structure/neutronics spatial mesh overlays mapping schemes in radial and axial plane)?

One-to-one mapping. One fuel rod modelled for each fuel assembly with the same axial nodalisation.

d) Temporal coupling scheme?

Thermal-hydraulics and neutronics iterated during each time step inside the same outer iteration loop (equal time step).

e) Coupling numerics – explicit, semi-implicit or implicit?

Implicit.

f) Coupling method – external or internal?

Internal.

g) Coupling design – serial integration or parallel processing?

Serial integration.

IV. General

a) User assumptions?

b) Specific features of the used codes?

c) Number of solutions submitted per participant and how they differ?

One solution.

OECD PUBLICATIONS, 2 rue André-Pascal, 75775 PARIS CEDEX 16
Printed in France.